Doctoral Dissertation

Novel nanobiotechnology platforms based on photochromic molecules

Doctoral Program in Science and Technology of Chemistry and Materials
Curriculum: Drug Discovery and Nanobiotechnologies
(32nd Cycle)
a.a. 2016-2019
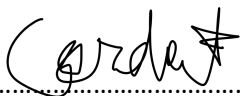
Francesca Cardano
* * * * * *

Supervisors
Prof. Silvia Giordani
Prof. Françisco M. Raymo
Prof. Gabriele Caviglioli

Doctoral Examination Committee:
Prof. Olga Bruno, University of Genoa
Prof. Santina Bruzzone, University of Genoa
Prof. Anna K.H. Hirsch Helmholtz Institute for Pharmaceutical Research Saarland (HIPS)

I hereby declare that, the contents and organisation of this dissertation constitute my own original work and does not compromise in any way the rights of third parties, including those relating to the security of personal data.

Francesca Cardano

March 2020

Summary

The development of new nano-biotechnologies is a promising and ever demanding research field. In particular, the possibility to use the organic chemistry tools to build molecules sensitive to a wide range of external stimuli, responsible of a switching between their two isomers, represents an interesting area of investigation with suitable applications in novel nano-technologies. The use of photochromic molecular switches in applications ranging from drug delivery to the probing of biochemical parameters, passing through their uses in material science, in polymer and carbon nano materials realms, constitute the main research subject of my PhD course. In this manuscript I'll report in Chapter 3 investigations upon Spiropyrans molecular switches in their metal complexations attitude for the Visible light regulated delivery of pharmaceutical active compounds. Chapter 4 will be dedicated to the study I conducted on hybrid mesostructures prepared combining Azobenzenes molecules and Graphene Oxide in order to apply these modified materials in the biological context. Chapter 5 will be instead dedicated to the study of photochromic Oxazines and Oxazolidines in their modifications with fluorophores to have ratiometric Temperature and pH sensing tools and in their use as switchable blocks in photo-modulable polymers.

List of Outputs

The experimental research activities conducted during this three-year grad school have led to the production of 5 manuscript here reported. My contribution in each of them is clearly highlighted. Moreover, I have presented my research activities with posters and oral contributions attending national and international conferences. During my PhD I have also attended a training summer school. All the details are reported below.

Publications:

- M. M. A. Mazza, F. Cardano, J. D. Baker, S. Giordani and F. M. Raymo Switchable Coumarins for Ratiometric pH Sensing_ *in preparation*

Contribution: synthesis and characterization of compounds, draft in preparation.

- F. Cardano, E. Del Canto and S. Giordani. Spiropyrans for light-controlled drug delivery. Dalton Trans., 2019,48, 15537-15544.

Contribution: All the experimental data (only exception MS measurements *E.Del Canto), draft preparation and elaboration during all the editing process (included revised version and referees' reply).

- M. M.A. Mazza, F. Cardano, J. Cusido, J.D. Baker, S. Giordani and F. M. Raymo. Ratiometric temperature sensing with fluorescent thermochromic switches. Chem. Commun., 2019,55, 1112-1115.

Contribution: synthesis and characterization of compounds, draft preparation.

- F. Cardano, M. Frasconi and S. Giordani. Photo-responsive graphene and carbon nanotubes to control and tackle biological systems. Frontiers in Chemistry, 2018, 6, 102.

Contribution: literature search and independent manuscript composition and elaboration during all the editing process (included revised version and referees'reply).

- J. Sun, F. Morales-Lara, A. Klechikov, A. V. Talyzin, I. A. Baburin, G. Seifert, F. Cardano, M. Baldrighi, M. Frasconi and S. Giordani. Porous graphite oxide pillared with tetrapod-shaped molecules. Carbon N. Y., 2017, 120, 145-156.

Contribution: synthesis of compounds and materials.

Conferences & Workshops:

- 27th IUPAC International Symposium in Photochemistry, University College Dublin, Dublin, 8-13 July 2018_"Photochemical and Photophysical Studies of Coumarin and Carbazole Fluorophores Conjugated with Photochromic Subunits". *Poster*
- Technological Workshop SCI_Chemistry of graphene and applications in catalysis and polymer_Politecnico of Milan, Milan, 13 June 2019_"Assembly of pillared graphene oxide mesostructures". *Poster*
- XXXIX Convegno Nazionale della Divisione di Chimica Organica della Società Chimica Italiana, Società Chimica Italiana, University of Turin, 8-12 September 2019 "A Spiropyran Molecule for the Delivery of Aspirin". *Oral*

Training Schools:

- COST ACTION 1507 Training School on Spectroscopy for the Characterization of Carbon- Related Materials_University of Wien, 5-8 June 2018.

Content

List of Figures

List of Tables

Chapter 1

Introduction

1.1 Photochromism

The property of some chemical compounds to reversibly change their absorption spectra, in response to an incident optical input, was defined by Hirshberg in the '50s with the term photochromism.[1] Clearly, from the macroscopic view point, the phenomenon corresponds to the visible detection of a different color.

A basic photochromic reaction can be represented by the following equation (Figure 1.0).
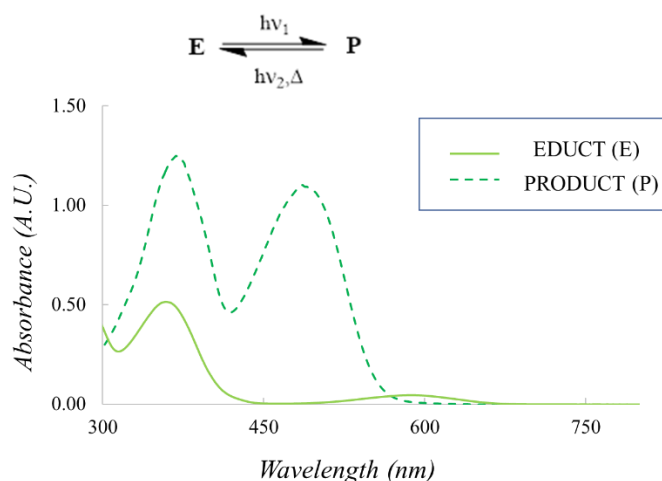
Figure1.0. Representative UV-Vis absorption spectrum and equation of a photochromic process.

Where the educt (E) is the material, a single molecule in many cases, in its not-switched and more stable state, and the product (P) is the same entity in its switched, less stable form.[2] It is clear that the photochromic molecule presents a precise and typical absorption in its more stable isomer and a different one in the metastable form. Moreover, the excitation wavelength to determine the phenomenon is usually in the UV region.[3] Commonlly, the product can be obtained by the excitation of the educt with a selected wavelength in its

absorption region and it can be re-converted in E by the exposure to another appropriate wavelength or to a heating source.[4] During the photo-reaction the molecule is moved to its excited states and the phenomenon usually consists of a photochemical process followed by a photophysical one and it is a first order process.[5] The photochromism is defined normal if the educt absorbs at shorter wavelength than the product, while an inverse photochromism occurs if the absorption's wavelength of the educt is longer than the one of the products.[6] The reactions responsible of photo-processes at the molecular level are usually due to ring closing/ring opening modifications, *trans/cis-cis/trans* isomerizations, or intramolecular charge transfer phenomena.[7] The photoisomerism is characterized by specific and intrinsic properties: fatigue, quantum yield of the photoreaction, cyclability and photostationary state, which have peculiar values depending on the type of molecules involved and in the specific reaction: their rates are representative and specific for any process.[8] The different chemical-physical properties that characterize the molecule before and after the photochromic process involve several properties as fluorescence emission, dipole moment, polarizability and the absorption of visible light. These effects are translated from the molecular level to the macroscopic one, affecting also the refractive index, the color and the solubility properties among the others.[9] Several classes of organic molecules are photochromes and they are classified by the two main mechanism of the photoreaction:

- Ring closing/ring opening: Spiropyrans, Spyroxazines and Oxazolidines, Fulgides, Diarylethenes, Dihydroindolizines, Chromenes.
- *Trans/cis-cis/trans* isomerization: Azobenzenes.

For several photochromes the ring opening/closing mechanism is followed by a *cis/trans-trans/cis* re-arrangement that contribute in the photochromic process.[10] The reversible photoconversion of these molecular switches can be used to develop new systems with specific chemical modifications that are responsible of the generation of an optical response to a guest presence.[11] If the photochromes are functionalized with ionophores' moiety, cationic or anionic receptors can be obtained, and they can be controlled in their sensing capabilities with different wavelength's irradiation stimuli.[12,13] The reversibility features due to the photochromic substrate of those sensors represent a key role in the systems. Moreover, in some cases, with particular functional groups in the molecule's scaffold, the

presence of a guest entity is sufficient to switch the molecule to its metastable isomer and the back reaction to the more stable isomer in these situations is achieved removing the guest species or applying a light stimulus or a heating source.[14] The switching at the molecular level of compounds affected by photochromism can be obtained by the application of other stimuli over light and specific guests. In particular, some switches are sensitive to pH variations showing an halochromic behavior.[15] In many systems where the isomerization process occurs *via* ring opening and closing processes, the bond breakages can be obtained inserting an acidic source in the molecular environment (i.e. decreasing the pH), this phenomenon is effective for molecules as spiropyrans and spiroxazines-oxazolidines and the reverse reaction to return to the educt moiety is achieved with an increase of the pH values.[16] These evidences allowed the use of these compounds also as pH sensors. The spectroscopic properties of the isomer obtained by the application of different external stimuli can be different depending on the nature of the applied stimulus and on the type of molecule involved, this means different chemical/physical properties of the systems, suitable for the final applications.[17-19] The variety of photochromic molecules in terms of chemical scaffolds, the possibility to change their properties through synthetic strategies and the possibility to use several classes of stimuli have paved the use for different purposes. Firstly, the chromophoric properties of these molecules have allowed their use as dyes and pigments,[20] while, after the discovery of their photochromic behavior, they have been applied in several area: from photo-switchable materials to sensing materials or molecular sensors.[21-23] Molecular photo-switches act at the micrometer level, the isomerization process mainly occurs at the nanosecond/microsecond time scale from E to P, while the reverse reaction is usually slower.[24] They have been introduced as building blocks for molecular logic gates because they are able to reproduce logic functions.[25] Unfortunately, the fatigue and the limits in the cyclability of the switching after a certain numbers of cycles have reduced the potential applications in this field. The photostability is crucial for the applications and uses of these compounds. The assembly, mainly *via* covalent attachment or strong interactions to polymeric backbones, materials and surfaces represent the current strategy to have suitable photochromic compounds with an enhanced stability overtime and environmental conditions because in these conditions the molecules are more photostable than in solutions. The assembly of these switchable entities has been indeed successful for

applications in polymer chemistry as well as in CNMs chemistry. They have indeed been used for the assembly of photo-responsive materials with applications in material science[26,27] and in life science through the conjugation with bio-molecules[28,29] as well as they have been used to design systems to regulate physical processes to develop smart tools.[30,31] Modifications in the chemical scaffolds, have opened the way to photoactivation processes achievable with different type of light stimuli, and in particular, considering the possibility of application in the biological context, the possibility to use Visible light as stimulus, instead of UV light, opens the use of these systems for the development of no-dangerous and safe devices. During my PhD course I have focused the study on three classes of photochromic molecular switches: Spiropyrans, Azobenzenes and Spyroxazines-Oxazolidines with the goal to develop new nanotechnologies with potential final applications for many of them in the biological context.

1.1.1 Spiropyrans
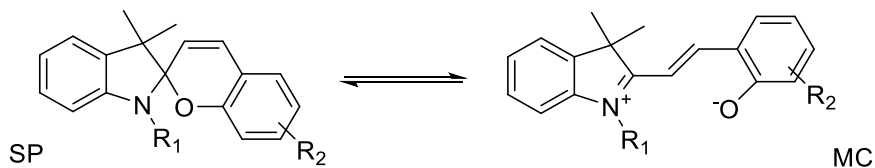
Figure 1.1. Schematic representation of a Spiropyran molecule in its two isomers_SP(left) and MC (right).

Spiropyrans[32,33] are also known as spirochromenes, they are characterized by a twisted structure made of two heterocyclic units linked to each other through a tetrahedral carbon atom: the spiro-junction. In this conformation, the two halves of the molecule lie in two orthogonal planes (Figure 1.1). The closed stable isomer form is named spiropyran (SP) and, due to its geometrical conformation, the π-electron conjugation between the two heterocycles (indolenine and benzopyran) doesn't occur; the spiro C-O bond breaks and the cis-trans isomerization of the double bond occurs upon exposure to UV radiation. The open metastable isomer is called merocyanine (MC) and it shows a planar conformation and a delocalized π electron system[34]SP and MC present well known different chemical-physical properties: firstly the MC isomer in solution shows a strong absorption in the visible region with a maximum around 550 nm, the SP isomer absorbs intensely in the UV region usually

between 200 and 300 nm. Moreover, MC isomers show fluorescence emission in the visible range.[35] As already mentioned, the switching process is reversible and the MC conversion to the stable SP form is restored with the usual conditions: exposure to visible light or heating the sample without applying light sources.[36-37] Furthermore merocyanine can be stabilized through coordination with metal ions allowing the SP-MC isomerization to occur also in the dark.[38] The improvement of the complexation of spiropyrans with metal cations by chemical modifications of the substituents on the spiropyran moiety[39,40] has allowed the development of this class of photochromic molecules for sensing.[41] In terms of synthesis of the molecular scaffold: two main approaches can be followed for the synthesis of spiropyrans: 1) the condensation of an indolenine base presenting an active methylene group with an o-hydroxy aromatic aldehyde[42] 2) the condensation of o-hydroxy aromatic aldehyde with the salts of heterocyclic cations and the following removal of the elements of the acid from the obtained stiryl salt with amines or gaseous ammonia.[32]

1.1.2 Azobenzenes
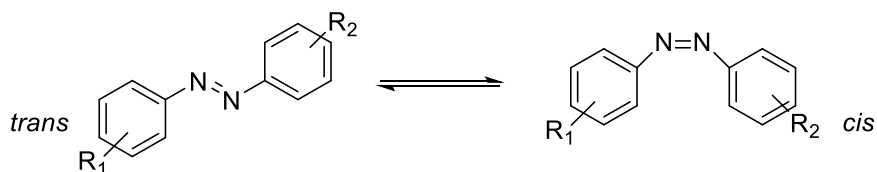
Figure 1.2. Schematic representation of an Azobenzene molecule in its two *trans* (left) and *cis* (right) isomers.

Di-aza stilbenes, better known as azobenzenes (AB), have been discovered and used as dyes and pigments since the end of XIX century[43] while their photochromic properties and their reversible isomerization have been elucidated in the first half of 1900s[44,45] (Figure 1.2). The reversible isomerization process of these derivatives involves the switch of the geometry of the N=N double bond that could shift between the *trans* and *cis* conformations. When the more thermodinamically stable *trans* (or E) isomer is exposed to UV light, it converts to the *cis* (or Z) metastable form,[46] that, being the less stable, reverts spontaneously back to the trans form with a high quantum yield. This re-isomerization can be gained in less time by heating or by exposition of the *cis* form to VIS light. The kinetic of both isomerization

reactions, i.e. *trans/cis* and *cis/trans*, are dependent on the substituents present on the molecules and their relative positions respect to the phenyl rings.[47] The presence of a lone pair electron on nitrogen atoms of the AB molecules is responsible of a n-π* electronic transition, in addition to the π-π* one. The first transition, at lower energy, occurs between 430 and 440 nm for both AB isomers, while the second occurs in the UV region. These bands are very sensitive to the presence of substituents on the AB backbone as well as to the solvent's effects, such as the interaction between the solvent and functional groups or bathochromic shifts due to the polarity of the solvent itself.[48] Several synthetic strategies have been proposed for the preparation of the AB's photo responsive scaffolds. The most frequently used approach involves the azo coupling reactions,[49] but also the Wallach and Mills reactions are good synthetic routes to obtain these compounds. The methodology of the azo coupling is a well-established procedure to prepare AB derivatives and it is based on the diazotization of an aromatic primary amine at temperature under $0°$ C where the diazonium species is stable, then it can react with an electron rich aromatic nucleophile to give the desired azobenzene.[50] The yields of these kind of reactions are good and the reaction's time is usually in the order of 1-2 hours.[51] Mills reaction occurs between aromatic nitroso derivatives and anilines in glacial acetic acid at room temperature: the lone pair on the nitrogen of aniline attacks the nitroso derivative in acid media, allowing the formation of an intermediate that after the removal of a molecule of water give the desired product.[52] The Wallach reaction implies a rearrangement sequential to a conversion, in acidic condition, of the nitrobenzene into the azoxybenzene. The reduction's agents involved in the formation of the azoxy species are several as the Wallach's mechanisms proposed[53] and the final treatment with the acid results in the formation of a mixture of azobenzene products. Several are the applications of ABs molecule due to the possibility to insert chemical modifications in the main scaffold, this peculiarity has paved the way for the applications in material science, and in particular we have focused our interest on the applications in the Carbon Nanomaterials environment.

1.1.3 Oxazines and oxazolidines
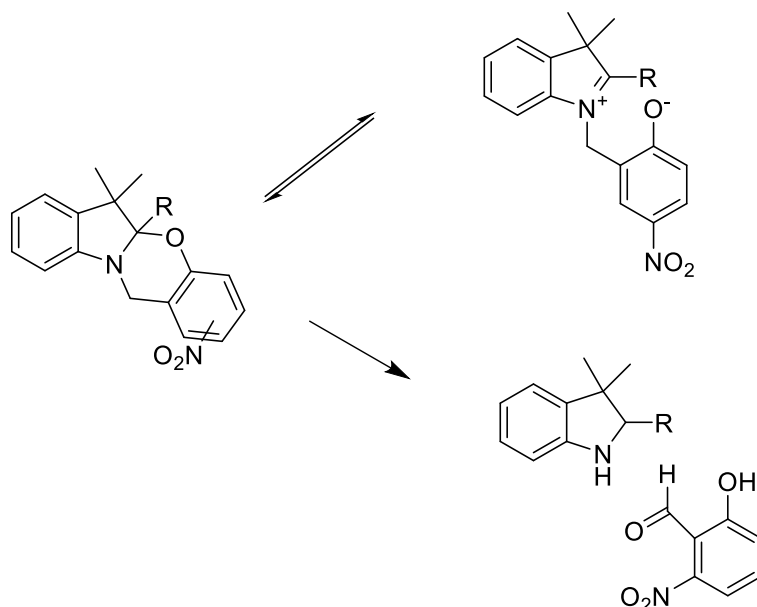
Figure 1.3. Schematic representation of Oxazines scaffolds in their reversible and irreversible forms.

2H,4H-benzo[1,3]oxazine, i.e. Oxazines (Figure 1.3) have been designed and studied to improve the switching fastness and the fatigue resistance of the previously described spiropyrans to obtain molecular switches systems with better performances.[24] The goal has been achieved designing and synthesizing molecules with a scaffold where a 2H,4H-benzo[1,3]oxazine and a 2H,3H-indole heterocycle are fused together by a [C-N] bond.[54] In this way the photochromic conversion of the molecule is achieved just through the cleavage and the formation of the [C-O] bond upon the exposition to wavelength in the absorption area of the 4-nitrophenoxychromophore.[55] This stimulus is responsible of ring opening and ring closing phenomena without the need to switch the *trans/cis-cis/trans* configuration of a [C=C] linkage, that was instead necessary for the photochromic switching of spiropyrans.[54] The results are a faster switching to the metastable charged isomer on a picosecond time scale and the possibility to repeat the switching process for a higher number of cycles without evidence of degradation, indeed commonly the molecules in their zwitterionic form are spontaneously reverted to the original isomer after few milliseconds in the worse cases.[56] In addition, the photochromic switches of these systems don't happen through a triplet state as for spiropyrans: this means systems not affected by singlet oxygen species that are instead formed during the photoconversion of spiropyrans, representing an

advantage for their applications in particular in terms of stability and degradation.[57] The oxazine systems present also an halochromic behavior, indeed the opening of the ring can be achieved by the exposition to acidic conditions: this process cause the formation of the protonated form of the opened isomer.[55] In this situation the system is reverted to the initial isomer through neutralization with bases *via* a 4-nitrophenolate intermediate. The possibility to modify from the synthetic view point the scaffold of these molecules allow to prepare systems with different switching speeds and with different functional groups for different uses; in particular the possibility to insert different groups at the chiral center of the ring closed oxazine is fundamental for their applications. This C atom present a sp^3 hybridization in the close conformation that isolate any substituent attached in this position from the electronically view point from the indole heterocycle, when the ring is instead opened, this carbon atom presents an sp^2 hybridization that allow a conjugation with the linked heterocycle.[56,57] This interesting aspect has been extensively used to insert chromophoric groups in that position with the goal to selectively control and activate several of their intrinsic properties.[31,58] Moreover, it is interesting to highlight that modification in the position of the nitro group can have severe effects on the switchability and reversibility of the system. The first class of designed Oxazines showed this group in para position in respect to the oxygen: the switching process is reversible. Dr. Raymo's research group recently synthesized molecules where this group is relocated to the meta position: the switching process change from reversible to irreversible.[59-60] The illumination in the same region is responsible of a total cleavage of the oxazine structure with the release probably of a nitrosobenzaldehyde species without any possibility of reversibility. These features have allowed the development of interesting system to control-regulate and activate several chemical-physical properties at the single molecule level and in material applications with the final possibilities to develop in particular photoactivatable fluorescent system to develop bio-imaging and sensing tools.

A similar phenomenon can be achieved using 2H,3H-indole heterocycle modified with a 2H,3H,4H,5H-[1,3]oxazole (oxazolidine) heterocycle instead of a oxazine ring (Figure 1.4).
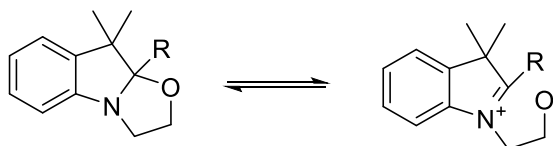
Figure 1.4. Schematic representation of Oxazolidine structures.

With this chemical scaffold the photochromic switchable properties of the system can be achieved upon the exposure to light or other stimuli and they can be used for the same purposes of the above described reversible oxazines and the functionalization of the quaternary sp^3 carbon is also in this situation the key point for the use of these molecules.[61] Oxazines and Oxazolidines are usually synthesized in few steps: the synthetic route usually starts from the indole entity, if some modifications are requested in this scaffold they usually occurs in position 5 and they can be achieved in the early steps, before the Oxazine formation or after the formation of the switchable scaffold. This chemical strategy represents one of the most promising strategies when photoremovable protecting groups are needed.[62] To build the oxazine itself, the opportune N-H indole is usually reacted with a 2-bromo or 2-chloro phenol derivative with the $-NO_2$ substitution in *meta* or *para* position in respect to the OH group. When the $-NO_2$ group is in *para* position, an additional treatment with base could be necessary to complete the cyclization and to have the molecule in the close form.[54] In the case of oxazolidine the process is achieved using a 1-alogenated ethanol derivative, and also in this case the basic treatment is necessary to close the ring. The functionalization at the spiro junction is usually obtained through a conjugation in strong acidic conditions between a highly reactive methyl group in position 2 of the indole portion and an aldehyde functionality in the subunit with the desired substituent. These molecules have been intensely applied in material science for the development of photo-switchable materials involving mainly polymers and they have been used for their sensing capabilities for the detection of several chemical, physical and biological parameters and to create caged photoactivable compounds.[59,63,64]

1.2 Carbon Nano Materials (CNMs)

Carbon Nano Materials (CNMs) are a family of particles and materials characterized by a composition of carbon atoms with sp^3 and or sp^2 hybridization and dimensions in the nanoscale frame,[65] these materials show interesting properties from the physical and chemical view point and the assembly of hybrid structures through the combination with small molecules represent a good compromise to improve the property of these materials, transferring the properties of the molecules to the materials or the properties of the materials to the molecules. Members of this group of materials are fullerenes, carbon nanotubes (CNTs), carbon nano-onions (CNOs), graphene, nano diamonds (NDs), carbon dots (CDs) and carbon nano-horns (CNHs). The assembly of these mesostructures can be achieved though chemical strategies implying covalent and non-covalent approaches exploiting mainly the high surface area and the direct link to sp^2 carbons or the π-π interactions between molecules and the materials.[66,67] CNMs have been intensely applied for the development of many technologies from electronic and optoelectronic technologies[68] to energy storage and production purposes[69] passing through bioengineering and biomedical applications.[70,71] The achieved results are interesting and numerous considering how the similarity in the composition and the differences in the final structures assembled have paved the way to the use for several applications (Figure 1.5).
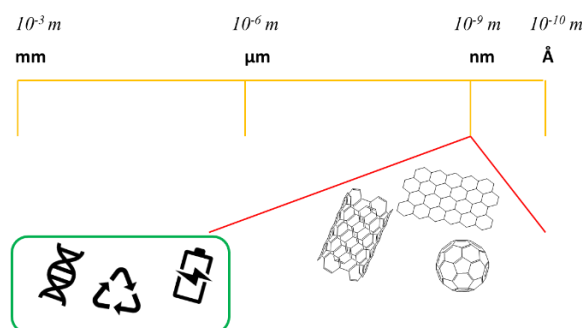
Figure 1.5. An overview on the CNMs realm and their applications in biology and low cost and renewable energy.

The functionalization of these materials with photochromic organic molecules represent the possibility to tune the properties of the hybrid structures through the simple application of

an external stimulus, this have allowed their use as molecular junctions, or transistors and electronic devices.[72] As examples: the conjugation of carbon nanotubes, with azobenzene units has resulted[73] in the development of photo-controlled transistors, diodes, electrodes and color detectors. Here the azobenzene units act as junctions and charge transporter between two electrodes and the resulting device presents stability both under mechanical stress and after many reversible photo-switching cycles.[74] A nanoscale color detector based on a single-walled carbon nanotubes (SWCNTs) non-covalently functionalized with photochromic azobenzenes, has showed that the change in the dipole moment of the photochromic molecule upon adsorption of photons results in the charge transfer between the molecule the material. Recently, the Grossman group[75] has harnessed the combination of CNTs with azobenzenes in order to achieve energy storage hybrid materials; they have found that the amount of energy stored per AB molecule was redoubled when the ABs were linked to the CNTs. Significant are the applications of CNMs in the bio environment, among them I have focused the attention on the assembly of GO based structures.

Biocompatible graphene oxide functionalized with spiropyrans or other molecular switches[76,77] have been studied for sensing of ions in cells. Photo-controllable SWCNTs have been proposed as promising scaffolds for the controlled release of zinc (II) cation, indeed preliminary investigations have evidenced the possibility to use spiropyran-functionalized SWCNT for a light controlled release of this anti-inflammatory agent.[78,79] Fluorescent nanoparticles of reduced graphene oxide, functionalized with hyaluronic acid (HA), as targeting subunit, doxorubicin as drug and SPs, as fluorescent probes, have been prepared for cellular imaging and drug delivery applications.[80] GO coupled with spiropyran-BODIPY conjugated multifluorescent polymers[81] have been prepared for bioimaging. Multifunctional materials[82] such as photo and pH tunable materials as SWCNTs modified with SP and azadipyrromethene moieties have been prepared for bioimaging applications. The developmephont of systems by combining different photochromes allows (i) the application of different wavelengths and (ii) the modulation of the properties of the different units in the system by applying the proper stimuli; the obtained materials present different tunable colors, superior photo-stability and brightness for bioimaging applications. GO coupled with spiropyran-BODIPY conjugated multifluorescent polymers[81] have been prepared for bioimaging purposes. The properties of AB have also been applied as tools for

the preparation of CNMs, in particular AB molecules and their isomerization processes upon the exposure to UV light and heating sources have been used for the exfoliation of graphite to produce graphene; indeed the significant conformational change associated with the trans–cis photochemical isomerization of alkyl-substituted azobenzenes seems to improve the efficiency of liquid-phase exfoliation, because the photochromic molecules act as dispersion-stabilizing agents.[72,83]

I herein briefly discuss the properties of the members of this family while I will dedicate a more detailed description for GO.

1.2.1. Carbon Nanotubes

Carbon nanotubes (CNTs)[84] are rolled-up cylinders of sp^2 hybridized carbon atoms organized in one sheet of graphene (single-walled carbon nanotubes, SWCNTs) or in multiple graphene layers (multi-walled carbon nanotubes, MWNTs).[85] They are usually prepared by arc discharge of graphite, laser ablation, or gas-phase catalytic growth from carbon sources, they usually need a purification process after the synthesis to eliminate carbonaceous or metallic traces that can interfere with their properties and/or uses. SWCNTs possess excellent mechanical properties: a high Young modulus accompanied by high tensile strength and elasticity, moreover they present thermal conductivity and they can also be metallic or semi conductive depending on their vector. They are used for a wide range of applications, from electronics to gas storage and sensing devices but also in nanobiotechnology, and nanomedicine.[86]

1.2.2. Graphene and Carbon dots

Graphene quantum dots (GQDs) and carbon dots (C-dots) are zero-dimensional (0D) materials with nanometric size. They both show interesting properties as photostability, absorbance and intrinsic photoluminescence (PL) that can also be photoconverted, moreover they show electrochemiluminescence and catalytic properties after opportune doping process but they have a different composition.[87] The first ones are made of hybridized sp^2 carbon and they present a crystalline structure, while the second are usually smaller and with a spherical shape primarily composed of sp^3 hybridized carbon, usually amorphous or nano-crystalline with sp^2 carbon clusters.[88] They are synthesized with 2 possible approaches

involving "top-down" methods that regard mainly breaking down or cleaving of carbonaceous materials with chemical/electrochemical and physical processes and "bottom-up" approaches that are performed through pyrolysis and carbonization or by the chemical fusion of organic molecules. Due to their optical intrinsic features these materials have seen many applications as bioimaging or gene/drug delivery tools but they are also used in the sensing realm and to conduct photoreduction and catalytic reactions and in the optoelectronic environment to prepare solar cells and supercapacitors.[89]

1.2.3 Fullerenes

Fullerene (C60), is a zero-dimensional (0D) CNM, it consists of sp^2-hybridized carbon atoms organized in 12 pentagonal and 20 hexagons rings to form a spherical structure they are produced by different techniques: chemical vapor deposition, radio-frequency or arc discharge methods and chemical synthesis. There are also other types of fullerenes characterized by an higher or smaller diameter and, accordingly, by a different number of carbon atoms.[90] Fullerenes are characterized by photoluminescence and good dispersibility and biocompatibility, they are applied in the biomedical field as bioimaging tools or photosensitizer agents, but they found applications also for the assembly of solar cells and gas storage devices.[91]

1.2.4 Nanodiamonds

Nano diamonds (NDs) consist of sp^3 carbon atoms only, which give them rigidity and strength. Nano diamonds can be prepared with different techniques: pulsed laser ablation, chemical vapor deposition and explosives' molecules detonation. The defect' centers present in the structure are responsible of their optical properties, in particular, nitrogen vacancies confer emission properties. These materials show also hardness and interesting Young's modulus, biocompatibility, high thermal conductivity and electrical resistivity. Nano diamond additives have been used for metal plating electrochemical applications, while recently they have been used for magnetic resonance imaging applications, chromatography, proteomics and mass spectrometry.[92]

1.2.5 Carbon Nano-onions

Carbon nano-onions (CNOs) are made of sp^2 carbon atoms organized in multi concentric shells of fullerenes.[93] Carbon nano-onions can be synthetized by different methods, among these, the more important are: chemical vapour deposition, pyrolysis, arc discharge and thermal annealing of detonation nano diamonds. These nanoparticles present a diameter between 2 and 50 nm and a high surface area that allow an easy functionalization, they don't show intrinsic optical properties but unfortunately they tend to aggregate in solution. They have been used for several applications[94] in electronic tribology and catalysis and due to their biocompatibility, their small size, and the possibility to functionalize them both covalently and not-covalently in order to overcome the stability issues and to introduce modification with active molecules or with compounds that can confer them optical properties they have been studied and applied mainly for bioimaging and biomedical applications.[95,96]

1.2.6 Graphene Oxide

Graphene is a two-dimensional (2D) carbon-based nanomaterial[97] made of an atom thin layer of sp^2 hybridized carbon atoms, organized hexagonally to form a honeycomb structure. It can be synthesized by different techniques, ranging from mechanical or chemical exfoliations, un-rolling of carbon nanotubes, bottom-up chemical synthesis and epitaxial growth. Graphene is particularly interesting due to its mechanical and electronic characteristics.[98] Even more useful in terms of properties and applications is its oxidized form i.e. graphene oxide (GO). GO was first discovered in 1859, obtained from graphite through an oxidative treatment.[99] The most common method to synthetize GO are the Hummers and the Brodie methods.[100] GO shows optical properties and several theories have been proposed to explain their origin: as example it seems that the electronic transition (i.e. a band gap) between the non-oxidized sp^2 carbon domain and the oxidized sp^3 one of GO sheet cause fluorescence[101] the photoluminescence properties in addition to the ultrafast optical dynamics and the nonlinear optical ones pave the way for uses as in optoelectronic devices. GO presents electronic properties such as conductivity are related to the chemical structure and its disorder due to the presence of sp^3 carbon fractions, that are mainly due to the sp^3 C-O moieties that made the material almost insulating, indeed only reduction

processes convert the material up to a semiconductor.[102,103] GO shows also electrochemical and electrocatalytic properties moreover it has an enhanced chemical activity and a good capacity for chemical functionalization. The fact that in its pristine form it already shows functional groups that are responsible of its characteristics and are useful for the additional functionalization, that can occur both covalently and no-covalently,[104,105] indeed the presence of epoxy, hydroxy, carboxylic acid groups on the surface and at the edge of the material itself and a large surface area, that promote the building of p-p interactions, represent an useful tool for the functionalization with molecules or the assembly of hybrid materials to tune and improve the properties of the material to address interesting applications. GO is also a good oxidizing agent and a carbocatalyst. GO represents a versatile substrate for uses as the assembly of GO-based electrodes to develop electrochemical technologies,[106] electrocatalytic substrates and sensors or electroluminescent devices,[107] this material is also used as substrate for the assembly of membranes to achieve filtration and separation processes,[108] hybrid GO based structures are also useful substrates for environmental and energy storage applications through the development of sponge-like assembly to achieve these results[109] but in particular its good water dispersibility and its biocompatibility have significantly indicated this material for applications in the bio context, in particular in its nano form (nano graphene oxide NGO).[71] NGO has been proposed for bio-imaging using its fluorescence in the NIR-I spectral wavelengths range and as platform for the delivery of drugs, active agents and biomolecules.

1.3 Summary

Molecular switching compounds are molecules which respond to a bunch of external stimuli exhibiting macroscopic changes due to variation in their geometrical structure. They are usually photochromic substrates which respond to electromagnetic radiation at precise wavelengths, but they have shown sensitivity also to pH variation/solvents'polarity change and guest interactions. The isomerization process is mainly reversible and the two generated species differ from each other because of their structural conformation that allow different photochemical reactions, this clearly occurs in different absorption spectra and usually different emission properties. The possibility to design and modify the molecules from the synthetic view point has allowed the development of tools for the control of phenomena and

processes. These small molecules can be applied singularly or conjugated to materials in order to address their intrinsic properties also to the material science environment paving the way to new discovery and applications in nanobiotechnologies.

1.4 Aims of the Thesis

The development of new nanotechnologies is an ever-increasing field of investigation, indeed the possibilities to develop nano-devices to address useful tasks represent a promising way to improve the technology results especially in the biological realm. To address these needs, I believe that the possibility to use photochromic compounds represents an interesting choice indeed these molecules respond to a vartiety of external stimuli, they are easy to be synthesized, they can transfer property to materials, they are efficient in terms of cyclability and they can be used as ON/OFF systems. For these reasons I have studied three different families of molecular switches with different purposes:

1.4.1 Spiropyrans

A spiropyran moiety was investigated in its chelating properties through a cationic species, using the abilities of the MC isomer in combination to a pharmaceutical active compound. I have studied the assembly of a ternary system between a Spiropyran, Zinc (II) cation, and Aspirin (ASA) to study a drug delivery system photo modulable with Visible Light that represents a potential tool for bio-medical applications (Figure 1.6).
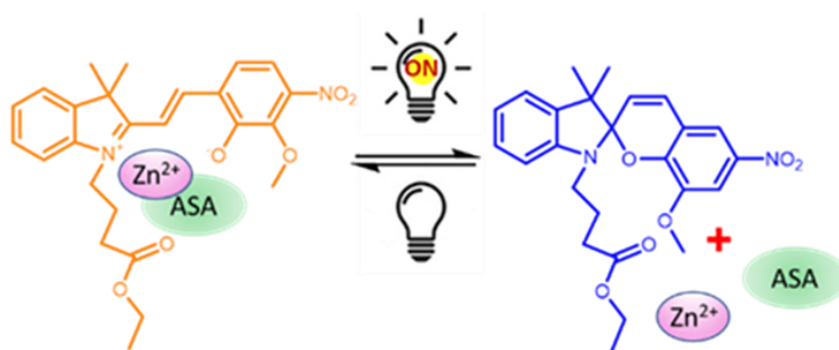
Figure 1.6 A simplified representation of the SP-based drug delivery system.

1.4.2 Azobenzenes

An azobenzene moiety represented by 2 different azobenzene structures have been applied for the assembly of hybrid photo-responsive structures through the conjugation with GO in order to develop photo-responsive materials with potential uses in the biological environments (Figure 1.7).
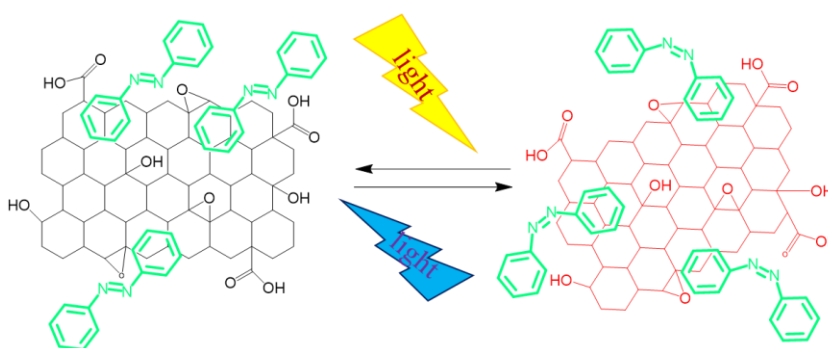
Figure 1.7 An overview upon the hybrid GO-AB based material.

1.4.3 Oxazines and Oxazolidines

Oxazines and Oxazolidines scaffolds were used as switchable units to develop fluorescent probes and sensors for chemical and physical parameters as temperature and pH with high resolution and ratiometric properties that can gain application in the biological realm. Other oxazines molecules were synthesized and studied to build switchable polymers conjugating them with not photoactivatable subunits in order to extend the properties of the switchable monomers (Figure 1.8).
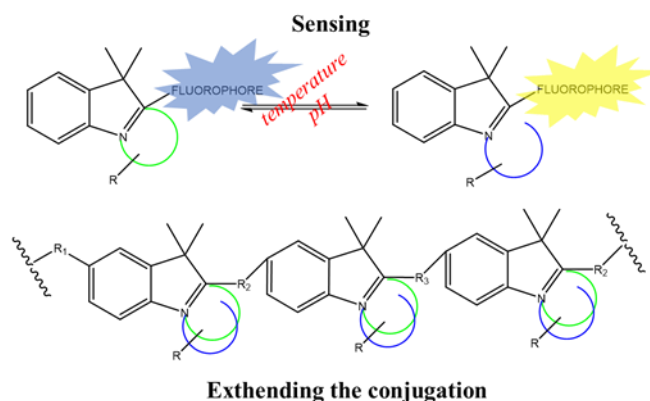
Figure 1.8 Application in sensing and polymer assembly of Oxazines and Oxazolidines.

Chapter 2
Materials and Methods

2.1 Organic Synthesis and Functionalization of CNMs

Chemicals and solvents were purchased in high-purity grade from commercial sources (Merck, TCI, VWR, Matrix Scientific, Acros Organics, Carlo Erba Reagents, Cambridge isotope Laboratories) and used as received, dry solvents were obtained through addition of molecular sieves to commercial solvents in air free containers bubbled with Argon. CNMs: graphene oxide was purchased from Graphenea as Graphene Oxide dry powder Graphenea C-132. H_2O (18.2 MΩ cm) was purified with a Sartorius Arium Advance or a Barnstead International NANOpure Diamond analytical system. Sonication was performed using an ultra sound sonic bath Elmasonic P serie.

2.2 NMR Spectroscopy

<u>Chapters 3-4-5</u>

NMR spectra were recorded with Bruker Avance 400 MHz spectrometers (400.13 MHz for ^{1} H and 100.62 MHz for ^{13}C) solubilizing the samples in the desired deuterated solvents (i.e. CD_3CN, $CDCl_3$ chapter 3_$CDCl_3$, chapter 4_$CDCl_3$, CD_3CN, DMSO-d6, CD_3OD Chapter 5).

Temperature NMR measurements were conducted measuring compound **a** 15mM in CD_3CN at 5 different temperatures: 283, 298, 308, 318 and 328 K. The sample is refrigerated to 283 K inserting the sample in an ice bath and then proceeding with the measurement, 318 and 328 K are instead reached warming the sample using the warming system of the instrument itself. (Chapter 5)

The spectra were analyzed with Mestrenova software

2.3   MS Spectrometry

HRMS spectra were recorded by MALDI-TOF MS; spectra were acquired using a Waters MALDI-Q TOF Premier spectrometer. The instrument was operated in positive or negative reflectron mode as required, all samples consisted of MeCN solutions used for the UV-Vis absorption and fluorescence emission spectroscopies (Chapter 3 and 4)

Electrospray ionization mass spectra (ESIMS) were recorded with a Bruker micrOTO-Q II spectrometer (Chapter 5)

2.4   Spectroscopies

Solvents for UV/Vis absorption and fluorescence emission spectroscopic studies were purchased in spectrophotometric or HPLC grade. 1 cm x 1 cm path length quartz cuvettes were used for UV/Vis absorption and fluorescence emission analyses.

The data collected are analyzed with Excel (Office 365) software.

2.4.1 Absorption

Absorption spectroscopy studies were performed on an Agilent Cary 8454 UV/Vis diode array spectrophotometer.

For solution spectroscopy studies, 1.00×10^{-2} M mother solutions of the SP-E_spiropyran molecule, acetylsalicilic acid (ASA) and the metal salt in MeCN were freshly prepared the day of the experiment and diluted to the appropriate concentration prior to the analysis. The experiments were performed using a 5×10^{-5} M concentration of the titrated compounds and progressive addition of 1×10^{-2} M solution of the titrant compounds. The prepared samples presented the appropriate concentration of 5×10^{-5} M for each component in MeCN solution, that was the one used for all the measurements.

The effect of visible irradiation/dark cycles were repeated three times to test the system's stability and was evaluated by means of absorption spectroscopy by using a Cary 6000i UV/Vis/NIR spectrophotometer; the solutions were exposed to broadband visible-light

illumination by using and were allowed to equilibrate in the dark inside the spectrometer chamber while performing the measurement. Data were acquired every 5 min for 36 consecutive turns.

<u>Chapter 4</u>

The Uv-Vis Spectroscopy measurements were conducted for material samples and for the AB molecules alone. Pristine GO, GO-AB1 and GO-AB2 samples were performed using 100 µg/ mL DMSO solutions of the material, the necessary samples were prepared diluting 1mg/mL principal concentrated solutions after their sonication for 5 min. AB1 and AB2 solutions were measured as $3 * 10^{-5}$ M DMSO solutions prepared by opportune dilution of concentrated batches. For the AB cis-trans isomerization studies a 4watt UV-lamp at 365 nm usually used for TLC detection, a low-power LED torch (Varta EasyLine Trilogy, white LED, 150 mW, 12 lumen) and a Steinel HL2010-E heat gun were used. In the UV measurements the samples were measured up to 5 min of exposure of the source, the exposure to Vis light/heat source to check the reversibility of the process was monitored every 5 min, as well as the exposure to the heat source. For sample AB1, the spectra reported after heating is upon maximum condition of heating exposure tested for sample AB2. The measurements performed in UV conditions for the GO, GO-AB1 and GO-AB2 samples were conducted with the same UV source with a UV exposure up to 2h.

2.4.2 Emission

Fluorescence spectra were recorded on a Horiba Jobin Yvon Fluoromax-4 spectrofluorometer with 3 nm excitation and emission slits, 1 nm resolution, 0.1 nms-1 scan speed.

<u>Chapter 3</u>

The solutions analyzed contain the three interacting elements at 5×10^{-5} M concentration in 1:1:1.5 SP-E:ASA:Zn^{2+} ratio in MeCN they are equilibrated in the dark for 4h and them measured, with the opportune excitation wavelengths reported in the text.

2.5 Fourier Transform Infrared Spectroscopy (FTIR)

Chapter 4

FT-IR spectra were measured in the solid state on a PerkinElmer FT-IR Spectrometer Spectrum 100 with universal equipment for transmittance measurements. The spectra were recorded at 32 scans with a 4 cm^{-1} resolution in a region between 4000 and 500 cm^{-1}. Samples were analyzed in KBr disks, prepared with 1% of sample and 99% of KBr. The measurements were conducted in Vacuum condition, and the control background was measured with disk made only with KBr. For the disk preparation a press with a pressure of around 8 tons was used applying it for 1.30 mins. The data were collected and analyzed with Origin 9.0 software.

2.6 Raman Scattering Spectroscopy (RAMAN)

Chapter 4

Raman mapping measurements were collected at room temperature on a Horiba Jobin Yvon HR 800 UV LabRam Raman microscope. The samples were deposited directly on silicon wafer and excited with a built-in 633 nm laser. The laser spot was focused on the sample surface using a 100x or a 50x objective. Raman maps were taken with 0.2 s of exposure time, one accumulation and total number of points 128x128 in a region between 500 and 2500 cm^{-1}. The data were collected and analyzed with Origin 9.0 software. The measurements performed in UV conditions for the samples were conducted with 4watt UV-lamp at 365 nm usually used for TLC detection with a UV exposure up to 2h, the consequential exposure to Vis light were performed for 1h with ambient light and 30 min with direct vis light.

2.7 X-ray Photoelectron Spectroscopy (XPS)

Chapter 4

XPS measurements were performed in XPS analysis was carried out using an X-ray photoelectron spectroscopy microprobe (PHI Quantes,ULVAC-PHI) with a monochromatic

Al Kα (1486.6 eV) radiation source. The powder samples were fixed on indium substrates. The ionizing AI(mono) source, with a charge neutralizer ON. For the recording of wide spectra PE was fixed at 160 eV with step of 1 eV, high resolution spectra were measured at PE of 10 eV with step of 0.1 eV.

2.8   X-ray Diffraction (XRD)

Chapter 4

A Panalytical X' pert X-ray diffractometer with Cu-Ka radiation (ʎ: 1.5418 Å) was used to record the diffraction patterns. The samples were prepared depositing a thin powder's film of the materials over a glass slide without the use of solvents. The already dried samples were measured with a vacuum equipment to remove any effect of humidity.

Chapter 3

Spiropyrans: preliminary investigations for drug delivery applications

3.1 Introduction

The study of new stimuli-responsive nano-devices is gaining great attention in the nanomedicine realm. The careful design of nano-carriers opens new opportunities for smart platforms responsive to different endogenous or exogenous stimuli.[110] In this context the development of new light-controlled systems is a challenging and promising field of investigation for new applications in the biological and biomedical fields. The possibility of regulating systems with a low invasive tool like visible light is promising for photo-pharmacological purposes.[111] Light stimuli can be controlled in space and time with high precision and can be easily modulated in terms of intensity and precise operation wavelength. Moreover, the assembly of coordination complexes of light-controlled scaffolds with ligands, presenting intrinsic properties itself represents a new way to study multi stimuli-responsive materials for applications in the biological realm.[112] Among photochromic and photo-switchable molecules, spiropyrans (SP)[37,113] have attracted a lot of attention for these purposes, indeed their isomerization from SP to MC can be achieved using a variety of external stimuli such as light, heat, protons and metal ions.[11] Spiropyrans have been investigated in the last decade for the formation of metal complexes with several metal ions differing in softness/hardness, coordination or binding properties that are responsible for the final geometry of the complex.[114] Many spiropyran derivatives can act as sensors for biologically important cations with the goal to obtain probes selective for specific cations, with increased chelating stability, but maintaining the ON/OFF switchability's properties fundamental for the development of multi-use sensors. I have focused my attention on derivatives that don't need UV light for the isomerization, as UV

light could represent an invasive stimulus for applications in the biological realm. Recently, the coordination chemistry of a spiropyran ester derivative: Ethyl 4-(8-methoxy-3,3'-dimethyl-6-nitrospiro-[chromene-2,2'-indo-line]-1'-yl)butanoate(SP-E), containing an N-substitution in the indolenine moiety and a NO_2 group in the benzopyran portion which stabilize the formation of MC isomer has been studied.[115] This obtained information constitute an essential starting point for the development of more complex assemblies for potential drug delivery systems. With this in mind, I investigated the possible coordination chemistry and the behavior of this molecules complexed with Zn^{2+} in presence of acetylsalicylic acid (ASA), completing several chemical and physical studies that constitute a preliminary investigation for the development of potential prodrug's delivery system (Figure 3.0).
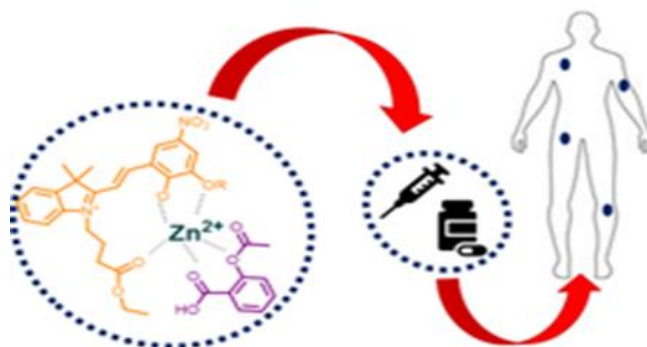
Figure 3.0. The proposed Vis-light regulated photochromic drug delivery system.

For this project Zinc was selected as cation because it represents an essential element for human being: it presents an antioxidant role and it is the cofactor for more than 200 enzymes, moreover it is a structural element for several proteins; its deficiency is responsible of issues involving the regular biochemical processes of cells and these effects can clearly show influence over the immune system and the production of hormones among the others.[116] Zinc cation has shown anti-inflammatory properties and its use has been tested as adjuvant agent in cancer prevention.[117] Recently, chronic inflammation, has been connected to the development of many forms of cancer, and for this reason the possibility to control the inflammatory response to tissue damage has become a key factor for cancer treatment and prevention.[118] ASA has been chosen as nonsteroidal anti-inflammatory drug (NSAID) because of its anti-inflammatory activity also in combination with zinc.[119] This Active

Pharmaceutical Ingredient (API), has shown to decrease the incidence of several tumor types[120] and its geometry allows its interaction with metal ions and in particular with zinc.[121]

3.2 Design of the Project

The proposed system, summarized in the scheme (Figure 3.1), presents a photo-switchable subunit that is characterized by isomerization properties already investigated by our group in presence of Zn^{2+}. The presence of a methoxy group and an O^- in the nitro-phenyl portion of the SP-E molecule in its MC form contributes to the coordination with metal cations.[115] The location of the strong electron-withdrawing nitro group in the 6' position, that stabilizes the open MC form, has highlighted SP-E as a promising candidate for my goal. ASA coordinates with Zn^{2+} in an already studied way.[122] These three compounds can be used to assembly a ternary reversible drug delivery system that can be formed in dark conditions and disassembled under visible light stimulus, allowing the controlled release of both APIs.
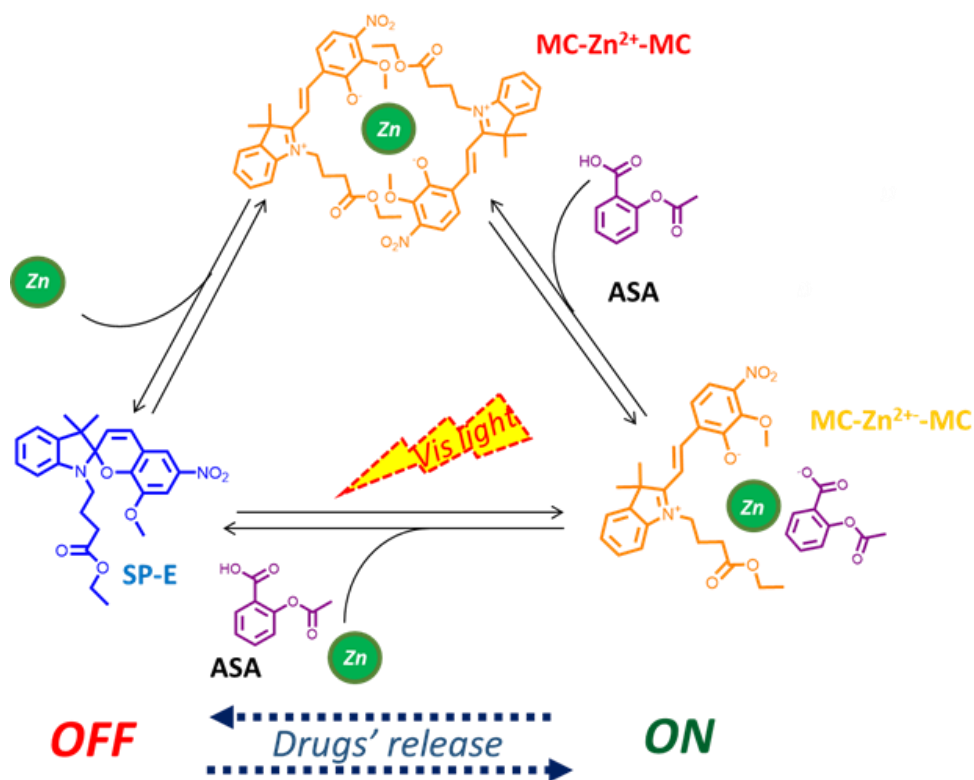
Figure 3.1 Design of the light-modulable spiropyran based molecular platform for drug delivery.

3.3 Experimental Results

3.3.1 Synthesis

The SP-E molecule was synthesized following a published procedure optimized by our group with two-steps consisting of the N-alkylation of the appropriate indolium moiety followed by the condensation with 3-methoxynitrosalicyaldheyde.[115] (Figure 3.2)
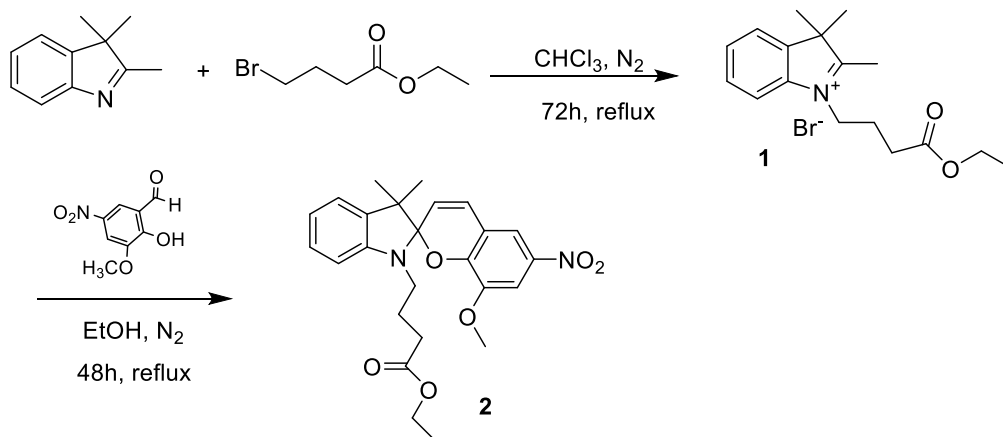
Figure 3.2 Synthetic scheme for the studied SP molecule.

1. ^{1}H NMR (400 MHz, CDCl$_3$): δ ppm = 1.24 ppm (t, 3H), 1.64 (s, 6H), 2.25 (dq, 2H), 2.72 (t, 2H), 3.19 (s, 2H), 4.10 (q, 2H), 4.80-4.97 (m, 2H), 7.45-7.67 (m, 3H), 7.97 (d, 1H); ESIMS: m/z = 274.1826 [M$^+$] (m/z calcd for C$_{17}$H$_{24}$NO$_2^+$ 274.3804).

2.^{1}H NMR (400 MHz, CD$_3$CN): δ ppm = 1.16 (s, 3 H) 1.19 (t, J=7.15 Hz, 3 H) 1.26 (s, 3 H) 1.79-1.94 (m, 2 H) 2.33 (td, J=7.15, 2.86 Hz, 2 H) 3.15-3.35 (m, 2 H) 3.79 (s, 3 H) 4.06 (q, J=7.19 Hz, 2 H) 5.97 (d, J=10.56 Hz, 1 H) 6.69 (d, J=7.7 0.7 Hz, 1 H) 6.87 (td, J=7.37, 0.88 Hz, 1 H) 7.02 (d, J=10.56 Hz, 1 H) 7.14 (dd, J=7.26, 0.88 Hz, 1 H) 7.19 (td, J=7.70, 1.32 Hz, 1 H) 7.69 (d, J=2.42 Hz, 1 H) 7.79 (d, J=2.64 Hz, 1 H); ESIMS: m/z = 453.4087[M$^+$] (m/z calcd for C$_{25}$H$_{28}$N$_2$O$_6^+$ 453.2026).

^{1}H NMR spectra are reported in the Appendix Chapter.

3.3.2 UV/Vis absorption spectroscopy

The UV/Vis absorption spectra of spiropyrans can provide precise information related to the isomerism between the close and the open form of the molecule, they are also a useful tool to indicate and control binding phenomena.

The isomerization and binding events, that generate the MC isomer in solution, are highlighted by a significant change in the photochromic properties of the compounds: the system in solution shows an absorption band in the Visible region that is absent when SPs are alone in the same pure solvent.[113]

I found that a MeCN solution containing SP-E, ASA and Zn(II) cation in 1:1:1 ratio with a $5x10^{-5}$ M concentration each, presents a significant absorption area in the Visible region (yellow line Figure 3.3).
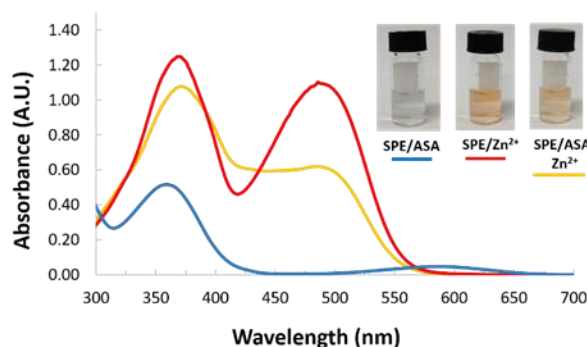
Figure 3.3 Absorption spectra of MeCN solutions of SP-E in presence of equimolar, $5x10^{-5}$ M, amount of Zn^{2+} (red line); ASA (blue line); ASA/Zn^{2+} (yellow line).

In this region, between 400 nm and 500 nm, the complexes between MC and metal complexes are usually found. The shape of the absorption in this area is different compared to the one recorded for a MeCN solution containing SP-E and Zn(II) cation in 1:1 ratio (red line Figure 3.3) at the same concentration. The absorption spectrum of a solution containing SP-E and ASA in 1:1 ratio (blue line Figure 3.3) doesn't show any absorption in this region, just a very weak band around 585 nm was found, due to the small fraction of the MC isomer present, which increases when the solution is exposed to UV light. For these reasons, I decided to investigate the highlighted area around 430 nm, that appears only in the

absorption spectra where SPE/ASA/Zn are present in solution. Additionally, the three solutions presented different colors (photo insets in Figure 3.3). Increasing the amount of ASA equivalents added the color of the solution changed significantly from orange to yellow, as evidenced in the figure below, where 0 (A), 10 (B) and 30 (C) equivalents of ASA, in respect to the MC-Zn^{2+}, were added (Figure 3.4).
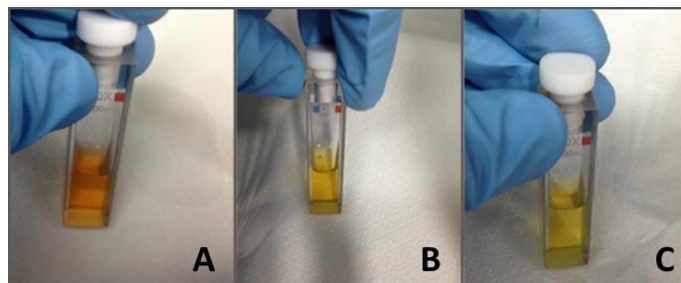
Figure 3.4 Visible color changes upon addition of increasing amounts of ASA, in details 0-10-30 equivalent of ASA added in titration (ii). The experiment is performed in a 5×10^{-5} M MeCN solution of the titrated compounds (SP-E:Zn^{2+} 1:1) with following additions of the titrant compound (ASA).

The new absorption shoulder observed at around 430 nm presented an hypsochromic shift compared to the MC-Zn^{2+} band with its maximum at 490 nm. This is a first evidence of the formation of a new species that I investigated through titration experiments for the whole system.

The experiments were performed using a 5×10^{-5} M concentration of the titrated compounds and progressive addition of 1×10^{-2} M solution of the titrant compounds to maintain the necessary equivalents ratios. The analyzed samples presented a concentration of 5×10^{-5} M for each component in MeCN solution. Two strategies were followed: (i) addition of increasing amount of $Zn(ClO_4)_2 \cdot 6H_2O$ to a 1:1 ratio of SP-E and ASA; (ii) addition of increasing amount of ASA to a 1:1 ratio of SP-E and $Zn(ClO_4)_2 \cdot 6H_2O$ (consisting in a MC-Zn^{2+} solution previously equilibrated overnight). The obtained data were reported respectively in Figure 3.5a and 3.5b. Moreover, considering the results obtained by the strategies (i) and (ii) I have performed another titration experiment (iii) achieved by the addition of increasing amounts of $Zn(ClO_4)_2 \cdot 6H_2O$ to a 1:10 ratio of SP-E and ASA (Figure 3.5c).
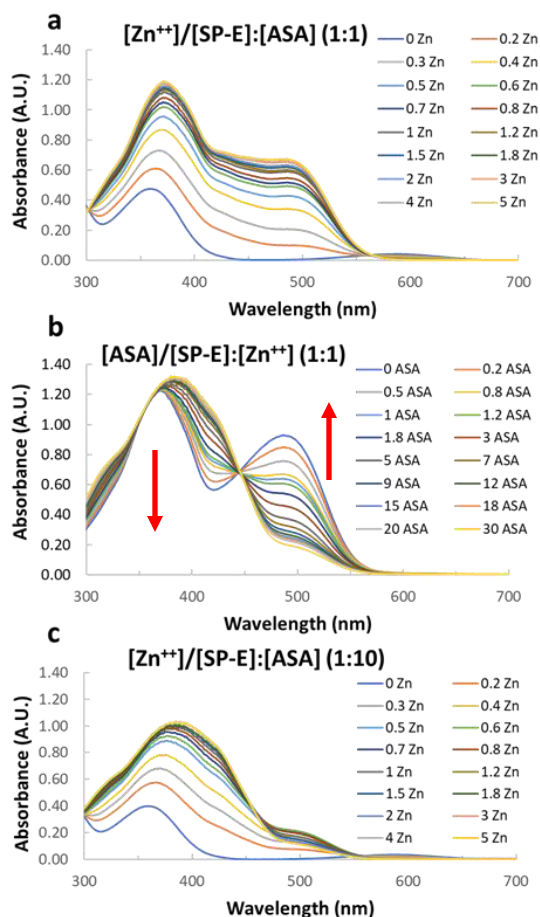
Figure 3.5 UV/Vis absorption spectra changes upon the addition of increasing amounts (equivalents) of titrating agents a) $Zn(ClO_4)_2*6H_2O$ to a 1:1 ratio of SP-E and ASA; b) ASA to a 1:1 ratio of SP-E and $Zn(ClO_4)_2*6H_2O$; c) $Zn(ClO_4)_2*6H_2O$ to a 1:10 ratio of SP-E and ASA.

The spectra were measured after the equilibration of the ternary system with the aim to prove also its stability overtime. The formation of the complex is not immediate; this process is correlated to the rate of isomerization from the SP to the MC isomer and is reported in the irradiation experiments shown in the next paragraph. For this evidence, I measured the spectra after 3 h from the addition of the titration agent to be sure to investigate the whole complex after its complete formation. Moreover, the whole complex is stable up to 1 month (with no signs of precipitation, no variation in absorption spectra or in color). The following spectra confirm these results (Figure 3.6)
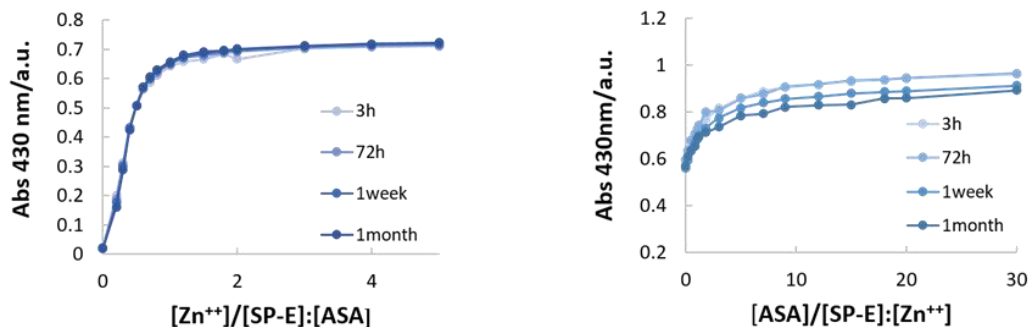
Figure 3.6 Titration experiments were performed preparing the MeCN solutions containing the necessary components (i.e. SP-E and ASA or SP-E and Zn^{2+}), the titrations agents (i.e. Zn^{2+} or ASA) were added to those solutions and the samples were stored in dark condition for 3h to allow the systems' equilibration, then the spectra were recorded. The same samples for the titration Zn^{2+}/SP-E:ASA (1:1) and ASA/SP-E:Zn^{2+} (1:1) were kept and monitored in time and they don't show any variation up to one month after the samples' preparation.

During the titrations I have analyzed the spectroscopic behavior of the two absorption bands at 430 nm and at 490 nm, that could correspond to the ternary system and the MC complex with Zinc(II) cation respectively.

It is clear from Figures 3.7 how the presence of ASA influences the equilibria in solution of the whole environment, indeed the titration's spectra, analyzed at the selected wavelength of 430 nm and 490 nm, highlight how the equilibria are different.
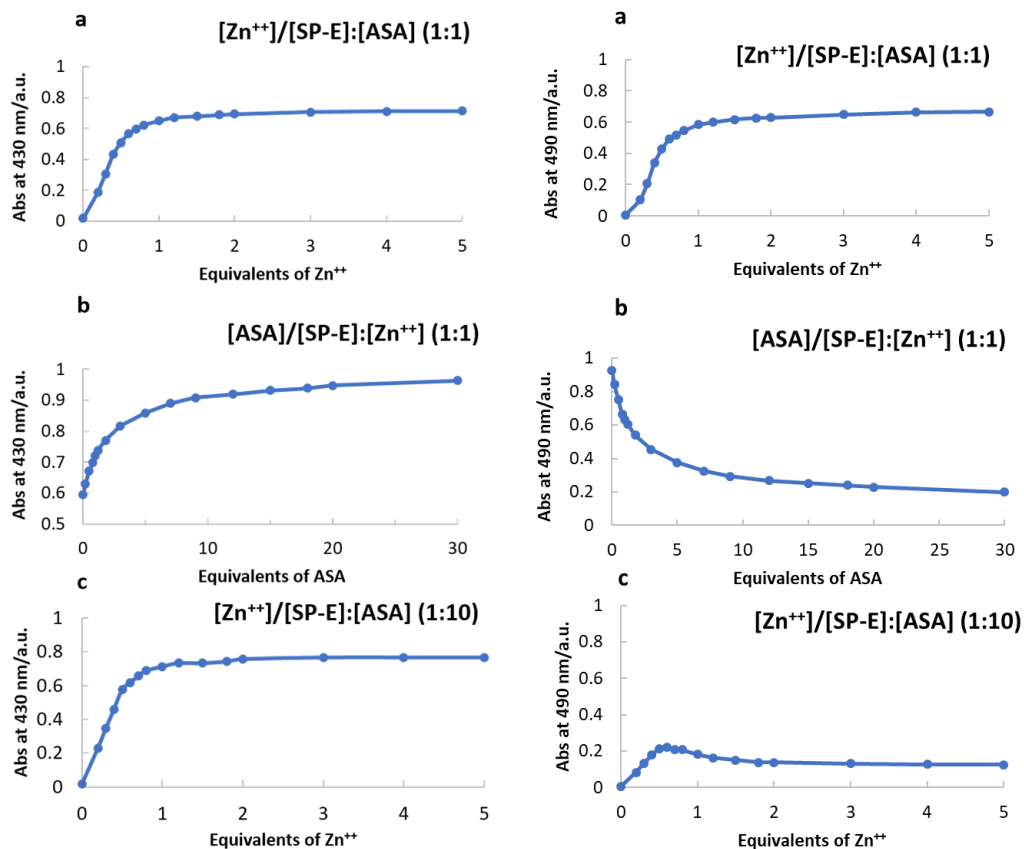
Figure 3.7 Titration curves for the performed experiments analyzed at 430 nm and 490 nm upon the addition of increasing amounts of a) $Zn(ClO_4)_2*6H_2O$ to a 1:1 ratio of SP-E and ASA; b) ASA to a 1:1 ratio of SP-E and $Zn(ClO_4)2*6H_2O$; c) $Zn(ClO_4)_2*6H_2O$ to a 1:10 ratio of SP-E and ASA.

The absorbance spectra (Figure 3.6) show different shapes depending on which titration agent was added. The different titration tests present different features and the comparison of the two selected wavelengths (430 nm and 490 nm) confirmed these different trends. The (**3.5c**) titration experiment was conducted in order to define the properties of the system in a situation where the ASA component was in excess compared to the others considering that in titrations (**3.5a-b**) it seemed that it was needed 10 times more the amount of ASA to achieve the stability of the titration.

In particular, the UV-Vis absorbance spectroscopy data collected, and the titration curves analyzed at 430 nm and 490 nm highlight how, in the titration performed using ASA as titrating agent, the two species shown a competitive formation's feature. While the absorption shoulder at 430 nm increased during the experiment the band at 490 nm decreases

(Figure 3.7): this can be interpreted as the formation of a new ternary system between the three elements despite the MC-Zn^{2+} complex. A deeper analysis on the plotted data shows that the stability, i.e. the plateau region, was achieved at different values depending on the titrating agents. In case of zinc titration, the amount of equivalent needed to reach the plateau is around 1.2, while in the case of the ASA titration, the equivalents' amount is ten times more, indeed about 12 equivalents were necessary to reach a stabile value. These data show how the binary system (SP-E:Zn^{2+}) and the ternary one (SP-E:ASA:Zn^{2+}) were in competition for their formation, where the one with two components was more favorite. Zinc titrations performed in samples containing ASA in excess (10:1 ratio to SP- E) shown the expected trends. By the plotted data we can observe that in this experiment, while the species at 430 nm increased until a plateau constant region, the species at 490 nm presented a slight increase until around 0.6 equivalents, it then decreased to a constant value at around 1.8 equivalents (as we can clearly observe from the enlargement here reported to highlight the phenomena, figure 3.8).
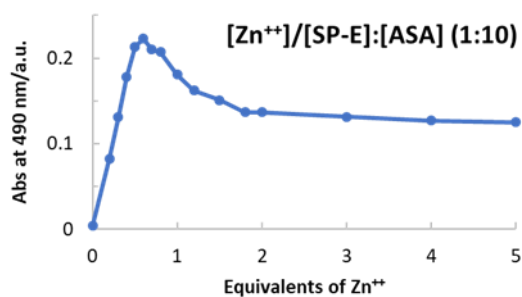
Figure 3.8 Enlarged version of Figure 2.7c in absorbance between 0 and 0.25. The absorbance at 490 nm increase until 0.6 equivalents, then it decreases to a stable value at around 1.8 equivalents, where the plateau region begins.

This trend could be an additional information that in presence of an excess of ASA, in case of zinc titration, the species at 490 nm seems to be limited in its formation because zinc is involved in the formation of the ternary system that is in competition with the formation of the binary one.

To conduct a deeper investigation of the system, UV-Vis measurements were conducted also in MeCN solutions containing the SP-E molecule and a preformed acetylsalycilic acid-

Zinc(II) salt. These comparison's measurements were performed with the aim to highlight how is important to insert in the systems all the components without pre-interactions/pre-complexes formation, with the goal to allow the formation of the systems between the three necessary elements i.e SP-E, ASA and Zn(II) cation which represents the object of this study, these measurements enforced my results. These additional data are accompanied by a visual colorimetric overview of the photochromic features of all the possible combinations between the three elements in MeCN solutions: it is evident also just observing the samples and their color difference, how the species in solutions were different in the various scenario (Figure 3.9).

MC:Zn (1:1)   SP:ASA:Zn (1:1:1)   SP:ASA:Zn (1:1:12)   SP:ASA (1:1)   ASA:Zn (1:1)   SP-E:ASAZnsalt (1:1)   SP:ASAZnsalt (1:50)

Figure 3.9 Representative solutions of different combinations of the three analyzed components with 5×10^{-5} M concentration.

Titration experiments conducted between SP-E and ASA and between ASA and Zn^{2+}, indicate that the new highlighted species was formed only in the simultaneous presence of the three components. Moreover, additional titration experiments were conducted with a preformed ASA-Zinc (II) salt that was synthesized accordingly to a reported procedure,[123] with the only variation of the salt's source ($Zn(ClO_4)_2 \ast 6H_2O$ instead of $Zn(SO_4)_2 \ast 7H_2O$). The titration experiments were conducted adding this pre-synthesized salt to a constant amount of SP-E at 5×10^{-5} M concentration, following the same procedure used for all the reported titrations experiments. MeCN solutions' colours looked different compared to the previous one: in these last analyses the solution looks pink coloured, while in the previous the colour was orange. This analysis shows a different behavior compared to the already performed ones as we can clearly observe in the spectra (Figure 3.10).
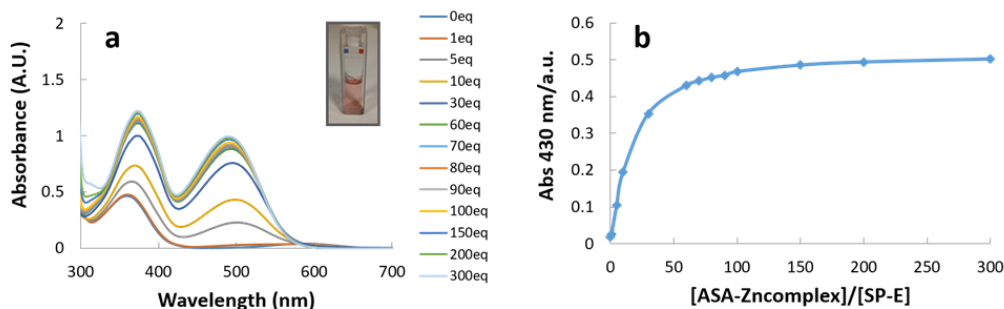
Figure 3.10 Titration experiments in a 5x10-5 M solution of SP-E with equi-molar amounts of ASA-Zn (II) complex. The experiment was conducted up to 300 equivalents, it reached a plateau region at around 120 equivalents.

The new ternary species is slower in its formation and the amount of ASA-Zn(II) complex needed to reach a plateau region is higher (around 120 equivalents), moreover the system is not stable over time (precipitation was observed). The measurements were performed after 5h from the samples' preparation. The system was not stable: after 8h from the samples' preparation, the sample containing 300 eq. of ASA-Zn (II) complex contains some precipitated material, after 24 hours also the samples containing 200-150-100 eq. of ASA-Zn (II) complexes were precipitated, in the consequent 24 hours the samples containing 90 and 80 equivalents showed precipitation. The precipitated material in the samples was analyzed by MS Spectrometry and basically consisted in ASA, the residual solutions analyzed after the precipitation phenomena shown absorbance spectra comparable to the one before the precipitation that mainly show only the presence of the MC-Zn^{2+} complex. The results of these analyses suggest that the three components were not in the right ratio to form the ternary system we want to investigate, indeed probably the zinc contribution was too low to form the ternary system and the zinc present was mainly involved in the formation of the salt with ASA and in the formation of the binary system. These data underline how our proposed ternary system shows better properties. I conducted further control's experiments to prove that only in the reported conditions the studied system was present, indeed in presence of only ASA and $Zn(ClO_4)_2$, i.e. titration in a $5x10^{-5}$ M solution of ASA with equi-molar amounts of $Zn(ClO_4)_2*6H_2O$ up to 20 equivalents and SP-E and ASA, i.e. titration in a $5x10^{-5}$ M solution of SP-E with equi-molar amounts of ASA up to 2 equivalents, no species characterized by absorbance at 430 nm were detected (Figure 3.11).
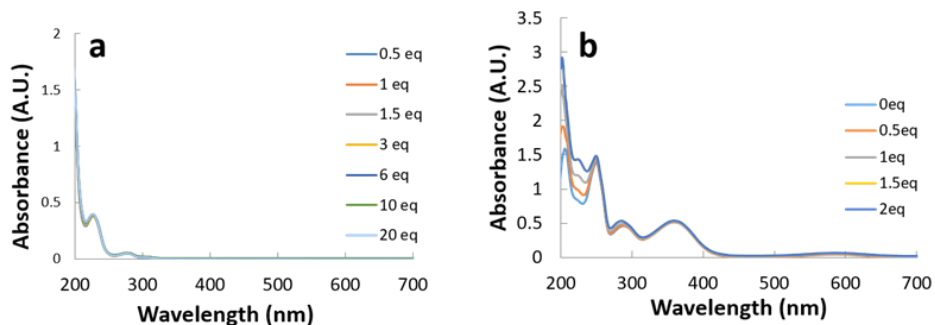
Figure 3.11 Control experiments. a) titration in a 5x10^{-5} M solution of ASA with equi-molar amounts of Zn(ClO$_4$)$_2$*6H$_2$O up to 20 equivalents b) titration in a 5x10^{-5} M solution of SP-E with equi-molar amounts of ASA up to 2 equivalents. In both cases no species characterized by absorbance at 430 nm are detected.

The results obtained by MS spectrometry, that I will show in the next paragraphs, highlighted the presence of a SP-E:Zn^{2+}:ASA species in 1:1:1, therefore we believe the SP-E and ASA 1:1 ratio represent a good starting point to demonstrate qualitatively the presence of the ternary system in solution in its co-presence with the MC-Zn^{2+} complex. My investigations pointed out how an excess of ASA increased the formation of the ternary species from the quantitative view point, these data will be taken into consideration in future analyses where the goal will be to have the system in the higher quantity possible in order to conduct deeper studies preliminary to the production of a potential device.

3.3.3 Light-responsiveness of the system

The species in solution were studied to analyze their kinetic properties and the reversibility features that constitute a key point for the development of a light-triggered release. For these purposes I prepared solutions containing respectively SP-E, ASA and Zn(ClO$_4$)$_2$* 6H$_2$O in 1:1:1.5 ratio and SP-E, Zn(ClO$_4$)$_2$*6H$_2$O and ASA 1:1:15 ratio respectively (Figure 6a-b). This corresponds to the plateau region in the titration experiments and ensures the presence of the ternary system from the spectroscopic view point. After the sample's preparation I allowed its equilibration storing the sample in the dark overnight, enabling the formation of the system. After the first measurement, the solution was irradiated for 5 min with a low-power LED torch (150 mW, 12 lumen) to evaluate the conversion of the SP moiety from the open to the close isomer, resulting in the disappearance of the absorption in the visible region and the photochromic change of the solution. After the removal of the visible light

source the samples were maintained in dark conditions and the re-formation of the complex was registered by measuring the sample every 5 minutes for 3 hours. The systems were completely reformed in 2 hours and they didn't look degraded during these dark/light cycles, as showed respectively in Figure 3.12 and figure 3.13 where 3 consequential dark/light cycles are reported.

Figure 3.12 The spectra a-b-c-d show the irradiation experiments for 3 sequential cycle for the sample containing SP-ASA-Zn^{2+} (1:1:1.5) as a representative example of the kinetic studies conducted. In details a, the spectrum for the sample after its equilibration overnight; spectra b, c, d show the reformation of the systems monitored for 3h (form clearer to darker color's intensity).

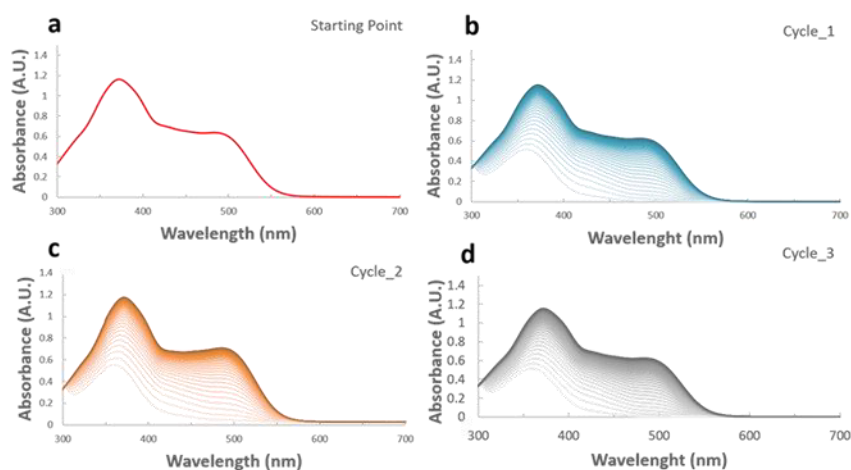**Figure 3.13** The spectra a-b-c-d show the irradiation experiments for 3 sequential cycles for the sample containing SP-E:Zn^{2+}:ASA (1:1:15) as a representative example of the kinetic studies conducted. In details a, the spectrum for the sample after its equilibration overnight; spectra b, c, d show the reformation of the systems monitored for 3h (form clearer to darker color's intensity).
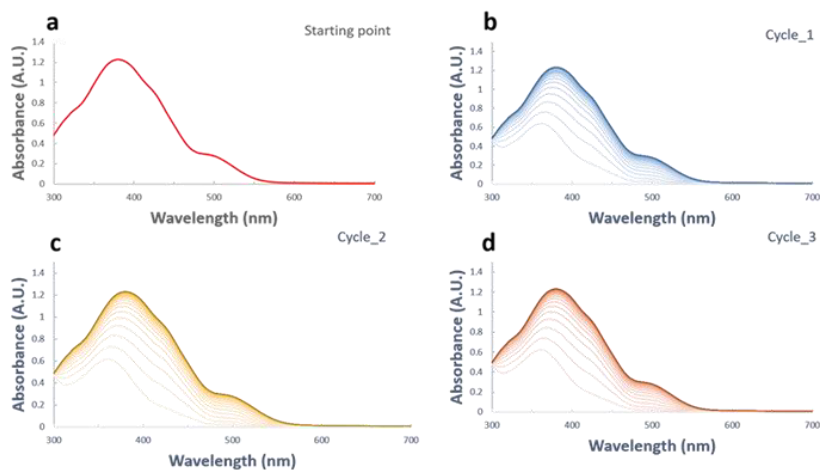
It is interesting to observe how the monitored reaction of re-formation of the system was faster in presence of ASA excess, indeed the plateau region was achieved after around 70 min, while without the excess of ASA it was reached after 120 min, this behavior suggest that an excess of ASA helps the formation the ternary system. (Figure 3.14)
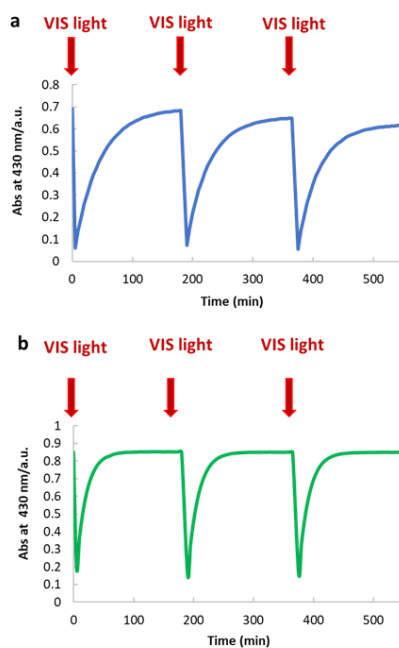
Figure 3.14 The formation of the new ternary system is monitored at 430 nm for 3 hours in three consequential dark/light cycles for both the plateau region of the titration experiments a) SP-E:ASA:Zn^{2+} 1:1:1.5 and b) SP-E:Zn^{2+}:ASA 1:1:15).

These cyclic experiments were repeated on 3 different samples for the sample SP-E:ASA:$Zn(ClO_4)_2$ 1:1:1.5 to prove the repetitiveness in the formation of the ternary system and the results showed a high rate of reproducibility with no significant statistical variation (details of the three measurements and the recorded spectra (The additional measurements repeated for the 2 samples are reported in Appendix Figures S1-S2).

3.3.4 Fluorescence Spectroscopy

The MC isomer of spiropyran molecule presents a π-electron delocalized system: this generates fluorescence emission in the visible region. In our design the ternary system is formed with the spiropyran in its MC isomer, to demonstrate its presence I analyzed the emission properties of the whole system. A solution containing the three interacting

elements at 5×10^{-5} M concentration in 1:1:1.5 SP-E:ASA:Zn^{2+} ratio in MeCN was equilibrated in the dark for 4h and the fluorescence was evaluated using a λ_{exc} = 430 nm, that corresponds to the absorption region of the ternary system and λ_{exc} = 490 nm, that correspond to the absorption region of the complex between SP-E and Zn^{2+} (Figure 3.15).
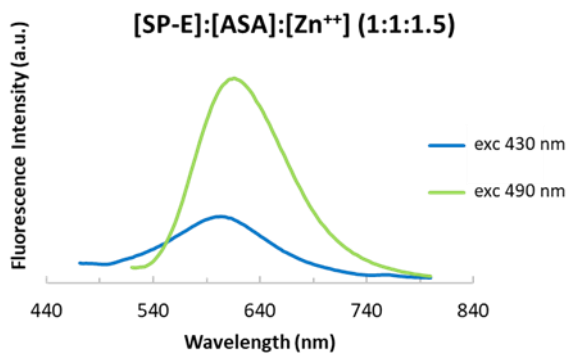
Figure 3.15 Fluorescence emission spectrum of SP-E:ASA:Zn2+ sample in 1:1:1.5 ratios, concentration 5x10-5 M, λexc: 430 nm and 490 nm.

The resulting spectrum shown fluorescence in the Visible region with emission at λ_{max}= 603 nm with the excitation at 430 nm and λ_{max}= 616 nm with the excitation at 490 nm. An analogue measurement was performed also for the sample containing SP-E:Zn^{2+}:ASA in 1:1:15 ratio in MeCN using the same excitation wavelengths 430 nm and 490 nm (Figure 3.16).

Figure 3.16 Emission spectra of the sample SP-E:Zn^{2+}:ASA (1:1:15), the analyzed sample presents a concentration of 5x10-5 M for each component which is analyzed at λexc 430 nm and λexc 490 nm, the obtained emission spectra present λmax at 566 nm and 622 nm respectively.

The collected data suggest that the ternary system is present in its MC isomer form in co-presence to the SP-E: Zn^{2+} complex as showed also in the absorption spectra, while the MC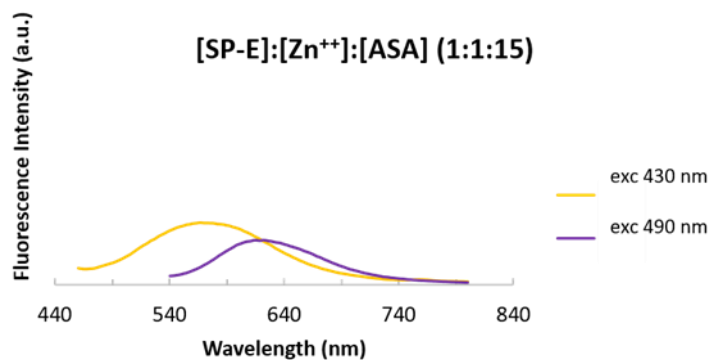 isomer alone in MeCN solution presents an emission with λ_{max} at 670 nm, after its excitation with a wavelength of 585 nm that corresponds to the MC absorption maximum for the molecule alone in its MC form in MeCN.

The emission spectra seemed to be affected by complexation phenomena, indeed the excitation at 430 nm and 490 nm caused an excitation of both complexes (binary and ternary) that could represent the reason of the slightly different positions of the peaks' maximum position. Moreover, I performed further experiments, in more diluted solutions: the fluorescence measurements reported in the previous figures (Figure 3.15-3.16) red line and the measurements conducted in the same condition of excitation wavelengths diluting the solution of the half of their initial concentration (blue line). The reported data (Figure 3.17) don't show any variation in the position of the maximum value of emission's peaks, and this is useful to prove that if some phenomena of reabsorption of emitted light occur it seem that they don't affect this parameter.
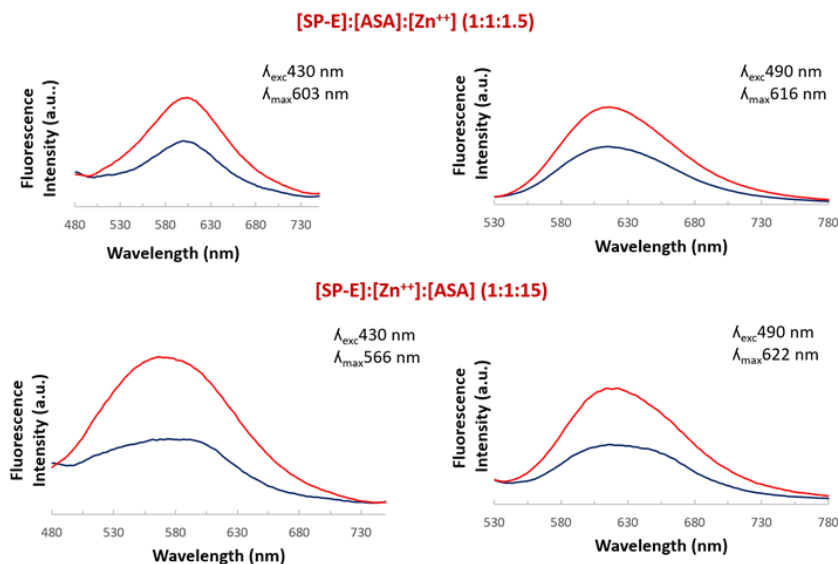

Figure 3.17 Fluorescence emission spectra in original and diluted MeCN solutions.

3.3.5 High Resolution Mass Spectrometry (HRMS)

MALDI-TOF mass spectrometry studies were conducted to proof the existence of the ternary system. This soft ionization technique was chosen because it allows the detection also of fragile complexes. The data here shown, (Figure 3.18), highlight how in a solution of SP-E:Zn(ClO$_4$)$_2$:ASA in MeCN the peaks indicating the presence of 2SP+Zn+ClO$_4^-$ and SP+Zn+ClO$_4^-$ entities were found at 1067 *m/z* and 615 *m/z* respectively.
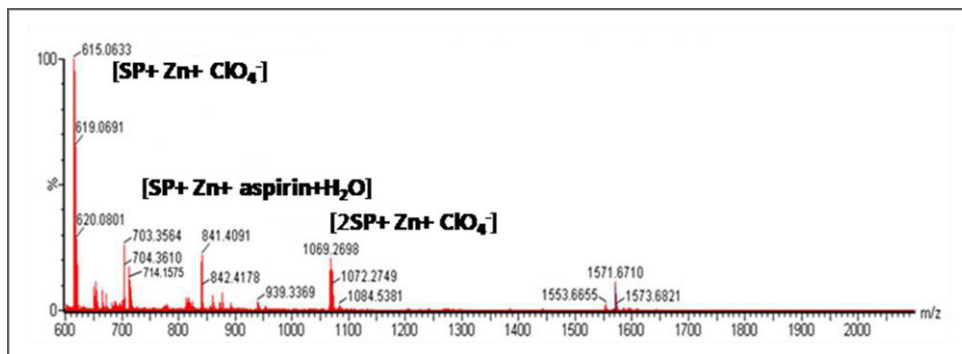
Figure 3.18. High resolution mass spectrum of the sample containing SP-E/ASA/Zn^{2+}.

The same peaks were found in a solution of SP-E+Zn(ClO$_4$)$_2$ in MeCN, that represents the control experiment for this investigations. The presence of the peak at 714 m/z in the SP-E+Zn(ClO$_4$)$_2$+ASA sample suggested the presence of a SP-Zn:ASA:H$_2$O system, indeed this *m/z* peak presented the exact value required for the precise SP:Zn:ASA:H$_2$O system itself and it was not found in the sample containing only SP-E+Zn(ClO$_4$)$_2$ (Figure 3.19).

Figure 3.19 High resolution mass spectrum of the sample containing MC-Zn^{2+} complex in MeCN. In this MALDI-TOF spectrum the m/z peaks belonging to the MC-Zn^{2+} systems are highlighted. It is useful to compare this spectrum with the one reported in the main text, to evidence the formation of the ternary system in presence of ASA.

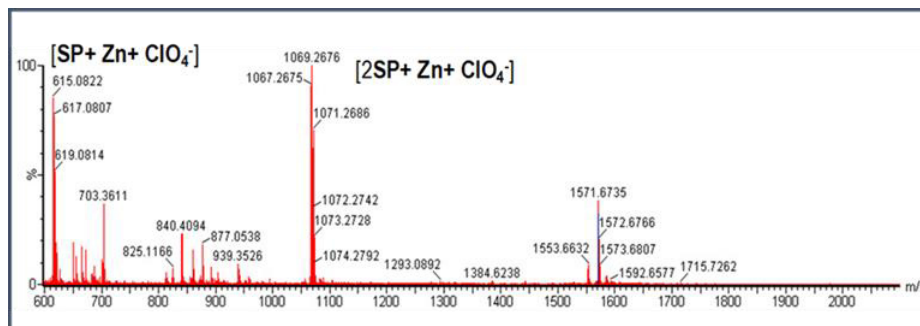Moreover, analyzing this preliminary information, the investigated multi component system seems to contain several entities in solution and the investigations of their equilibria is useful for the final application of this unit.

3.4 Conclusions and Future Perspectives

The reported preliminary investigations highlight the great potentialities of this photo-responsive drug-delivery system.[124] The assembly of a photochromic system, structured by the interactions between a metal cation, correlated to a pharmaceutically active compound, and its binding geometry with a spiropyran moiety, constitutes a promising scaffold for the simultaneous light-regulated delivery of two active agents (ASA and Zinc (II) cation). The techniques used to perform the analysis provided the fundamental preliminary data necessary to start deeper investigations. The system shows good spectroscopic features and its essential visible light reversibility was proven. Further investigations involving X-ray crystallography and NMR spectroscopy could represent the next steps to define the formation of a three-component complex system in its whole feature and space orientation. These systems could be used as APIs for new medical devices as bandages that could release the medicaments over the necessary areas only when the strips are removed from their envelope and they are applied over the skin under visible light. Moreover, they could be investigated also for internal body medicaments and their release and consequently activation can be obtained by the co-operation of optical fibers driving visible light stimuli.

Chapter 4

Hybrid GO-Azobenzenes based mesostructures

4.1 Introduction

Azobenzene photochromic compounds, with their intrinsic *trans-cis* isomerization conformation have been deeply studied for the assembly of photo and stimuli responsive CNMs.[125,126,77] Indeed, azobenzene molecules are interesting switchable cores with high sensitivity, good manufacturing properties and a fully reversible conversion between the two isoforms, that presents itself different chemical and physical properties useful for several applications that can be easily managed.[19,47] The properties of CNMs and the possibility to functionalize with covalent and no-covalent strategies their surface with the aim to have materials with new performances have opened the research to new field of investigations.[74] For this reason, we have decided to assemble a hybrid structure combining GO and two different azobenzene molecules bringing amino groups in their scaffolds to easily link them in a covalent way to the material. Amino-linkers molecules have already been used to intercalate between GO sheets.[127] Indeed, we have recently prepared a GO hybrid structure by intercalation of Tetrakis(4-aminophenyl)methane, bringing -NH_2 groups at the extremities;[128] the assembled structure presents a 3D conformation and it was tested in gas sorption applications. This material can be employed also for other applications, such as for the assembly of filtering membranes or sponges-like structures for the removal of pollutants agents. With the same rational idea I decided to intercalate, azobenzene moieties, investigating the different behavior of the molecules in respect to the material depending on the substituents present that can have an influence both in the assembly of the material and in the eventually optical final properties of the hybrid structures. In particular, it is interesting to evaluate the different intercalation within GO and evaluate the switching behavior of azobenzene in the assembled structures. Finally, we aim to drive these systems to application in the biological realm.

4.2 Design of the Project

Two azobenzene molecules i.e. 4-(phenyldiazenyl) aniline (**AB1**) and 4,4-diazene-1,2-dianiline (**AB2**), differing for the presence of an amino entity in their scaffold were linked to GO. The goal is to prepare two materials presenting the same components, but with different assembly modes and final photo responsive properties (Figure 4.0).
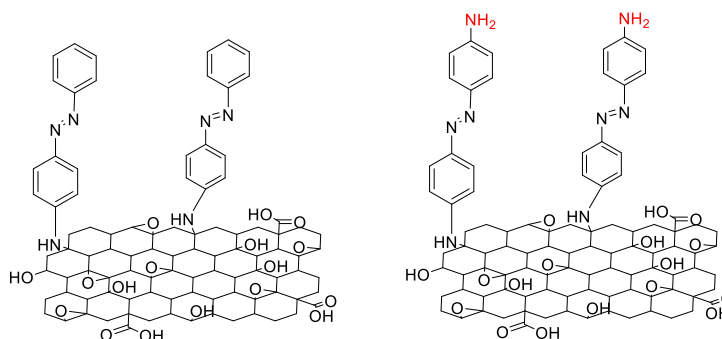

Figure 4.0 Schematic representation of the two proposed GO-AB hybrid structures, which differs each other for the presence/absence of NH$_2$ groups at the extremity.

4.3 Experimental Results

The molecules were synthesized, and the hybrid material was prepared accompanied by a complete characterization of the material with several techniques to prove the effective assembly.

4.3.1 Synthesis of the Molecules and Preparation of the GO hybrid Materials

The desired azobenzene molecules were synthesized accordingly to reported procedures[129-131] with slight modifications in the purification's phase (Figures 4.1 and 4.2).
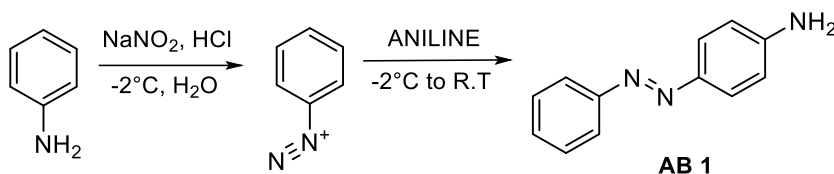

Figure 4.1. Synthetic scheme for compound **AB1**

AB1. The compound was prepared with typical diazonium chemistry procedure starting from aniline (1 mL,10.97 mmol) in H_2O with classical reagents: $NaNO_2$ (757.2 mg, 10.97 mmol) and HCl 12M (914.5 µL, 10.97 mmol) at low temperature (-2°C - 0°C) for 2h followed by the addition of the necessary second portion of aniline (1mL, 10.97 mmol). The purification was performed by column chromatography (Hex: EtOAc 8:2) to give the product as an orange solid (43%, 930 mg); ESIMS: m/z = 199.1095 [M$^+$] (m/z calcd for $C_{12}H_{11}N_3^+$ 199.2478); ^1H NMR (400 MHz, CDCl3): δ (ppm) = 4.07 (s, 2H), 6.80 (d, 8 Hz, 2H), 7.43 (t, 1 H), 7.52 (t, 2H), 7.83-7.88 (m, 4H).

The same molecule was also synthesized with equivalent results in terms of yield, synthesizing a diazoaminobenzene intermediate obtained by the addition of sodium acetate. Diazoaminobenzene was reacted with aniline hydrochloride to get the desired product by precipitation and recrystallization from CHCl3.
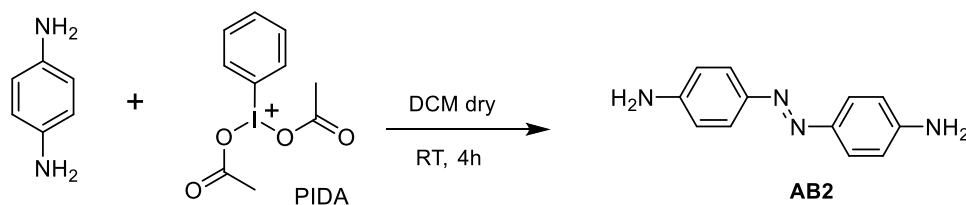

Figure 4.2 Synthetic scheme for compound **AB2**

AB2. 1,4-diaminobenzene (2g, 18.49 mmol) was treated with (diacetoxiodo)benzene (5.650g, 17.57 mmol) in dry DCM and stirred at RT for 4h. The product was purified through column chromatography (DCM) to get the product as a dark red solid (16%, 560 mg). ESIMS: m/z = 212.3152 [M$^+$] (m/z calcd for $C_{12}H_{12}N_4^+$ 212.1157); ^1H NMR (400 MHz, DMSO-d6): δ (ppm) = 5.70 (s, 4H), 6.64 (d,8 Hz, 4H), 7.51 (d, 8 Hz, 4H).

The synthesized molecules were used for the functionalization of the material with the following protocol (Figure 4.3) in order to obtain a covalent functionalization, in particular the reaction condition seemed to promote the interaction of the epoxy and carboxylic GO[132] groups with the -NH2 groups of the azobenzene's moieties through a nucleophilic addition of the amino moiety to the functional groups on the material:
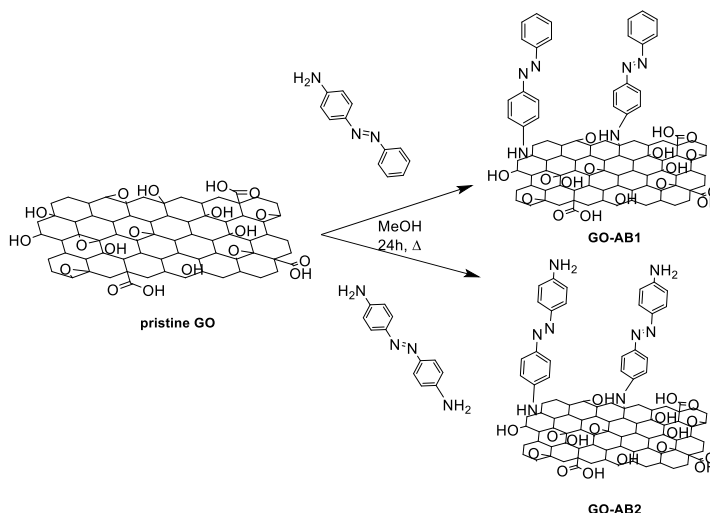
Figure 4.3 Schematic representation of the 2 hybrid systems investigated.

GO-AB1/GO-AB2. GO (50 mg) was dissolved in MeOH (50mL) and sonicated for 10 min, **AB1** (50 mg) or **AB2** (50 mg) was added, the mixture was sonicated for additional 10 min and the reaction was heated at reflux for 24h. The work-up was performed through several washing processes with ultracentrifugation (20K RPM for 20 min each cycle). The reaction's solvent was removed at the end of the reaction and was washed for 20 consequential centrifugation cycles with fresh aliquots of MeOH and Acetone alternatively to remove all the unreacted amounts of **AB1** and **AB2**. The work up was stopped when the washing solvent used for the washing cycle, checked by UV-Vis absorption measurement, didn't show any trace of unreacted **AB1** or **AB2**. The dried samples were then dried in an oven at 65°C for 24h and more to get the desired materials (around 35mg for each batch).

4.3.2 UV-Vis Absorption Spectroscopy

UV-Vis absorption measurements were performed to define the properties of the molecules and of the material considering the photochromic properties of azobenzene compounds.[75] **GO** samples presented a good dispersibility in DMSO that have been selected for these studies.

AB1 and **AB2** were tested as $3*10^{-5}$ M solutions in DMSO upon exposure to a 365nm UV source (4watt, 10 cm distance) to check the photochromic behavior and the variation of the absorption spectra and its reversibility properties. (Figure 4.4)
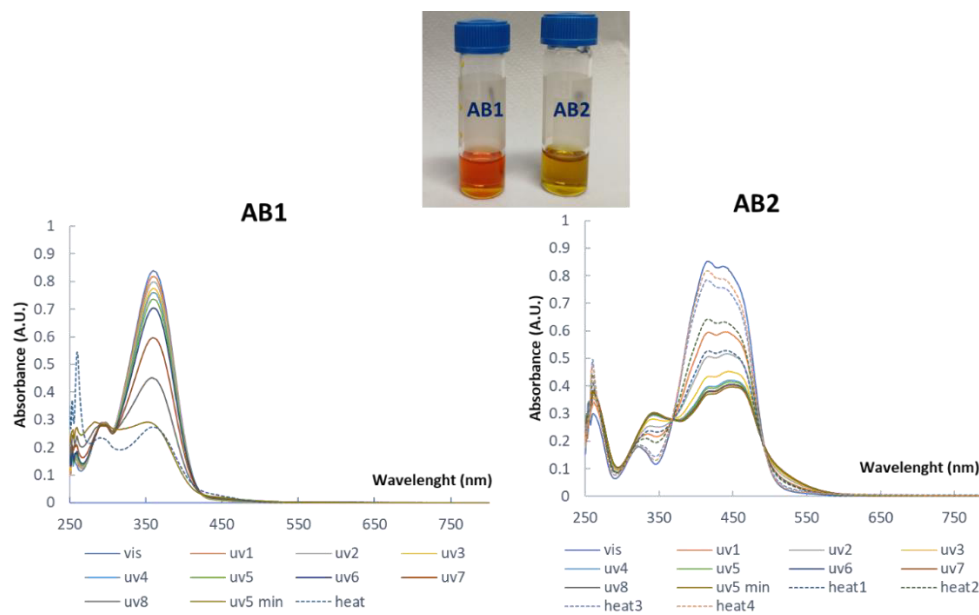
Figure 4.4 Uv-Vis absorption spectra of **AB1** and **AB2** in DMSO and samples' solutions.

Both the molecules in DMSO showed the expected π-π* shift after exposure to UV light, this correspond to a decrease in the absorption maxima respectively at 360 nm and 420 nm for both the samples, moreover the reversibility of the process was proved upon Vis light exposure or heating for **AB2**, while for **AB1** the process looks not completely reversible or slower than for **AB1**.

Pristine **GO**, **GO-AB1** and **GO-AB2** samples were prepared and measured as 100 µg/ mL DMSO solutions as reported in detail in chapter 2. (Figure 4.5-4.6)
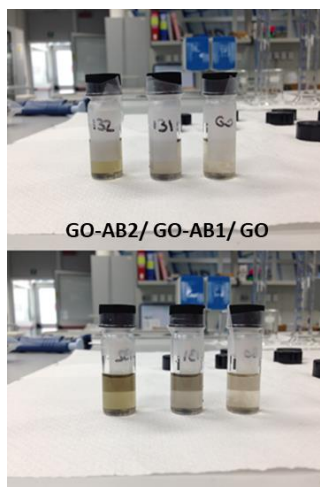

Figure 4.5 The 3 analyzed samples **GO**, **GO-AB1** and **GO-AB2** in DMSO.
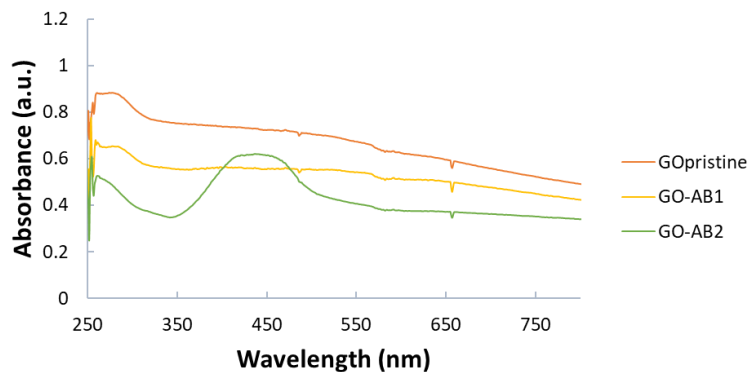
Figure 4.6 Uv-Vis absorption spectra of **GO**, **GO-AB1** and **GO-AB2** in DMSO.

The reported spectra evidenced a clear absorption for the sample **GO-AB2** that represented a prove of the effective functionalization of the material, unfortunately for sample **GO-AB1** any particular absorption related to the molecule was not observed

The same samples were analyzed upon exposure to UV light at 365 nm to understand if it was possible to observe the same behavior highlighted for **AB1**-**AB2** due to their azobenzene scaffold (Figure 4.7).
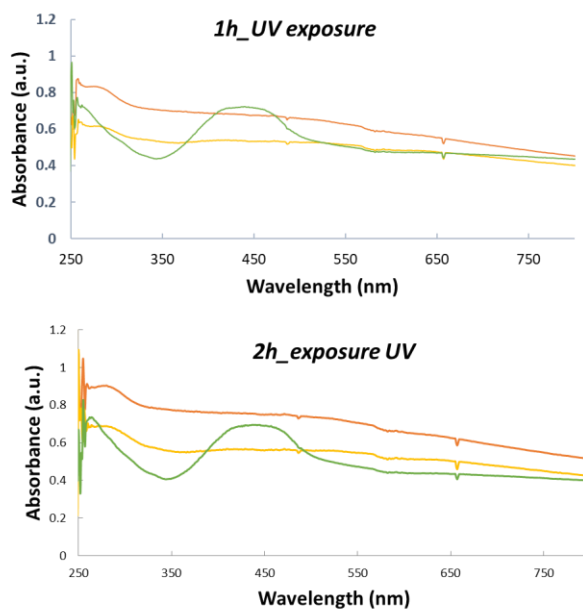

Figure 4.7 Uv-Vis absorption spectra of **GO**, **GO-AB1** and **GO-AB2** in DMSO upon exposure to UV light.

The samples were stored in dark conditions and irradiated with the UV 365 nm source up to 2 hours. Unfortunately, no variations were observed upon exposure to UV source as reported in Figure 4.7 especially for the sample **GO-AB2**, the normalized abs maximum observed at 433nm shifted just from 0.42 to 0.40 absorbance and this could be related not to a photo-responsive reaction but just to a normal operational/ instrumental variation.

4.3.3 FTIR_Fourier Transform Infrared Spectroscopy

FTIR measurements were conducted as a general characterization to prove the presence of the molecule in the functionalized material. The experiments were conducted on pristine **GO**, functionalized **GO-AB1** and **GO-AB2** and on **AB1** and **AB2** to define the expected typical bands for the molecules and to find them also on the functionalized material. Here I report the recorded spectra and in particular also their enlargements in significant regions that are useful to prove the functionalization with the molecules. (Figures 4.8 and 4.9)
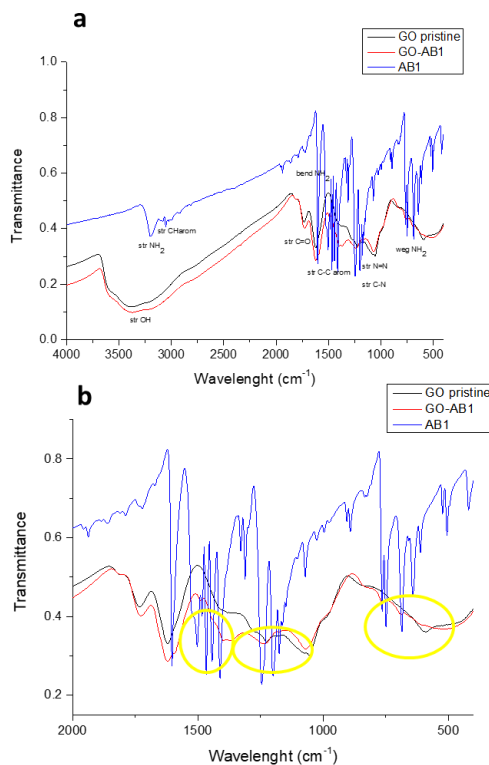
GO-AB1

Figure 4.8 FTIR spectra of **GO**, **GO-AB1** and **AB1 (a)** and enlargement in significant area (**b**).

Selected wavelengths: 3198 cm^{-1} str -NH$_2$, 3100-2955 cm^{-1} str CH arom, 1605 cm^{-1} bend -NH$_2$, 1400-1500 cm^{-1} str CH arom, 1244 cm^{-1} str C-N, 1198 cm^{-1} str, N=N, 750-680 cm^{-1} weg -NH$_2$_in the GO samples a huge band 3680-3000 cm^{-1} -OH str,was observed due to the presence of functional groups of the material itself.

GO-AB2
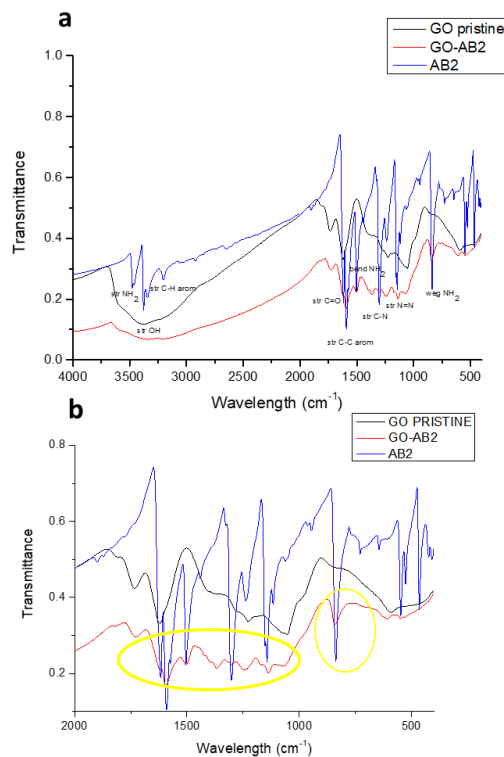
Figure 4.9 FTIR spectra of **GO**, **GO-AB2** and **AB2 (a)** and enlargement in significant area (b).

Selected wavelengths: 3470 cm^{-1} str -NH$_2$, 3370-3190 cm^{-1} str CH arom, 1620 cm^{-1} str C=O,1589 cm^{-1} str CH arom, 1501 cm^{-1} bend -NH$_2$, 1400-1500 cm^{-1} str CH arom, 1304 cm^{-1} str C-N, 1146 cm^{-1} str, N=N, 832 cm^{-1} weg -NH$_2$_in the GO samples a huge band 3600-3000 cm^{-1} -OH str,was observed due to the presence of functional groups of the material itself.

For both samples, the expected peaks at the wavenumbers typical for the functional groups present on the molecules were found, this typical material's characterization prove the successful functionalization of the material.

4.3.4 RAMAN_ Raman Scattering Spectroscopy

Raman measurements were performed to understand the surface properties of CNMs, many evidences are usually detachable after the functionalization because they influence the features of G and D peaks. These parameters are usually influenced by the modification due to covalent functionalization processes,[133] in the case of GO, the oxidation processes, necessary to modify the graphite into oxidized graphene already influence these parameters and not always it is possible to highlight by this technique a further functionalization with other molecules. This characterization techniques are anyway useful to define the material's properties and to check if there are variations upon exposure to a UV source as performed with other CNMs linked to AB units.[134,135]

I herein report the recorded spectra registered for all the samples in normal and UV light conditions. (Figures 4.10/4.14)
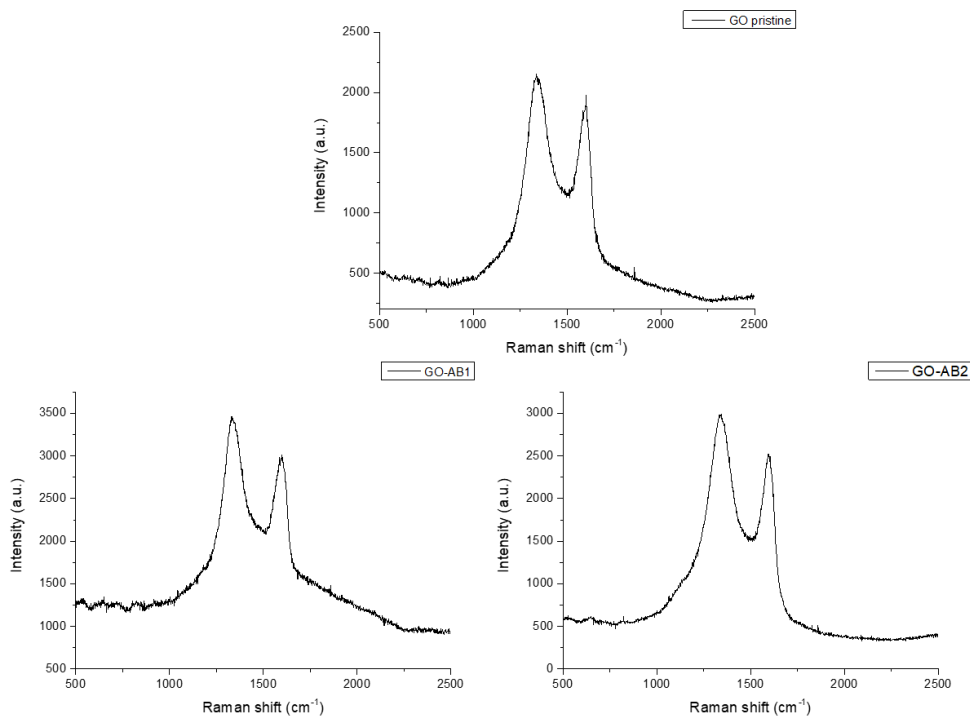
GO-AB1/AB2

Figure 4.10 Raman spectra for the samples **GO**, **GO-AB1** and **GO-AB2**.

		GO	GO-AB1	GO-AB2
no UV light	D (x axis)	1339.5	1335.6	1340.5
	G (x axis)	1596.2	1596.2	1597.2
	D/G ratio	1.13	1.16	1.18

Table 4.0 Analyses of the significant peaks of the RAMAN spectra.

GO-AB1 UV exposure

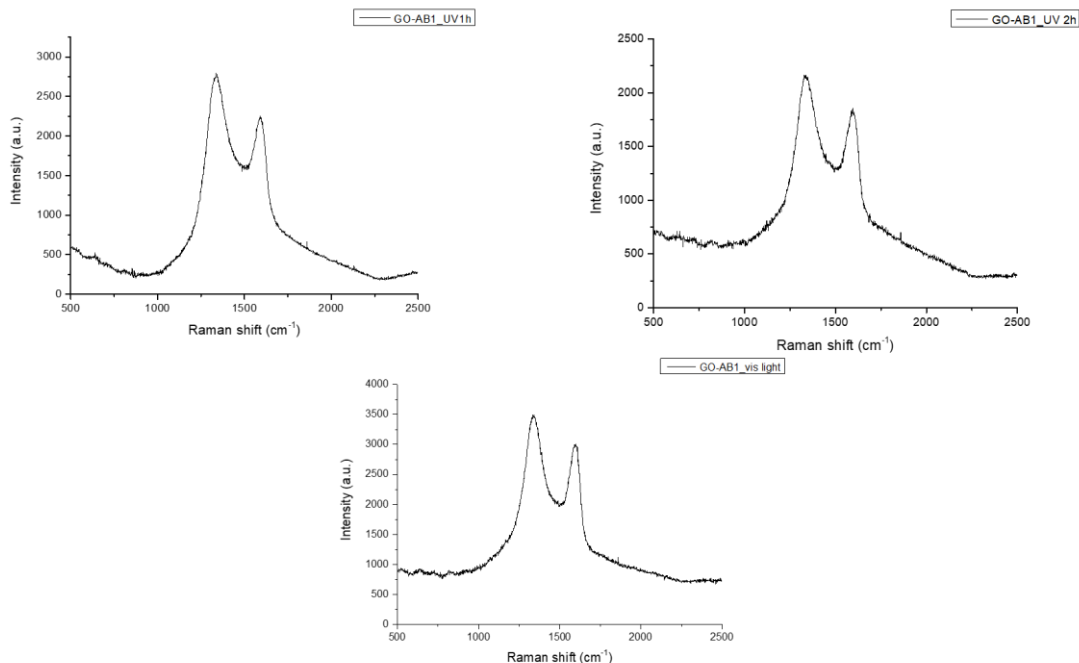**Figure 4.11** Raman spectra for the samples **GO-AB1** upon exposure to UV light and Vis light.

		1h UV	2h UV	Vis light after UV
GO-AB1 UVlight	D (x axis)	1337.5	1334.6	1340.5
	G (x axis)	1593.3	1594.3	1596.2
	D/G ratio	1.23	1.17	1.15

Table 4.1 Analyses of the significant peaks of the spectra for the samples **GO-AB1** in the 3 measurements conditions.
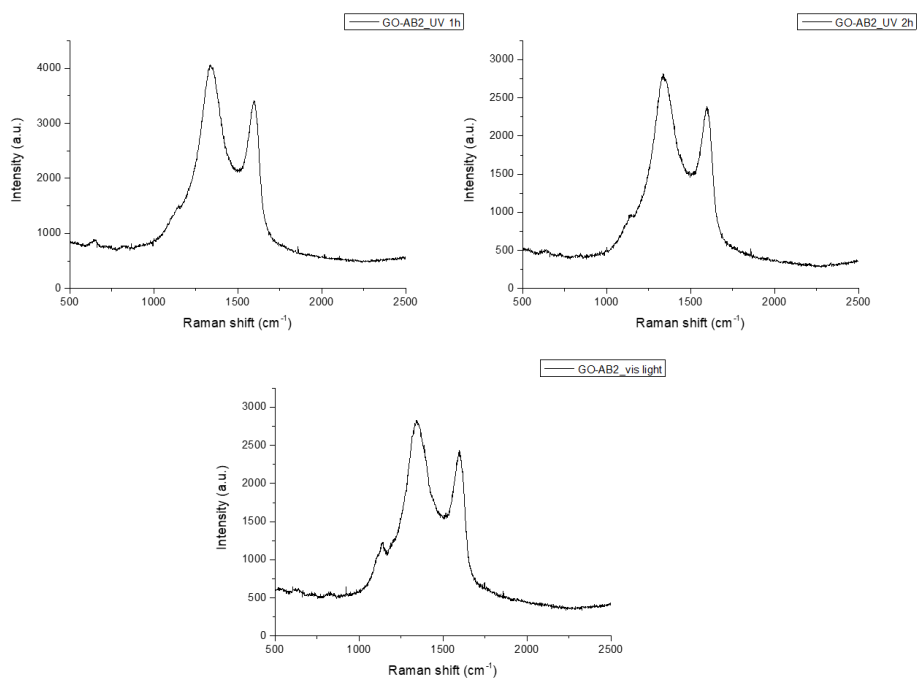
GO-AB2 UV exposure

Figure 4.12 Raman spectra for the samples **GO-AB2** upon exposure to UV light and Vis light.

GO-AB2 UVlight					
	D (x axis)	1338.5	1343.4		1344.4
	G (x axis)	1597.2	1595.2		1596.2
	D/G ratio	1.2	1.18		1.2

Table 4.2 Analyses of the significant peaks of the spectra of **GO-AB2** in the 3 measurements conditions.
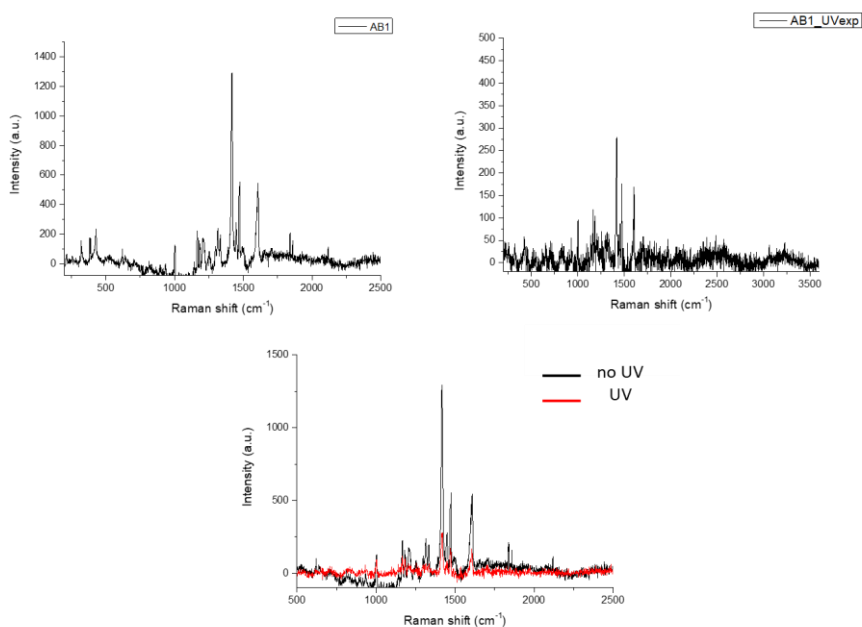
AB1

Figure 4.13 Raman spectra for the samples **AB1** without and upon exposure to UV light and comparisons of the 2 measurements.
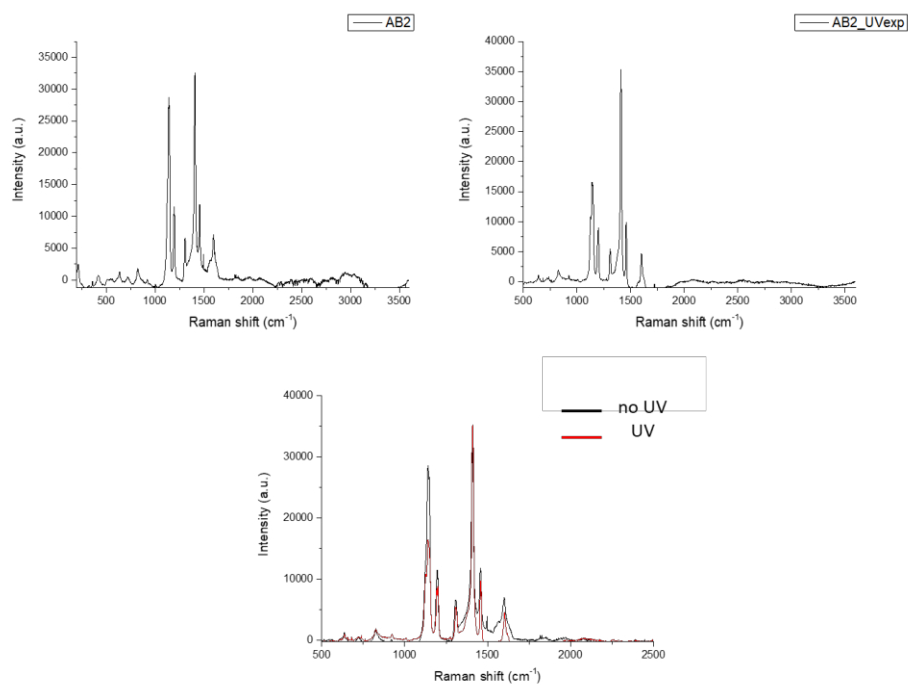
AB2

Figure 4.14 Raman spectra for the samples **AB2** without **and** upon exposure to UV light and comparisons of the 2 measurements.

53

The spectra recorded and the data obtained for the D and G peaks and their related ratios show the typical features of a GO functionalized materials. The comparison between the peak positions and the D/G ratios as showed in the tables, (in particular Table 4.4), showed a little shift around 2 cm^{-1} for both **GO-AB1** and **GO-AB2** samples, the literature data also report little downshift (around 3 cm^{-1}),[134,135] Moreover the exposure to the UV source for a prolonged time (2h) in environmental narrow dark conditions is responsible of an increase of the temperature that is not useful for the *trans-cis* isomerization process we would like to study. Additional studies conducted just on the molecules **AB1** and **AB2** don't show any variation on the peaks upon the exposure to UV light.

GO-AB1

	no UV	1h UV	2h UV	Vis light after UV	
	1596.2	1593.3	1594.2	1596.2	G peak position

GO-AB1

	no UV	1h UV	2h UV	Vis light after UV	
	1597.2	1597.2	1595.2	1596.2	G peak position

Table 4.3 Summary of the analyses of the significant peaks of the spectra of **GO-AB1** and **GO-AB2** in the 3 measurements conditions.

4.3.5 XPS_X-ray Photoelectron Spectroscopy

XPS measurements on the two functionalized samples **GO-AB1** and **GO-AB2** were performed to define the surface composition of the assembled materials on the powder samples directly deposited over an Indium substrate.
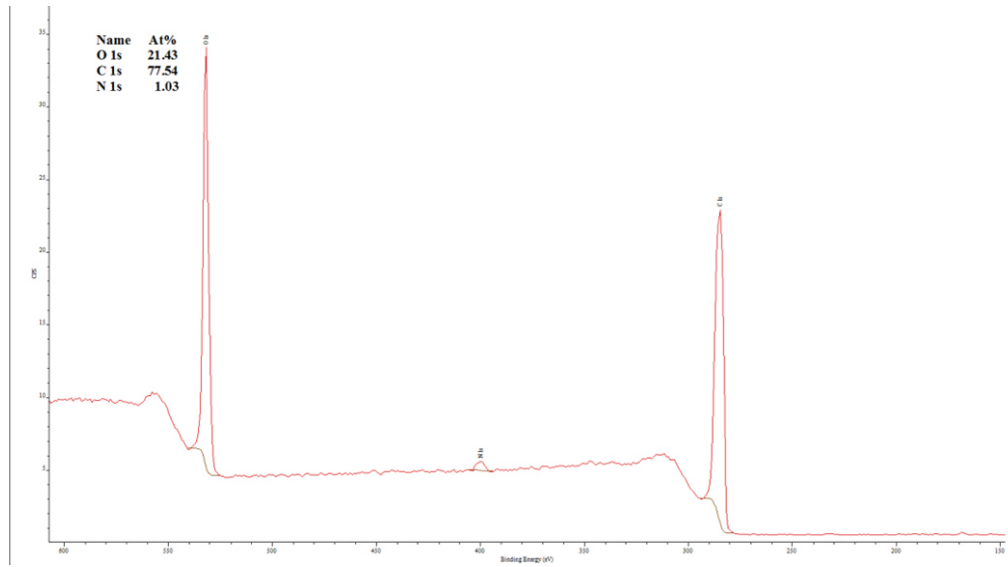
Wide Spectra

GO-AB1

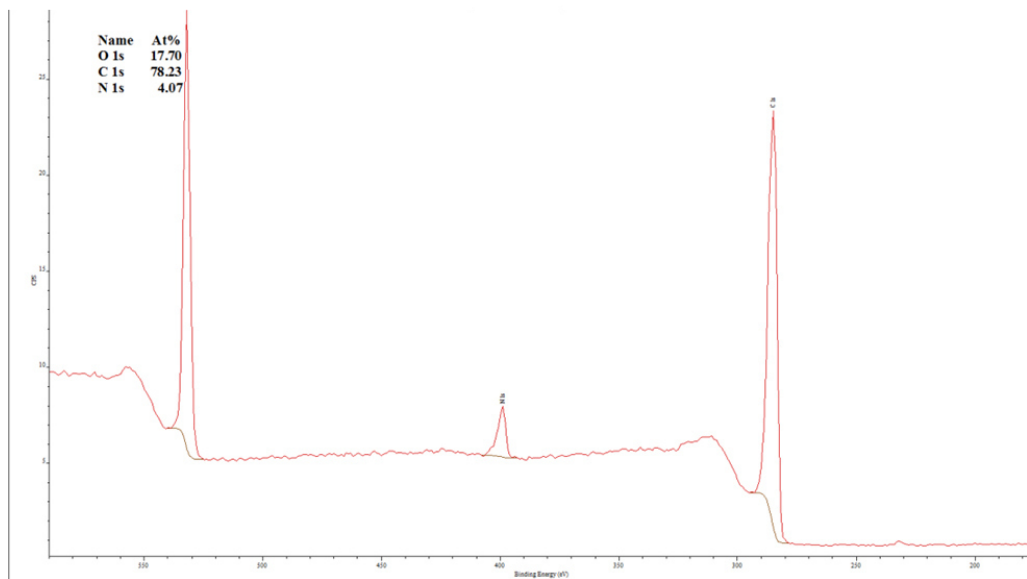**Figure 4.15** XPS wide spectrum for sample **GO-AB1.**

GO-AB2

Figure 4.16 XPS wide spectrum for sample **GO-AB2.**

The spectra (Figure 4.15 and 4.16) highlighted the presence of all the expected species, in particular: Nitrogen, in addition to Carbon and Oxygen, this represent the opportune functionalization of the material with molecules containing Nitrogen as **AB1** and **AB2**. C and O are respectively 77.54% and 21.43% for **GO-AB1**, 78.23% and 17.70% for **GO-AB2** which belong to the GO material itself. The comparison of the percentage of elements found highlight that the sample **GO-AB2** has about 4 times more nitrogen than the sample **GO-AB1**, i.e. 4.07% vs 1.03% probably the presence of the double amine functionality of **AB-2** leaded to more molecules bounded on GO.
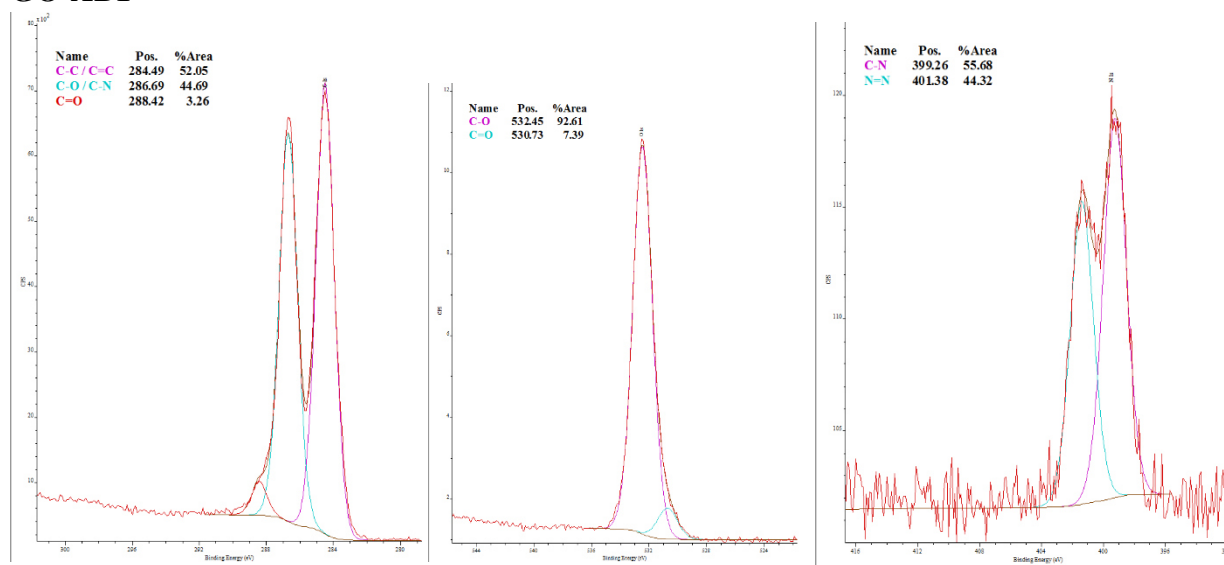
High resolution spectra

GO-AB1

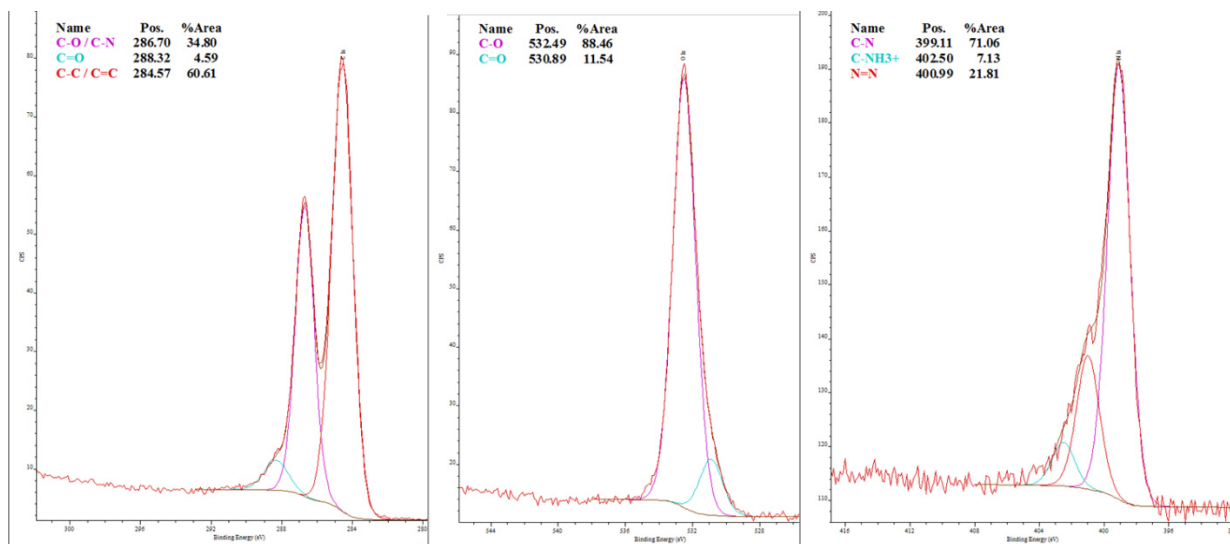**Figure 4.17** XPS High-resolution spectrum for sample **GO-AB1.**

GO-AB2

Figure 4.18 XPS High-resolution spectrum for sample **GO-AB2.**

The high-resolution spectra (Figure 4.17-4.18) and the analyses, the deconvolution of peaks and the following analysis of the functional groups, represent a prove of the functionalization with the selected **AB1 and AB2** molecules

Considering in particular the N peak (third column) for **GO-AB1** the values are C-N 55.68% and N=N 44.32%, observing the hypothesized structure of the material, reported in figures 4.17 and 4.18 , the results confirmed the supposed functionalization, the amount of C-N is more than the N=N (in the structure there are more C-N than N=N) and the fact that almost the 50% of the N is related to the N azobenzene could be a prove of a good functionalization. Moreover, the absence of N-H components in the N peak could be the prove that all the molecules present are attached to the material and there are no free amino groups in the material itself.

The same analysis (third column) for **GO-AB2** showed C-N 71.06% C-NH3$^+$ 7.13% and N=N 21.81 %, values, the different percentage for the C-N and N=N components could allow to draw the same conclusions found for **GO-AB1**. The presence of a N-H components in the N peak could prove that not all the **AB2** molecules are attached by both their -NH$_2$

groups to the material, observing the percentages and the chemical structures the N=N group is made of two N atoms while the NH only by one N atom (21.8% vs 7.13%), the 1:1 ratio considering the different N contributions could be: 10.9% vs 7.13%, I could conclude only that the molecules preferentially are attached to the material only by one NH_2 group, but there is a little percentage of molecules that are attached by both the $-NH_2$ groups.

XPS measurements proved the expected functionalization for the materials.

4.3.6 XRD_X-ray diffraction

The XRD measurements were conducted with the goal to understand the properties of the material and to prove the interlayer distance of **GO-AB** samples and the possibility to assemble pillared structures with **AB1** and **AB2** molecules as linkers or spacers between the GO sheets.

The evidences found during these measurements (Figures 4.19) showed typical pattern for GO materials and I highlighted the importance to conduct *in vacuum* measurements, indeed in these conditions the samples are completely dried and the interference due to the intercalation of water molecules is eliminated because it can interfere with the measurements, altering the measured values and providing unreal results.[136]
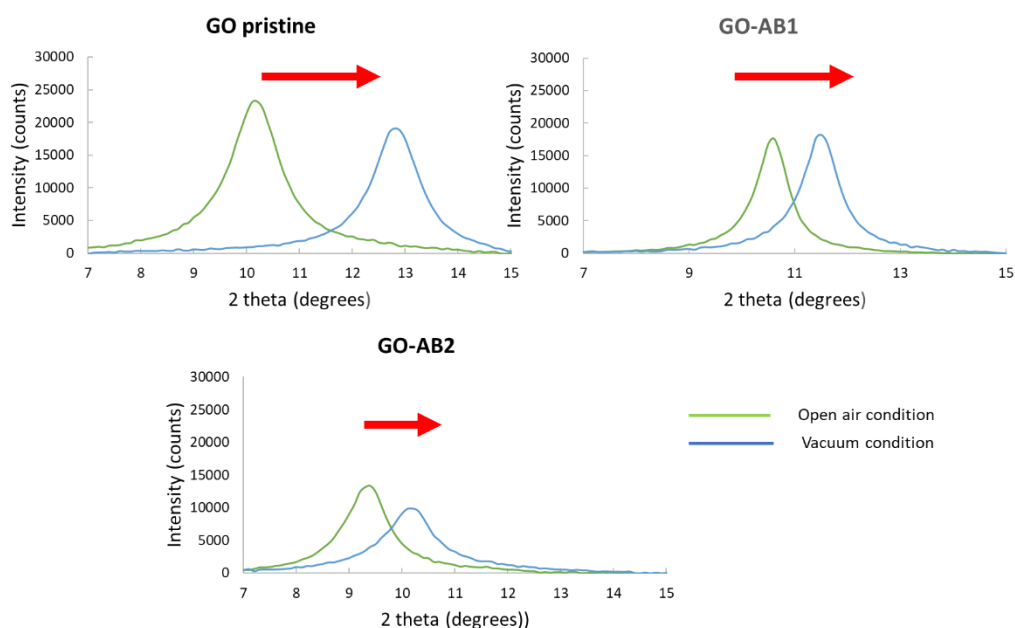

Figure 4.19 XRD measurements for pristine **GO**, **GO-AB1** and **GO-AB2** in air and in vacuum conditions.

The comparisons between the pristine and the functionalized materials in vacuum conditions (Figures 4.20) evidenced interesting different properties that are representative of different intercalations obtained by the different molecules.
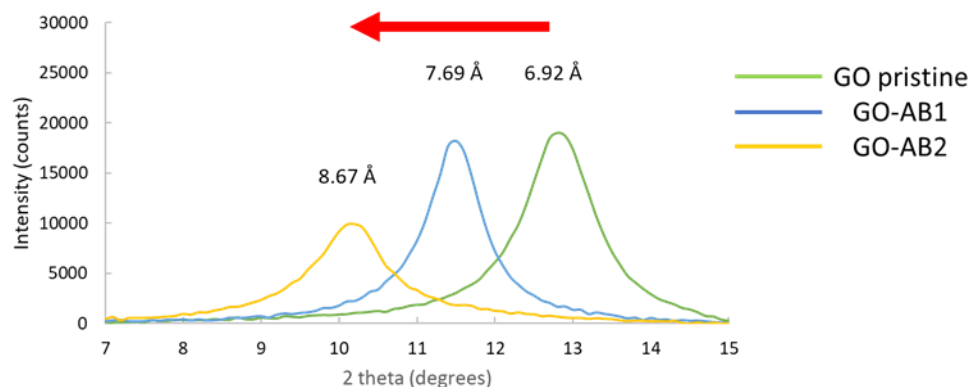

Figure 4.20 Comparisons of XRD measurements for pristine **GO**, **GO-AB1** and **GO-AB2** in vacuum conditions**.**

The possibility to apply the Bragg's equation:

$$2d\sin\theta = n\Lambda$$

Where θ can be read by the spectra, n and Λ are respectively 1 and 1.5418 Å.

It is useful to extrapolate from the spectra the d-spacing between GO planes achieved by the presence of the AB molecules. The obtained values obtained for d respectively of 6.92 Å for pristine **GO**, 7.69 Å for **GO-AB1** and 8.67 Å for **GO-AB2** are in line with the 2 different intercalated molecule, and **AB2** molecule, with 2 -NH$_2$ functional groups is responsible of an increased spacing between the GO planes.

4.3.7 Films Preparation and Solvent Dispersibility

Considering the huge ranges of applications of these hybrid materials and our interest in the biological realm, I have performed several dispersibility tests using H$_2$O as solvent to check the dispersion's rate and also the deposition features with the goal to obtain uniform films useful both for additional characterization techniques that for the eventual final applications.

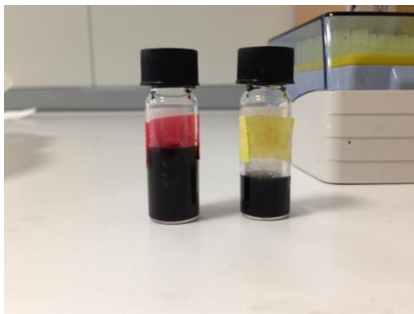- 1 mg/mL   left **GO-AB1**, right **GO-AB2**

Shaken suspensions

Figure 4.21 Suspensions of **GO-AB1** and **GO-AB2** in 1 mg/mL in H_2O after shaking**.**
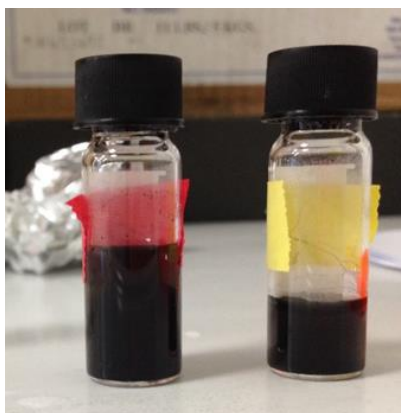
After 10 min of sonication in ultrasonic bath

Figure 4.22 Suspensions of **GO-AB1** and **GO-AB2** in 1 mg/mL in H_2O after 10 min of sonication**.**

- 50 µg/mL   left **GO-AB1**, right **GO-AB2**

Shaken suspensions

Figure 4.23 Suspensions of **GO-AB1** and **GO-AB2** in 50 µg/mL in H_2O after shaking**.**

After 10 min of sonication in ultrasonic bath

Figure 4.24 Suspensions of **GO-AB1** and **GO-AB2** in 50 µg /mL in H_2O after 10 min of sonication**.**

- 100 µg/mL   left **GO-AB1**, right **GO-AB2**
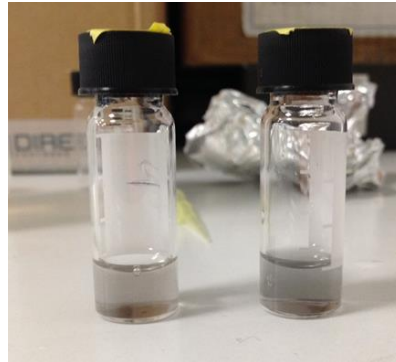
Shaken suspensions

Figure 4.25 Suspensions of **GO-AB1** and **GO-AB2** in 100 µg/mL in H_2O after shaking**.**
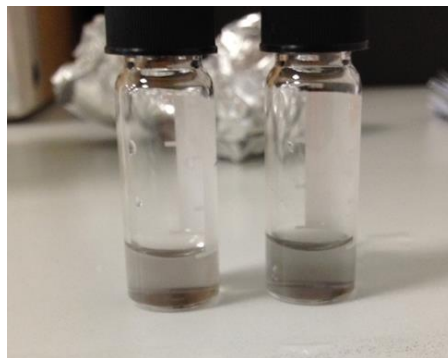
After 10 min of sonication in ultrasonic bath

Figure 4.26 Suspensions of **GO-AB1** and **GO-AB2** in 100 µg /mL in H_2O after 10 min of sonication**.**

- 200 µg/mL   left **GO-AB1**, right **GO-AB2**

Shaken suspensions

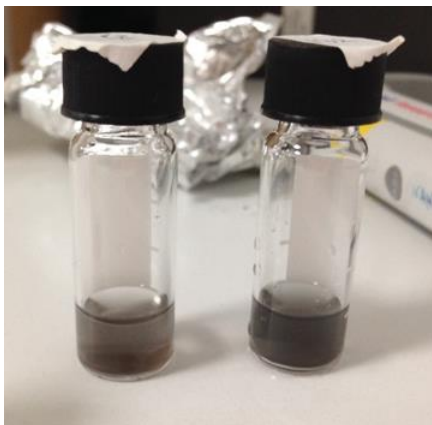**Figure 4.27** Suspensions of **GO-AB1** and **GO-AB2** in 200 µg/mL in H_2O after shaking.

After 10 min of sonication in ultrasonic bath

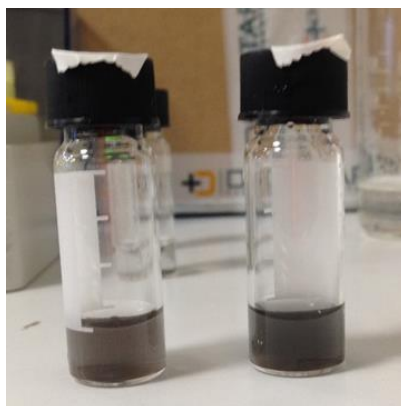**Figure 4.28** Suspensions of **GO-AB1** and **GO-AB2** in 200 µg /mL in H_2O after 10 min of sonication.

During the drop casting deposition's tests of 50 µL of the previously described suspensions, in many of the samples at lower concentration i.e. 50, 100 and 200 µg/mL, the materials contained into the drops was too low to observe the formation homogeneous films. For these drop casting analyses the sample with 1 mg/mL seems to be the only one which show good properties in terms of handling and applicability.
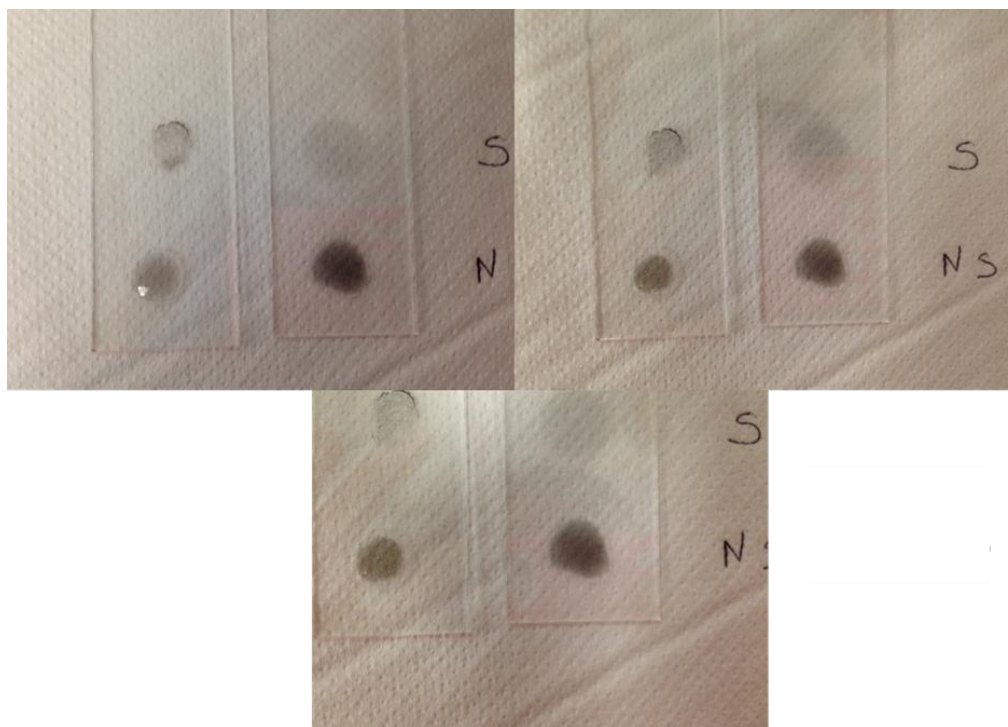
Figure 4.29 Drop casting of 50 µL of **GO-AB1** (above photos) and **GO-AB2** (bottom photo) of samples of 1 mg /mL in H_2O after 10 min of sonication

By eyes, the sample **GO-AB2** seemed to be well dispersed and the material seemed to be less aggregate, this could be a prove of a better functionalization as showed also by the other characterization techniques.

4.4 Conclusions and Future Perspectives

The two assembled hybrid materials **GO-AB1** and **GO-AB2** were prepared and fully characterized with the available and necessary techniques to prove the functionalization of GO and the fundamental characterization. The materials presented good interlayer distance, a functionalization in line with the expectation for the different functionalities of the molecules and good dispersibility in a bio compatible solvent like water. The equipment available unfortunately were not suitable to prove the photoresponsivity of the material, especially, the low power UV source should be replaced as well as the possibility to work in a dark or UV light friendly laboratory. In the future the material will be tested in its photo-responsive attitude and some experiments for the assembly of surfaces where to grow cells will be investigated.

Chapter 5

University of Miami_College of Art and Science

Oxazines and Oxazolidines for sensing applications and polymer synthesis.

5.1 Introduction

2H,4H-benzo[1,3]oxazine i.e. Oxazines molecules were studied and used as efficient photochromic subunits for a huge range of applications in the biological realm, in particular they have been highlighted as tools for bio-imaging purposes, photo-controllable polymers or activated-fluorescence related phenomena, using the ring closing/ring opening processes and combining these scaffolds also with opportune fluorophores' entities.[59] During my periods as visiting PhD student in Dr. Raymo Laboratory for Molecular Photonics at the University of Miami, I had the opportunity to collaborate at three different projects working mainly in the synthesis and characterization of molecules presenting Oxazines and Oxazolidines (i.e. *2H,3H,4H,5H*-[1,3]oxazole) scaffolds, in the same projects the spectroscopic chemical-physical characterizations of the elected compounds and materials were mainly performed by Dr. Mercedes Mazza, PhD student involved in the projects, these data will not be reported in this manuscript.

1. Ratiometric sensing of temperature with fluorescent Oxazines and Oxazolidines-based switches.
2. pH sensing with switchable Coumarins
3. Conjugated polymers assembled with Oxazine switching monomers.

5.2 Ratiometric sensing of temperature with fluorescent Oxazines and Oxazolidines-based switches

5.2.1 Introduction

The possibility to measure temperature at the sub-micrometer level is a useful tool, indeed this physical parameter is crucial and significant in several biological and chemical processes[137,138] and it is fundamental to understand many cellular events that are driven by endothermic or exothermic processes. The conventional systems used to measure temperature require the physical contact between the samples and the probes: this represent a limit in the temperature determination, indeed the miniaturization at this dimension level is not always possible.[139] On the other hand, optical measurements are useful to achieve these goals, and, among them, fluorescent-based methods seem to be the more promising candidates for micro-thermometry.[140,141] These probes can be usually divided into two categories depending on the output signals i.e. single or dual emission. The first category unfortunately can be affected by interfering factors as concentration of the probe, intensity or power of the excitation source and artefacts,[142,143] while the dual emission devices are not affected by these phenomena; for this reason, they are useful sensing systems where the temperature can be detected *via* the ratiometric comparison of two different signals.[63] These classes of probes can be designed with mechanisms of temperature-related geometrical conformation of the molecular scaffold used and the possibility to reach a dual emission from a single chromophore entity, represent an interesting purpose. It is known that some thermochromic compounds change in a reversible way their light absorption property in response to temperature's variation,[9] moreover these species can be assembled to emit in distinct spectral region allowing a ratiometric measurement. Oxazine heterocycles have been already investigated in terms of opening/closing phenomena under temperature influence,[144,145] we then decided to study their conjugation with a fluorescent unit to build new dual emission temperature probes.[61]

5.2.2 Design of the Project

Ring closed/ ring open isomers of the reported oxazine interconvert with a fast kinetic in MeCN changing the solvent's temperature.[145] (Figure 5.0)
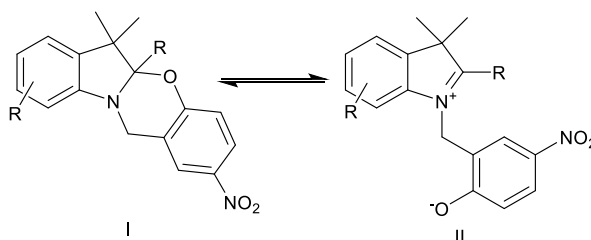

Figure 5.0 Schematic representation of the interconversion of the two oxazine forms.

In its open ring isomer the system presents electronic extended conjugation due to the presence of the indolium cation which shift the spectroscopic properties: the analysis of the absorption and emission's intensities, their shift and in particular the ratio between their value should change in response to temperature variations. For this purposes We studied four molecules in order to compare two different photochromic scaffolds (i.e. oxazine and oxazolidine) and two different fluorophores (i.e coumarin and carbazole) (Figure 5.1 **a**,**b**,**c**,**d**).

(*E*)-7-(diethylamino)-3-(2-(9,9-dimethyl-2,3-dihydrooxazolo[3,2-*a*]indol-9a(9*H*)-yl)vinyl)-2*H*-chromen-2-one

a

(*E*)-9,9-dimethyl-9a-(2-(9-methyl-9*H*-carbazol-3-yl)vinyl)-2,3,9,9a-tetrahydrooxazolo[3,2-*a*]indole

b

c

d

(*E*)-7-(diethylamino)-3-(2-(6,6-dimethyl-2-nitro-12*H*-benzo[5,6][1,3]oxazino[3,2-*a*]indol-5a(6*H*)-yl)vinyl)-2*H*-chromen-2-one

(*E*)-6,6-dimethyl-5a-(2-(9-methyl-9*H*-carbazol-3-yl)vinyl)-2-nitro-5a,6-dihydro-12*H*-benzo[5,6][1,3]oxazino[3,2-*a*]indole
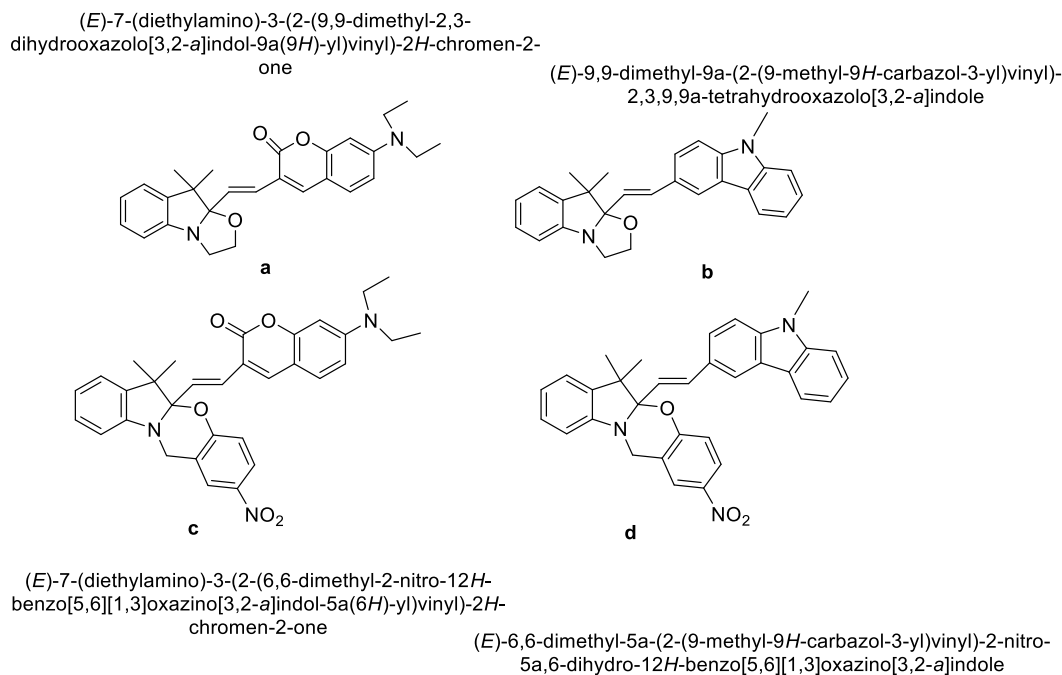
Figure 5.1 Chemical structures of the 4 compounds synthesized and tested for the project.

5.2.3 Content

The molecules were analyzed in their spectroscopic properties in a mixture of MeCN/H_2O (1:1 v/v), indeed the presence of H_2O and the consequential polarity's increase of the media, is useful to stabilize the molecules in their open/protonated forms (Figure 5.2).
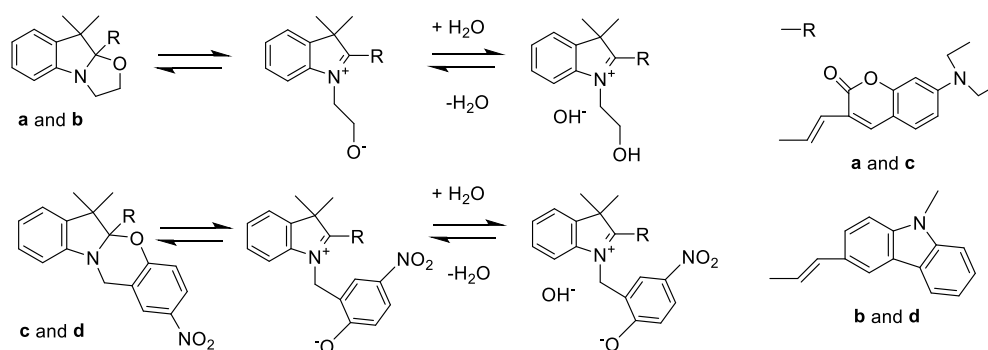

Figure 5.2 Equilibria in solution of the 4 compounds studied for the project.

In these conditions the compounds were analyzed in a temperature range between 281 K and 327 K, through UV-Vis absorption/emission spectroscopies. Moreover, compound **a**, that showed the best results in terms of absorption and emission spectroscopies, was studied through fluorescence microscopy *via* the incorporation into an alginate hydrogel in order to probe temperature at the micrometer level with spatial resolution. The same molecule (**a**) were also tested in NMR spectroscopy in the same temperature range to prove also with this technique the opening/closing phenomena.

5.2.4 Synthesis of the Molecules

Compounds **c** and **d** were synthesized following procedures already optimized by Dr. Raymo's research group.[146,147] Compounds **a** and **b**, were synthesized in their ring close forms i.e. **a**Cl and **b**Cl following the here reported procedure (figure 5.3) that consist in a condensation of an indolenine moiety bringing an active -CH_3 in position 2 with the aldehydic functional group of the fluorophores in acidic conditions:
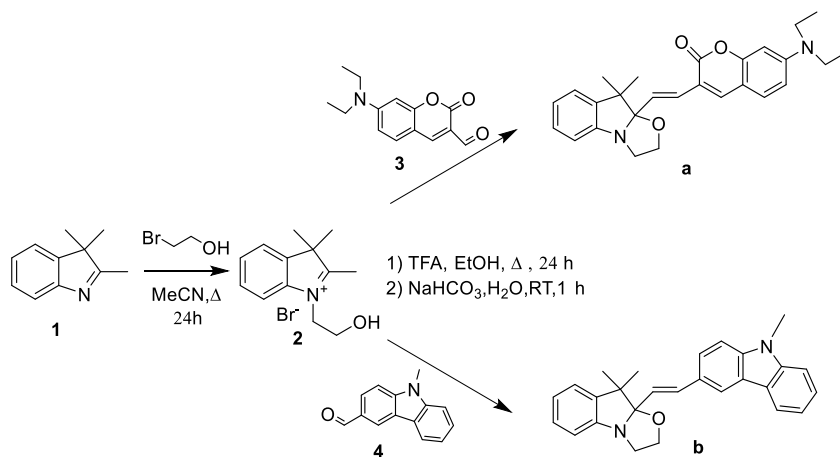
Figure 5.3 Synthetic scheme for compounds **a**Cl and **b**Cl.

Compounds **2**, **3** and **4** were synthesized following reported procedures to create the fluorophores coumarin and carbazole scaffolds and the *2H,3H,4H,5H*-[1,3]oxazole i.e. oxazolidine heterocyclic scaffold.[148-150]

<u>Synthesis of **a** Cl and **b** Cl.</u> Trifluoroacetic acid (TFA, 450 μL, 5.72 mmol) was added dropwise to a solution of 5 (250 mg, 0.87 mmol) and either 3 (216 mg, 0.88 mmol) or 4 (184 mg, 0.88 mmol) in EtOH (10 mL). The mixture was heated at reflux for 24 hours. After cooling down to ambient temperature, the solvent was distilled off under reduced pressure and the residue was dissolved in CH_2Cl_2 (5 mL). Addition of Et_2O (200 mL) and refrigeration for 12 hours caused the formation of a precipitate. After filtration, the solid residue was dissolved in aqueous $NaHCO_3$ (5% w/v, 20 mL) and stirred for 1 hour at ambient temperature. The aqueous mixture were extracted with EtOAc (3 × 40 mL). The organic phase was dried over anhydrous Na_2SO_4, filtered and the solvent was distilled off under reduced pressure to give either **a**Cl (68%, 264 mg), as a green solid, or **b**Cl (35%, 125 mg), as a red solid. **a**Cl: ESIMS: m/z = 431.2338 [M$^+$] (m/z calcd for $C_{27}H_{31}N_2O_3^+$ 431.2335); ^{1}H NMR (400 MHz, CDCl$_3$): δ (ppm) = 1.18 (s, 3H), 1.20–1.26 (t, 6H), 1.46 (s, 3H), 3.37–3.47 (m, 4H), 3.60–3.68 (m, 2H), 3.77–3.81 (m, 1H), 4.10–4.16 (m,1H), 6.51 (s, 1H), 6.55–6.61 (d, 9 Hz, 1H), 6.65–6.71 (m, 1H), 6.77–6.86 (m, 2H), 6.90–6.97 (t, 7 Hz, 1H), 7.05–7.11 (d, 7 Hz, 1H), 7.14–7.19 (m, 1H), 7.25–7.29 (m, 1H), 7.60 (s, 1H); ^{13}C NMR (100 MHz, CDCl3): δ (ppm) = 161.2, 155.8, 150.8, 150.6, 139.9, 139.4, 128.9, 128.0, 127.5, 126,7, 122.4, 121.5, 117.0, 112.0, 110.1, 109.0, 108.8, 97.1, 63.5, 50.2, 47.9, 44.8, 28.5, 20.4, 12.5. **b**Cl: ESIMS: m/z = 395.2111 [M$^+$] (m/z calcd for $C_{27}H_{27}N_2O^+$ 395.2123); ^{1}H

NMR (400 MHz, CDCl$_3$): δ (ppm) = 1.27(s, 3H), 1.54 (s, 3H), 3.54–3.59 (m,1 H) 3.67–3.76 (m, 2H), 3.88 (s, 3H), 4.11–4.16 (m, 1H), 6.32–6.38 (d, 16 Hz, 1H), 6.84–6.88 (d, 8 Hz, 1H), 6.96-7.02 (t, 7 Hz, 1H), 7.06 (s, 1H), 7.10–7.16 (m, 2H), 7.18–7.25 (t, 8 Hz, 1H), 7.35–7.45 (m, 2H), 7.48–7.55 (d, 7 Hz, 1H), 7.64–7.67 (d, 9 Hz, 1H), 8.10–8.16 (d, 8 Hz, 1H), 8.20 (s, 1H); ^{13}C NMR (100 MHz, CDCl$_3$): δ (ppm) = 150.8, 141.5, 140.9, 140.0, 133.1, 127.7, 127.6, 126.0, 124.7, 123.1, 122.9, 122.8, 122.5, 121.6, 120.4, 119.1, 118.9, 112.1, 110.2, 108.6, 108.5, 63.6, 50.2, 48.0, 29.2, 28.6, 20.4.

5.2.5 Temperature NMR Results

The here reported ^{1}H NMR spectra of compound **a** in CD$_3$CN (figure 5.4) present significant broadening in the region between 3 and 4 ppm for the resonances associated with the two pairs of diastereotopic ethylene protons. These observations are indicative of the opening and closing of the oxazolidine ring with fast kinetics on the NMR timescale, the data obtained are consistent and in accordance with the behavior reported previously for the oxazine reported in Figure 5.0.[31]
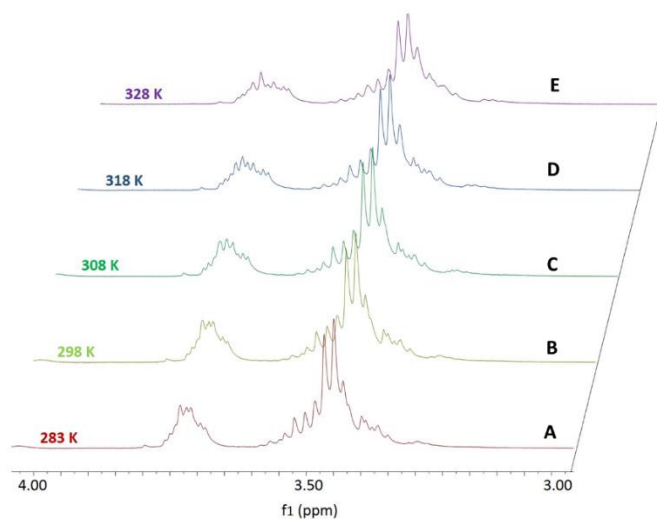
Figure 5.4 Partial ^{1}H NMR spectra (400 MHz, 15 mM, CD$_3$CN) of **a** at 283 (**A**), 298 (**B**), 308 (**C**), 318 (**D**) and 328 K (**E**).

5.2.6 Results

The experimental evidences obtained, showed the equilibration of two interconverting species with resolved fluorescence results in a ratiometric response to temperature in a temperature range, between 10 °C and 55 °C. This temperature's window is useful for the applications of these systems within the nano-biological realm. The ratiometric determination is allowed by the opening and closing of an oxazine or an oxazolidine heterocycle. The structural-geometrical changes related to these phenomena affect the electronic structure of two different fluorophores: carbazole and coumarin with influence upon the spectral position of the related absorption and emission bands. The resolved emissions of the two interconverting species can be probed into 2 way: spectroscopically in parallel or in an independent detection's channels of a single microscope. In both the experiments' setting eventual concentration effects and optical artifacts are overcome by the ratio between the detected intensities. The properties of these systems represent an advantage for the dual emission micro thermo-measurements in comparison to the single channel detection. In conclusion, the structural design of the investigated compounds allows to map temperature in a ratiometric mode at the microscale level with the acquisition of conventional fluorescence images.

5.2.7 Water Soluble Compounds

Considering the achieved results with compounds **a-d** and the promising applications of these molecules in new thermometric systems, we have proposed a modified version of probe **a**, which showed the best results, in terms of sensitivity and responsivity, with the goal to obtain a water-soluble molecule. These modifications could strength the uses of the probes in the biological realm. In accordance with the results achieved for a water-soluble version of compound **c** .[151] I synthesized molecule **e**. Figure 5.5
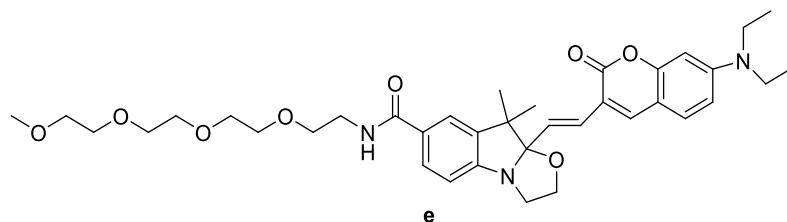

Figure 5.5 Chemical structure of the synthesized compound **e**Cl.

In this situation the polyethylene glycol (PEG) chain is useful to facilitate the solubility of the molecule in a solvent mixture containing a lower percentage of MeCN and a higher one of H_2O. The equilibria in solution of the compounds are reported in figure 5.6
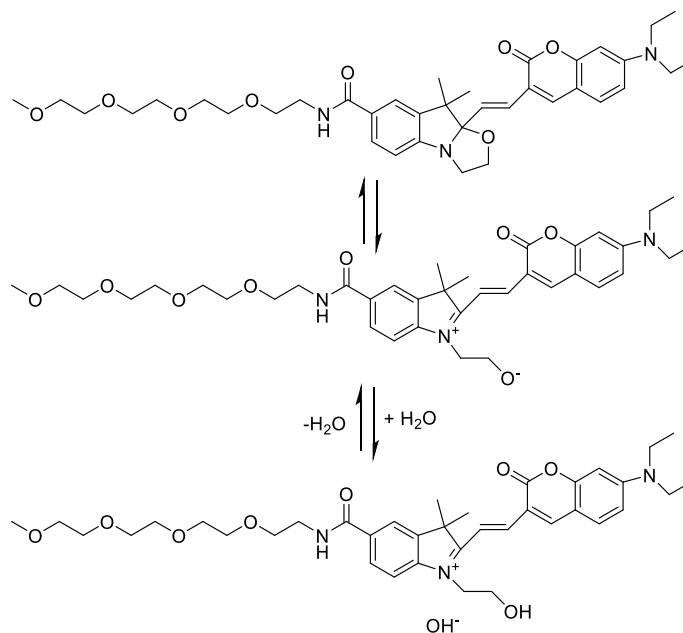

Figure 5.6 Equilibria in solution for compound **e**.

The photochromic auxochrome **c** have been already investigated in a more water-soluble version inserting the same PEG modification in position 5 of the indole scaffold.[58] This molecule will be tested in the same temperature conditions for the spectroscopic absorption and emission properties reducing or eliminating at all the amount of MeCN needed to solubilize the compound.

5.2.7.1 Synthesis of the Molecule
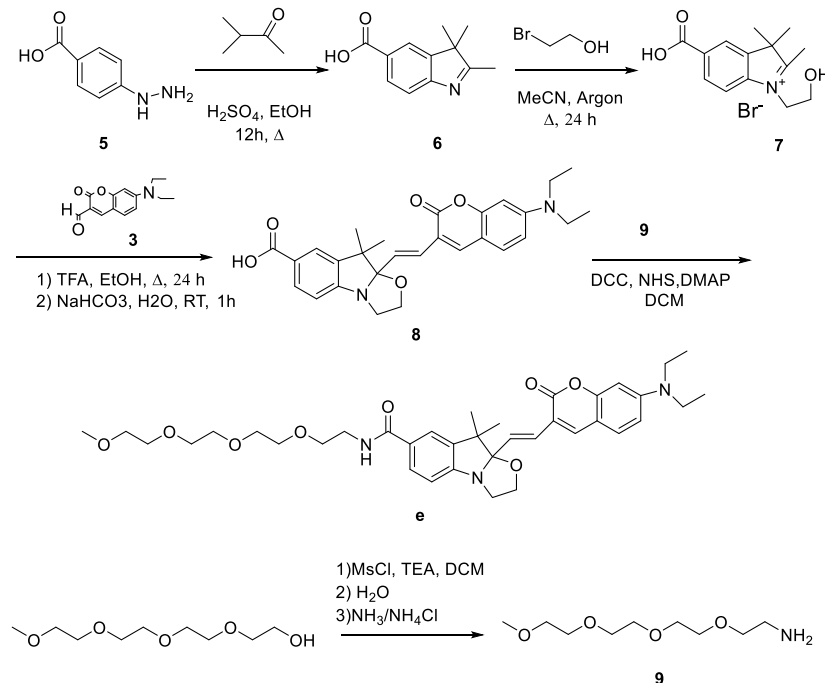
Figure 5.7 Synthetic scheme for compounds **e**Cl

<u>Synthesis of **e**Cl.</u> **8** (38mg, 0.08 mmol), N,N'-Dicyclohexylcarbodiimide (DCC, 33mg, 0.16 mmol), N-Hydroxysuccinimide (NHS, 19 mg, 0.16 mmol) and 4-Dimethylaminopyridine (DMAP, 2mg, 0.02 mmol) were dissolved in CH_2Cl_2 at 0 °C in Argon atmosphere, the reaction was warmed up to ambient temperature and stirred for 12 h. After 12h, **9** (33mg, 0.16mmol) was added to the mixture dropwise and the reaction was stirred at ambient temperature for other 12 h. The reaction was stopped, and the solvent removed in vacuum. The obtained crude product was purified with column chromatography (DCM:MeOH 98:2+0.8% TEA) to get **e**Cl (24%, 13mg) as a green solid. **e**Cl: ESIMS: m/z = 664.3660 [M+] (m/z calcd for $C_{37}H_{49}N_3O_8^+$ 664.8002); ^{1}H NMR (400 MHz, CD$_3$CN): δ (ppm) = 1.15 (s, 3H), 1.16-1.19 (m, 6 H), 1.44 (s, 3H), 3.28 (s, 3 H), 3.29-3.32 (m, 2H), 3.45-3.56 (m, 16 H), 3.73-3.75 (m, 2H), 6.55 (s, 1H), 6.71-6.77 (m, 2 H), 6.89 (d, 8 Hz,1H), 7.03 (bs, 1H), 7.37 (d, 8 Hz, 1H), 7.57 (s, 1 H), 7.67 (d, 9 Hz, 1H), 7.83 (s, 1H).

8. **7** (200 mg, 0.61mmol) and **3** (149mg, 0.61mmol) were dissolved in EtOH, trifluoroacetic acid (TFA, 310 µL, 3.96 mmol) was added dropwise to the mixture that was refluxed for 24h. After cooling down to ambient temperature, the solvent was distilled off in reduced

pressure and the residue dissolved in CH_2Cl_2 (5 mL). Addition of Et_2O (200 mL) and refrigeration for 12 hours caused the formation of a precipitate. The precipitated solid was filtered and dissolved in aqueous $NaHCO_3$ (5% w/v, 20 mL) and stirred for 1 hour at ambient temperature. The aqueous phase was extracted with EtOAc (3 x 40 mL). The organic phases were dried over anhydrous Na_2SO_4, filtered and the solvent was distilled off in reduced pressure to give **8** (33%, 96 mg) as a green solid. **8**: ESIMS: m/z = 475.2237 [M$^+$] (m/z calcd for $C_{28}H_{30}N_2O_5^+$ 475.5482); ^{1}H NMR (400 MHz, CD_3OD): δ (ppm) = 1.19-1.29 (m, 9 H), 1.44 (s, 1H), 3.49-3.55 (m, 4H), 3.62-3.65 (bs, 2H), 3.82 (bs, 1H), 4.09 (bs, 1H), 6.54 (s, 1H), 6.68 (d, 9 Hz, 1H), 6.73-6.78 (m, 1H), 6.90 (d, 8 Hz, 1 H), 7.43 (s, 1 H), 7.74 (s, 1 H), 8.07-8.38 (m, 3H), 8.55 (s, 1H).

7. **6** (500mg, 2.46 mmol) were dissolved in MeCN (10 mL), 2-Bromoethanol (210 µL, 2.95mmol) was added dropwise and the mixture heated at reflux in Argon atmosphere for 24 hours. After cooling down to ambient temperature, the solvent was distilled off in reduced pressure and the residue was dissolved in Hexane (10 mL) and sonicated for 30 min. Hexane was removed and the residue was rinsed and precipitated with CH_2Cl_2 (100 mL) to get compound **7** (yield 36%,184mg) as a pink/red solid. **7**: ESIMS: m/z = 248.1306 [M$^+$] (m/z calcd for $C_{14}H_{18}NO_3^+$ 248.1394); ^{1}H NMR (400 MHz, $CDCl_3$): 1.34 (s, 6 H), 2.30 (s, 3H), 3.47-3.50 (m, 2H), 3.78-3.80 (m, 2H), 7.55 (d, 7.5 Hz,1H), 8.02 (s, 1H), 8.04 (s, 1 H).

5.2.8 Future Perspectives

The obtained probes represent good tools for the ratiometric detection of temperature in aqueous media and they will be investigated for these applications in the fabrication of temperature controller devices. The project was developed within a National Science Foundation (NSF) grant (CHE-1505885), the other research group involved (University of Miami: Rosenstiel School of Marine and Atmospheric Science Department_ Prof. Peter J. Minnett) will be responsible of the production of the final temperature's controller system.

5.3 pH Sensing with Switchable Coumarins

5.3.1 Introduction

The capability to monitor pH values at cellular and sub-cellular levels with high spatial and time resolution is an essential tool in the biological realm.[151] pH has a determining role in the physiological activities of cells and cellular organelles, it is involved in the metabolism and internalization's processes within the cells itself.[152] For these reasons an accurate control of pH values is fundamental to detect regular and inappropriate functions of biochemical processes, to highlight the different cells' compartments and to study phenomena in tissues and systems.[153] The micro-scaled dimensions of cells in conjunction with the need to ensure minimal structural perturbations and the need of low invasive system restrict significantly the number of analytical methods compatible with these measurements.[154] Fluorescence microscopy is a convenient tool in this context indeed its key point are: the noninvasive character, the micrometric resolution accompanied by the fast response and the inherent sensitivity.[155] Usually, sensitive molecular probes are designed to change their fluorescence quantum yield in relation to pH: the measured emission intensity in the region of interest can be correlated to pH in a quantitative way. Unfortunately, this parameter can be affected by concentration and optical effects that can also have influence on the magnitude of the detected intensity. A solution to these issues is to use sensitive dyes engineered to produce dual emission in resolved spectral windows.[156,157] In these conditions, the intensity of one emission can be measured relative to the other to eliminate any possible artifact. Moreover, the sensitivity of these sensors needs to be regulated to a relatively wide range of pH values: usually between 4 and 8 (that represent respectively the acidic lysosomals' and the basic mitochondria's pH values). The aid of chemical synthesis is valuable to achieve all these properties to prepare efficient pH sensors. Oxazine's scaffolds have already been identified as tools for pH measurements: a ring opening mechanism based upon acidification have been investigated to activate the fluorescence of a coumarin fluorophore.[158] This opening process activate the fluorescence and it is responsible of a bathochromic shift in the coumarin absorption. The selective excitation of the ring-opened and protonated species resulted in an intense fluorescence signal. In addition, the linking of this pH activatable sensor to folate ligands consent the fluorescence's activation exclusively

in the endosomal compartments of cancer cells, allowing their discrimination from the normal ones at pH values under 5.

5.3.2 Design of the Project

The results already achieved with compound reported in Figure 5.8, the need to tune the pH sensitivity of this probe and the possibility of a ratiometric response suggested the possibility to generate with the organic chemistry tools structural modifications of the original oxazine heterocycle to obtain new pH probes (Figure 5.9).
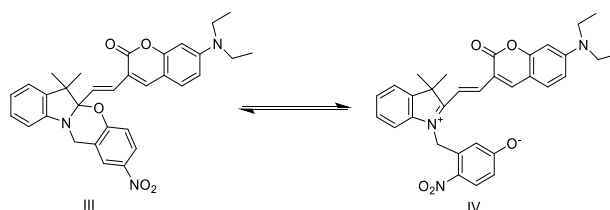

Figure 5.8 Equilibrium in solution upon pH variation for compound **c.**

Compounds **c**Cl and **f**Cl incorporate an oxazine heterocycle and differ in the position of a nitro substituent (Figure x). Compounds **a**Cl and **g**Cl have an oxazolidine heterocycle in place of the oxazine ring and differ in the substituent on 2H,3H-indole (indole) heterocycle, indeed compound **g**Cl was prepared with the goal to extend the conjugation of the system introducing a substituent in position 5 of the oxazolidine scaffold. The synthesis of **a**Cl and **c**Cl has been already reported while the synthesis of **f**Cl and **g**Cl was performed as follow.
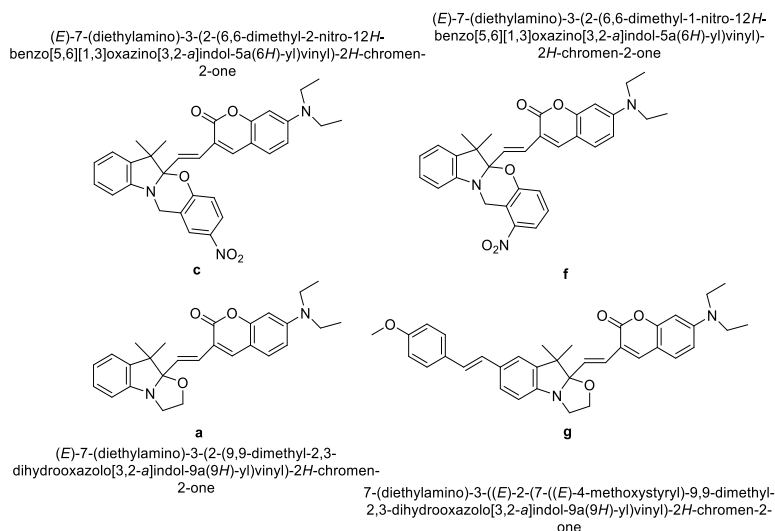
Figure 5.9 Chemical structures of the 4 compounds synthesized and tested for the project.

5.3.3 Content

The molecules were analyzed in their spectroscopic properties using MeCN as solvent through UV-Vis absorption/emission spectroscopies. The samples were analyzed in different pH conditions, changing the pH environment with addition of increasing amounts of trifluoroacetic acid (TFA) up to 1.75 equivalents. The elected compounds are relatively hydrophobic and essentially insoluble in aqueous environments. However, they easily dissolve in the presence of an amphiphilic polymer: Pluronic-123 because they associate with no-covalent interactions with the hydrophobic domains of the polymer itself. These nanoparticles were analyzed with the same spectroscopic techniques in a pH range between 2 and 8 in aqueous media highlighting the same results Moreover, compound **g**, that showed the best results in terms of absorption and emission spectroscopies, was studied through fluorescence microscopy *via* the incorporation into alginate hydrogel in a pH range between 4 and 7 in order to probe pH at the micrometer level in a ratiometric way.

5.3.4 Synthesis of the Molecules

Compounds **3**, **10**, **11** were synthesized accordingly to already reported procedures[16,60,149] Compound **f** was synthesized through the condensation of an oxazine moiety and an aldehyde substituted coumarin, compound **g** was synthesized with the same approach using an oxazolidine subunits instead of an oxazine one, moreover this moiety was prepared to allow a further Heck coupling reaction to introduce a further substitution to the molecule.
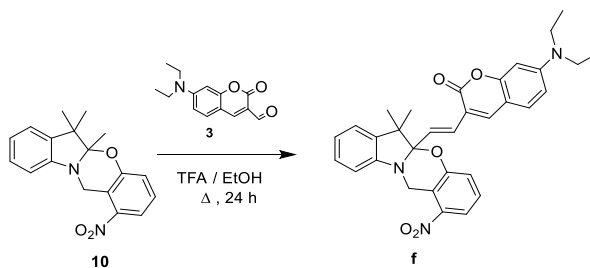
Figure 5.10 Synthetic scheme to synthesize compound **f**Cl.

Synthesis of **f**Cl. Trifluoroacetic acid (TFA, 160 µL, 2.09 mmol) was added dropwise to a solution of **10** (100 mg, 0.32 mmol) and **3** (79 mg, 0.32 mmol) in EtOH (10 mL). The

mixture was heated at reflux for 24 hours. After cooling down to ambient temperature, the solvent was distilled off in reduced pressure and the residue was dissolved in CH_2Cl_2 (50 mL) and washed with $NaHCO_3$ (5% w/v, 20 mL) and H_2O (20 mL). The organic phase was dried over anhydrous Na_2SO_4, filtered and the solvent was distilled off in reduced pressure. The residue was purified by column chromatography [SiO_2, CH_2Cl_2/MeOH (98:2, v/v)] to give **f**Cl (9%, 15 mg) as a green solid. ESIMS: m/z = 538.2359 [M + H]$^+$ (m/z calcd. for $C_{32}H_{32}N_3O_5$ = 538.6149); ^{1}H NMR (400 MHz, CD_3CN): δ (ppm) = 1.16-1.19 (m, 9H), 1.52 (s, 3H), 3.41-3.46 (m 4H), 4.78 (d, 19Hz, 1H), 5.02 (d, 19Hz, 1H), 6.51 (s, 1H), 6.67-6.72 (m, 2 H), 6.77-6.79 (m, 1 H), 6.82-6.89 (m, 1H), 6.98-7.09 (m, 2H), 7.17-7.19 (d, 5 Hz, 2H), 7.28-7.35 (m, 2H), 7.64-7.66 (d, 8 Hz, 1H), 7.81 (s, 1H).
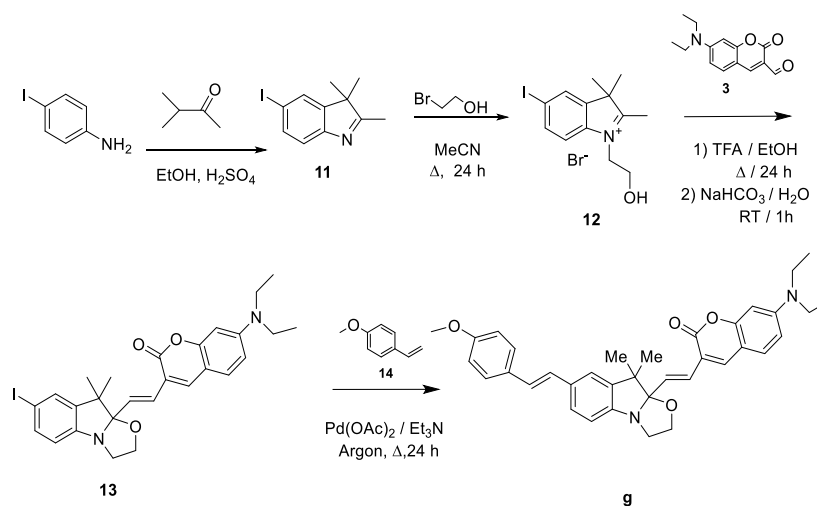
Figure 5.11 Synthetic scheme to synthesize compound **g**Cl.

Synthesis of **g**Cl. Palladium(II)acetate (18 mg, 0.07 mmol) was added to a solution of **13** (40 mg, 0.07 mmol) and **14** (20 mg, 0.14 mmol) in Et_3N (20 mL). The mixture was heated at reflux and in Argon atmosphere for 24 hours. After cooling down to ambient temperature, the reaction mixture was diluted with CH_2Cl_2 (20 mL) and washed with H_2O (2 × 20 mL). The organic phase was dried over anhydrous Na_2SO_4, filtered and the solvent was distilled off at reduced pressure. The residue was purified by column chromatography [SiO_2, CH_2Cl_2/MeOH (93:7, v/v) and Et_3N (1% v/v)] to give **g**Cl (25%, 10 mg) as a green solid. ESIMS: m/z = 563.2888 [M + H]$^+$ (m/z calcd. for $C_{36}H_{39}N_2O_4$ = 563.7072); ^{1}H NMR (400 MHz, $CDCl_3$): δ (ppm) = 1.19 (s, 3H), 1.25-1.23 (t, 6H), 1.49 (s, 3H), 3.41–3.49 (m, 4H), 3.66-3.67 (m, 2H), 3.81-3.85 (m, 4H), 4.30 (m, 1H), 6.51 (s, 1H), 6.59 (d, 8 Hz, 1H), 6.65-

6.72 (m, 1H), 6.75-6.81 (m, 2H), 6.87-6.92 (m, 2H), 6.96 (s, 1H), 7.24-7.31 (m, 4H), 7.44 (d, 8 Hz, 2H), 7.60 (s, 1H).

14. Methyltriphenylphosphonium bromide (2.19 g, 6.12 mmol) and K_2CO_3 (4.23g, 30.61 mmol) were added to 4-methoxybenzaldehyde (894 µL, 7.34 mmol) in N,N-dimethylformamide (DMF, 30 mL). The mixture was heated at reflux for 20 hours. After cooling down to ambient temperature, the reaction mixture was poured into H_2O (30 mL). The aqueous mixture was extracted with EtOAc (4 × 50 mL). The organic phase was dried over anhydrous Na_2SO_4, filtered and the solvent was distilled off at reduced pressure. The residue was purified by column chromatography [SiO_2, Hexane/EtOAc (9:1, v/v)] to give 12 (37%, 300 mg) as a colorless oil. ^1H NMR (400 MHz, CDCl$_3$): δ (ppm) = 3.84 (s, 3H), 5.18 (d, 8 Hz, 1H), 5.67 (d, 20 Hz, 1H), 6.72 (dd, 8 and 20 Hz, 1H), 6.91 (d, 8 Hz, 2H), 7.40 (d,8 Hz, 2H).

13. TFA (209 µL, 2.65 mmol) was added dropwise to a solution of **3** (100 mg, 0.41 mmol) and **12** (167 mg, 0.41 mmol) in EtOH (8 mL). The mixture was heated at reflux for 24 hours. After cooling down to ambient temperature, the solvent was distilled off at reduced pressure and the residue was dissolved in CH_2Cl_2 (5 mL). Addition of Et_2O (200 mL) and refrigeration for 12 hours caused the formation of a precipitate. After filtration, the solid residue was dissolved in aqueous $NaHCO_3$ (5% w/v, 20 mL) and stirred for 1 hour at ambient temperature. The aqueous mixture was extracted with EtOAc (3 × 40 mL). The organic phase was dried over anhydrous Na_2SO_4, filtered and the solvent was distilled off under reduced pressure to give **13** as a green solid (22%, 50 mg). ESIMS: m/z = 557.1293 [M + H] $^+$ (m/z calcd. for $C_{27}H_{30}IN_2O_3$ = 557.4442); ^1H NMR (400 MHz, CDCl3): δ (ppm) = 1.17 (s, 3H), 1.21-1.27 (m, 6H), 1.42 (s, 3H), 3.41-3.46 (m, 4H), 3.54-3.67 (m, 2H), 3.76-3.82 (m, 1H), 4.13 (q, 7 Hz, 1H), 6.51 (s, 1H), 6.56-6.63 (m, 2H), 6.64 (d, 17 Hz, 1H), 6.79 (d, 8 Hz,1H), 7.25-7.30 (m, 1H), 7.34 (s, 1H), 7.45 (d, 8 Hz, 1H), 7.59 (s, 1H).

12. 2-Bromoethanol (298 µL, 4.21 mmol) was added dropwise to a solution of **11** (1 g, 3.51 mmol) in MeCN (10 mL). The mixture was heated at reflux and in Argon atmosphere for 24 hours. After cooling down to ambient temperature, the solvent was distilled off in reduced pressure and the residue was dissolved in Hexane (10 mL), sonicated for 30 min and filtered. The residue was dissolved in CH_2Cl_2 (50 mL) and stored in fridge for 2 hours.

The resulting precipitate was filtered off, washed with CH_2Cl_2 (20 mL) and dried to give **12** (63%, 910 mg) as a pink solid.   ESIMS: m/z = 330.0349 [M – Br]$^+$ (m/z calcd. for $C_{13}H_{17}INO$ = 330.0349); ^{1}H NMR (400 MHz, CD$_3$CN): δ (ppm) = 1.58 (s, 6H), 2.79 (s, 3H), 3.99 (t, 5 Hz, 2H), 4.52 (t, 5 Hz, 2H), 7.59 (d, 8 Hz, 1H), 7.99 (d, 8 Hz, 1H), 8.13 (s, 1H).

5.3.5 Covalent functionalization of alginate hydrogel with a pH probe

To investigate the behavior of these coumarin based pH probes in the formation of alginate hydrogel beads, a covalent approach to link the molecule to the hydrogel material was proposed using compound **8** and an opportune modified alginate substrate (Figure 5.12) (i.e. alginate covalently functionalized with ethylene diamine (EA)) with the goal to investigate with biological experiments two forms of alginate hydrogel beads containing the coumarin probe.
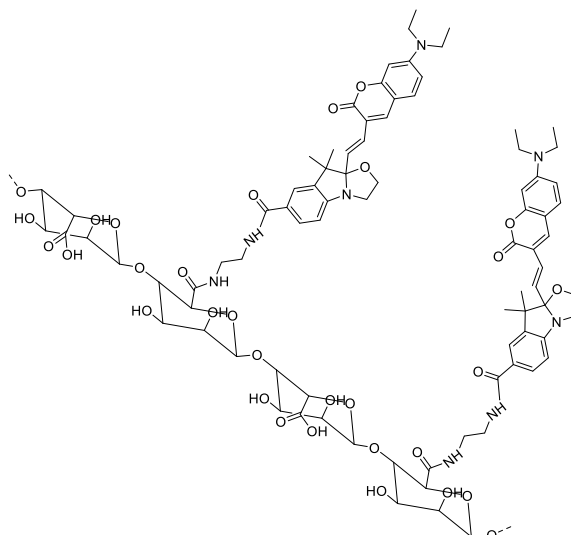
Figure 5.12 Schematic representation of the alginate composite.

5.3.5.1 Preparation of the Material

EA-alginate functionalized was prepared following a reported procedure with slight modifications.[159] Sodium Alginate (200 mg) was dissolved in H_2O, the pH of the solution is around 4. N-(3-Dimethylaminopropyl)-N′-ethylcarbodiimide hydrochloride (EDC*HCl, 200 mg) and N-Hydroxysuccinimide (NHS, 60 mg) were added to the mixture that was stirred for 15 mins. Ethylene diamine (EA, 50 mg) was added dropwise to the mixture that

was stirred at ambient temperature for 24 hours. The material was precipitated adding 50 mL of fresh acetone to solubilize the exceeded ethylenediamine and precipitate the functionalized alginate that was then washed with H_2O (50 mL). To prove the functionalization a portion of the material was analyzed adding few drops of Ninhydrin in EtOH, the functionalized material become blue colored due to the interaction between the amino functionalities and the Ninhydrin, while the pristine alginate remained colorless. 40 mg of the prepared EA-alginate was de-solved in 4 mL of H_2O, 40 mg of EDC*HCl and 12 mg of NHS were added to the solution that was stirred for 30 min, 12 mg of compound **8** in 500 µL of MeCN were then added dropwise. The solution became blue colored and the mixture was stirred at ambient temperature for 24 hours. The material was precipitated adding 50 mL of fresh Acetone to solubilize the exceeded compound **8** and precipitate the functionalized alginate that was washed with H_2O (50 mL), until the total transparency of the solution. The obtained material was blue colored, and this could be the confirmation of the functionalization with compound **8** in its open form, the close form can be obtained with the suspension of the material in a $NaHCO_3$ 5% solution, as indicated by a colour change to yellow (Figure 5. 13)
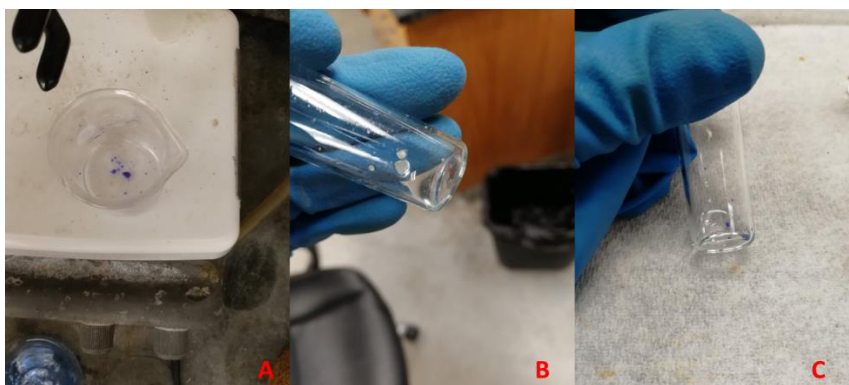
Figure 5.13 Few images of the prepared materials. A) the material after the preparation, B) the material treated with $NaHCO_3$ 5% solution to close the probe C) The material treated with TFA after the basic treatment (the open form is restored).

Alginate beads formed with this material will be tested spectroscopically and through fluorescence microscopy to analyze and investigate similarity and comparisons with the alginate beads incapsulated with the pre-formed polymeric nanoparticles described in the previous paragraph.

5.3.6 Results

The pH dependence of the equilibrium between the ring-closed and protonated ring-open forms of all the tested molecules observed from the absorption spectra translates into dual emission with a ratiometric response. This structural ring opening-ring closing transformation converts the hybridization of the carbon atom at the junction from sp^3 to sp^2 and brings the coumarin component in conjugation with the resulting 3H-indolium cation. This process generates an extended electronic delocalization in the molecule, which is responsible of the bathochromic shift of the main absorption of the coumarin chromophore. The resolved emission bands of the opened and closed forms of the compounds allow to probe pH ratiometrically through the acquisition of fluorescence images in different detection channels. Moreover, we proved that the compounds were not affected by any hydrolytic degradation or photobleaching phenomena at the experimental conditions, this aspect strengthens their potential use for pH sensing.

5.3.7 Future Perspectives

Investigations with a biological experiment (i.e. normal/cancer cell lines analyses/other species of microorganism) to test the probing properties of the compounds in real biological model in collaboration with University of Miami Biological departments)

5.4 Conjugated Polymers assembled with Oxazine Switching Monomers

5.4.1 Introduction

Molecular switches represent interesting and useful tools for the development of stimuli-responsive systems and materials including polymeric materials.[18,160] Among the photo-switchable molecules 2H,4H-benzo[1,3]oxazine (i.e. oxazine) compounds were used for the assembly of polymeric structures combining switchable subunits and polymeric substrates with covalent or no-covalent approaches, preparing materials with photoactivatable

properties.[161,162] Photo-responsive polymers were prepared incorporating photocleavable oxazines for fluorescence pattering applications, the obtained matrix requires just mild illumination's conditions and overcome many of the operations difficulties that usually characterize similar assemblies.[163] Oxazine monomers can be incorporated in polymeric materials either as pendants or main chain components in the structure with the goal to obtain conjugated polymers extending the optical and electronic properties of the assembled materials in a polymeric matrix. In particular the possibility to modify the position of a - NO_2 group in the 2H,4H-benzo[1,3]oxazine ring represent an useful tool to develop new polymeric conjugated material with photoactivatable properties that can be controlled in a reversible or not reversible way. The properties of the final composite polymers can be controlled and compared each other in their physical and chemical peculiarities.

5.4.2 Design of the Project

Design and synthesis of 2 small libraries of molecules presenting a 2H,4H-benzo[1,3]oxazine photoactivatable scaffold, the first, while the second shows molecules without a photoactivatable unit in their structure with opportune substituents in order to perform Heck Coupling reactions with the first class with photo-responsive monomers to obtain conjugated photo-switchable polymers. (Figure 5.14)
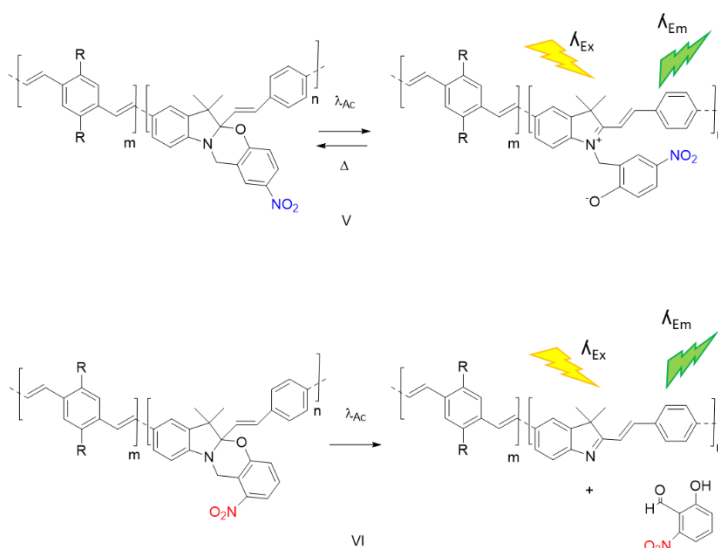
Figure 5.14 Schematic representation of the final conjugated polymer.

83

5.4.3 Content

Many of the necessary molecules were synthesized in order to assembly the final needed polymers to study the extended properties of the conjugated systems. The goal is to shift the absorbance and emission properties of the monomers as well as to modify other properties as optical and optoelectronic ones in the final polymers. In this context, the influence due to the position of the -NO$_2$ substituent, i.e. *meta* or *para* in respect to the oxygen atom, will be taken in consideration.

5.4.4 Synthesis of the Molecules

Two small libraries of molecules (figures 5.15 and 5.16) must be synthesized for the preparation of the final polymers.
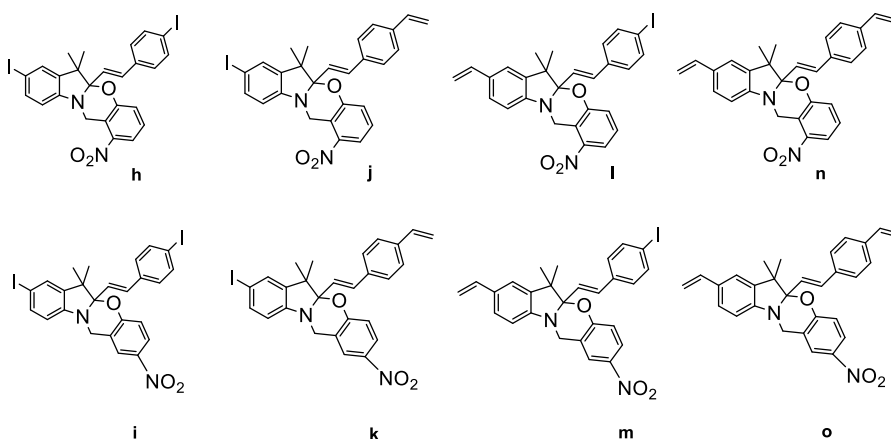
Figure 5.15 The small library of photo-switchable monomers.
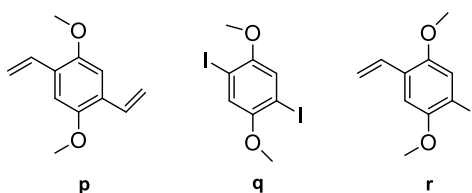
Figure 5.16 The small library of complementary monomers.

Compounds **h,i.j,k** were the novo synthesized, while compounds **p,q,r** were synthesized with slight modification of already reported procedures. Compounds **11** and **17** were

prepared accordingly to procedures optimized in the group.[16,60] Compound **16,** was synthesized with slight modification of a reported procedure.[164]

### 5.4.4.1 2H,4H-benzo[1,3]oxazine i.e. Oxazine Monomers
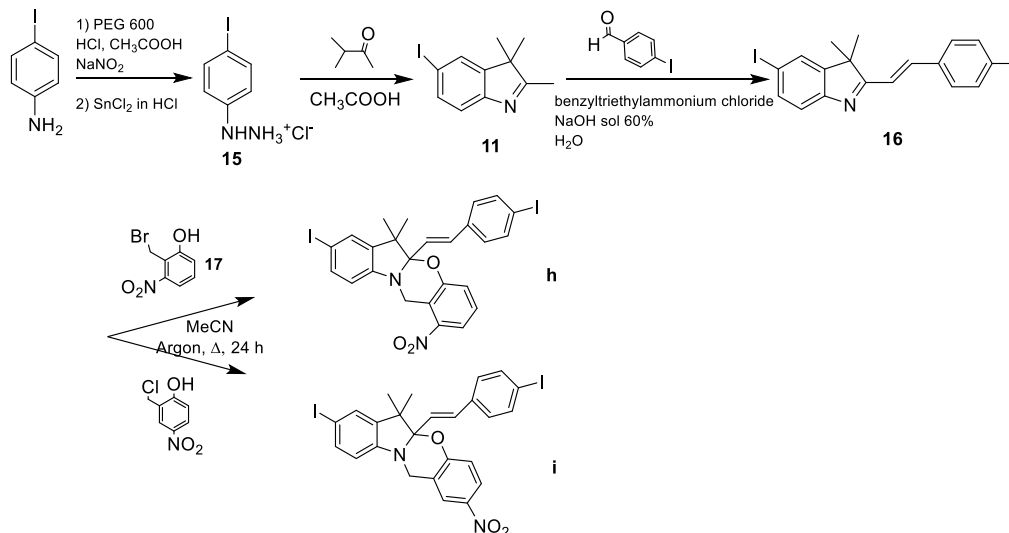
Figure 5.17 Synthetic scheme for compounds **h** and **i.**

<u>Synthesis of **h** and **i**.</u>

h. Compound **16** (200 mg, 0.40mmol) was dissolved in degassed MeCN (15 mL), **17** (232 mg, 1.00 mmol) was added to the mixture that has been stirred at reflux in Argon atmosphere for 24h. The solvent was removed in vacuum, the crude dissolved in CH$_2$Cl$_2$ (50 mL) and washed with NaHCO$_3$ 5% (50 mL) solution and H$_2$O (2 x 50 mL). The obtained residue was purified by column chromatography (Hex: EtOAc 9:1) to give **h** (25%, 65 mg). as a yellow solid. ESIMS: m/z = 650.9641 [M $^+$] (m/z calcd. for C$_{25}$H$_{20}$I$_2$N$_2$O$_3$ = 650.2476); ^{1}H NMR (400 MHz, CDCl$_3$): δ (ppm) 1.19 (s, 3 H), 1.50 (s, 3H), 4.73 (d, 16 Hz, 1 H), 4.99 (d, 8 Hz, 1 H), 6.32 (d, 8 Hz, 1 H), 6.38 (d, 9 Hz, 1H), 6.73 (d, 7 Hz,1 H), 7.08,7.18 (m, 4 H), 7.38-7.42 (m, 2H), 7.61-7.68 (m, 3 H).

i. Compound **16** (100mg, 0.20 mmol) was dissolved in degassed MeCN (10 mL), 2-chlorophenyl-4-nitro-phenolo (113mg, 0.60 mmol) was added to the mixture that was stirred at reflux in Argon atmosphere for 24h. The solvent was removed in vacuum, the crude dissolved in CH$_2$Cl$_2$ (30 mL) and washed with NaHCO$_3$ 5% (30 mL) solution and H$_2$O (2 x 30 mL). The obtained residue was purified by column chromatography (Hex: EtOAc 9:1)

to give **i** (23%, 30mg). as a pale-yellow solid. ESIMS: m/z = 650.9669 [M$^+$] (m/z calcd. For C$_{25}$H$_{20}$I$_2$N$_2$O$_3$ = 650.2476); ^{1}H NMR (400 MHz, CDCl$_3$): δ (ppm) 1.23 (s, 3H), 1.52 (s, 3H), 4.56 (s, 2H), 6.32 (d, 8 Hz, 1H), 6.44 (bs, 1H), 6.74 (d, 16 Hz, 1H), 6.76 (s, 1H), 7.11-7.13 (m, 2H), 7.36-7.39 (m, 2H), 7.66-7.70 (m, 2H), 8.00-8.03 (m, 2H).

16. Compound **11** (2g, 7.01mmol), 4-iodobenzaldehyde (1.6g, 7.01 mmol) and benzyltriethylammonium chloride (395mg, 2.13 mmol) were suspended in H$_2$O (3 mL). 2 mL of an aqueous NaOH (60%) solution were added dropwise to the mixture, the reaction was stirred at 40°C for 30h. The reaction was diluted with H$_2$O (10 mL), the pH was adjusted with HCl 12 M (few drops) until neutral value. The residue was extracted with EtOAc (3x30 mL) to get a brown semisold residue that was purified by column chromatography (Hex:EtOAc 9:1) to get **16** as a yellow solid. ESIMS: m/z = 499.9374 [M$^+$] (m/z calcd. for C$_{18}$H$_{15}$I$_2$N = 499.1273); ^{1}H NMR (400 MHz, CDCl$_3$): δ (ppm) 1.42 (s, 6 H), 7.04 (d, 9 Hz 1H), 7.33 (d, 8 Hz, 2H), 7.39 (d, 8 Hz, 1H), 7.65-7.71 (m, 3H), 7.73-7.79 (m , 2H).

11.4-iodoaniline (2g, 9.13 mmol), PEG 600 (100 mg,5 %, mass), CH$_3$COOH 4.6 mL and HCl 12 M, 2.3 mL were mixed in a round bottom flask. The mixture was heated until the total dissolution of 4-iodoaniline. The mixture was cooled to 0 °C in an ice bath, an aqueous solution of NaNO$_2$ (630 mg, 9.13mmol, in 2 mL of H$_2$O) was added dropwise and the mixture was stirred for 1h. A In the mean time a Tin(II)chloride solution was prepared dissolving(SnCl$_2$, 7 g) in 7 mL of HCl 12 M, the solution was cooled to 0 °C. This solution was added dropwise to the reaction mixture and stirred at room temperature for additional 2 h. The solution was filtered, the residue washed with water and dried in vacuum to obtain compound **15** as a grey solid (80%, 1.878g). 3-methylbutan-2-one (435 µL, 4.07 mmol) was added dropwise to a solution of **15** (1g, 3.68 mmol) in CH$_3$COOH (15 mL). The reaction mixture was heated at reflux for 17 h. The reaction was cooled to ambient temperature, CH$_3$COOH was partially removed in vacuum, the residue was dissolved in EtOAc or Et$_2$O (80 mL) and washed for several times with solutions of NaHCO$_3$ 20% in H$_2$O(80 mL each) or KOH 40% H$_2$O (80 mL each), the organic layers were dried over Na$_2$SO$_4$ and concentrated in vacuum to get **11** (88%, 1.140g) as a dark red oil. ^{1}H NMR (400 MHz, CDCl$_3$): δ (ppm) 1.30 (s, 6H), 2.29 (s, 3H), 7.30 (d, 8 Hz, 1H), 7.60 (s, 1H), 7. 64 (d, 9 Hz, 1H).
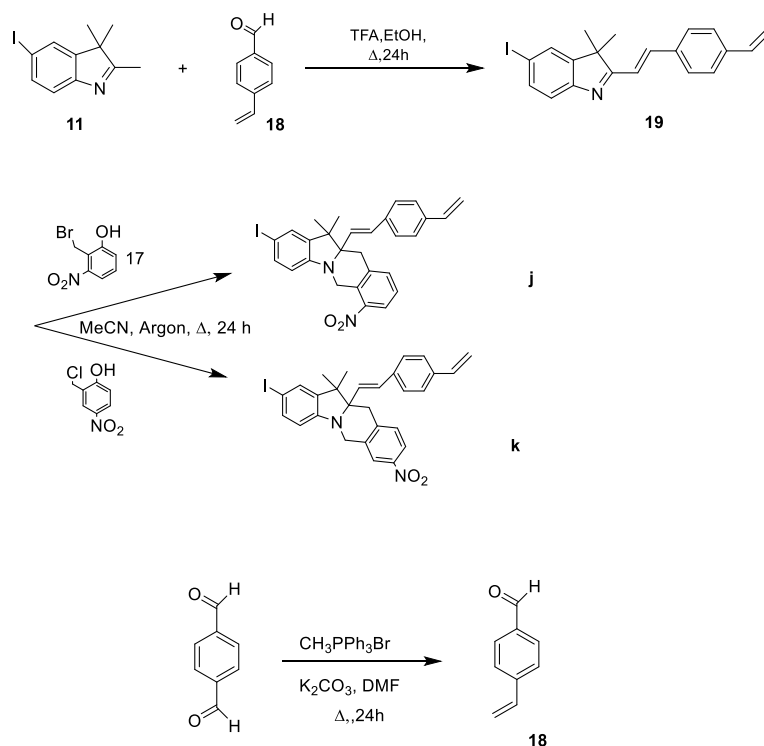
Figure 5.18 Synthetic scheme for compounds **j** and **k.**

Synthesis of **j** and **k.**

j. Compound **19** (150 mg, 0.38 mmol) was dissolved in degassed MeCN (15 mL) and **17** (218mg, 0.94 mmol) was added to the mixture that was stirred at reflux in Argon atmosphere for 24h. The solvent was removed in vacuum, the product was dissolved in CH_2Cl_2 (60 mL) and washed with $NaHCO_3$ 5% solution (50 mL) and H_2O (2x50 mL). The obtained residue was purified by column chromatography (Hex: EtOAc 9:1) to get **j** (19%, 40 mg) as a yellow solid. ESIMS: m/z = 551.0824 [M^+] (m/z calcd. for $C_{28}H_{25}IN_2O_2$ = 551.1257); ^1H NMR (400 MHz, $CDCl_3$): δ (ppm) 1.24 (s, 3H), 1.54 (s, 3H), 4.79 (d, 16 Hz, 1H), 5.01 (d, 8 Hz 1H), 5.30 (d, 7Hz, 1H), 5.77 (d, 8 Hz,1H), 6.32 (d, 9 Hz,1H), 6.40-6.42 (m, 1H), 6.68-6.77 (m, 1H), 6.80 (d, 8, Hz, 1H), 7.11-7.16 (m, 1H), 7.23-7.29 (m, 1H), 7.38-7.44 (m, 6H), 7.69 (s, 1H).

k. Compound **19** (140mg, 0.35mmol) was dissolved in degassed MeCN (15 mL) and 2-chlorophenyl-4-nitro-phenolo (263 mg, 1.40mmol) was added to the mixture that was stirred at reflux in Argon atmosphere for 24h. The solvent was removed in vacuum, the product

dissolved in CH_2Cl_2 (60 mL) and washed with $NaHCO_3$ 5% solution (50 mL) and H_2O (2x50 mL). The obtained residue was purified with column chromatography (Hex: EtOAc 9:1) to get **k** (16%, 30 mg) as an orange solid. ESIMS: m/z = 551.0805 [M$^+$] (m/z calcd. for $C_{28}H_{25}IN_2O_2$ = 551.1257); ^{1}H NMR (400 MHz, CDCl$_3$): δ (ppm) 1.30 (s, 3H), 1. 52 (s, 3H), 4.52 (bs, 2H), 5.30 (d, 16 Hz,1H), 5.76 (d, 8 Hz,1H), 6.34 (d, 9 Hz, 1H), 6.44 (d, 7 Hz, 1H), 6.75-6.88 (m, H), 6.80 (d, 7 Hz, 1H), 6.90 (d, 9 Hz, 1H), 7.19-7.21 (m , 2H), 7.27-7.31 (m, 1H), 7.39-7.42 (m, 3H), 8.01-8.808 (m, 2H).

19. **11** (648mg, 2.27 mmol) and **18** (300mg, 2.27mmol) were dissolved in EtOH (25 mL), trifluoroacetic acid (TFA 1.130 mL, 14.76 mmol) was added dropwise to the mixture, the reaction was refluxed for 24h. The solvent was removed in vacuum, the crude dissolved in in CH_2Cl_2 (60 mL) and washed with $NaHCO_3$ 5% solution (50 mL) and H_2O (2x50 mL). The obtained residue was purified by column chromatography (Hex:EtOAc 9:1) to give **19** (22%, 300mg) as an orange semisolid. ESIMS: m/z = 400.0573 [M$^+$] (m/z calcd. for $C_{20}H_{18}IN$ = 400.0588); ^{1}H NMR (400 MHz, CDCl$_3$): δ (ppm) 1. 46 (s, 6H), 5.32 (d, 16 Hz, 1H), 5.82 (d, 9 HZ, 1H), 6.69-6.82 (m, 1H), 7.03 (d, 8 Hz, 1H), 7.39 (d, 7 Hz, 1H), 7.45 (d, 9 Hz, 2H), 7.58 (d, 8 Hz, 2H), 7.65-7.68 (m , 2H), 7.74 (d, 7 Hz, 1H).

18. Terephtaldehyde (2g, 14.91 mmol) was dissolved in DMF (200 mL) in Argon atmosphere, $CH_3PPh_3^+Br^-$ (4.439g, 12.43mmol) and K_2CO_3 (8.587g, 62.13mmol) were added to the mixture the reaction was stirred at reflux for 3h. The obtained suspension was poured into H_2O (200 mL) and extracted with Et_2O (3x 200 mL), the crude product was purified by column chromatography (Hex: EtOAc 9:1) to get the desired product **18** (66%, 1.300g) as a colorless oil. This compound easily self-polymerize, for this reason it must be immediately used for the following reaction's step ^{1}H NMR (400 MHz, CDCl$_3$): 5.45 (d, 8 Hz, 1H), 5.92 (d, 7 Hz, 1H), 6.74-6.79 (m, 1H), 7.55 (d, 9 Hz, 2H), 7,84 (d, 8 Hz, 2H), 9.99 (s, 1H).

Synthesis of the appropriate indole derivative (**21**) to synthesize monomers **l**, **m**, **n**, **o** (figure 5.19).
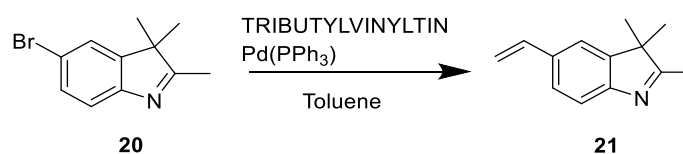
Figure 5.19 Synthetic scheme for compound **21**.

Compound **20** was synthesized following the same procedure used to synthesize **11**, using 4-bromo aniline instead of 4-iodo aniline as starting material. Compound **21** was synthesized adapting.[165]

21. 20 (1g, 4.2 mmol) was dissolved in Toluene (20 mL), Tributylviniyltin (1.350 mL, 4.6mmol) and Pd(PPh$_3$)$_4$ (146 mg, 0.01 mmol) were added with the addition of few crystals of 2,6-diterbutyl-4methyl phenolo. The reaction was refluxed for 4h and cooled to ambient temperature. Pyridine (2 mL) and pyridine fluoride solution (4 mL) were added, the mixture was stirred at R.T. for 12h. The reaction mixture was poured into Et$_2$O and the organic phases were washed with H$_2$O, HCl 10% solution and NaHCO$_3$ 5% solution (20 mL each). Organic phases were dried over Na$_2$SO$_4$, and the solvent was removed in vacuum. The obtained residue was purified with column chromatography (Hex: EtOAc 6:4) to get compound **21** (20%, 160 mg) as a red-brown oil. ESIMS: m/z = 186.1291 [M + H] $^+$ (m/z calcd. for C$_{13}$H$_{15}$N = 186.1452); ^{1}H NMR (400 MHz, CDCl$_3$): δ (ppm) 1.30 (s, 1H), 1.32 (s, 3H), 2.30 (s, 3H), 5.23 (d, 8 Hz, 1H), 5.75 (d, 9 Hz, 1H), 6.78-6.84 (m, 1H), 7.39 (s, 1H), 7.49 (d, 7 Hz, 1H), 7.35 (d, 8 Hz, 1H).

The same reaction was performed also using Pd(II)Acetate and PPh$_3$ catalysts obtaining the same results in terms of yields and reaction's performance.

5.4.4.2 Model compounds for Oxazine Monomers

These additional syntheses were performed to have model compounds of the Oxazines' monomers without the photo-activatable/modulable portion of the molecule in order to prepare also a model polymer as control material for the study of the photo-conjugation phenomena.

The synthesis of model compounds for compounds **i** and **k** (PF$_6^-$ salts) is here reported, while model compounds for **h** and **j** compounds are synthesis' intermediates (i.e. compounds **16** and **19**)

These syntheses were designed adapting and modifying,[60] the I$^-$ salts were always substituted at the end of the synthesis with PF$_6^-$ counterions not to have interferences with a a halogen anion, as I$^-$, during the spectroscopic measurements. Figures 5.20 and 5.21
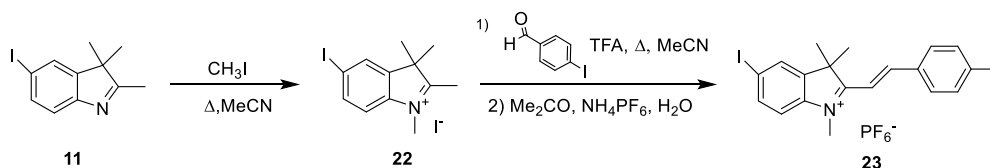
Figure 5.20 Synthetic scheme for compound **23**.

23. **22** (200 mg, 0.47 mmol) was dissolved in MeCN,(50 mL), 4-Iodobenzaldehyde (99mg, 0.43 mmol) was added followed by trifluoroacetic acid (TFA, 50 µL) the mixture was stirred at reflux for 24h, the reaction was monitored through MS spectrometry: the desired product was forming but **22** was still present, another amount of trifluoroacetic acid (TFA, 200 µL) was added, the reaction was stirred at reflux up to 12 days and checked by MS analysis, **22** seemed to remain in the reaction mixture until the stop of the reaction. After 12 days, the solvent was removed in vacuum, the crude product was purified through column chromatography (DCM:Hex 7:3 to DCM:MeOH 9:1) to give the I$^-$ salt of **23** as a yellow solid. The product was dissolved in Acetone (5 mL) and a concentrated solution of NH$_4$PF$_6$ in H$_2$O (5 mL) was added, the volume was reduced to its half and the obtained precipitate was filtered and washed with H$_2$O (10 mL) to give **23** (29%, 69 mg) as a yellow solid. ESIMS: m/z = 513.9502 [M-PF$_6$] $^+$ (m/z calcd. for C$_{19}$H$_{18}$I$_2$N$^+$ = 513.9826); ^{1}H NMR (400 MHz, CD$_3$CN): δ (ppm) 1.76 (s, 6H), 3.98 (s, 3H), 7.12 (d, 8 Hz, 1H), 7.42-7.50 (m, 2H), 7.76 (bs, 2H), 8.01 (bs, 2H), 8.16-8.25 (m, 2H)

22. **11** (1 g, 3.5 mmol) was dissolved in MeCN (10 mL), CH$_3$I (262 µL, 4.20 mmol) was added, the mixture was stirred at reflux for 3h. After cooling down to R.T. the obtained precipitate was filtered and washed with Et$_2$O, to get **22** as a brown solid (60%, 900 mg). ^{1}H NMR (400 MHz, DMSO-d6): δ (ppm) 1.50 (s, 6H), 2.73 (s, 3H), 3.93 (s, 3H), 7.71 (d, 7 Hz, 1H), 8.01 (d, 8 Hz,1H), 8.30 (s, 1H).
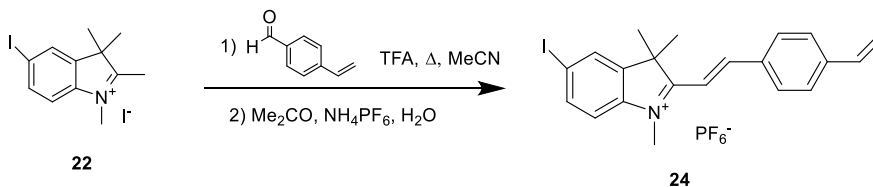
Figure 5.21 Synthetic scheme for compound **24**.

24. Compound **22** (200mg, 0.47 mmol) was dissolved in MeCN (50 mL),**18** (62mg,0,47 mmol) and was added followed by trifluoroacetic acid (TFA, 50 µL) the mixture was stirred at reflux for 24h, the reaction was monitored through MS spectrometry: the desired product was forming but **22** was still present, another amount of trifluoroacetic acid (TFA, 200 µL) was added, the reaction was stirred at reflux up to 6 days and checked by MS analysis, **22** seemed to remain in the reaction mixture until the stop of the reaction. After 6 days, the solvent was removed in vacuum and the product was purified through column chromatography (DCM:MeOH 99:1 to 9:1) to give the I$^-$ salt of **24** as a yellow solid. The product was dissolved in Acetone (5 mL) and a concentrated solution of NH$_4$PF$_6$ in H$_2$O (5 mL) was added, the volume was reduced to its half and the obtained precipitate was filtered and washed with H$_2$O (10 mL) to give **24** (57%, 150 mg) as a yellow solid. ESIMS: m/z = 414.0722 [M-PF$_6$]$^+$ (m/z calcd. for C$_{21}$H$_{21}$IN$^+$ = 414.3198); ^{1}H NMR (400 MHz, CD$_3$CN): δ (ppm) 1,78 (s, 6H), 4.03 (s, 3H), 5.51 (d, 16 Hz, 1H), 6.06 (d, 8 Hz, 1H), 6.85-6.91 (m, 1 H), 7.41 (d, 7 Hz,1H), 7.48 (d, 9 Hz, 1H), 7.67 (d, 8 Hz, 1H), 8.00-8.03 (m, 3H), 8.16 (s, 1H), 8.28 (d, 8 Hz, 1H).

5.4.4.3 Complementary Monomers

These monomers were synthesized as follow, referring to already reported procedures[166-168] with modifications. (Figures 5.22, 5.23 and 5.24).
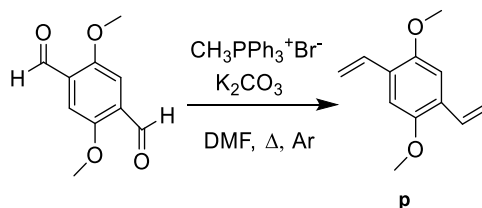
Figure 5.22 Synthetic scheme for compound **p**.

p. 2,5-dimethoxyterephtaldehyde (350 mg, 1.80 mmol) was dissolved in DMF (40 mL) in Argon atmosphere, $CH_3PPh_3^+Br^-$ (1.545g, 4.33 mmol) and K_2CO_3 (2.491 mg, 18.03 mmol) were added to the mixture that was stirred at reflux for 2h. The obtained suspension was poured into H_2O (50 mL) and extracted with Et_2O (3x 80 mL), the crude product was then purified by column chromatography (Hex: EtOAc 95:5) to get the desired **p** (67%, 230 mg) as a white/pale yellow solid. ^1H NMR (400 MHz, $CDCl_3$): δ (ppm) 3.85 (s, 1H), 5.28 (d, 8 Hz, 2H), 5.76 (d, 9 Hz, 2H), 7.01 (s, 2H), 7.05-7.10 (m, 2H).
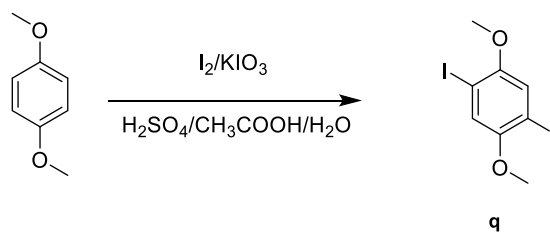
Figure 5.23 Synthetic scheme for compound **q**.

q. 1,4-dimethoxybenzene (2G, 14.47 mmol), iodine I_2 (4,40g, 17.37 mmol) and potassium iodate KIO_3 (3.717g, 17.37 mmol) in an acid solution $CH_3COOH:H_2O:H_2SO_4$ (90:7:3_12.6 mL, 0.98 mL, 0.42 mL). The mixture was stirred at reflux for 24h, it was poured into H_2O (50 mL) and the obtained precipitate was filtered and re-crystallized by THF/H_2O to give **q** (61%, 3.46g) as a light-yellow solid. ^1H NMR (400 MHz, $CDCl_3$): δ (ppm) 3.85 (s, 1H), 7.19 (s, 2H).

Alternative work up: the cooled reaction was poured into H_2O (50 mL), then addition of a saturated solution of Na_2SO_3 (30 mL), the precipitate was filtered and re-crystallized from $CHCl_3$/EtOH 1:1 to give the desired product.
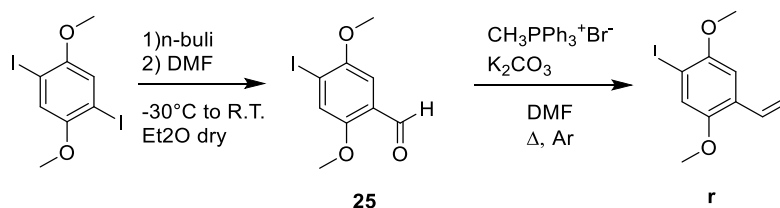
Figure 5.24 Synthetic scheme for compound **r**.

r. **25** (200 mg, 0.69 mmol) was dissolved in DMF (20 mL) in Argon atmosphere, $CH_3PPh_3^+Br^-$ (294 mg, 0.82 mmol) and K_2CO_3 (474 mg, 3.424 mmol) were added, the reaction was stirred at reflux for 4h. The obtained suspension was poured into H_2O (30 mL) and extracted with Et_2O (3x 60 mL). Organic phases were dried over Na_2SO_4, and removed in vacuum. The crude oily product obtained was purified by column chromatography (Hex: EtOAc 95:5) to give **r** (30%, 60 mg) as a transparent oil which spontaneously crystallize in a white solid. ^1H NMR (400 MHz, $CDCl_3$): δ (ppm) 3.80 (s, 3H), 3.88 (s, 3H), 5.31 (d, 8 Hz, 1H), 5.78 (d, 9 Hz, 1H), 6.94 (s, 1H),6.95-7.03 (m, 1H), 7.29 (s, 1H).

25.q (1g, 2.56 mmol) was suspended in dry Et_2O (30 mL), the reaction was cooled to -30° C, n-buli (2.5 M in Hexane, 1.030 mL) was added slowly to the mixture, the reaction was stirred at -30°C for 1h, dry DMF (1 mL, 12.82 mmol) were added and the mixture was allowed to reach RT and stirred for 4h. The product was poured into H_2O (50 mL) and aqueous phases were extracted with fresh Et_2O (3x 60 mL), organic phases were dried over Na_2SO_4, and the solvent was removed in vacuum to get a fluorescent yellow residue that was purified by column chromatography (Hex: EtOAc 9:1/ DCM:Hex (8:2 to 1:1) to give **25** (27%, 200 mg) as a white solid. ^1H NMR (400 MHz, $CDCl_3$): δ (ppm) 3.87 (s, 3H), 3,92 (s, 3 H), 7.23 (s, 1H), 7.46 (s, 1 H), 10.42 (s, 1 H).

5.4.5 Synthesis of the Polymer_preliminary synthesis

Two polymerization reactions were tested to prove the formation of the conjugated polymers. (figure 5.25)
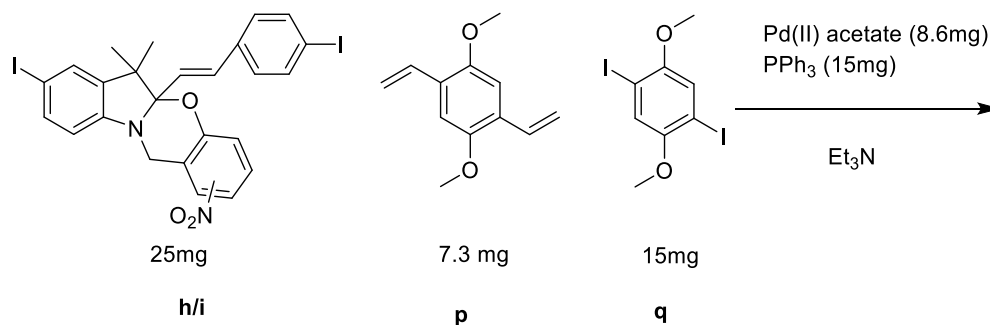
Figure 5.25 Synthetic scheme for polymers' assembly.

The reaction was set up in 10 mL Et₃N_ The ratio between the monomers used was 1:1:1 in equivalents corresponding to 0.04 mmol i.e. 25 mg of compound **h/i**, 7.3 mg of compound **p** and 15 mg of compound **q**. The catalyst and the solvents were used in excess (respectively, 1 and 2 eq of Pd(OAc)₂ and PPh₃), with the goal to facilitate polymerization's reaction_ The reaction was stirred at 140°C in a high pressure flask for 48 h and then at ambient temperature for 24 h. A precipitate was formed. The precipitate and the solution were collected separately, the solvent was removed in vacuum while de precipitate was dissolved in CHCl₃ and filtered through celite to remove the residue of catalysts. The filtered material was recovered with fresh CHCl₃ and precipitated with MeOH (3x CHCl₃ volume) to wash the expected polymers. The washing phases were checked by MS spectrometry and the process was repeated 3 times, each of them lasted 24h, in MS analysis no traces for the single monomers in MW were highlighted. The MS measurements were performed on the washed polymer just to check that this was not just one of the monomers with some dirtiness, but also in this case no MS value referred to the monomers were highlighted. The precipitated was dried and characterized by NMR.

5.4.5.1 Preliminary Considerations

NMR analyses on the two synthesized polymers evidenced that the oxazines entity are frequent in the polymer's structure, as we can observe from figure 5.26, where the enlarged NMR spectrum in the region between 2 and 5 ppm for the polymer with **h** as monomer.

Indeed, analyzing the peaks belonging to the 2 aliphatic protons of the oxazines portion (4.00-5.00 ppm) of the polymer and the methoxy region for the monomers (3.00-4.00 ppm) the integration shows an abundance of oxazines monomers compared to the not switchable portions. Considering the goal of extending the conjugation for the photo-switchable polymer, the next polymerization reactions, after this first (1:1:1) test should be performed using different ratios with lower ratio of photo-activatable monomers and higher ratios of no photo-activatable monomers. GPC (gel permeation chromatography) measurements will be planned in order to define the properties in terms of molecular weight and polymeric features of the final photo-switchable polymers.
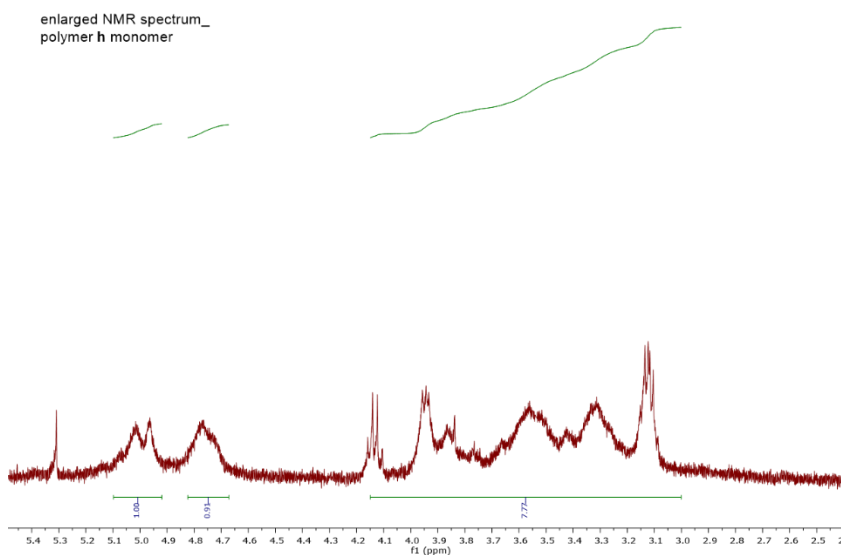
Figure 5.26 Partial NMR spectrum of the polymer containing monomer **h** in the structure.

5.4.6 Results

The molecules synthesized represent many of the necessary building blocks for the development and the preliminary polymerization experiments, the Heck coupling conditions seemed to work properly for the preparation of the desired polymers. The ratios between the SM (1:1:1) used for the polymerization's reactions represent a good starting point to check the reactivity of the molecules and the effectiveness of the polymerization's reaction conditions. By NMR analysis on the polymerized material the obtained polymer seemed to contain a significant amount of the Oxazine monomer. The goal of the project to extend the polymer's conjugation seem to drive the next synthesis to the use of different ratios of the

building blocks, i.e. increasing the amount of the complementary monomers and decreasing the equivalents of complementary monomers

5.4.7 Future Perspectives

Proceed with the remaining synthesis to have all the necessary monomers to start the whole study for the conjugated system in terms of chemical and physical parameters. After the whole study of the conjugated polymer the complementary monomers could be synthesized with an appropriate different -R portion, to prepare polymers with good water solubility properties. The -R portion, for example can be modified as an ethylene glycol side chain protected in its -OH termini with a *t*-butyl ester portion, useful to assembly the conjugated polymer, the protection can be then easily removed after the polymerization reaction to have a polymer with ensured aqueous solubility.

The ^{1}H NMR spectra for compounds **2,3,4, a, b, c, d, e, 6,7,8.9, 12, 13, 14, f, g, 11, 16, 18, 19, 21, 22, 23, 24, 25, h, i, j, k, p, q, r** and for the 2 assembled polymers and the ^{13}C NMR spectra for compounds **a** and **b** are reported in the appendix chapter.

References

1.   Hirshberg, Y.; Fischer, E. *J. Chem. Phys.* **1955**, *23*, 1723.

2.   Nakatani, K.; Piard, J.; Yu, P.; Métivier, R. Introduction: organic photochromic molecules. *Photochromic Materials: Preparation, Properties and Applications*, **2016**.

3.   Dürr, H.; Bouas-Laurent, H.; *Photochromism: molecules and systems*. Elsevier. **2003.**

4.   Dorion, G. H.; Wiebe, A. F. *Photochromism*, Focal Press, New York, **1970**.

5.   G. H. Brown, ed., *Photochromism*, Wileyinterscience, New York, **1971**.

6.   Irie, M.; Yokoyama Y.; Seki T. *New Frontiers in Photochromism*, Springer Japan, **2013**.

7.   Natali, M.; Giordani, S. *Chem. Soc. Rev.* **2012**, *41*, 4010-4029.

8.   Garcia, A. A.; Cherian, S.; Park, J.; Gust, D.; Jahnke, F.; Rosario, R. J. Phys.Chem. A. **2000**, *104*, 6103-6107.

9.   Crano, J.C.; Guglielmetti, R.J. *Organic Photochromic and Thermochromic Compounds Vol.2: Physicochemical Studies, Biological Applications, and Thermochromism*. Springer US, **2002**.

10.   Aramaki, S.; G. H. Atkinson. *J. Am. Chem. Soc.* **1992**, *114(2)*, 438-444.

11.   Natali, M.; Giordani, S. *Org Biomol Chem.* **2012**, *10(6)*, 1162-1171.

12.   Fedorova, O. A.; Gromov S.P.; Pershina, Y.V.; Sergeev S.S, Strokach, Y.P.; Barachevsky, V.A.; Alfimov, M.V.; Pèpe, G.; Samat, A.; Guglielmetti, R. *J. Chem. Soc. Perkin Trans 2.* **2000**, *3,* 563-570.

13.   Shinkai, S.; Shigematsu, K.; Kusano Y.;Manabe, O. *J. Chem. Soc. Perkin Trans.1* **1981**, 3279-3283.

14.   Natali, M.; Aakeröy, C.; Desper, J.; Giordani, S. *Dalton Trans.* **2010**, *39*(35), 8269-8277.

15.   Raymo, F.M.; Giordani, S. *J. Am. Chem. Soc.* **2001**, *123*(19), 4651-4652.

16.   Tomasulo, M.; Sortino S.; F.M. Raymo. *J. Org. Chem.,* **2008**, 73, 118–126.

17.   Raymo, F. M.; Giordani, S.. *J. Am. Chem. Soc.* **2002***, 124*(9), 2004-2007.

18.   Klajn, R. *Chem. Soc. Rev.* **2014**, *43(1)*, 148-184.

19.   Klajn, R. *Pure Appl. Chem.* **2010**, *82(12)*, 2247-2279.

20.   H. Zollinger, Color Chemistry: Syntheses, Properties and Applications of Organic Dyes and Pigments, VCH, NY, **1987**.

21.   Amdursky, N.; Kundu, P.K.; Ahrens, J. Huppert, D.; Klajn, R. *ChemPlusChem*, **2016** *81(1)*, 44-48

22.   Bain, C. D.; Troughton, E. B.; Tao, Y. T.; Evall, J.; Whitesides, G.M.; Nuzzo, R. G. *J. Am. Chem. Soc.* **1989**, 111(1), 321-335.

23.   Sakamoto, H.; Takagaki, H.; Nakamura, M.; Kimura, K. *Anal. Chem.* **2005**, *77*, 1999-2006.

24.   Tomasulo, M.; Sortino, S.; Raymo, F. M. *Org. Lett.* **2005**, 7(6), 1109-1112.

25.   Raymo, F.M.; Giordani, S. *Org. Lett.* **2001**, *3(12)*, 1833-1836.

26.   Zhu, M. Q.; Zhu, L.; Han, J. J.,;Wu, W.; Hurst, J. K.; Li, A. D. *J. Am. Chem. Soc.* **2006**, *128(13),* 4303-4309.

27.   Kundu, P. K.; Samanta, D.; Leizrowice, R.; Margulis, B.; Zhao, H.; Börner, M.; Udayabhaskararao,T.; Manna, D.;Klajn, R. *Nat. Chem.* **2015**, 7(8), 646.

28.   Bartels, E.;Wassermann, N. H.;Erlanger, B. F. *Proc. Nat. Acad. Sci. U.S.A.* **1971**, *68*, 1820-1823.

29.   Kocer, A.; Valko, M.; Meijberg, W.; Feringa, B. L. *Science*, **2005**, *309*, 755-758.

30.   Swaminathan S.; Garcia-Amoros, J.; Thapaliya, E.R.; Nonell, S.; Captain B.; Raymo, F.M. *ChemPhysChem,* **2016**, *17*, 1852-1859.

31.   Deniz, E.; Tomasulo, M-; Cusido, J.; Yildiz, I.; Petriella, M.; Bossi, M.L;Sortino, S.;.Raymo, F.M. *J. Phys. Chem. C*, **2012**, *116*, 6058–6068.

32.   Lukyanov, B. S.;Lukyanova, M. B. *Chem. Heterocycl. Compd.* **2005**, *41*, 281-311.

33.   Vandewyer, P. H.; Hoefnagels, J.; Smets, G. *Tetrahedron* **1969**, *25*, 3251-3266.

34.   Ernsting, N.P.; Arthen-Engeland, T. *J. Phys. Chem.* **1991**, *95*, 5502-5509.

35.   Barachevsky, V.A. *J. Fluoresc.* **2000**, *10*, 185-191.

36.   Görner, H. Phys. *Phys. Chem. Chem. Phys*. **2001**, *3*, 416-423.

37.   Minkin, V.I. *Chem. Rev*. **2004**, *104*, 2751-2776.

38.   Zakharova, M. I.; Pimienta, V.; Minkin, V. I.; Metelitsa, A. V.; Micheau, *J. C. Russ. Chem. Bull*. **2009**, 58, 1329-1337.

39.   Chibisov, A. K.; Görner, H. *Chem. Phys*. **1998**, *237*, 425-442.

40.   Sakata, T..; Jackson, D. K.; Mao, S.; Marriott, G. *J. Org. Chem*. **2008**, *73*, 227-233.

41.   Winkler, J. D.; Bowen, C. M.; Michelet, V. *J. Am. Chem. Soc*. **1998**, *120*, 3237-3242.

42.   Wizinger, R.; Wenning, H. *Helv. Chim. Acta*. **1940**, *23*, 247-271.

43.   Zollinger, H. *Color Chemistry: Syntheses, Properties, and Applications of Organic Dyes and Pigments*. Verlag Helvetica Chimica Acta Zurich. **2003**.

44.   Hartley, G. S. *Nature* **1937**, *140*, 281-281.

45.   Krollpfeiffer, F.; Potz, H.; Rosenberg, *A. Eur. J. Inorg. Chem*. **1938**, 71, 596-603.

46.   Tamai, N.;Miyasaka, H. *Chem. Rev*. **2000**, *100*, 1875-1890.

47.   Garcìa-Amoròs, J.; Velasco, D. Beilstein *J. Org. Chem.* **2012**, *8*, 1003-1017.

48.   Griffiths, J. *Chem. Soc. Rev*. **1972**, *1*,48-493.

49.   Merino, E. *Chem. Soc. Rev*. **2011**, *40*, 3835-3853.

50.   Szele, I.; Zollinger, H. *Top. Curr. Chem*., **1983**, *112*, 1-66.

51.   Haghbeen, K.; Tan, E.W. *J. Org. Chem*. **1998**, *63*, 4503-4505.

52.   Ueno, K. Akiyoshi, S. *J. Am. Chem. Soc*., **1954**, *76*, 3670-3672.

53.   Bacon, E.S.; Richardson, D.H. *J. Chem. Soc.,* **1932**, 884-888.

54.   Tomasulo, M.; Sortino, S.; White A.J.P.; F. M. Raymo, *J. Org. Chem*., **2005**, *70*, 8180-8189.

55.   Tomasulo, M.; Sortino, S.; Raymo, F.M. *Adv. Mater*., **2008**, *20*, 832-835.

56.   Beaujean, P.; Bondu, F.; Plaquet, A.; Garcia-Amorós, J.; Cusido, J.; Raymo, F.M.; Castet, F.; Rodriguez, V.; Champagne, B. *J. Am. Chem. Soc*. **2016**, *138(15)*, 5052-5062.

57.   H. Goerner, *Phys. Chem. Chem. Phys*. **2001**, *3*, 416-423.

58. Cusido, J.; Battal, M.; Deniz, E.; Yildiz, I.; Sortino, S.; Raymo, F.M. *Chem. Eur. J.,* **2012**, *18*, 10399-10407.

59. Zhang, Y.; Tang, S.; Thapaliya, E.R.; Sansalone, L., Raymo, F.M. *Chem Comm*. **2018**, *54(64)*, 8799-8809.

60. Zhang, Y.; Swaminathan, S.; Tang, S.; Garcia-Amoros, J.; Boulina, M.; Captain, B.; Baker, J.D.; Raymo, F.M. *J. Am. Chem. Soc*. **2015**, *137*, 4709-4719.

61. Mazza, M.M.A.; Cardano, F.; Cusido, J.; Beker, J.D.; Giordani, S.; Raymo, F.M. *Chem. Commun.* **2019**, *55*, 1112-1115.

62. Klán, P; Solomek, T.; Bochet, C.G; Blanc, A.; Givens, R.; Rubina, M.; Popik, V.; Kostikov, A.; Wirz, J. *Chem. Rev*. **2012**, *113(1)*, 119-191.

63. Mazza, M.M.A.; Raymo, F.M. *J. Mater. Chem. C* **2019**, *7*, 5333-5342.

64. Sansalone, L.; Bratsch-Prince, J.; Tang, S.; Captain, B.; Mott, D.D.; Raymo, F.M. *PNAS* **2019**,*116(42),* 21176-21184.

65. Jeevanandam, J.; Barhoum, A.; Chan, Y.S.; Dufresne, A.; Danquah, M.K. *Beilstein J. Nanotech*. **2018**, *9(1)*,1050-1074.

66. Kemp, K. C.; Georgakilas, V.; Otyepka, M.; Bourlinos, A.B.; Chandra, V.; Namdong Kim, K.; Kemp, C.; Hobza, P.; Zboril, R.; Kwang S.K. *Chem. Rev*. **2012**, *112*, 6156-6214.

67. Goenka, S.; Sant, V.; Sant, S. *J. Control. Release.* **2012**, *173*, 75-88.

68. Guo, X.; Huang, L.; O'Brien, S.; Kim, P.; Nuckolls, C. *J. Am. Chem. Soc*. **2005**, *127*, 15045-15047.

69. Lamari, D.P.; Malbrunot, F.; Tartaglia, G.P. *Int. J Hydrogen Ener*. **2002**, *27(2)*, 193-202.

70. Saito, N.; Usui, Y.; Aoki, K.; Narita, N.; Shimizu, M.; Hara, K.; Ogiwara, N.: Nakamura, K.; Ishigaki, N.; Kato, H. Taruta, S. *Chem. Soc. Rev*. **2009**, *38*, 1897-1903.

71. Goenka, S.; Sant, V.; Sant, S. *J. Control. Release*. **2014**, *173*, 75-88.

72. Xiaoyan, Z.; Hou,,L.; Samorì, P. *Nature Comm*. **2016**, *7*, 11118.

73. Simmons, J. M.; In, I.; Campbell, V.E.; Mark, T.G.; Léonard, F.; Gopalan, P.; Eriksson, M.A. *Phys. Rev. Lett*. **2007,** *98(8)*, 086802.

74.   Zhou, X.; Zifer, T.; Wong, B.M., Krafcik, K.L.; Léonard, F.; Vance, A.L. *Nano Lett*. **2009**, *9*, 1028-1033.

75.   Kucharski, T.J.; Ferralis, N.; Kolpak, A.M.; Zheng, J.O.; Nocera, D.G.; Grossman, J.C. *Nat. Chem*. **2014**, *6*, 441-447.

76.   Li, Y.; Duan, Y.; Zheng, J.; Li, J.; Zhao, W.; Yang, S.; Yang, R. *Anal. Chem*. **2013**, *85(23)*, 11456-11463.

77.   Wang ,C.; Yang, S.; Yi, M.; Liu, C.; Wang, Y. Li, J.; Li, Y.; Yang, R. *ACS Appl Mat. Interf.* **2014**, *6(12)*, 9768-9775.

78.   Del Canto, E.; Flavin, K.; Natali, M.; Perova, T.; Giordani, S. *Carbon, N.Y.* **2010**, 48, 2815-2824.

79.   Del Canto, E.; Natali, M.; Movia, D.; Giordani, S. *Phys. Chem. Chem. Phys.* **2012**, *14*, 6034-6043.

80.   Al Nahain, A.; Lee, J. E.; Jeong, J. H.;Park, S.Y. *Biomacromol*. **2013**, *14*, 4082-4090-

81.   Sharker, S.M.; Jeong, C.J.; Kim, S.M.; Lee, J.E.; Jeong, J.H.; In, I:; Lee, H.; Park, S.Y. *Chem. Asian J*. **2014**, *9(10),*2921-2927.

82.   Flavin, K.; Kopf, I. Murtagh, J. Grossi, M. O'Shea, D. F. Giordani, S. *Supramol. Chem.* **2012***, 24*, 23-28.

83.   Ciesielski, A.; Samorì, P. *Adv. Mater*. **2016**, *28(29)* 6030-6051.

84.   Iijima, S. *Nature*. **1991**, *354(6348),* 56.

85.   Georgakilas, V.; Kordatos, K.; Prato, M.; Guldi, D.M.; Holzinger, M.; Hirsch, A. *J. Am. Chem. Soc.* **2002**, *124(5),* 760-761.

86.   Jorio, A.; Dresselhaus, G.; Dresselhaus, M.S. *Carbon nanotubes: advanced topics in the synthesis, structure, properties and applications.* Springer Science & Business Media **2007**.

87.   Zheng, X.T.; Ananthanarayanan, A.; Luo, K.Q.; Chen, P. *Small.* **2015**, *11(14),*1620-36.

88.   Baker, S.N.; Baker, G.A. *Angew. Chem. Int. Ed*. **2010,** *49(38),*6726-6744.

89.   Wang, Y.; Hu, A. *J. Mater. Chem. C*. **2014**, *2(34)*, 6921-6939.

90.   Mojica, M.; Alonso, J.A. Méndez, F. *J. Phys. Org. Chem*. **2013**, *26(7),*526-539.

91.   Yadav, B.C.; Kumar, R. *Int. J. Nanotech. Appl*. **2008**, *2(1)*,15-24.

92.   Mochalin, V.N.; Shenderova, O.; Ho, D.; Gogotsi, Y. *Nature Nanotech*. **2012,** *7(1)*,11.

93.   Camisasca, A.; Giordani, S. *Inorg. Chim. Acta*. **2017**,*468*, 67-76.

94.   Bartelmess, J.; Quinn, S.J.; Giordani, S. *Chem. Soc. Rev*. **2015**, *44(14)*, 4672-4698.

95.   Bartelmess, J.; Baldrighi, M.; Nardone, V.; Parisini, E.; Buck, D.; Echegoyen, L.; Giordani, S. *Chem.: Eur. Jour*. **2015**, *21(27)*,9727-9732.

96.   Lettieri, S.; d'Amora, M.; Camisasca, A.; Diaspro, A.; Giordani, S. *Beilstein J. Nanotech*. **2017**, *8(1)*,1878-88.

97.   Novoselov, K.S.; Jiang, D.; Schedin, F.; Booth, T.J.; Khotkevich, V.V.; Morozov, S.V.; Geim, A.K. *PNAS*. **2005,** *102(30)*,10451-10453.

98.   Mao, H.Y.; Laurent, S.; Chen, W.; Akhavan, O.; Imani, M.; Ashkarran A.A.; Mahmoudi, M. *Chem. Rev*. **2013**, *113*, 3407–3424.

99.   Hummers, Jr W.S.; Offeman R.E. *J. Am. Chem. Soc*. **1958**, *80(6)*,1339.

100.   Brodie BC. Phil. *Trans. Royal Soc. London*. **1859**,*149*, 249-259.

101.   Shang, J.; Ma, L.; Li, J.; Ai, W.; Yu, T.; Gurzadyan G.G. *Sci. Rep*. **2012**, *2*,792.

102.   Yan ,J.A.; Chou, MY. *Phys. Rev. B*. **2010**, *82(12)*, 125403.

103.   Saxena, S.; Tyson, T.A.; Shukla, S.; Negusse, E.; Chen, H.; Bai, J. *Appl. Phys Lett*. **2011**, *99(1)*, 013104.

104.   Georgakilas, V.; Otyepka ,M.; Bourlinos, A.B.; Chandra, V.; Kim, N.; Kemp, K.C.; Hobza, P.; Zboril, R.; Kim, KS. *Chem. Rev*. **2012**, *112(11)*,6156-6214.

105.   Dreyer, D.R.; Park, S.; Bielawski, C.W.; Ruoff, RS. *Chem. Soc. Rev*. **2010**, *39(1)*, 228-240.

106.   Chen, D.; Feng, H.; Li, J. *Chem. Rev*. **2012**, *112(11)*, 6027-6053.

107.   Zhu, Y.; Murali, S.; Cai, W.; Li, X. Suk, J.W.; Potts, J.R.; Ruoff, R.S. *Adv. Mater*. **2010**, *22(35),* 3906-3924.

108.   Joshi, R.K.; Carbone, P.; Wang, F.C.; Kravets, V.G.; Su ,Y.; Grigorieva, I.V.; Wu H.A.; Geim, A.K.; Nair R.R. *Science*. **2014**,*343(6172)*,752-754.

109.   Chabot, V.; Higgins, D.; Yu, A.; Xiao, X.; Chen, Z.; Zhang, J. *Energy Environ. Scie.* **2014**,*7(5)*,1564-1596.

110.   Mura, S.; Nicolas, J.; Couvreur, P. *Nat. Mater*. **2013**, *12*, 991-1003.

111.   Velema, W.A.; Szymanski W.; Feringa, B.L. *J. Am. Chem. Soc.***2014**, *136*, 2178-2191.

112.   McConnell, J.; Wood, C.S.; Neelakandan P.P.; Nitschke, J.R. *Chem. Rev*. **2015**, *115*, 7729-7793.

113.   Berkovic, G.; Krongauz, V.; Weiss, V.; *Chem. Rev*. **2000**, 100, 1741-1754.

114.   Natali, M.; Soldi, L.; Giordani S. *Tetrahedron*. **2010**, *66(38)*,7612-7617.

115.   Baldrighi, M.; Locatelli, G.; Desper J.; Aakeröy C.B.; Giordani, S.; *Chem. A Eur. J.* **2016**, *22*, 13976-13984.

116.   Salgueiro, M.J.; Zubillaga, M.;.Lysionek D.Ph.A.; Sarabia, I. *Nutr. Res*. **2000**, *20*, 737-755.

117.   Prasad, A.S.; *Front. Nutr*. **2014**, *1*, 1–10.

118.   Moore, MM.; Chua, W.; Charles K.A.; Clarke S.J.; *Clin. Pharmacol. Ther*. **2010**, *87*, 504-508.

119.   Chohan, Z.H.; Iqbal, M.S.; Iqbal, H.S.; Scozzafava, A.; Supuran, C.T.; *J. Enzyme Inhib. Med. Chem*., **2002**, *17*, 87-91.

120.   Mahdi, J.G.; Mahdi, A.J.; A. J. Mahdi, Bowen, I.D. *Cell Prolif*., **2006**, 39, 147-155.

121.   Singla, A.K.; Wadhwa, H.; *Intern. J. of Pharm*.,**1994**, 108, 173-185.

122.   Lemoine, P.; Viossat, B.; Dung, N.H.; Tomas, A.; Morgant, G.; Greenaway, F.T.; Sorenson, J.R.J.; *J. Inorg. Biochem*., **2004**, 98, 1734-1749.

123.   Lambi, J.N.; Nsehyuka, A.T.; Egbewatt, N.; Cafferata, L.F.R.; Arvia, A.J. *Thermochim. Acta*, **2003**, *398*, 145-151.

124.   Cardano, F.; Del Canto, E.; Giordani, S. *Dalton Trans*.,**2019**, *48*, 15537-15544.

125.   Cardano, F.; Frasconi, M.; Giordani S. *Front. Chem.* **2018**, *6*,102.

126.   Feng, W.; Luo, W.; Feng, Y. *Nanoscale.* **2012**, *4(20)*, 6118-6134.

127.   Lerf, A.; He, H.Y.; Forster, M.; Klinowski, J. *J. Phys. Chem. B.* **1998**,*102(23)*, 4477-4482.

128. Sun,J.; Morales-Lara, F.; Klechikov, A.; Talyzin, A.V.; Baburin, I.A.; Seifert, G.; Cardano, F.; Baldrighi, M.; Frasconi, M.; Giordani, S. *Carbon*. **2017**,*1(120)*, 145-156.

129. Fischer, E.; Stanford, RV. *Introduction to the preparation of organic compounds.* **1922**.

130. Rajaganesh, R.; Gopal, A.; Mohan Das, T.; Ajayaghosh, A. *Org. Lett*. **2012** *14(3)*,748-751.

131. Ma, H.; Li, W.; Wang, J.; Xiao, G.; Gong, Y.; Qi, C.; Feng, Y.; Li, X.; Bao, Z.; Cao, W.; Sun, Q.; Veaceslav, C.; Wang, F.; Lei, Z. *Tetrahedron*, **2012**, *68*, 8358-8366.

132. Bourlinos, A.B.; Gournis, D.; Petridis, D.; Szabo, T.; Szeri, A.; Dekany, I. *Langmuir*. **2003,** *19(15),* 6050-6055.

133. Ferrari,A.C.; Basko D.M. *Nature Nanotech*. **2013**, *8(4)*, 235.

134. E. Margapoti, E.; Strobel, P.; Asmar, M.M.; Seifert, M.; Li, J.; Sachsenhauser, M.; Ceylan, O.; C. Palma, A.; Barth, J.V.; Garrido, J.A.; Cattani-Scholz, A.; Ulloa, S.E.; Finley, J.J *Nano Lett*., **2014**, *14*, 6823-6827.

135. Kim, M.; Safron, N.S.; Huang, C.; Arnold, M.S.; Gopalan, P.; *Nano Lett.,* **2012**, *12*, 182-187.

136. Cerveny, S.; Barroso-Bujans, F.; Alegria, A.; Colmenero, *J. Phys. Chem. C*. **2010**,*114(6),*2604-2612.

137. Bai, T.T.; N. Gu. *Small* **2016**, *12*, 4590-4610.

138. Uchiyama, S.; Gota, C.; Tsuji, T.; Inada, N. *Chem. Commun*. **2017**, *53*, 10976-10992.

139. Quintanilla, M.; Liz-Marzan, L.M. *Nano Today*, **2018**, *19*, 126-145.

140. Zhou, H.Y.; Sharma, M.; Berezin, O.; Zuckerman, D.; Berezin, M.Y.; *ChemPhysChem*, **2016**, *17*, 27-36.

141. del Rosal, B.; Ximendes, E.; Rocha, U.; Jaque, D. *Adv. Opt. Mater*. **2017**, *5*, 1600508

142. McLaurin, E.J.; Bradshaw, L.R.; Gamelin, D.R. *Chem. Mater*. **2013**, 25, 12831292.

143.   Cheng, Y.; Gao, Y.; Lin, H.; Huang, F.; Wang, Y.S. *J. Mater. Chem. C*, **2018**, *6*, 7462-7478.

144.   Tomasulo, M.; Sortino, S.; Raymo, F.M., *J. Photochem. Photobiol., A*, **2008**, *200*, 44-49.

145.   Deniz, E.; Tomasulo, M.; Cusido, J.; Sortino, S.; Raymo, F.M. *Langmuir*, **2011**, *27*, 11773-11783.

146.   Deniz, E.; Sortino, S.; Raymo FM. *J. Phys. Chem. Lett*. **2010**, *1(24)*,3506-3509.

147.   Garcia-Amorós, J.; Swaminathan, S.; Sortino, S.; Raymo, FM. Chem. Eur. *J.* **2014**,*20(33),*10276-10284.

148.   Raymo, F.M; Giordani, S.; White, A.J.P.;Williams, D.J. *J. Org. Chem.* **2003**, *68*, 4158-4169.

149.   Wu, J.; Liu, W.; Zhuang, X.; Wang, F.; Wang, P.; Tao, S.; Zhang, X.; Wu, S.; Lee, S.T. *Org. Lett*. **2007**, *9*, 33-36.

150.   Grigoras, M.; Antonoaia, N.C. *Eur. Polym. J*. **2005**, *41*, 1079-1089.

151.   Han, J.; Burgess, K.; *Chem. Rev*. **2010**, *110*, 2709-2728.

152.   Casey, J.R.; Grinstein, S.; Orlowski, *J. Nat. Rev: Mol. Cell Bio*. **2010**, *11(1)*, 50.

153.   Wike-Hooley, J.L.; Haveman, J.; Reinhold, H.S. *Radiother. Oncol*. **1984** *2(4)*, 343-366.

154.   ThermoFisherScientific Catalogue_ Overview of pH Indicators_*Section 20*

155.   Yue, Y.; Huo, F.; Lee, S.; Yin, C.; Yoon, J. *Analyst*. **2017**,*142(1)*,30-41.

156.   Bassnett, S.T.; Reinisch, L.; Beebe, D.C. *Am. J. Phys-Cell Phys*. **1990**, *258(1),*171-178.

157.   Whitaker, J.E.; Haugland, R.P.; Prendergast, F.G. *Anal. Biochem*. **1991**, *194(2),* 330-344.

158.   Tang, S.; Zhang, Y.; Thapaliya, E.R.; Brown, A.S. Wilson J.N.; Raymo, FM. *ACS Sensors* **2016**, *2(1),*92-101.

159.   Huang, Y.; Wang, Z. *Int. J. Bio. Macromol*. **2018**, *107*,741-747.

160.   Peters, G.M.; Tovar, J.D. J. Am. Chem. Soc. **2019**,*141(7)*,3146-3152.

161.	Cusido, J.; Ragab, S.S.; Thapaliya, E.R.; Swaminathan, S.; Garcia-Amorós, J.; Roberti, M.J.; Araoz, B.; Mazza, M.M.A.; Yamazaki, S.; Scott, A.M.; Raymo, FM. *J. Phys. Chem. C*. **2016,***120(23)*,12860-12870.

162.	Swaminathan, S.; Garcia-Amorós, J.; Fraix, A.; Kandoth, N.; Sortino, S.; Raymo FM. *Chem. Soc. Rev*. **2014**, *43(12),*4167-4178.

163.	Thapaliya, E.R.; Zhang, Y.; Raymo FM. J. Mater. Chem. C. **2017,***5(5)*,1179-1183.

164.	Cui, J.; Kim, S.H. *Chi. Scie. Bull*. **2004**, *49(8)*,797-802.

165.	McKean, D.R.; Parrinello, G.; Renaldo, A.F.; Stille, JK. *J. Org. Chem*. **1987** *52(3)*,422-424.

166.	Scottwell, S. Ø.; Barnsley, J.E.; McAdam, C. J.; Gordon, K.C.;Crowley, J.D. *Chem. Comm*. **2017**, *53(54)*, 7628-7631.

167.	Sontag, B.; Rüth, M.; Spiteller, P.; Arnold, N.; Steglich, W.; Reichert, M.; Bringmann. *Eur. J. Org. Chem*. **2006**, *2006(4)*, 1023-1033.

168.	Kim,M.J.; Yu, Y.J.; Kim, J.H.; Jung, Y.S.; Kay, K.Y.; Ko, S.B.; Lee, C.R.; Jang, I.H.; Kwon, Y.U.; Park, NG. *Dyes and Pigments* **2012**, *95(1)*, 134-141.

Appendix

Chapter 3

- **Kinetic studies**
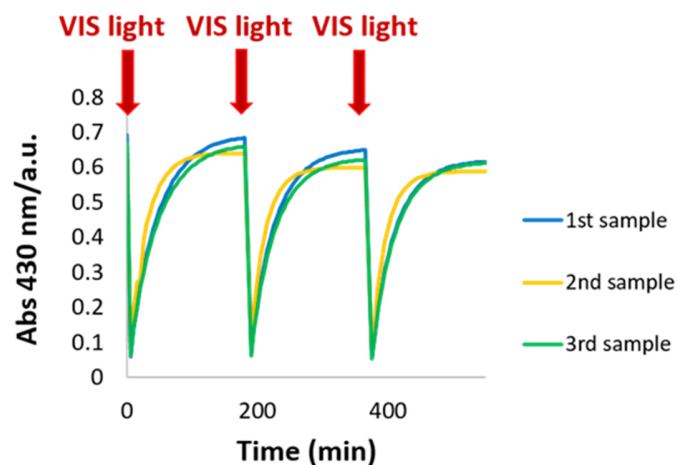
Figure S1. Three different examples of the sample containing SP-ASA-Zn^{++} (1:1:1.5) were tested to prove the repetitiveness of the formation of the new system over 3 consecutive cycles.
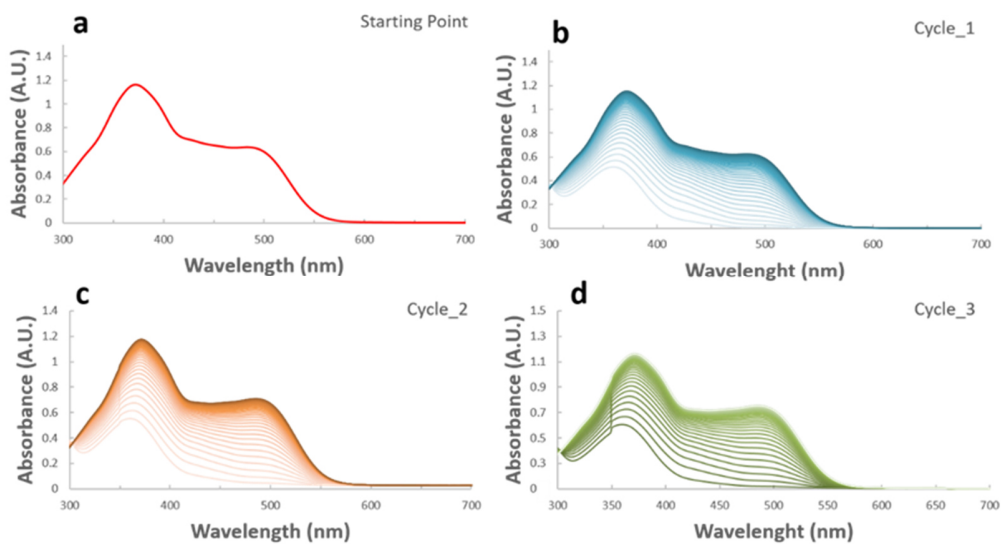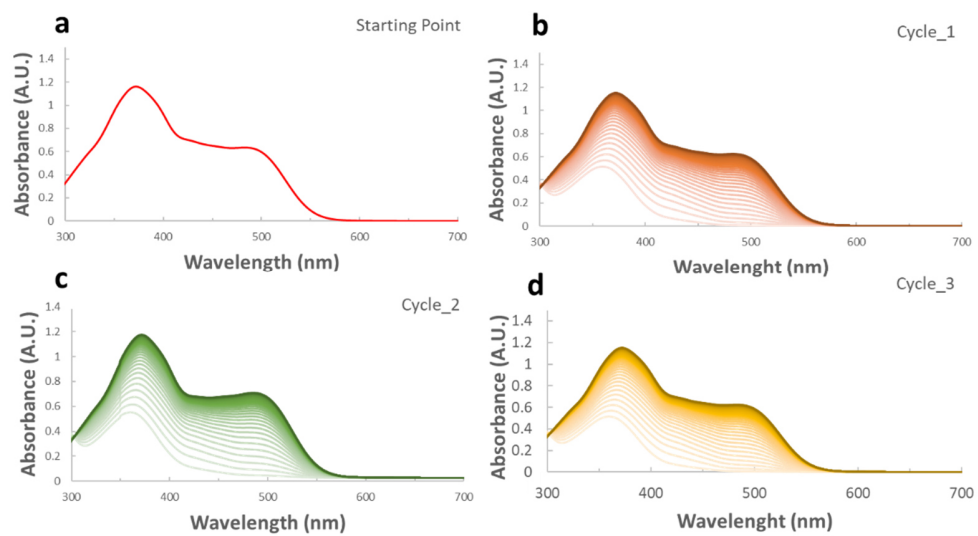
Figure S2. The two additional absorption spectra of the dark-light kinetic's experiments on the sample SP-ASA-Zn^{++} (1:1:1.5).

- **^{1}H NMR**

Compounds 1_2

1_CDCl₃
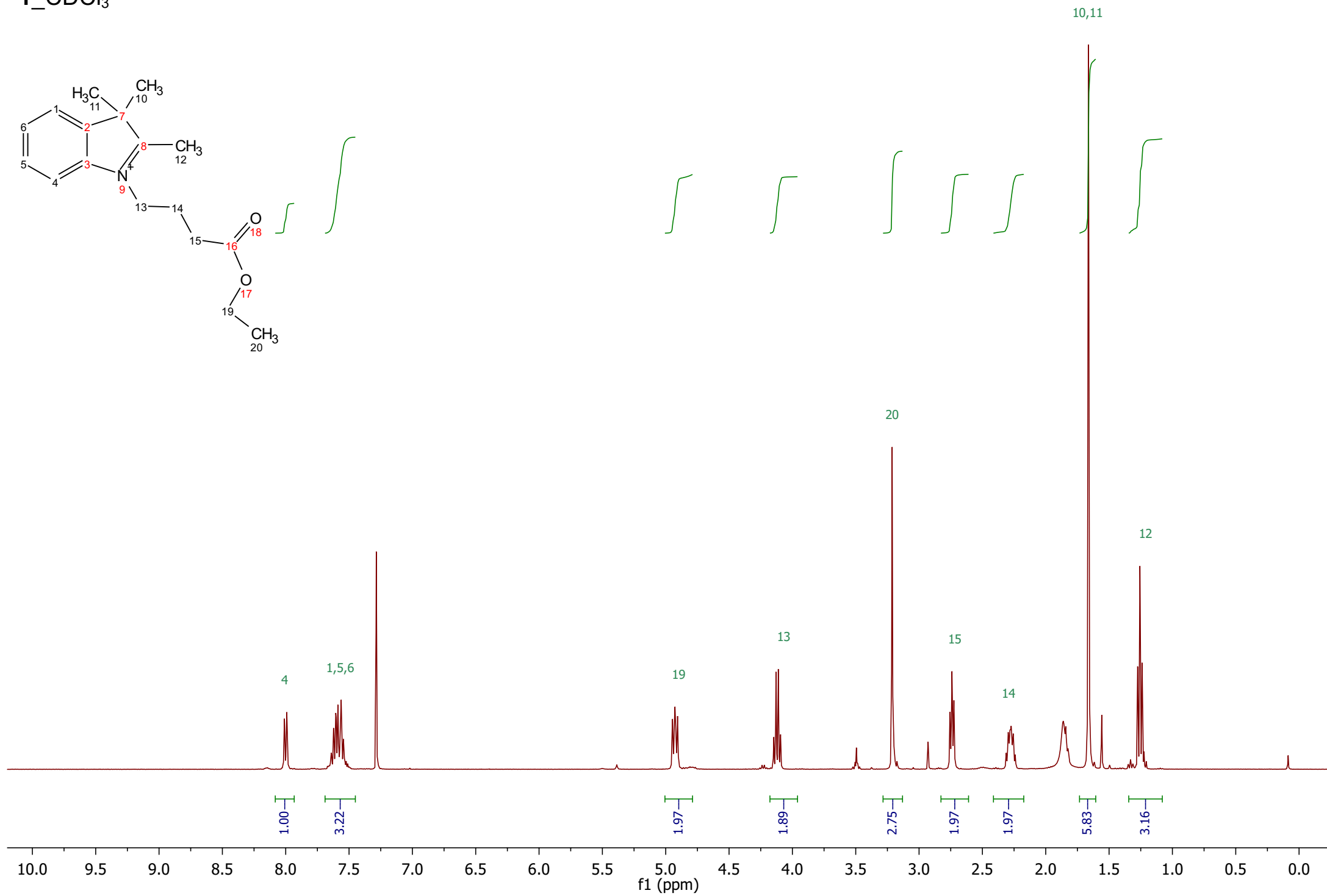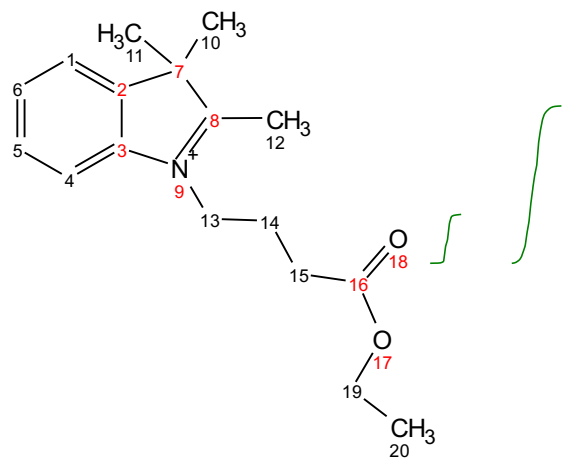
2_CD$_3$CN
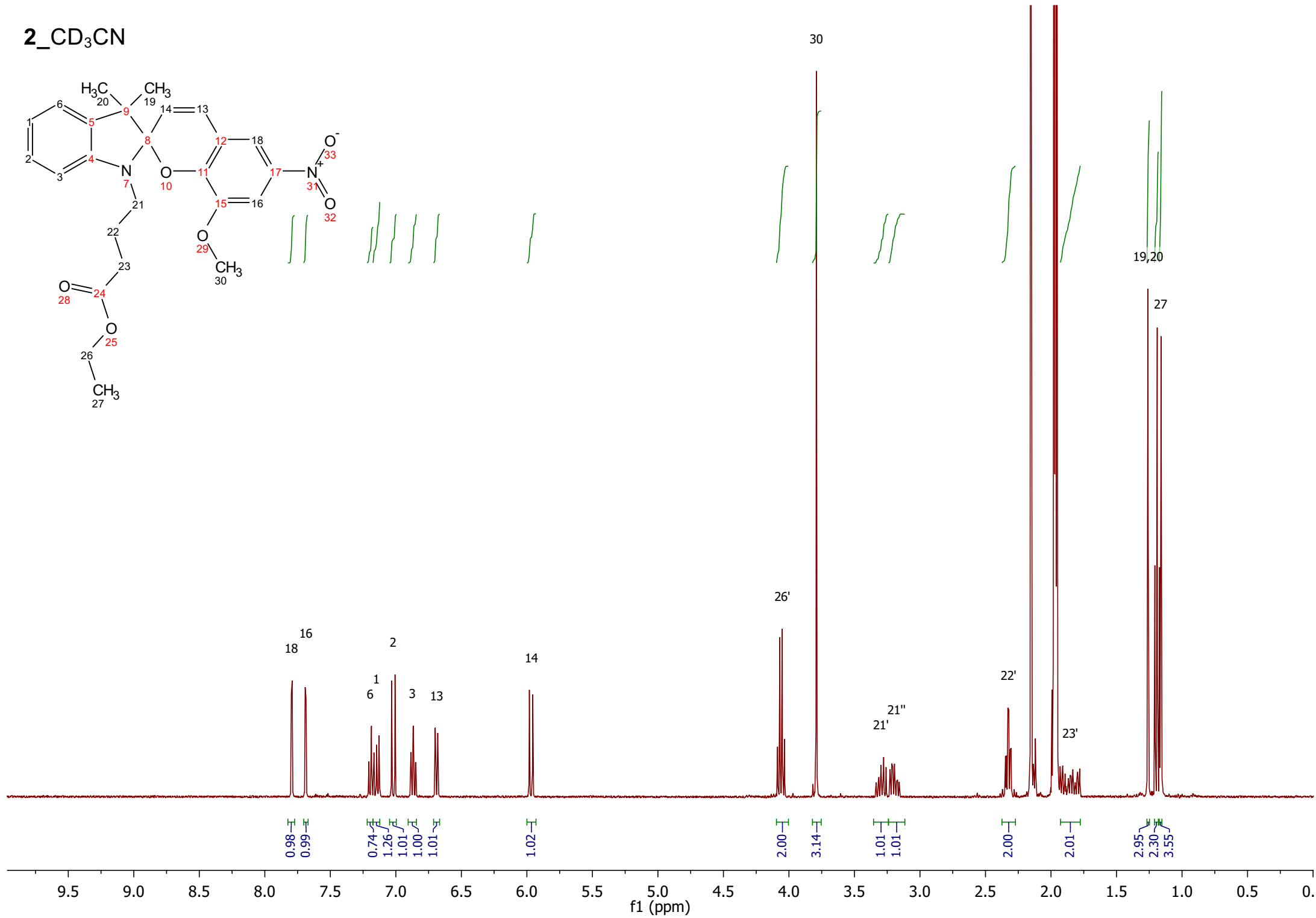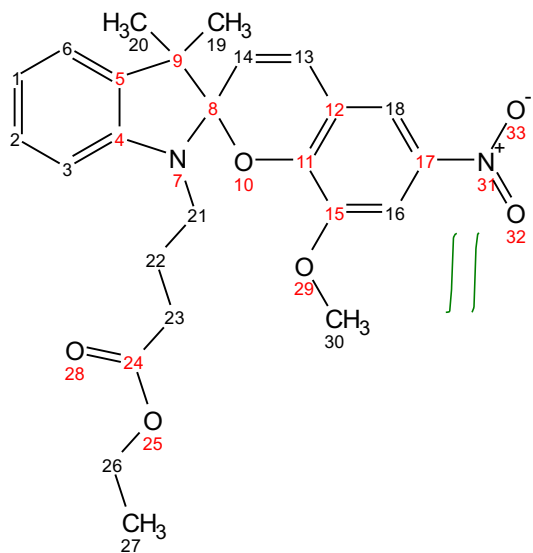
Chapter 4

- **¹H NMR**

Compounds AB1-AB2

AB1_CDCl$_3$

AB2_DMSOd-6

4,6,10,14

1,3,11,13

15,16

4.00

4.05

3.88

f1 (ppm)
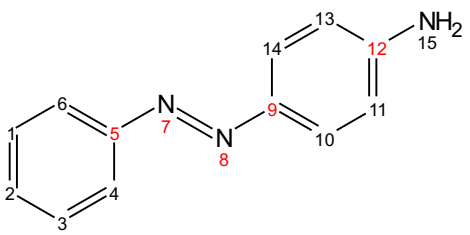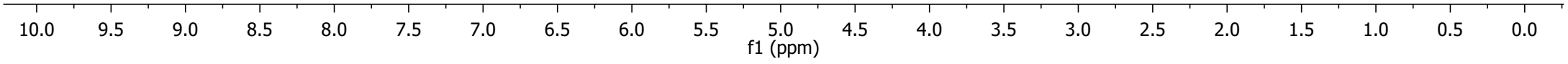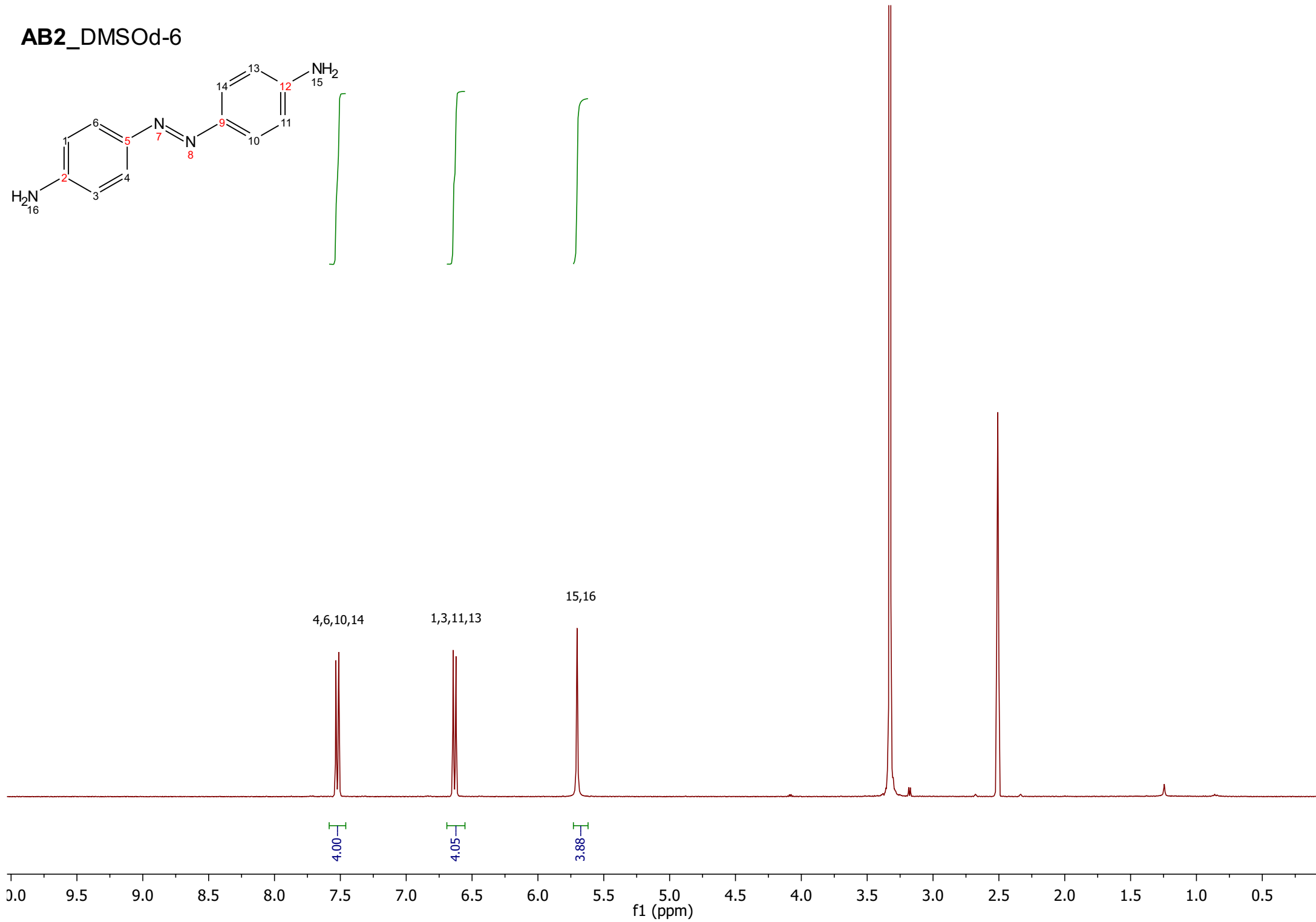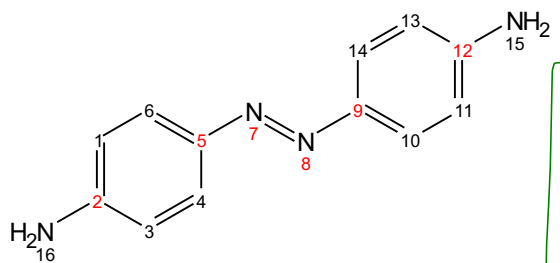
Chapter 5

1. *Ratiometric sensing of temperature with fluorescent Oxazines and Oxazolidines-based switches.*

    - **¹H NMR**

Compounds 2,3,4, a, b, c, d, e, 6,7,8.9.

    - **¹³C NMR**

Compounds a, b.

2. *pH sensing with switchable Coumarins*

    - **¹H NMR**

Compounds 12, 13, 14, f, g.

3. *Conjugated polymers assembled with Oxazine switching monomers.*

    - **¹H NMR**

Compounds 11, 16, 18, 19, 21, 22, 23,24, 25, h, i, j, k, p, q, r, polymer with h monomer, polymer with i monomer.

*the spectrum for compound c unfortunately is not well resolved, to confirm the purity of the product I herein attach the MS measurements performed on the same sample. The molecules showed purity also during all the chemical-physical characterizations performed.

**many of the spectra contain peaks belonging to residual of solvents used in the work up or to clean the NMR tubes.

4_DMSO-d6
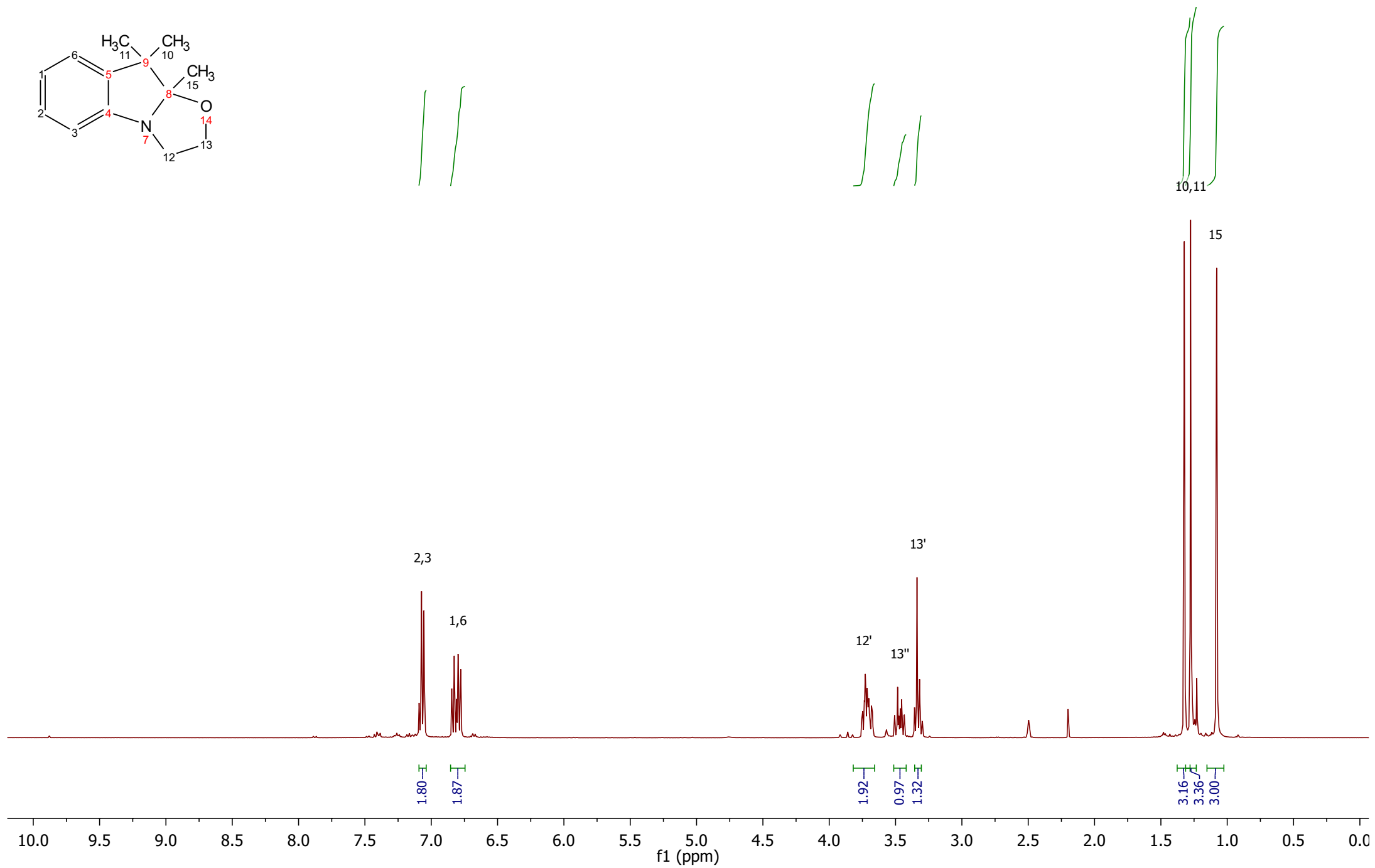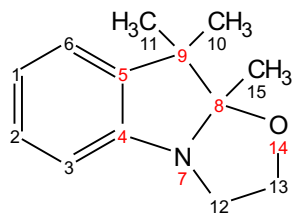
3_CDCl₃
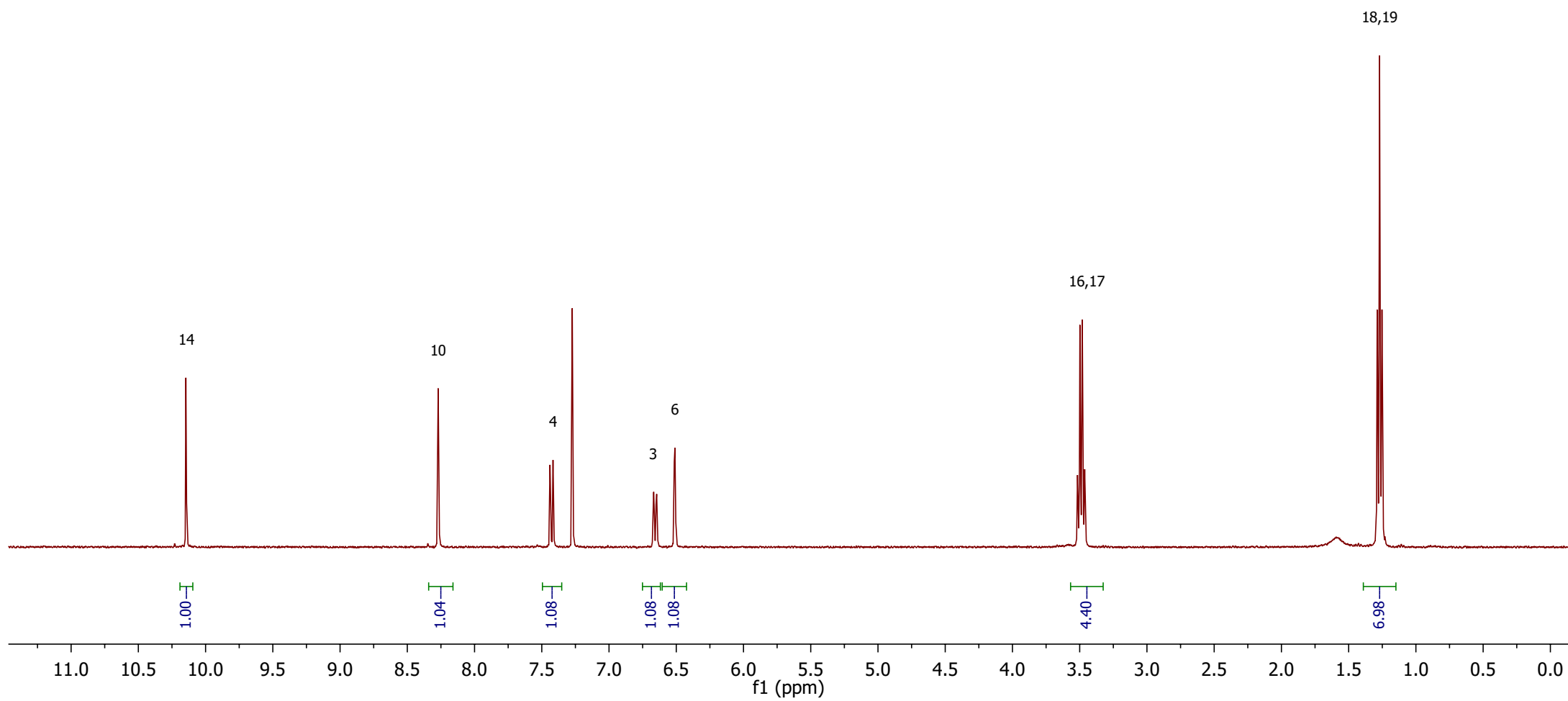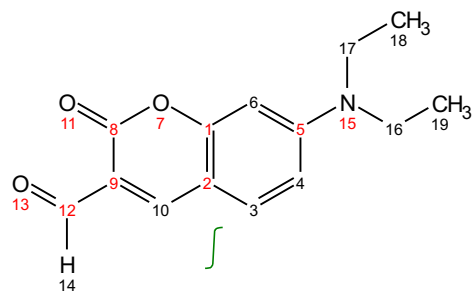
3_CDCl$_3$
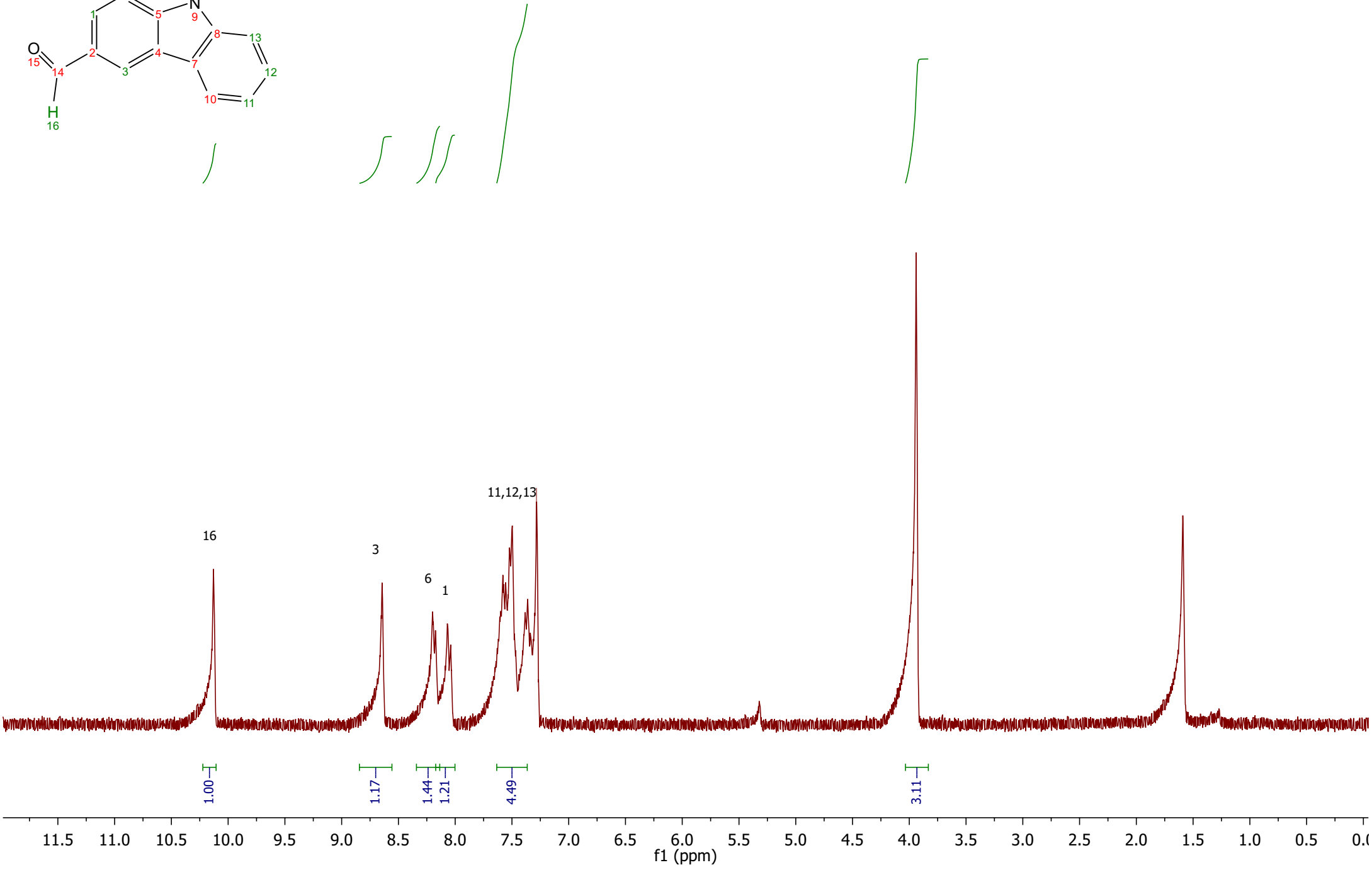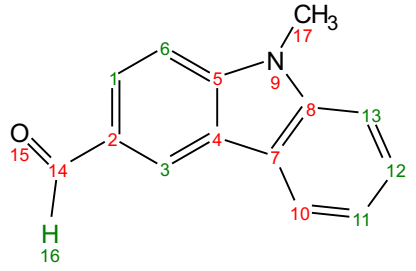
6_CDCl$_3$
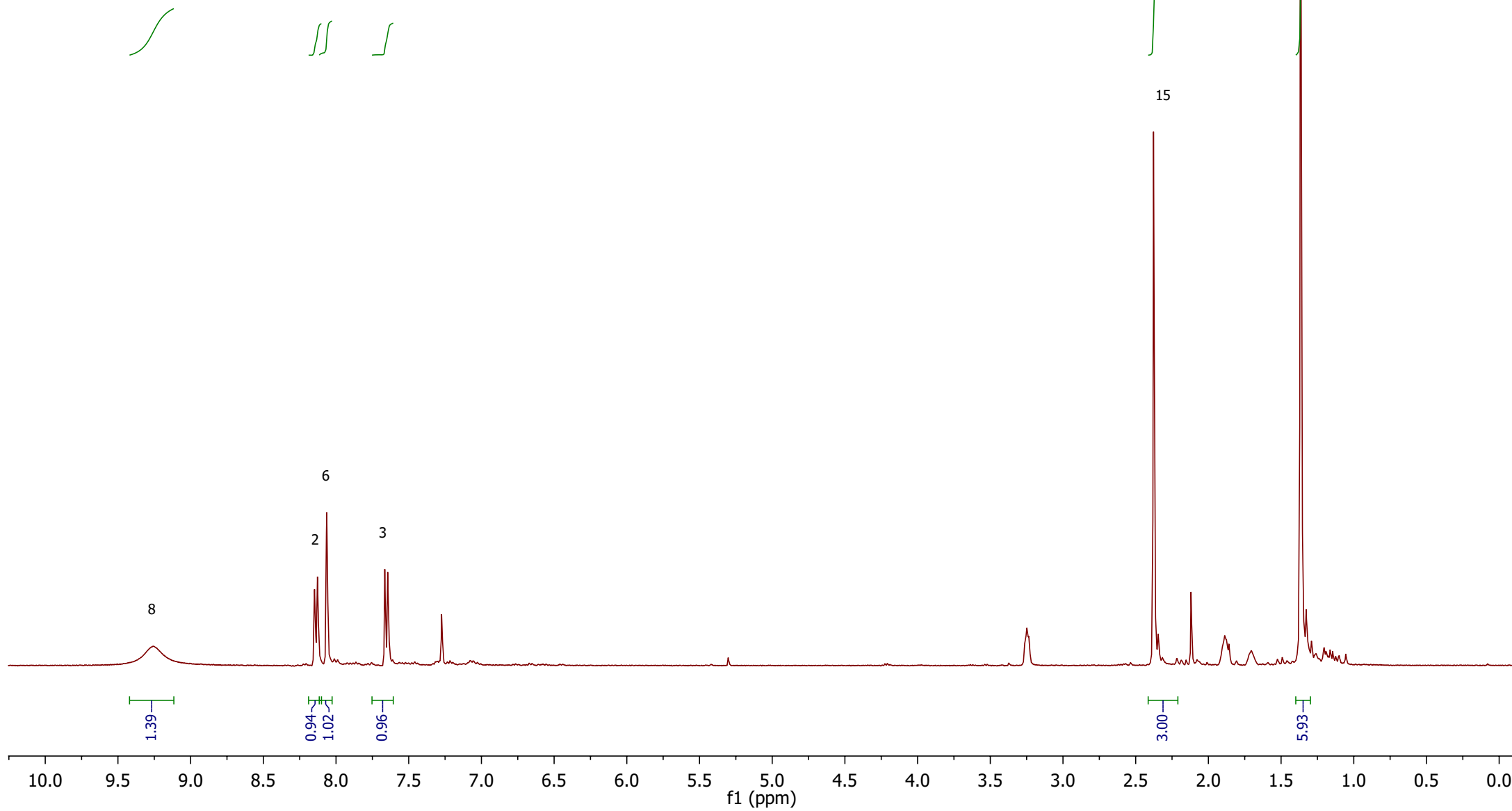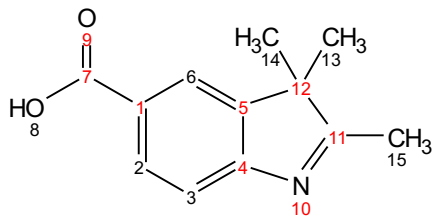
7. CD₃CN
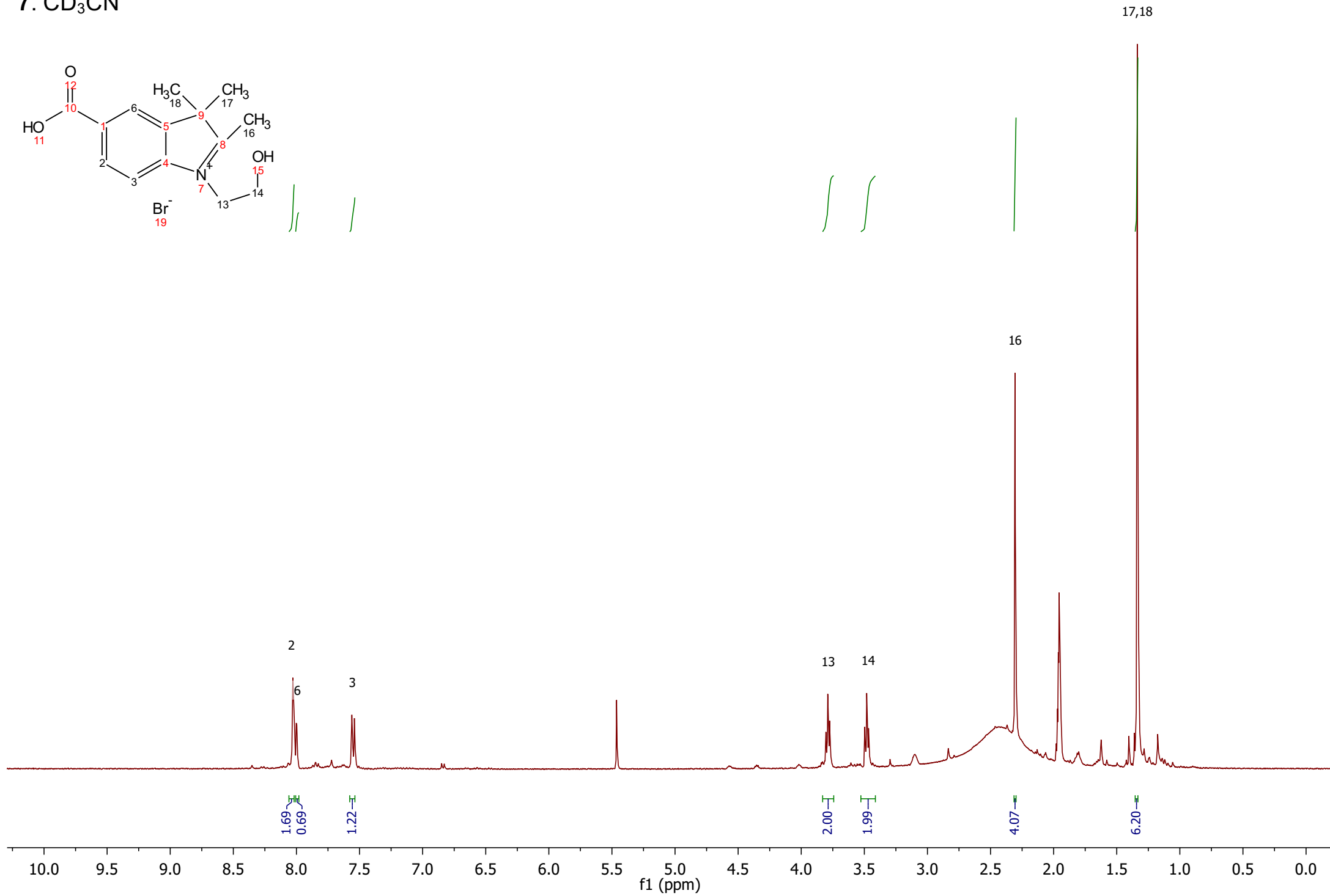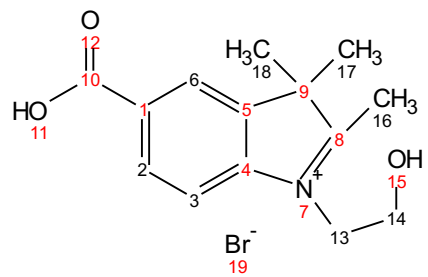
8. CD₃OD
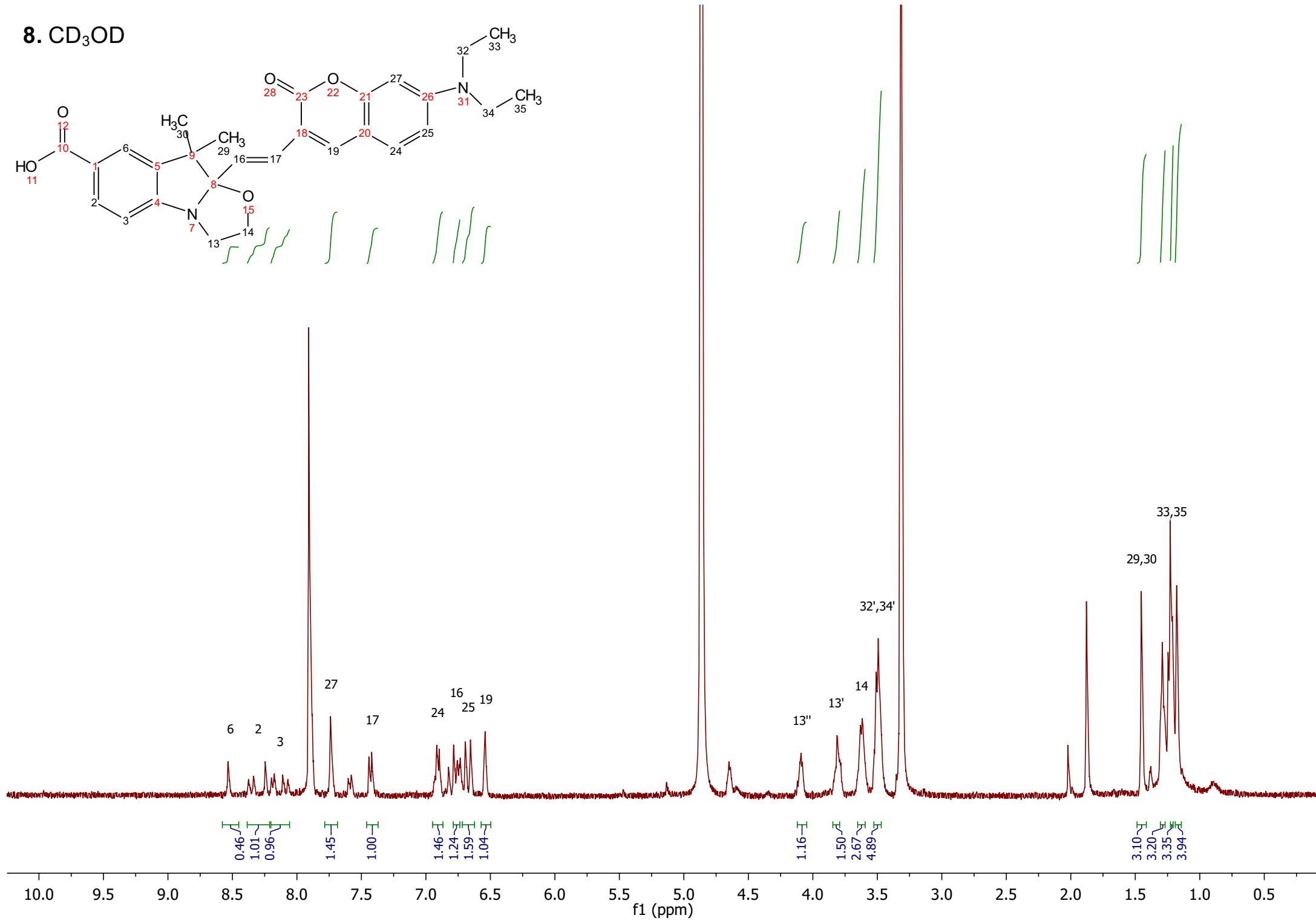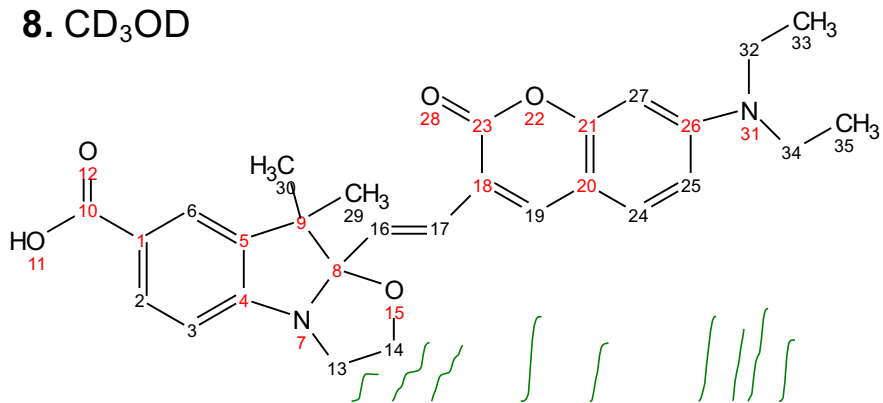
9_CDCl$_3$
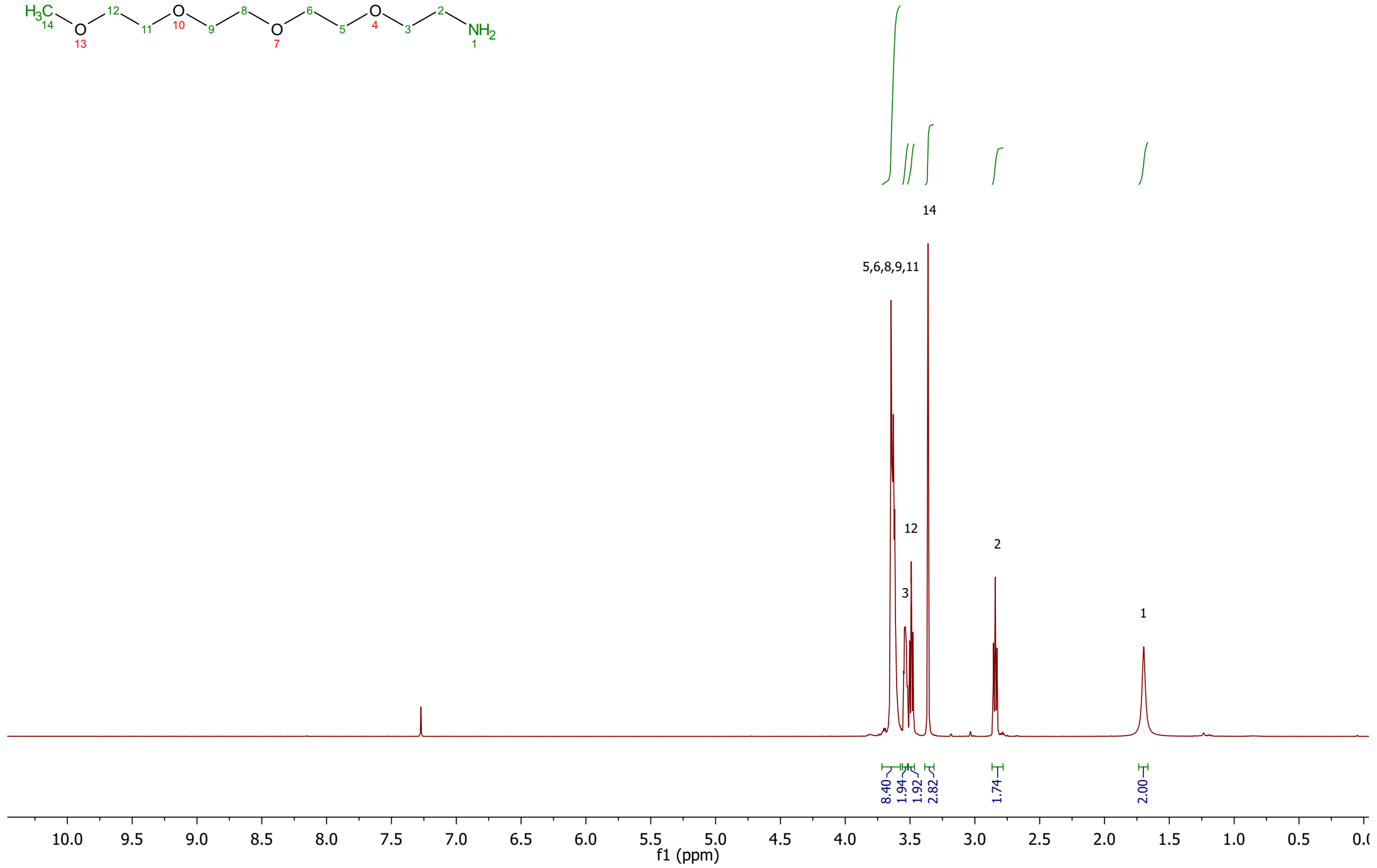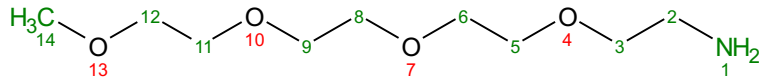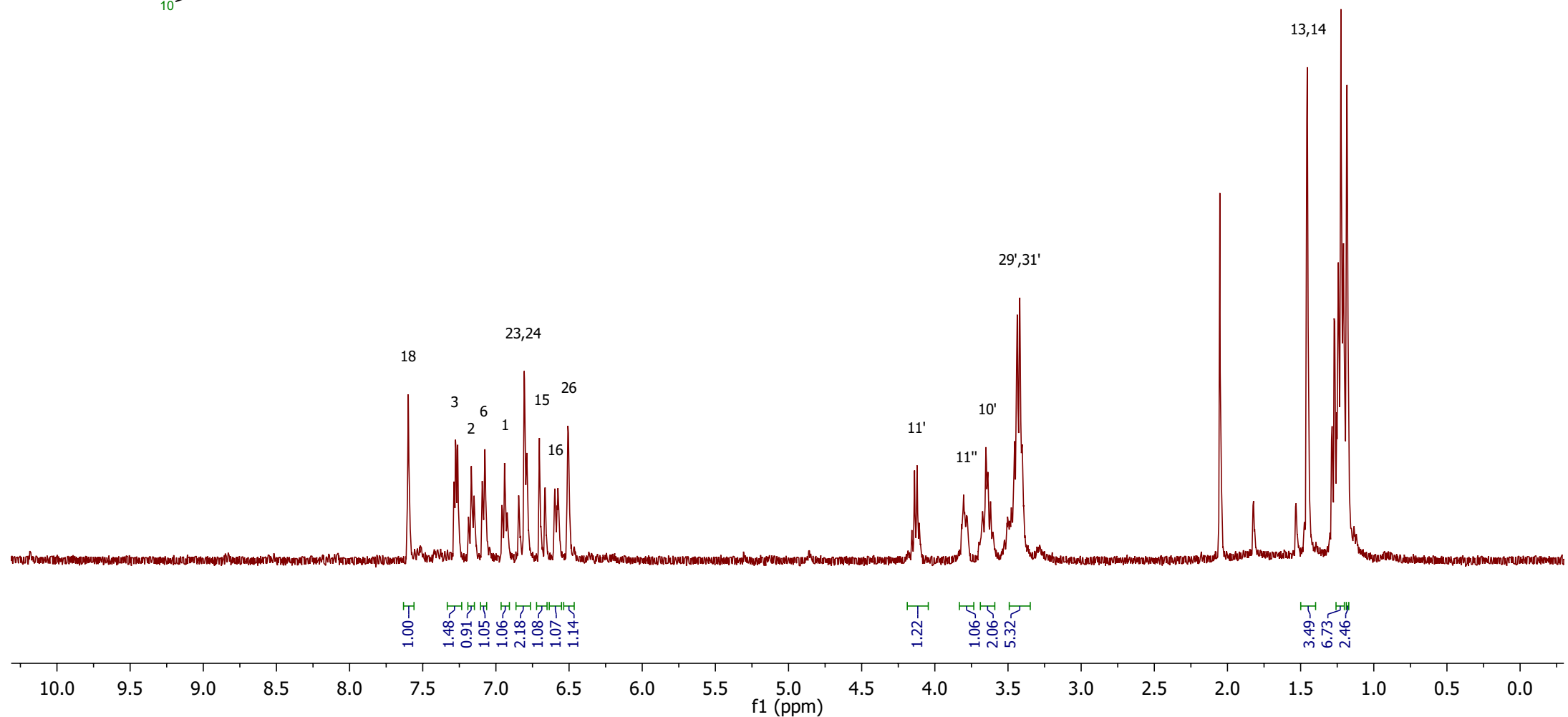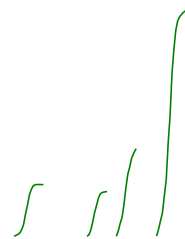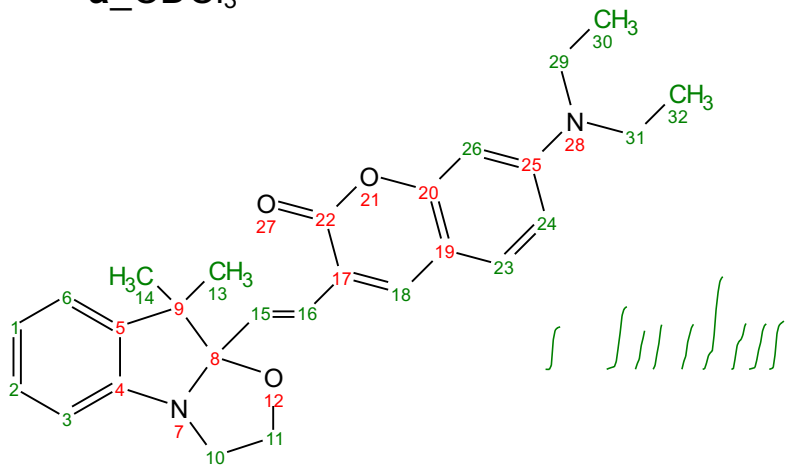
5,6,8,9,11

14

12

3

2

1

8.40 1.94 1.92 2.82 1.74 2.00

10.0 9.5 9.0 8.5 8.0 7.5 7.0 6.5 6.0 5.5 5.0 4.5 4.0 3.5 3.0 2.5 2.0 1.5 1.0 0.5 0.0
f1 (ppm)
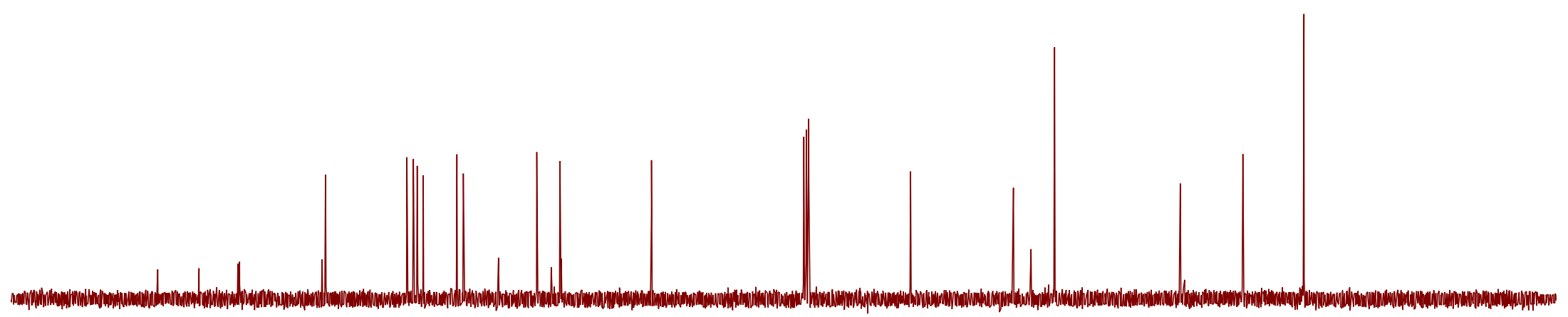
a_CDCl₃
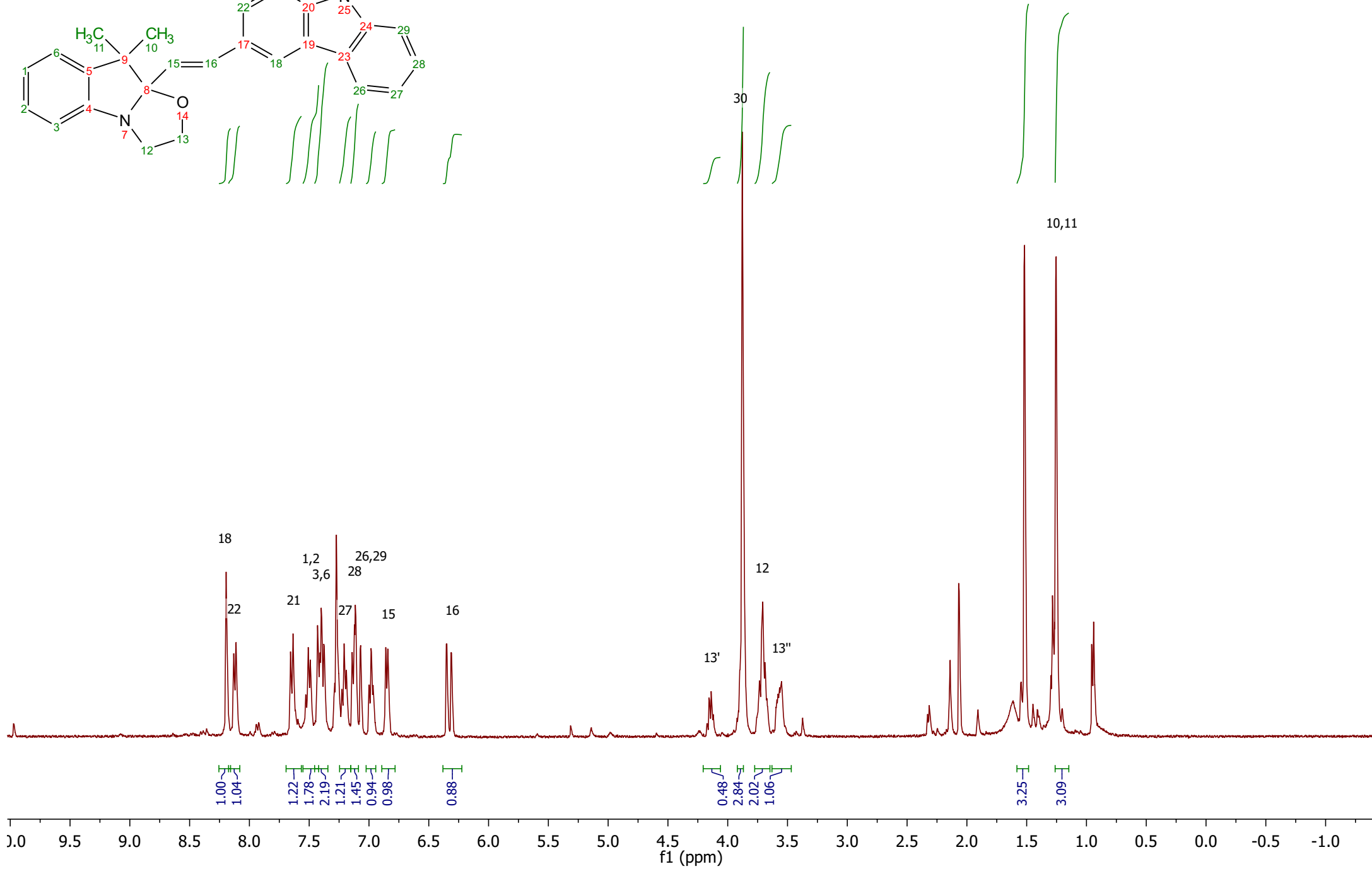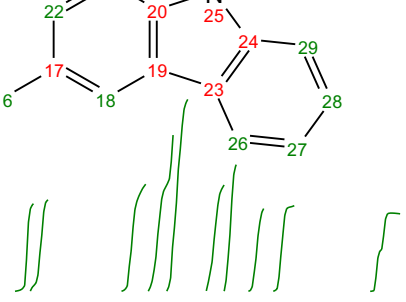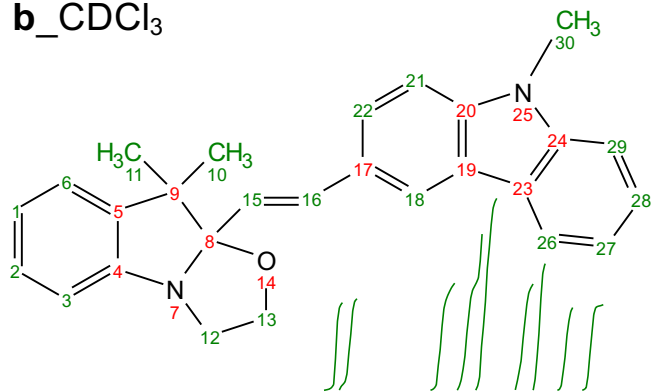
a_CDCl$_3$_^{13}C

b_CDCl$_3$

b_CDCl₃_¹³C
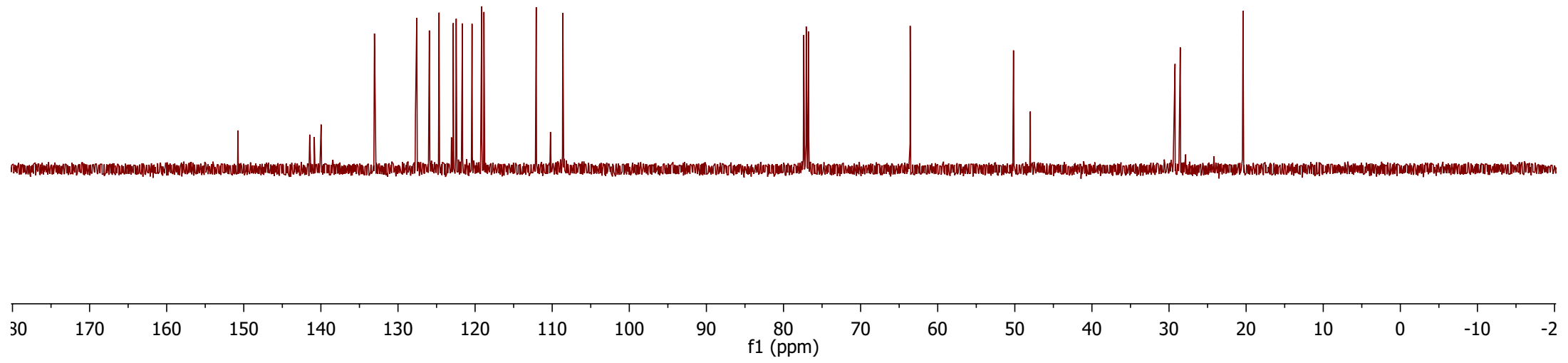
ESI-TOF Mass Spectrum Report

Analysis Name   D:\Data\UMiami\0410FrCa01_LOW_ACN_CHCL3_wFA_POS.d   Acquisition Date   4/10/2018 12:25:46 PM

Sample Name   FC108   Instrument   microOTOF-Q II

Comment   ACN_CHCL3 (50:50 0.1% FA)   Method   tune_low_Bruker_Calibration.m

OK = MS for the
desired
product –

+MS, 0.2-0.4min #(12-23)
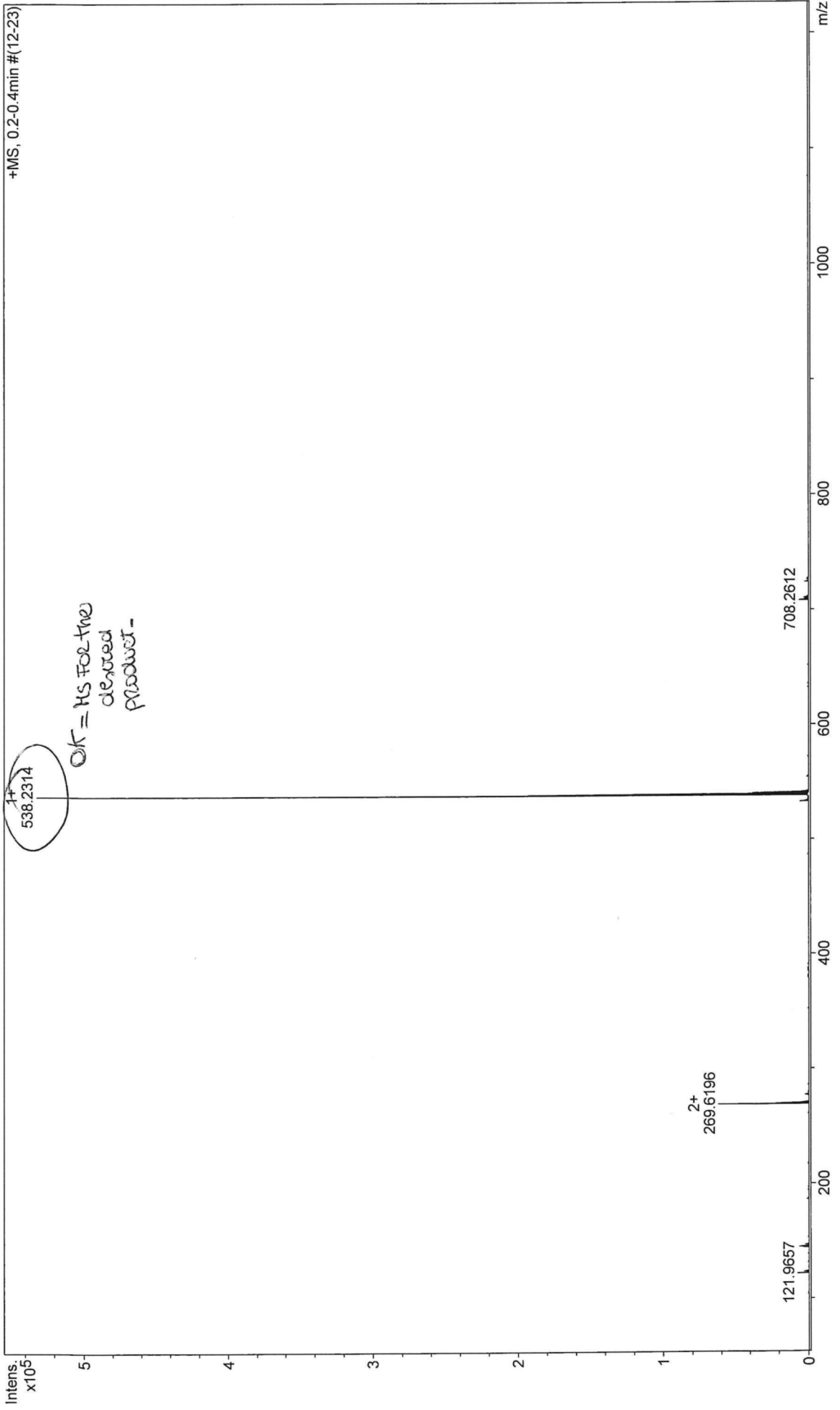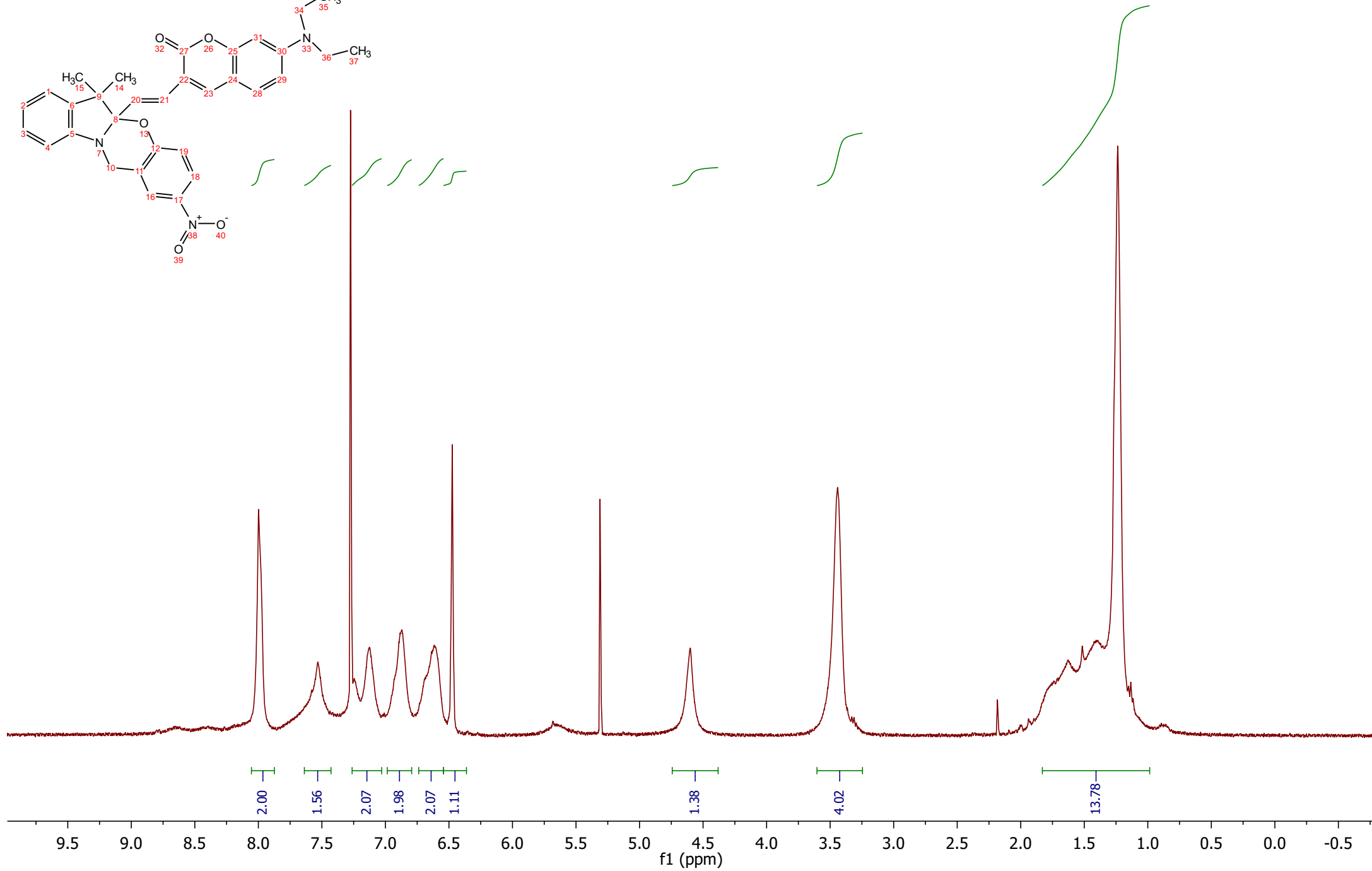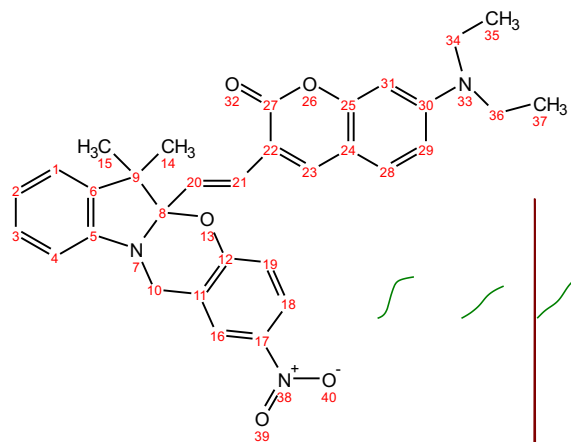
c_CDCl$_3$

c_CD$_3$CN

e_ CD₃CN
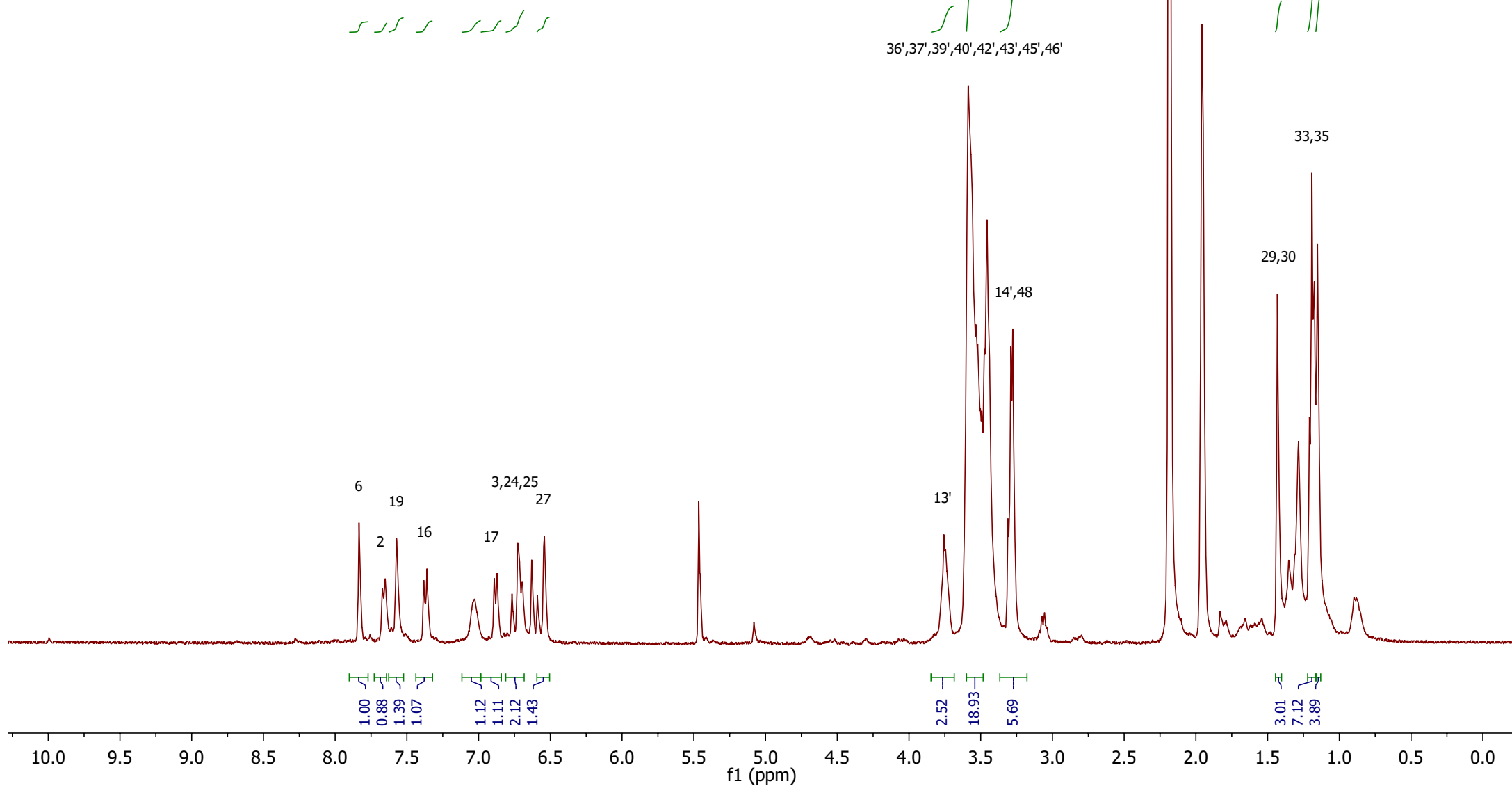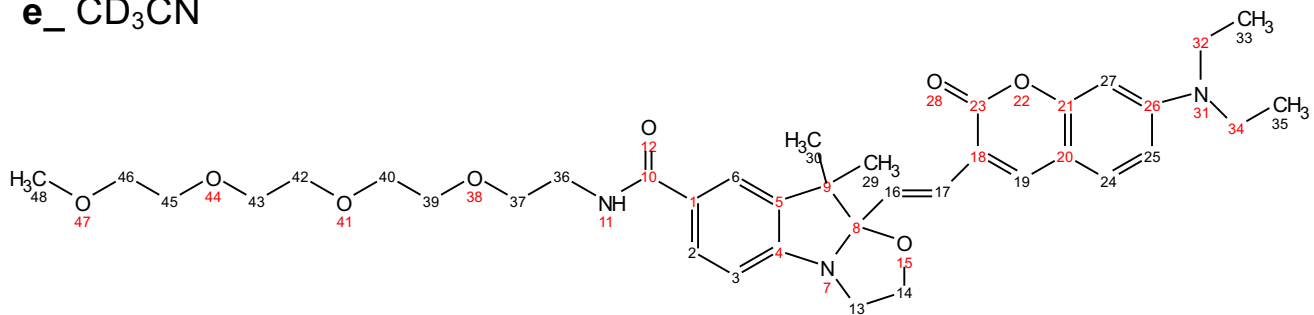
12_CD₃CN
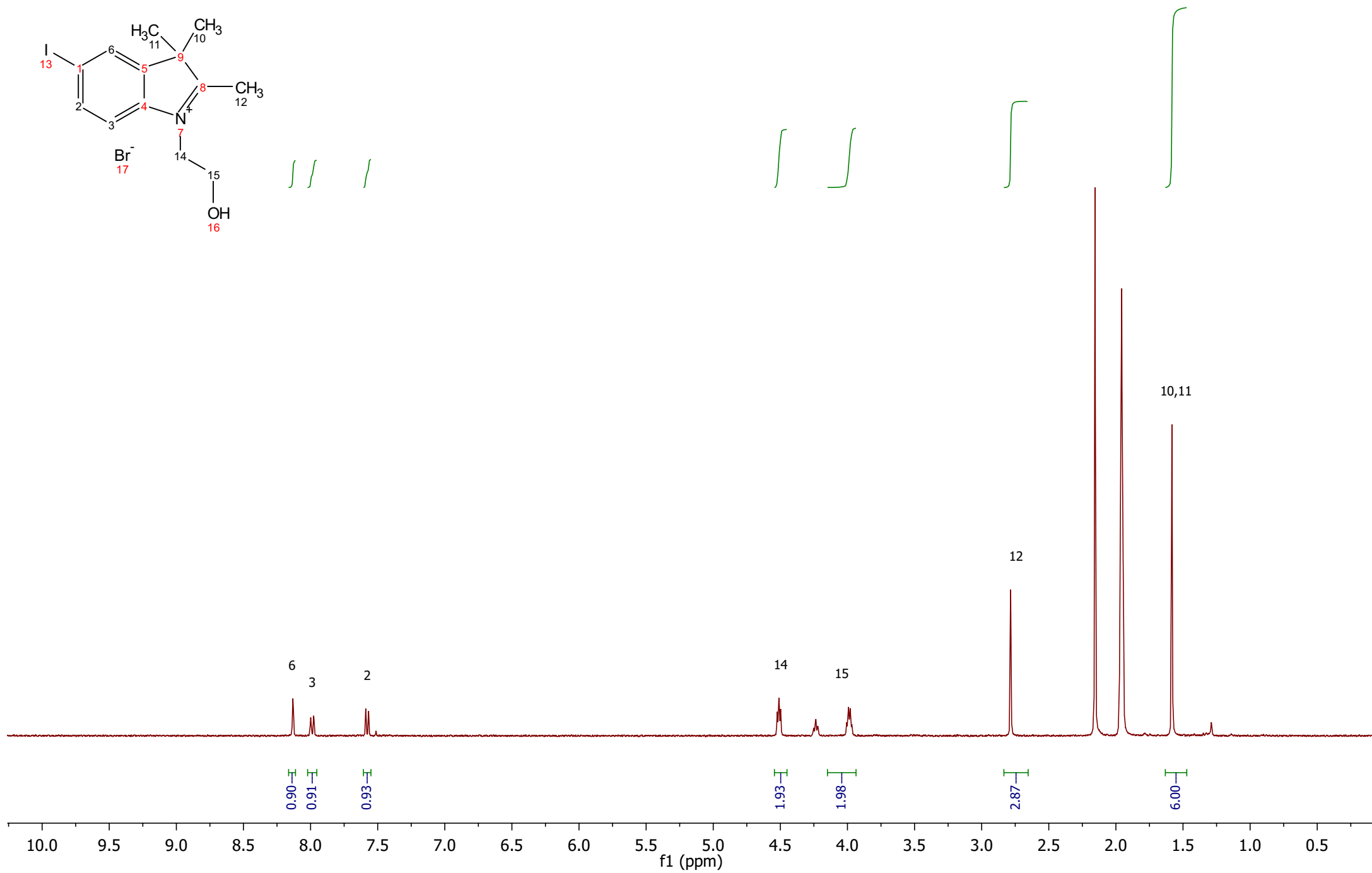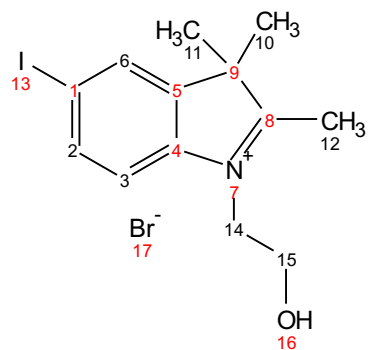
13_CDCl₃
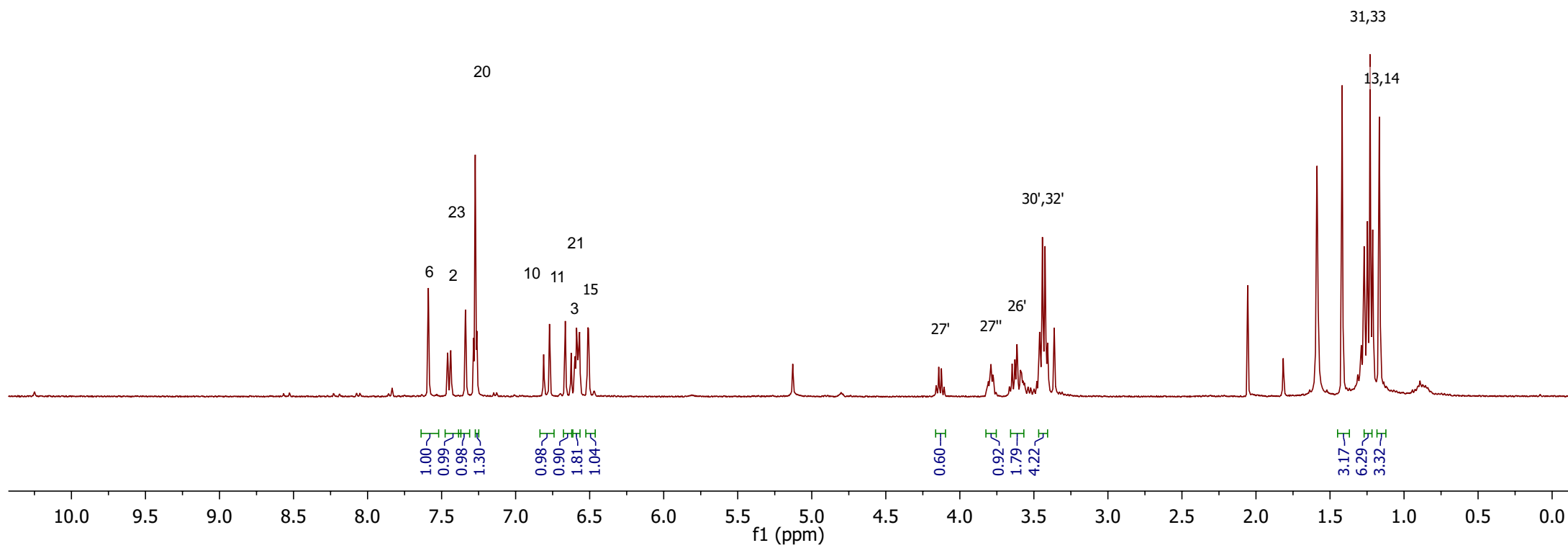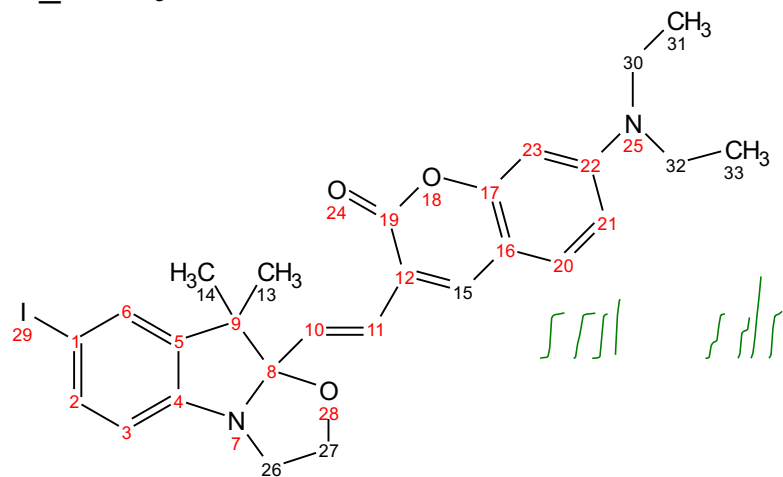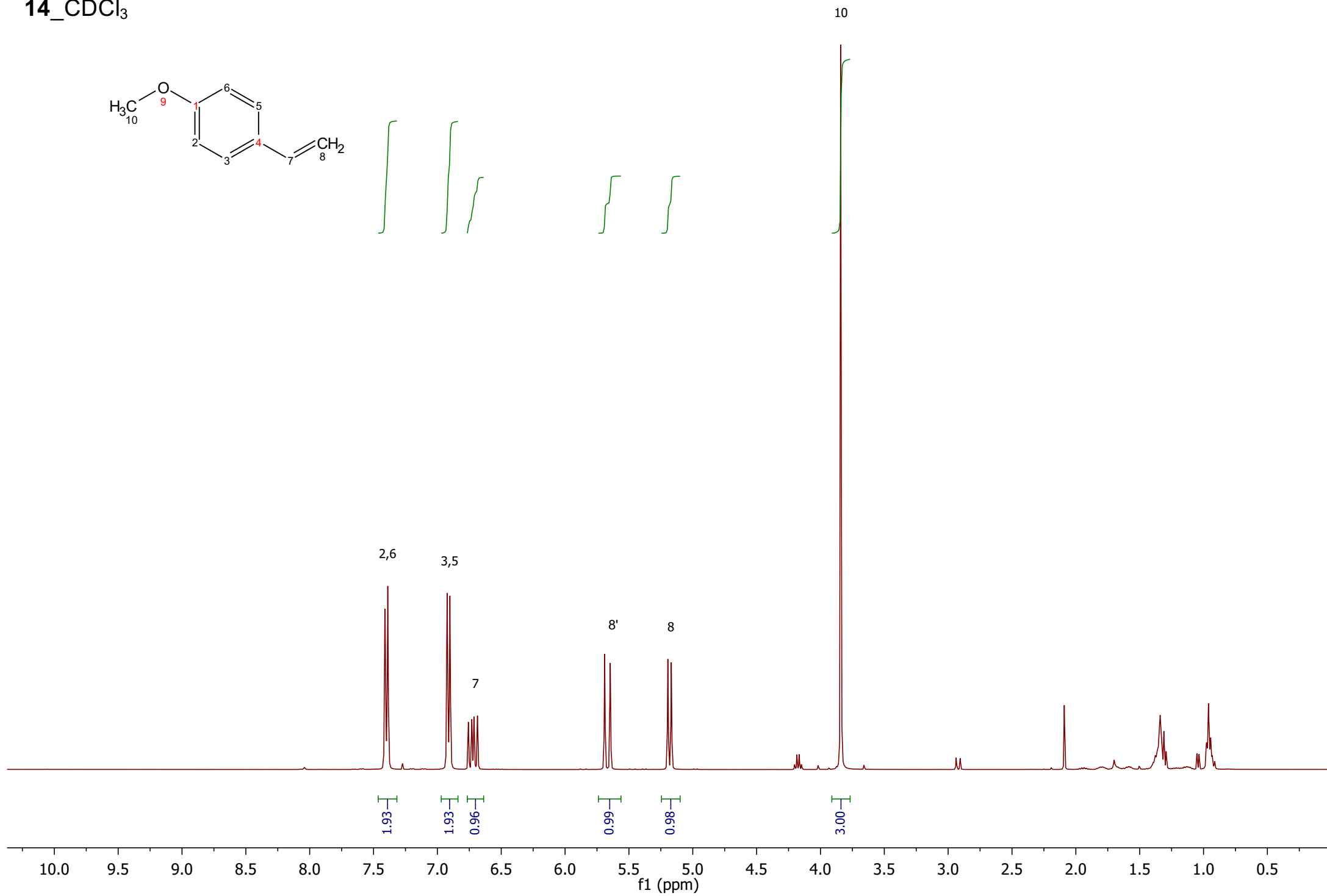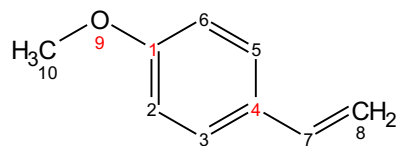
14_CDCl$_3$

f_CD$_3$CN
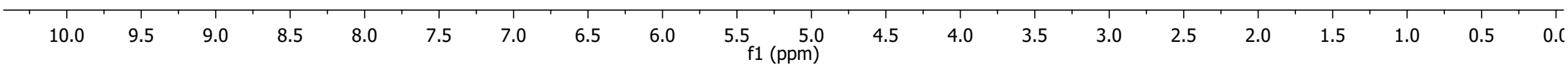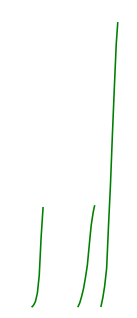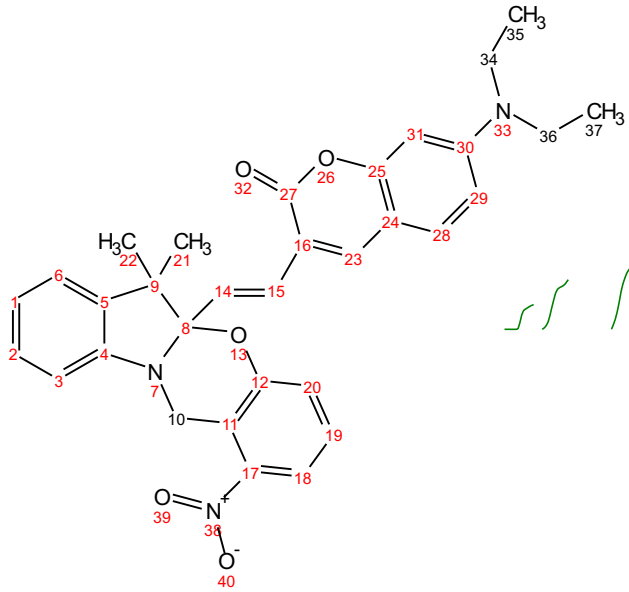
g_CDCl₃

11_CDCl$_3$

10,11

12

6

2

3

0.92
0.84

0.98

2.94

6.00

10.0   9.5   9.0   8.5   8.0   7.5   7.0   6.5   6.0   5.5   5.0   4.5   4.0   3.5   3.0   2.5   2.0   1.5   1.0   0.5   0.
f1 (ppm)

16_CDCl$_3$

18_ CDCl₃

19_CDCl$_3$

10,11

16,20
17,19

6

2 3

12

13

21

22

22'

6.51

1.05
2.14
1.99
2.10
1.18

1.01

1.00

0.99

1.00

10.0   9.5   9.0   8.5   8.0   7.5   7.0   6.5   6.0   5.5   5.0   4.5   4.0   3.5   3.0   2.5   2.0   1.5   1.0   0.5

f1 (ppm)
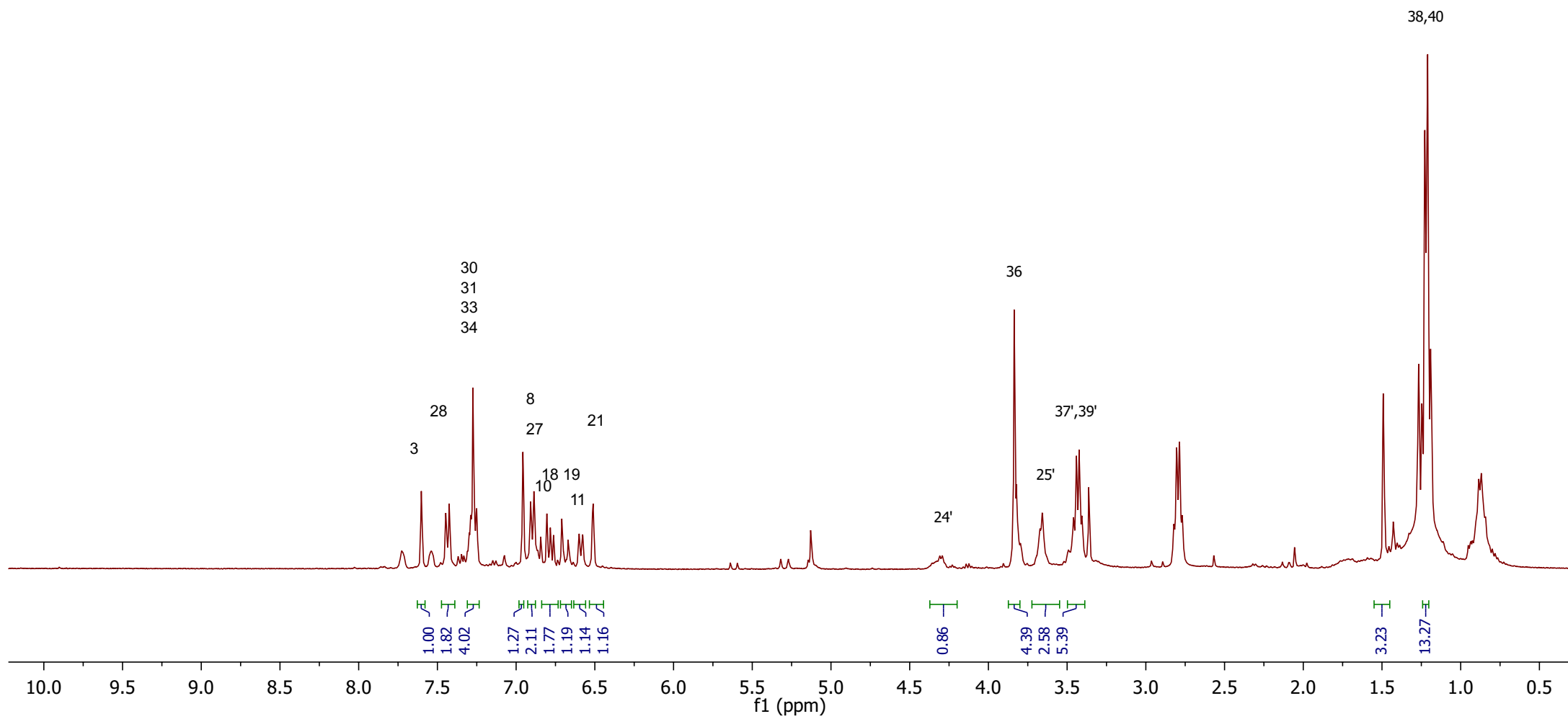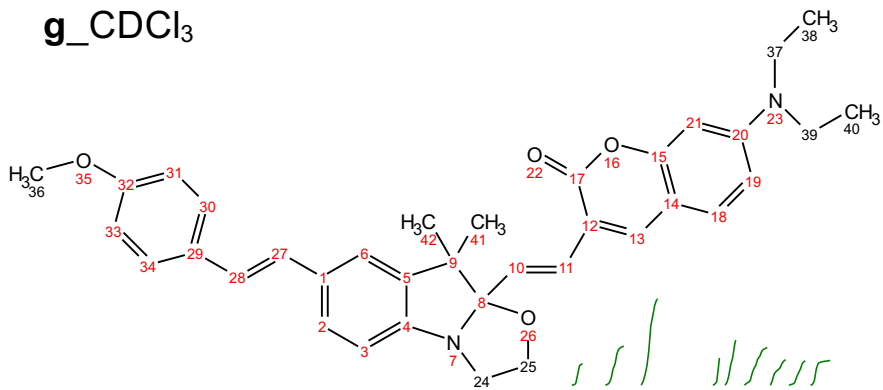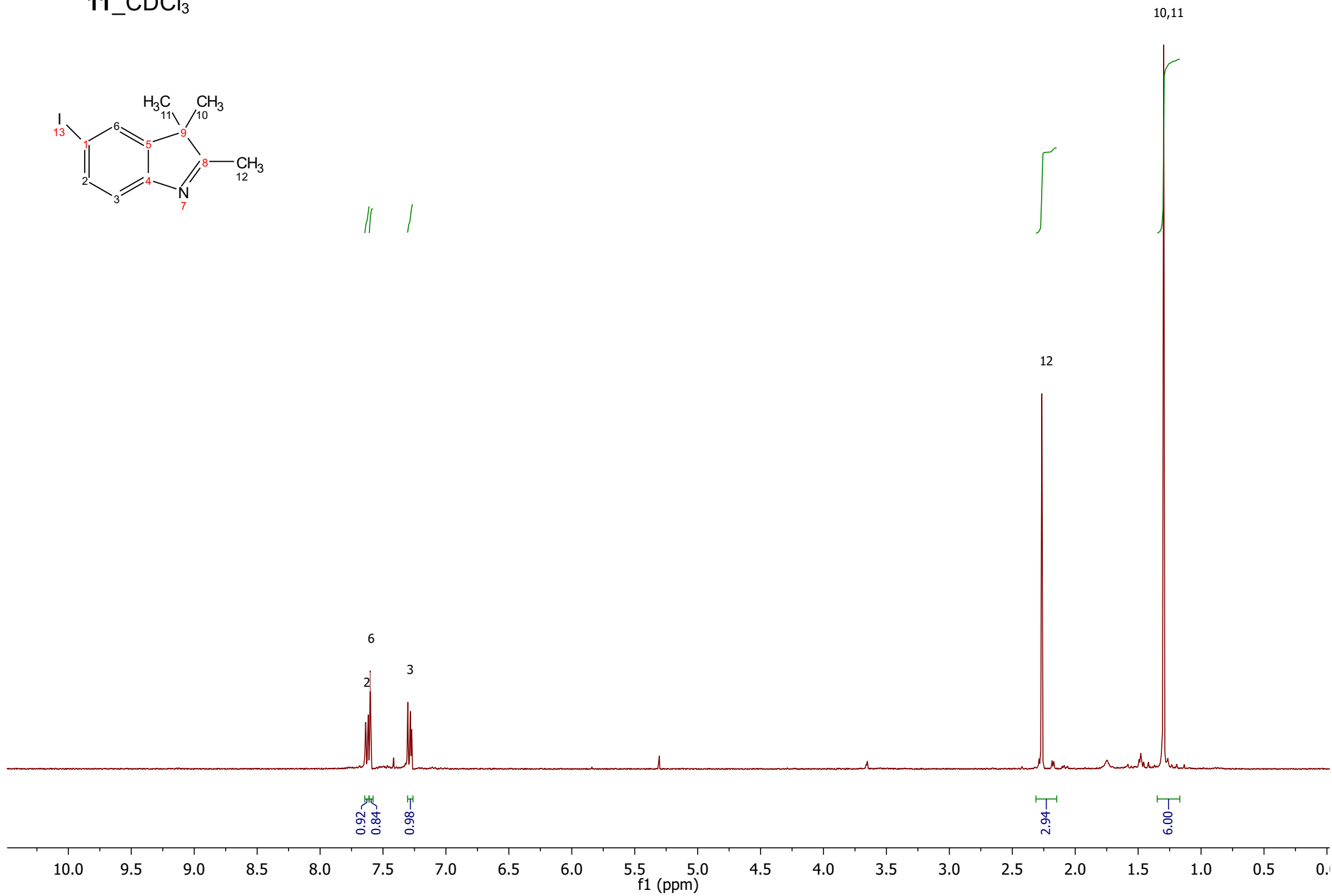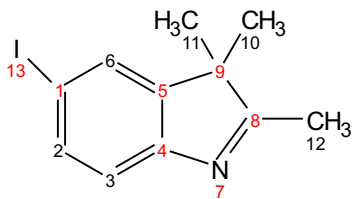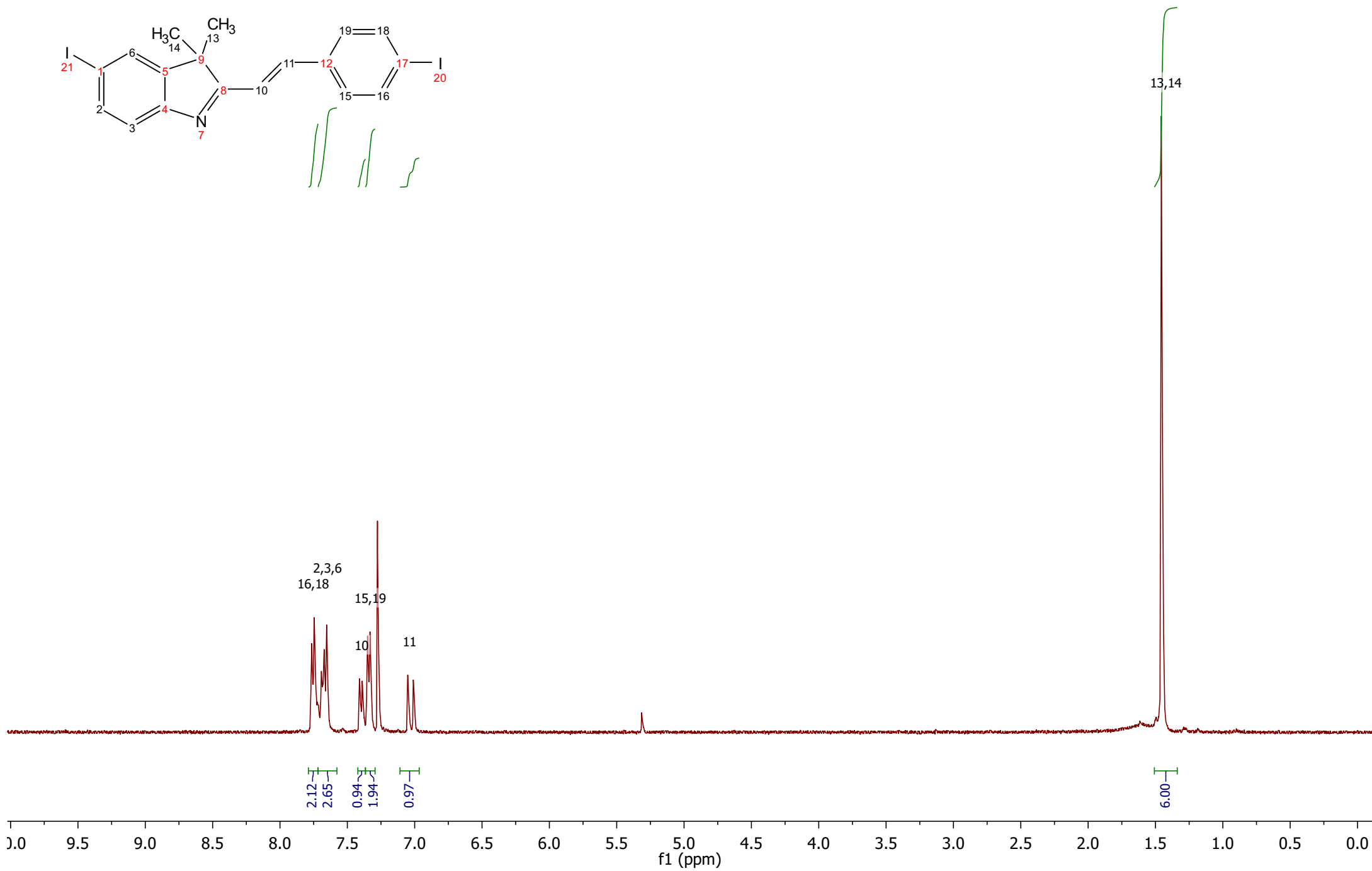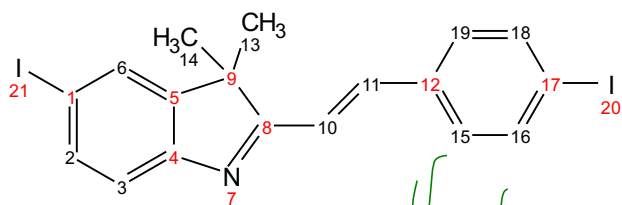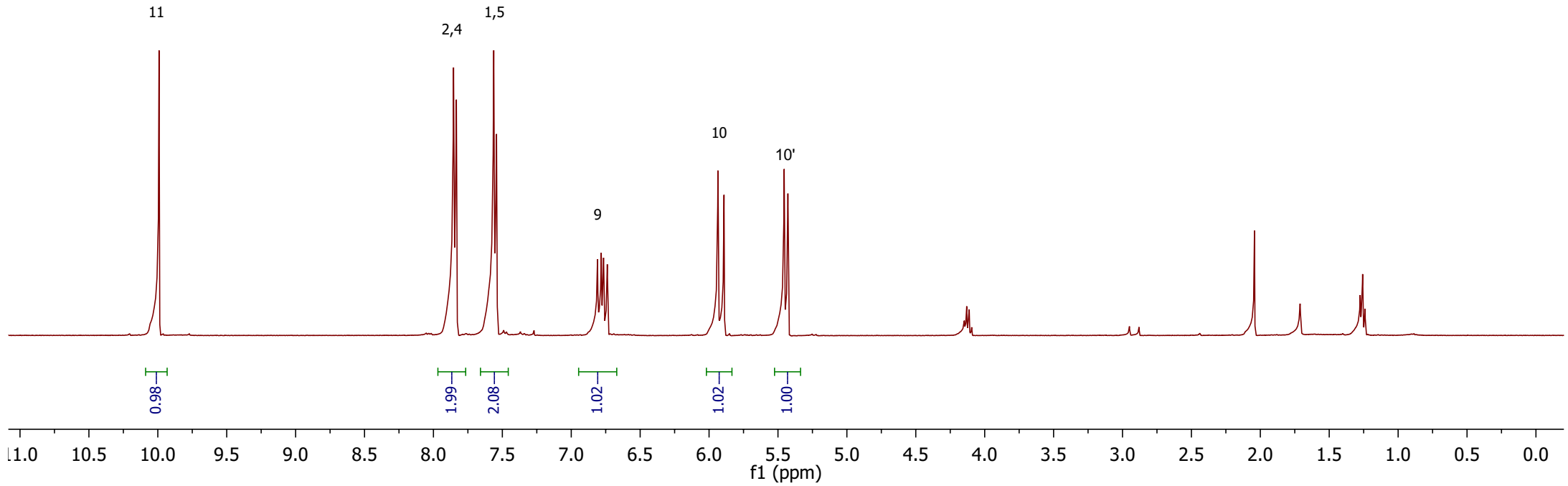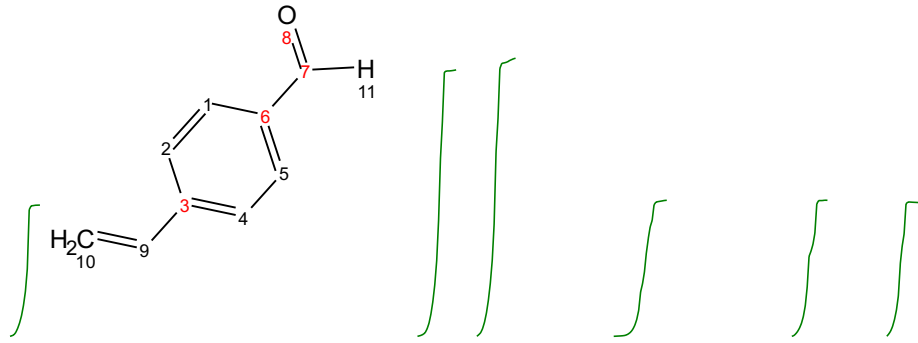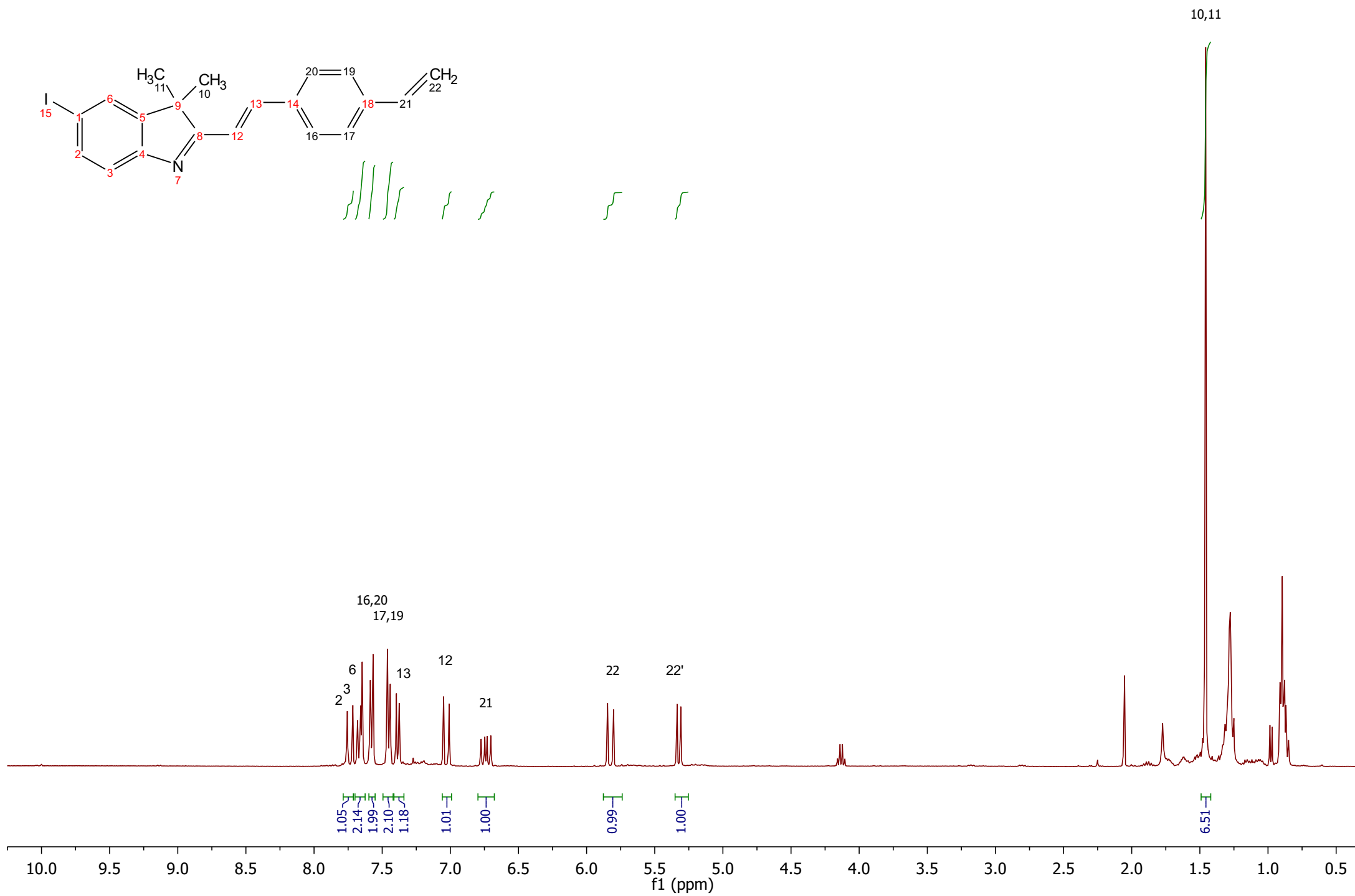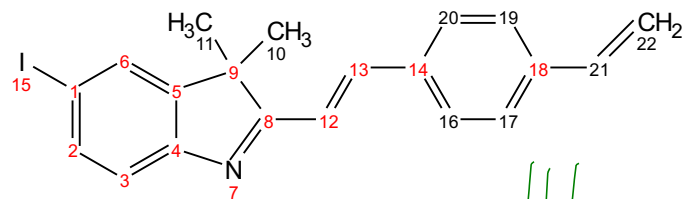
21_CDCl₃
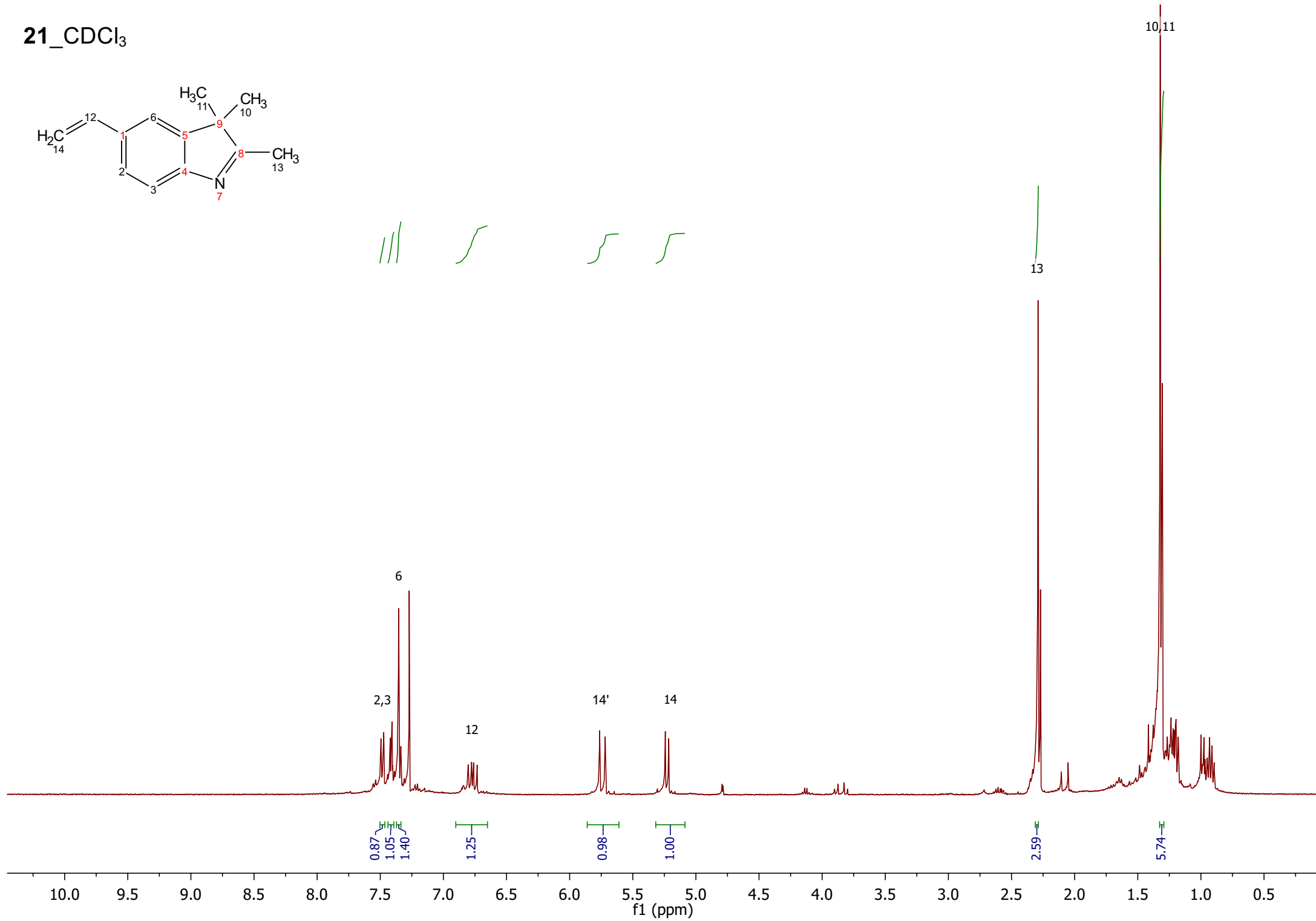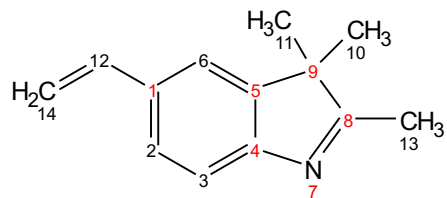
22_DMSO-d6
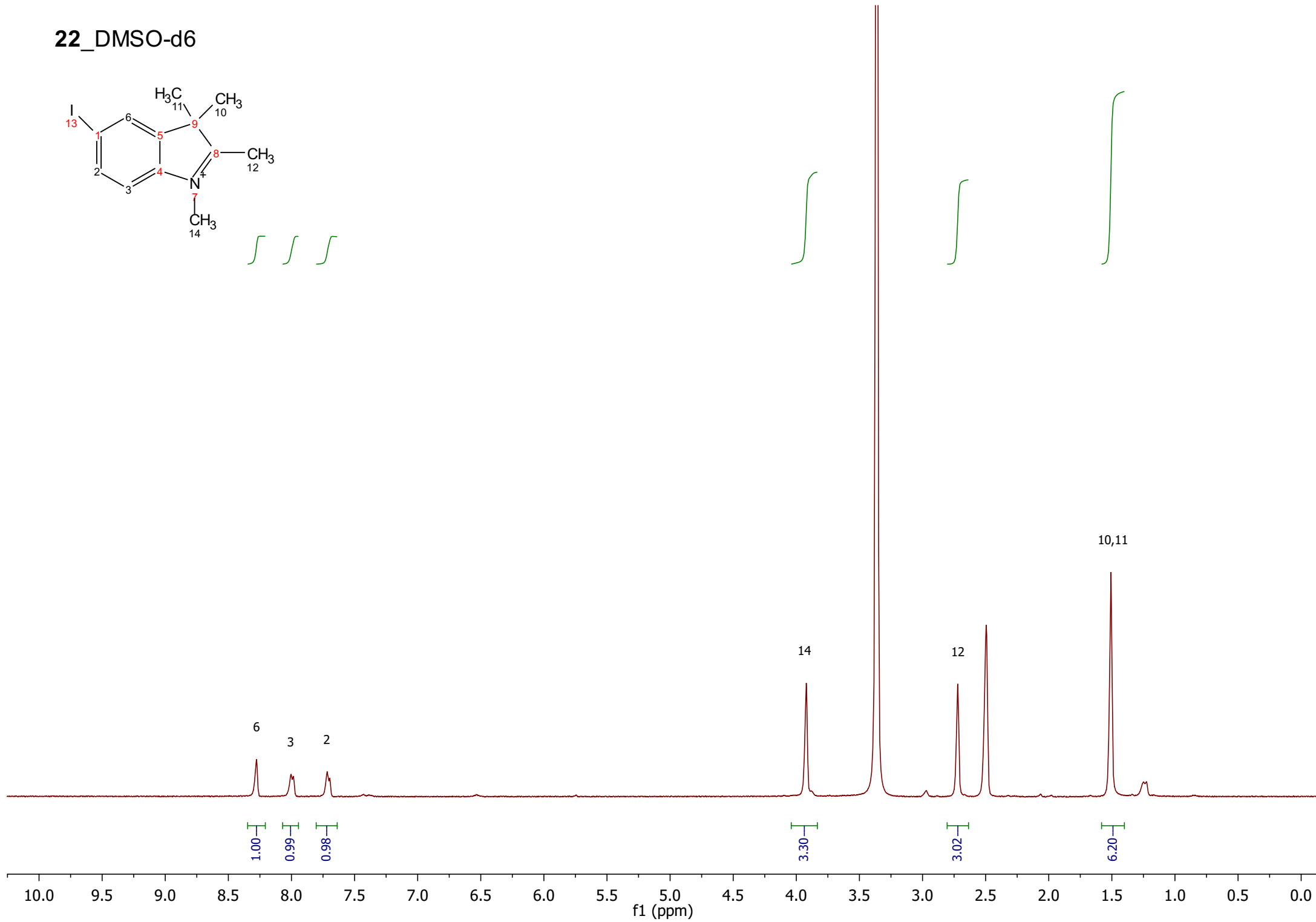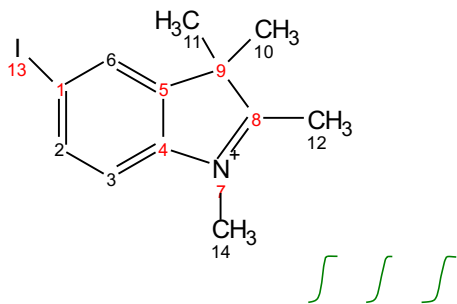
23_CD₃CN

24_CD₃CN

25_CDCl₃

h_CDCl₃

i_CDCl₃

j_CDCl₃

k_CDCl$_3$

p_CDCl$_3$

9,1

2,5

10',12'

10,12

13,14

1.45
2.31

1.97

1.98

6.00

10.0   9.5   9.0   8.5   8.0   7.5   7.0   6.5   6.0   5.5   5.0   4.5   4.0   3.5   3.0   2.5
f1 (ppm)
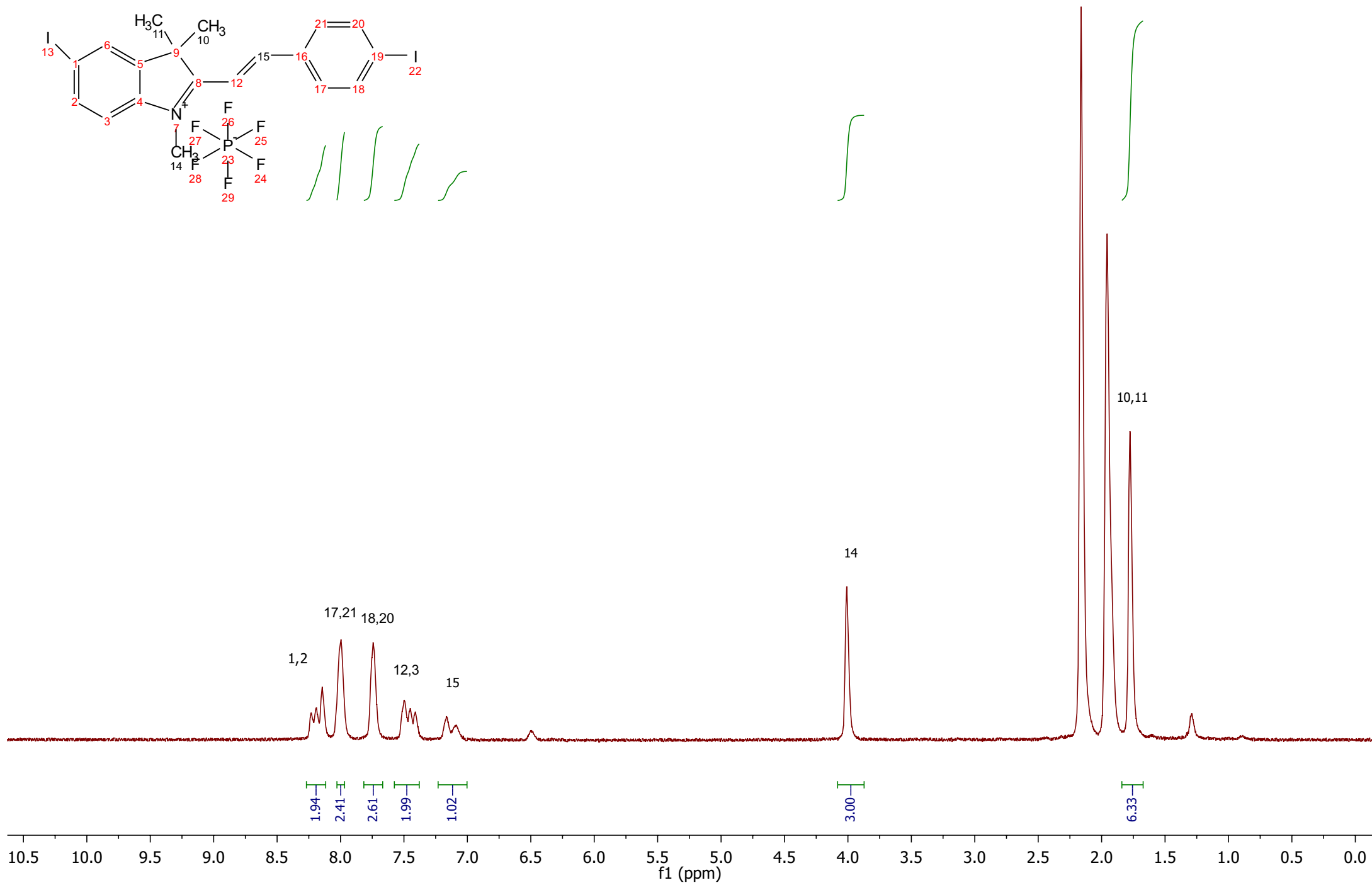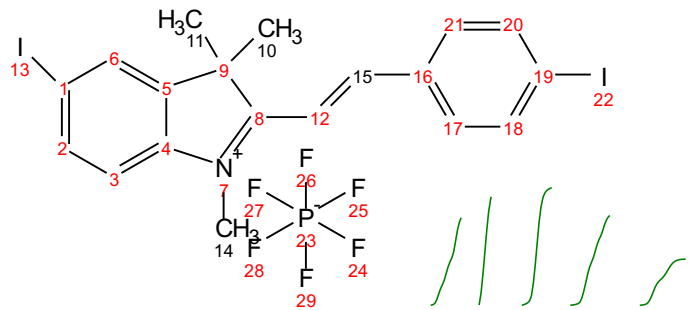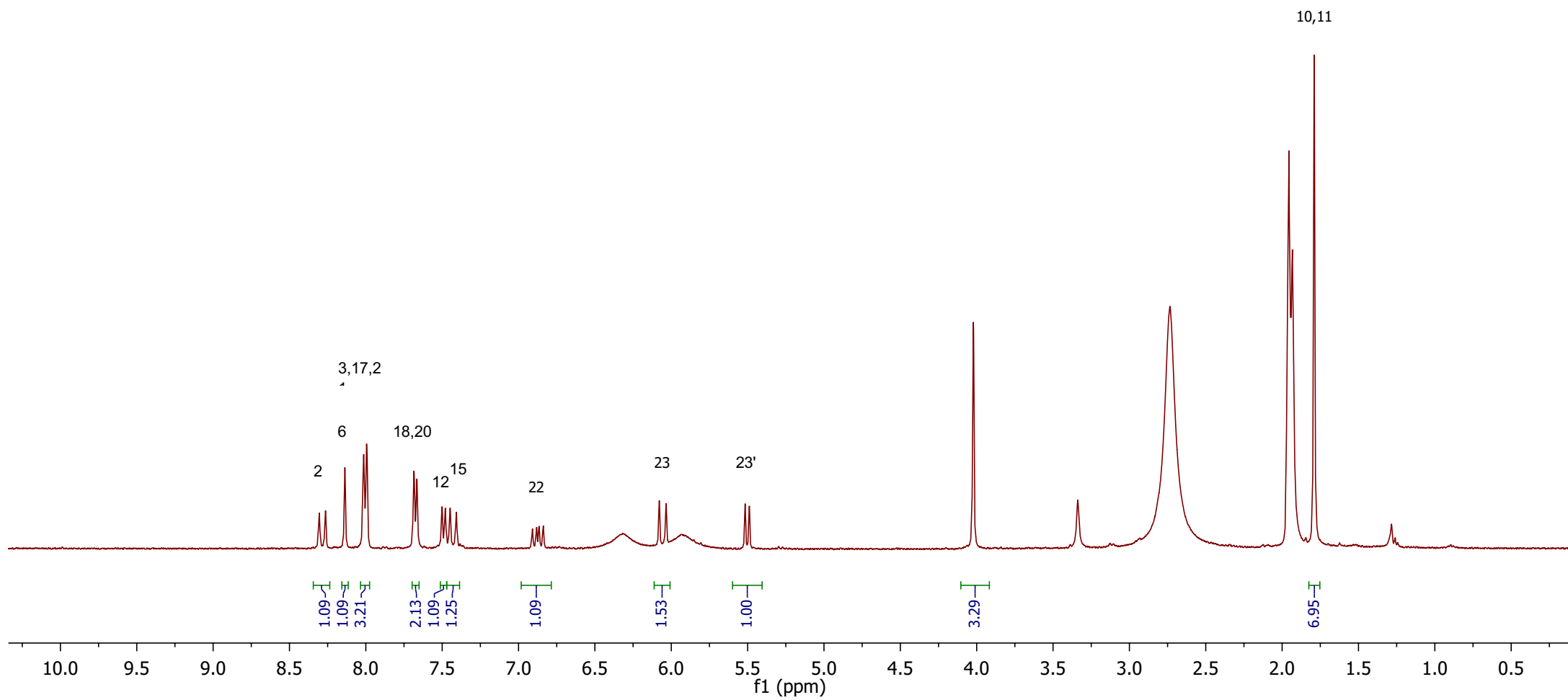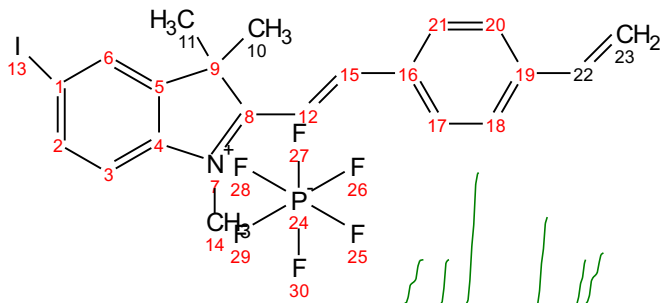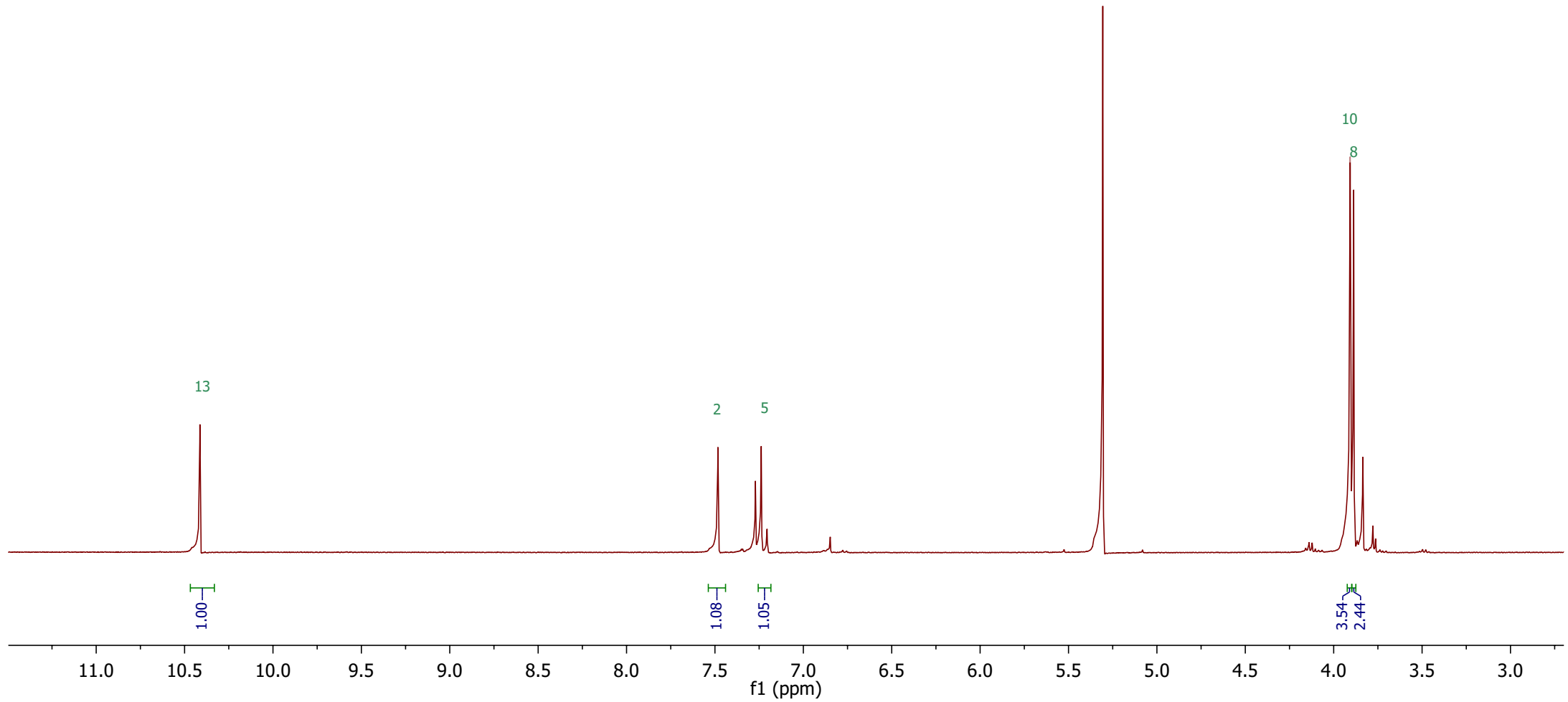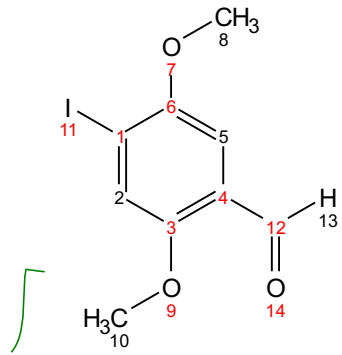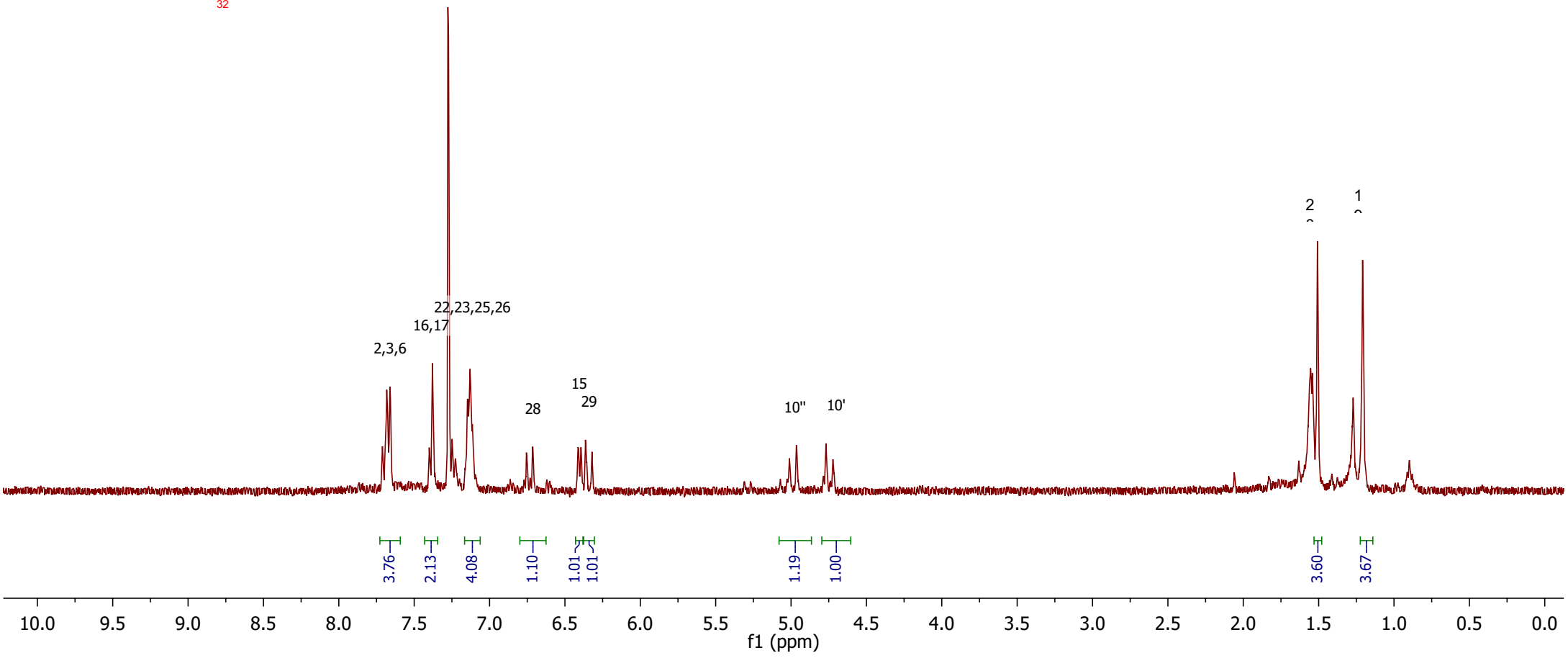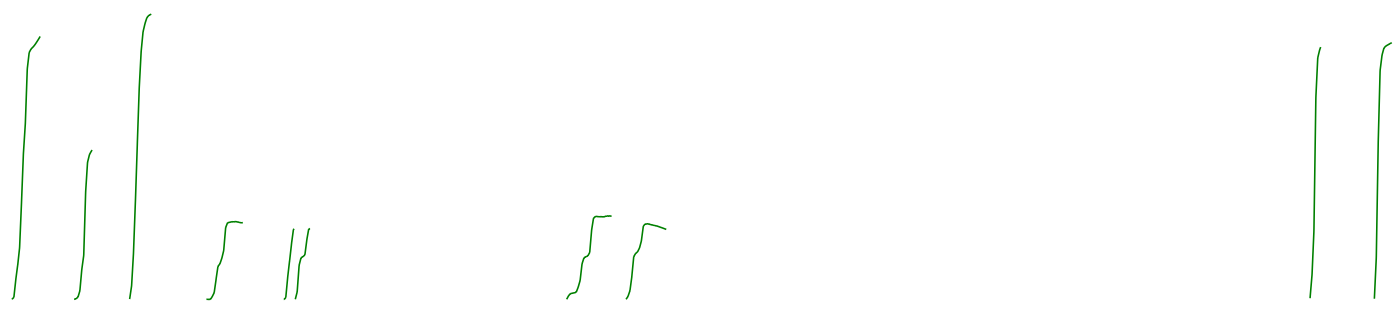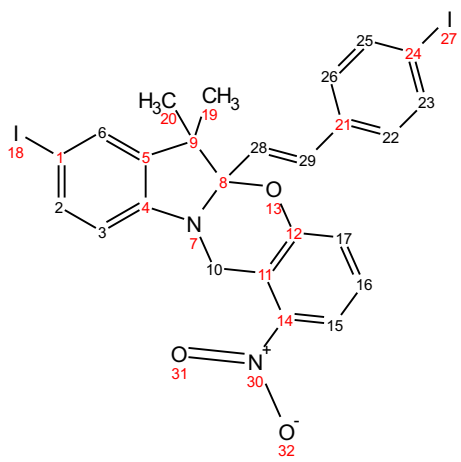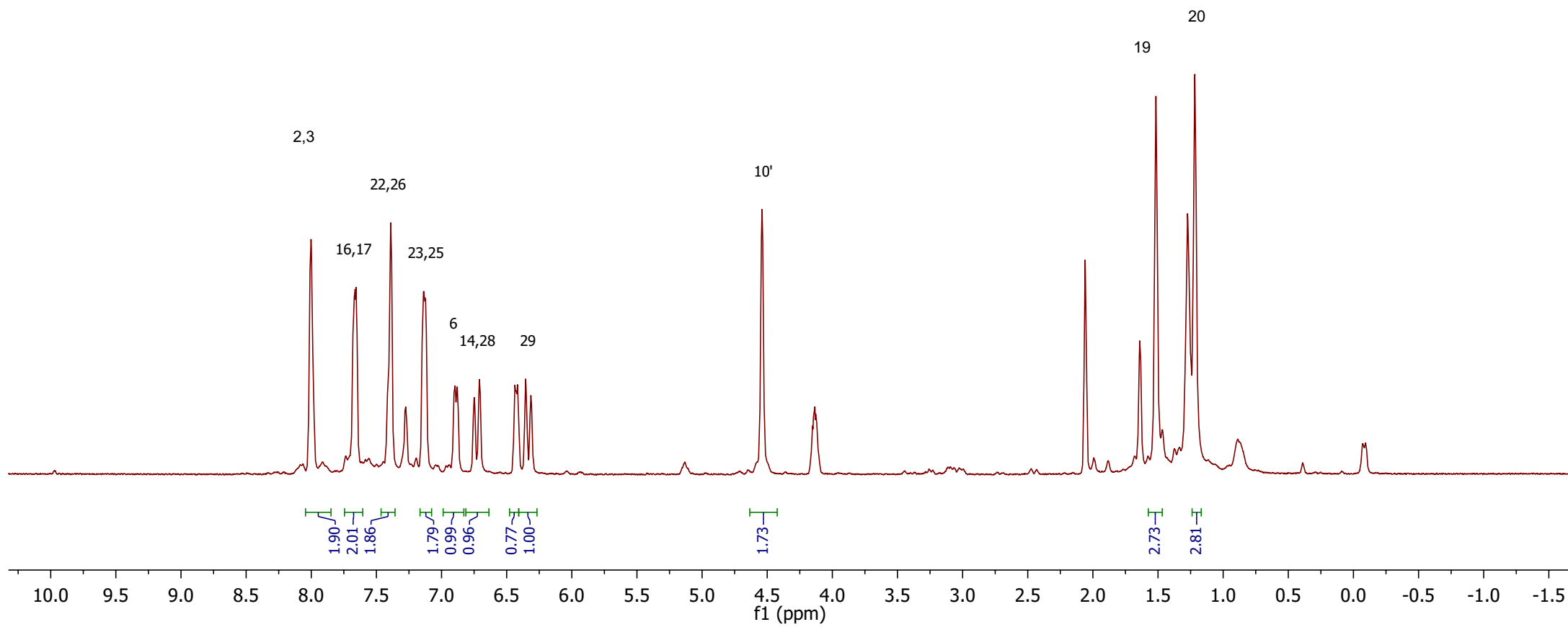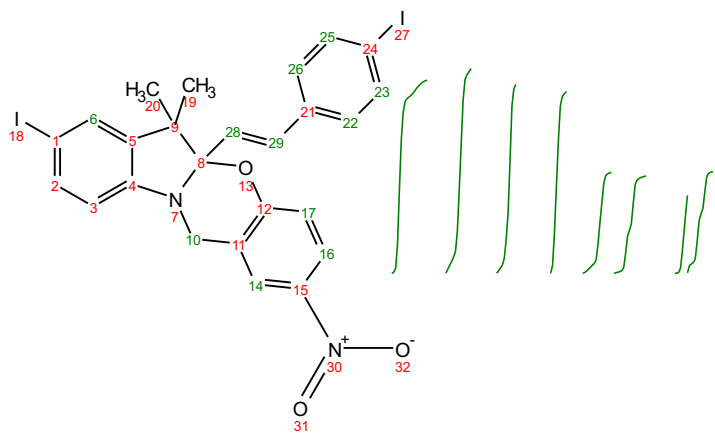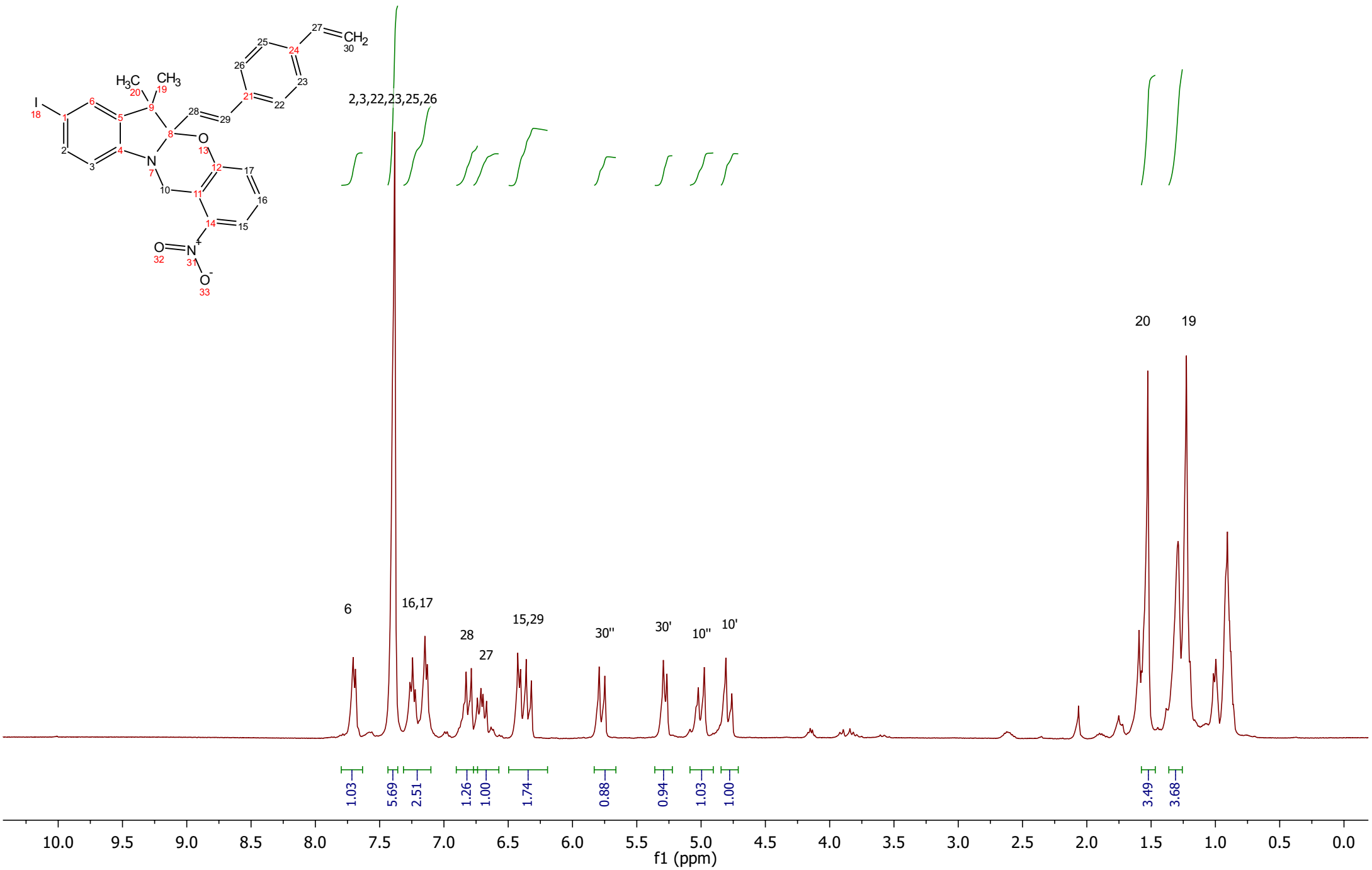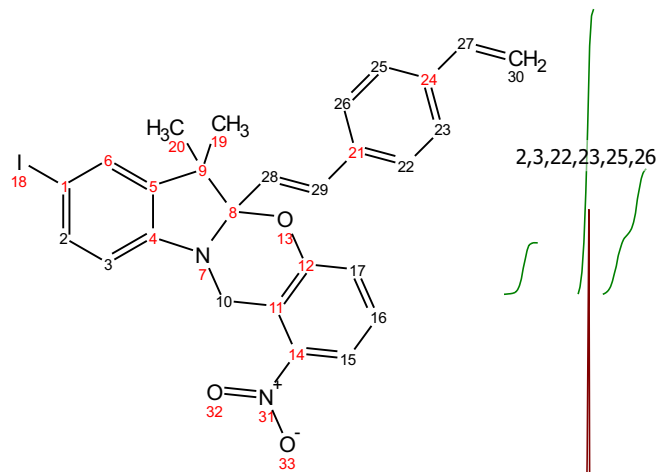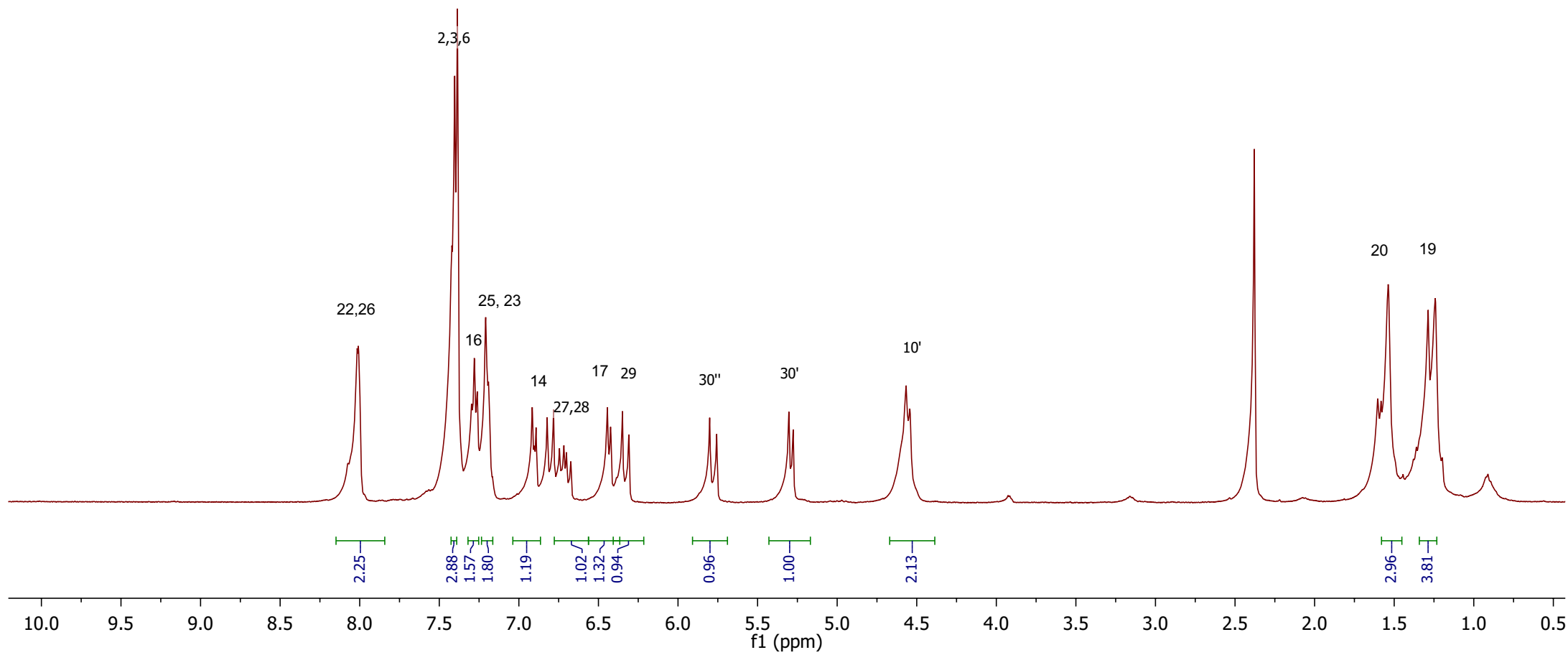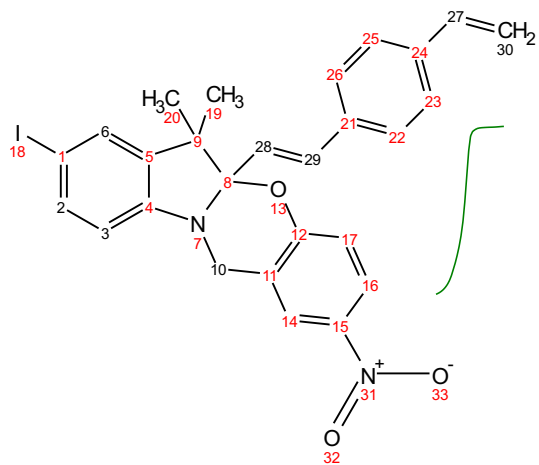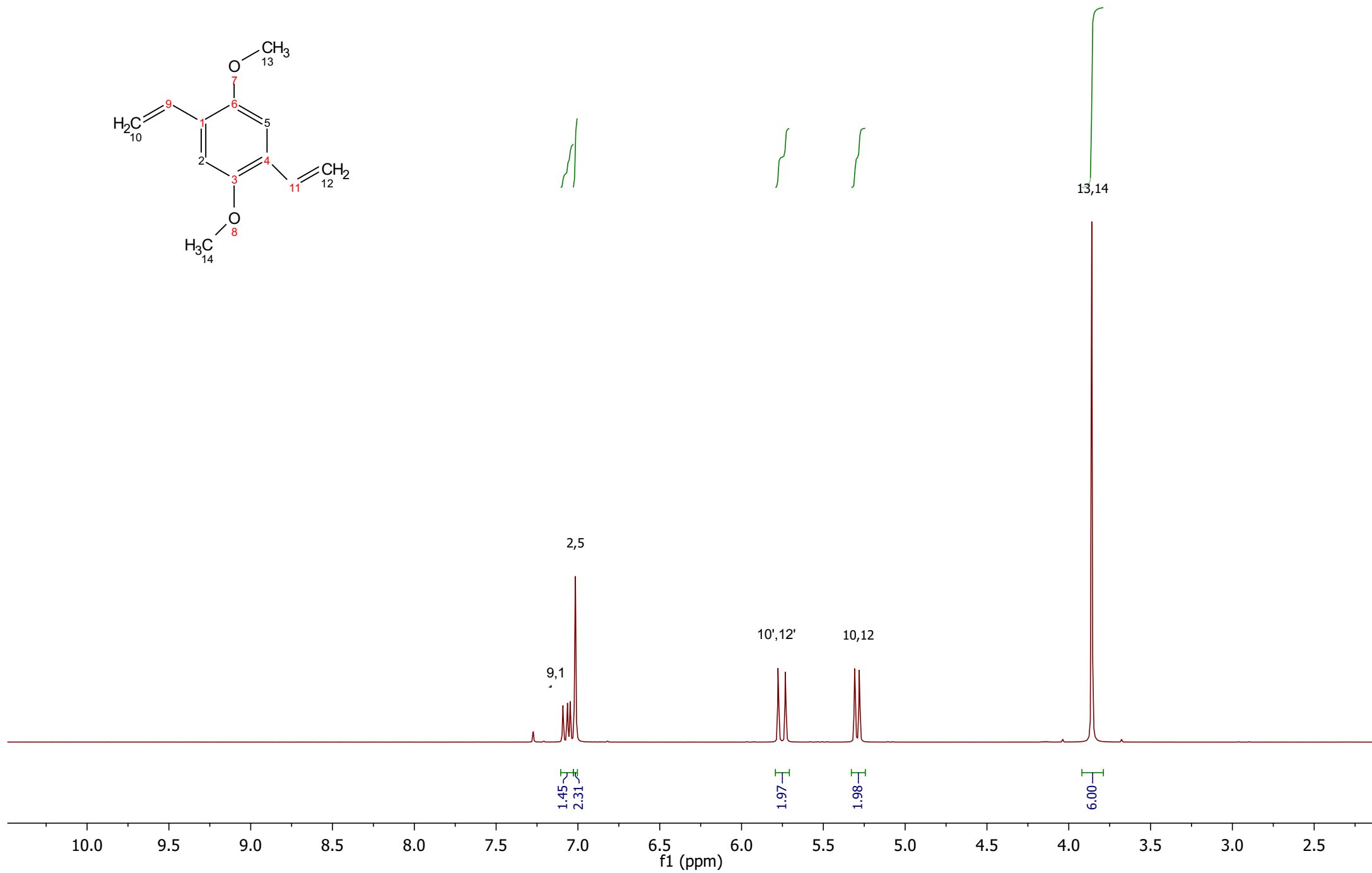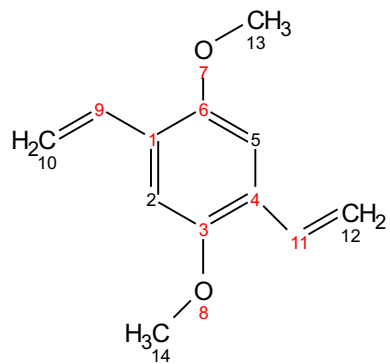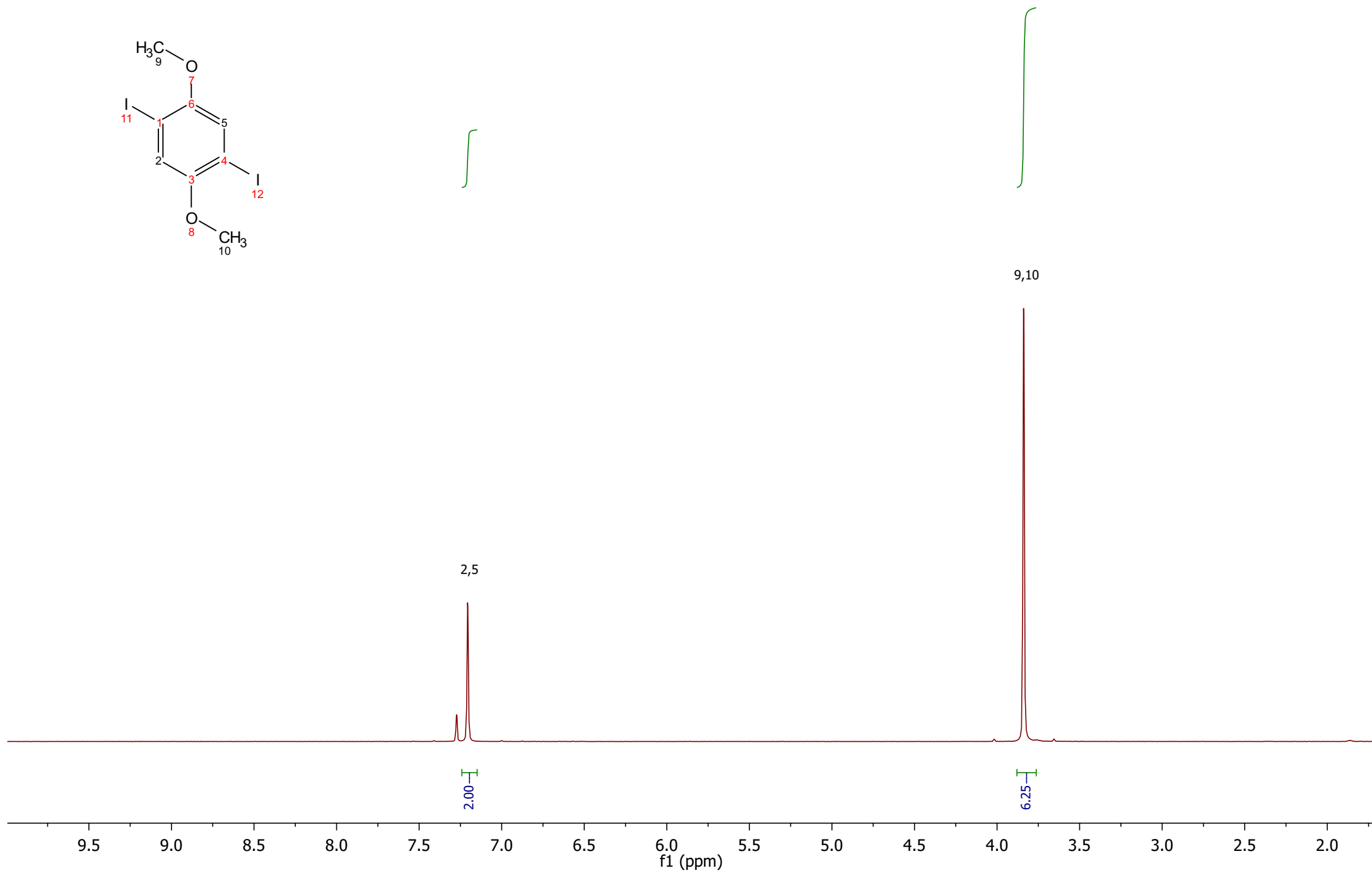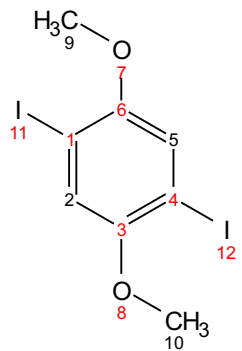
q_CDCl₃

r_CDCl
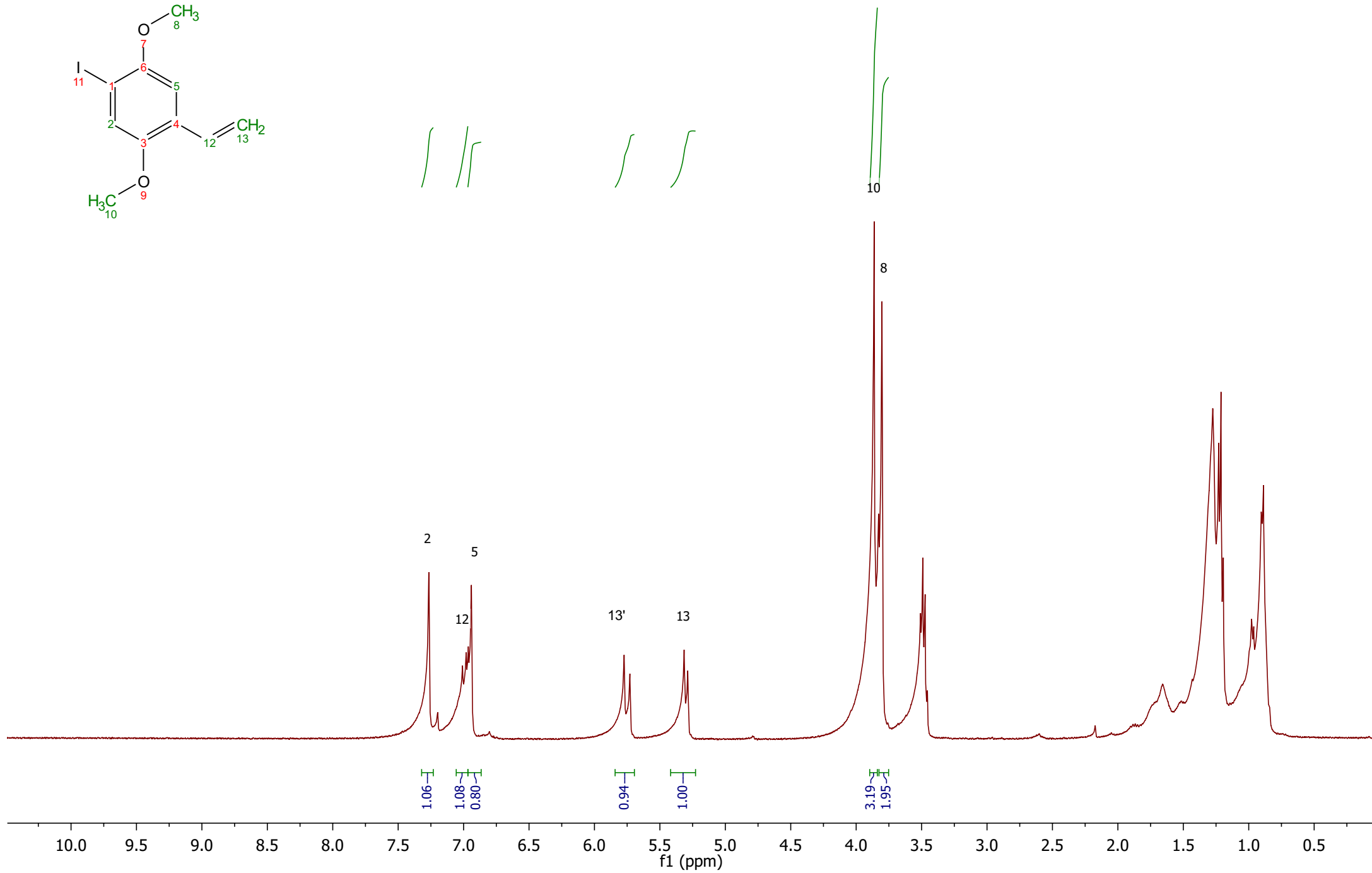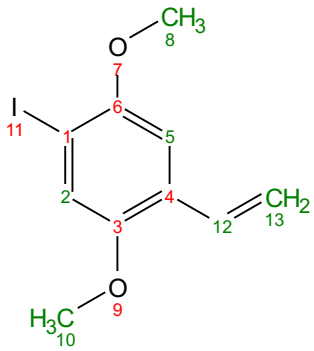
Polymer_monomer **h**_CDCl$_3$

Polymer_monomer **i**_CDCl$_3$